

**MOTOR CONTROL IN PERSONS WITH A TRANS-TIBIAL  
AMPUTATION DURING CYCLING**

A Dissertation  
Presented to  
The Academic Faculty

by

Walter Lee Childers

In Partial Fulfillment  
of the Requirements for the Degree  
Doctor of Philosophy in Applied Physiology in the  
School of Applied Physiology

Georgia Institute of Technology  
August 2011

**COPYRIGHT 2011 BY WALTER LEE CHILDERS**

**MOTOR CONTROL IN PERSONS WITH A TRANS-TIBIAL  
AMPUTATION DURING CYCLING**

Approved by:

Dr. Robert J. Gregor, Advisor  
School of Applied Physiology  
*Georgia Institute of Technology*

Dr. Boris I. Prilutsky  
School of Applied Physiology  
*Georgia Institute of Technology*

Dr. T. Richard Nichols  
School of Applied Physiology  
*Georgia Institute of Technology*

Dr. Lena H. Ting  
Department of Biomedical Engineering  
*Emory University and the Georgia  
Institute of Technology*

Dr. Geza F. Kogler  
School of Applied Physiology  
*Georgia Institute of Technology*

Date Approved: July 1, 2011

This dissertation is dedicated to any individual living with an amputation and my late Grandfather, Thomas Walter Reeves.

## ACKNOWLEDGMENTS

I have been very fortunate to have so many people that have advised and educated me along the way. A couple words in a thick dissertation are inadequate to fully express my gratitude toward those that have given of themselves to help me achieve this degree yet here goes anyway...

Big thanks to my adviser Robert Gregor. Coolest guy I've ever worked for in my life. Always supportive, always offering steady guidance while tactfully reminding me I can't do everything at once. I remember meeting Dr. Gregor through Dr. Prilutsky. I told Dr. Prilutsky I was interested in doing some research in cycling and he said there's this Gregor fellow down the hall that has done a little in that area (little was a bit of an understatement). I wandered in Dr. Gregor's office and said, "I want to study some cycling stuff, you do that?" Next thing I know I was digging through boxes of instrumentation and given a storage room to call a laboratory. After I graduated Georgia Tech (the first time), I mentioned to Gregor, "All I know now is that I don't know nuth'n." Next thing I know I was a PhD student. I think it was Gregor's plot to keep me all along because the secretary already had my paperwork ready when I came out of his office. Devious plan or not, I've enjoyed my time working with Dr. Gregor immensely.

I also appreciate the guidance of my other committee members, Geza Kogler, Boris Prilutsky, Richard Nichols, and Lena Ting. I thank Dr. Kogler for his support of me, especially during the design and fabrication of the ankle foot orthosis used in these experiments and for countless discussions on the state of prosthetic research. I thank Dr. Prilutsky because he introduced me to biomechanics, motor control and Dr. Gregor but I especially appreciate all the little talks we've had about two joint muscles, science, and dealing with reviewers. I thank Dr. Nichols for his endless encouragement, advice and for his time putting together the rehabilitation seminar and the ethics courses. I would not have taken those courses on my own yet they exposed me to different areas of

research and different ways of thinking through a problem that will continue to benefit me throughout my career. Finally, I really appreciate Dr. Ting for her time with me on discussion and interpretation of research, for being interested in my results when I thought they were uninteresting and for her advice on my proposal. Dr. Ting's influence through the proposal had an enormous impact on the final experiments for this dissertation and without her, I believe I would have missed and misinterpreted a lot of interesting data.

These experiments could not have been accomplished without all the wonderful people that volunteered for testing. They volunteered their time to be covered with electrodes, stuck on a bike and asked to pedal. They were patient, cooperated with everything (even if the equipment didn't) and generally dealt with my mayhem all without payment. I had an absolute blast working with all of them and consider them all dear friends. I hope what we've learned here can influence clinical practice and make a difference not only for my volunteers but everyone that has acquired an amputation. In addition to the eighteen subjects that volunteered for the experiments in this dissertation, I want to thank all the subjects used for pilot testing, many of them my classmates. They helped me work through all sorts of equipment, testing and methodological issues I could not have done on my own.

I want to acknowledge the master's students, DeLana Finney, Laura Clark-Jones, and Hosna Sharafi, that worked with me in the lab. I learned a lot from working with all of you, your projects and I enjoyed every minute of it. Each of you had the challenge of not only getting your own projects done but doing those projects amid the chaos of random equipment malfunction and whatever mess I was creating with my own project. I wish each of you the very best of luck as you enter the prosthetics and orthotics profession.

I would like to acknowledge the help, guidance and advice from others in the School of Applied Physiology, Beth Brown, Scott Conger, Rob MacDonald, Chris

Hovorka, Rob Kistenberg, Joy Daniel, Shay Powell, Kristy Wentz, Arick Auyang, Emma Hudson-Tole, Alexander Klishko, Christopher Mizelle, Guay-haur Shue, Stephen Sprigle, Mindy Millard-Stafford, Jill Rahnert, Mike Jones and everyone else I can't think of right now. All of you provided incredible support for me throughout my time in the masters and PhD program. A big thanks to Rob MacDonald for allowing me to raid material from the MSPO lab knowing I was never going to return anything. Maybe now that I'm leaving you can get your stuff back... Maybe...

I also acknowledge the Georgia Tech TI:GER program. This program taught me about the process of technology commercialization and introduced me to my incredible teammates, Stephen Kunen, Becky Rule, Jesse Sandlin, and Leslie Thomas. It was a joy to work with all of you.

None of this research or my PhD would have been possible without the support from the many businesses that donated material and the National Institute of Health. I thank Tracy Slemker and Prosthetic Design Inc. for the donations of prosthetic components, Mindy Millard-Stafford for the donation of space and a Lode cycle ergometer, Ray Browning and Serotta Custom Bicycles for the donation of my first cycle ergometer, Peter Harsch and Ossur Inc. for the donation of the prosthetic feet used for my masters project, and Pete Wicker and Outback Bikes for the donation of bicycle components and always giving me deals on bikes. I thank the National Institute of Health and the US taxpayer for funding three years of my education as well as providing money for lab equipment and travel to scientific conferences via a T32 training grant.

Another big thank you goes to Tracy Slemker. All of this, the prosthetics stuff, the PhD, the masters, everything, "It's all your fault!" Tracy introduced me to the Prosthetics industry back in 2003 when I was working in drag racing. Since then, he has been an incredible mentor to me and has helped me every step of the way being very generous with his time and his advice. I could not and would not have done any of this without his involvement. Thanks Tracy.

There have been many other people that deserve a big thank you as well. People that have mentored and advised me throughout life and have made me the person I am today. I thank my high school teacher, Barry Gillespie, for introducing me to engineering and the application of science. I thank Tex Layton and Jim Johnson of the Commemorative Air Force who took the time to teach a kid how to use a wrench and the importance of craftsmanship. I thank “Digger” Don Dixon for taking me as an intern in his racecar engine shop for several years allowing me to learn all about things made of oil and metal. I thank my professors at Southern Polytechnic State University, Millard Davis, John Logue, John Sweigart and Don Horton who encouraged, educated and advised me while providing fine examples academic professors. I thank Jin Lee for introducing me to cycling and all the crazy adventures we got into cycling across Europe and America. I thank John Proctor for advising me through all my major decisions while making sure I was always well fed. I thank Douglas Taylor for our many debates over drinks and providing a different perspective on the larger impact of my work. Another big thanks goes to Lance Larsen who advised me to get out of drag racing and pursue a pathway in the prosthetics profession. After all, top fuel dragsters and humans; it’s all the same equations just different application but also a different impact.

Finally, I want to thank my family. To my Mom, Nancy Childers, who curtailed her own pursuit of a PhD in order to help raise myself and my two brothers while my Dad, Chet Childers, attempted to start a software company. Their sacrifices always ensured my brothers and I could continue to pursue whatever subject struck our fancy. Lastly to my wife, Jamie Childers, who tirelessly dealt with all my late nights, last minute mayhem, and general non-sense. She was always there to help me through everything and I love her dearly.

# TABLE OF CONTENTS

	Page
ACKNOWLEDGEMENTS	i
LIST OF TABLES	xi
LIST OF FIGURES	xv
SUMMARY	xvii
 <u>CHAPTER</u>	
1 INTRODUCTION	1
Aim #1	3
Aim #2	6
Significance	10
Limitations	12
2 BACKGROUND	14
Integration of physiological systems for motor control	14
Trans-tibial Amputation	14
The Cycling Task	16
Biomechanics of Cycling with a Trans-tibial Amputation	23
3 METHODS	32
Subject Information	32
Experiment Protocol	35
Data Collection Protocol	46
Data Reduction	51

4	THE EFFECT OF CADENCE ON MUSCLE COORDINATION IN PERSONS WITH AN AMPUTATION AT CONSTANT OUTPUT	54
	Introduction	54
	Methods	55
	Results	57
	Discussion	67
5	MOTOR CONTROL IN PERSONS WITH AN AMPUTATION DURING CYCLING AT CONSTANT CADENCE	70
	Introduction	70
	Methods	72
	Results	73
	Discussion	88
6	THE EFFECT OF ALTERED MECHANICS ON LOWER LIMB OUTPUT DURING CYCLING	97
	Introduction	97
	Methods	98
	Results	104
	Discussion	119
7	THE EFFECT OF INTERFACE MECHANICS BETWEEN THE LOWER LIMB AND AN EXTERNAL DEVICE DURING CYCLING	124
	Introduction	124
	Methods	125
	Results	131
	Discussion	142

8	SYMMETRICAL KINEMATICS DOES NOT MEAN SYMMETRICAL KINETICS IN PERSONS WITH UNILATERAL TRANS:TIBIAL AMPUTATION	146
	Introduction	146
	Methods	147
	Results	148
	Discussion	157
9	SUMMARY, CLINICAL APPLICATIONS AND DIRECTION FOR FUTURE RESEARCH	159
	Summary	159
	Clinical Applications	163
	Conclusions and Future Directions	165
	APPENDIX A: DESCRIPTION OF EQUIPMENT	169
	Cycle Ergometer	169
	Force Pedal and Crank System	171
	Kinematic Instrumentation	175
	Surface Electromyography Instrumentation	176
	APPENDIX B: MEASUREMENT OF MOTION BETWEEN THE RESIDUAL LIMB AND THE PROSTHETIC SOCKET DURING CYCLING	177
	Introduction	177
	Methods	179
	Results	184
	Discussion	187

APPENDIX C: UNCERTAINTY AND SENSITIVITY ANALYSIS FOR THE CALCULATION OF INVERSE DYNAMICS DURING CYCLING	189
Introduction	189
Methods	190
Results	198
Discussion	201
REFERENCES	204
VITA	213

## LIST OF TABLES

	Page
Table 1: Major lower limb muscles involved in cycling	18
Table 2: Hip and Knee Angles derived from a computer simulation	27
Table 3: Results of pilot work performed on TTA comparing work asymmetry	28
Table 4: Inclusion Criteria	33
Table 5: Volunteer Information for the TTA group	34
Table 6: Volunteer Information for the Intact group	34
Table 7: Outline of Load/Cadence Conditions for all groups	37
Table 8: Electrode placement	51
Table 9: Timing of Peak Torque	57
Table 10: Variables quantified to answer Hypothesis 1.2	72
Table 11: Pedaling resistance and cadence calculated via the force pedals	73
Table 12: Mass, center of mass and moment of inertia calculations	74
Table 13: Magnitude and timing of Peak Torque	76
Table 14: Average Joint Moment	78
Table 15: Timing of Peak Moments	79
Table 16: Magnitude of Peak Moments	79
Table 17: Mass, center of mass and moment of inertia calculations	103
Table 18: Pedaling asymmetries in work and force about the crank spindle	104
Table 19: Cleat location	106
Table 20: Timing of Peak Torque	109
Table 21: Average Joint Moment	111
Table 22: Magnitude of Peak Moments	112

Table 23: Timing of Peak Moments	112
Table 24: Cleat location	132
Table 25: Average Joint Angle	132
Table 26: Joint Range of Motion	133
Table 27: Timing of Peak Torque	135
Table 28: Average Joint Moment	153
Table 29: Magnitude of Peak Moments	153
Table 30: Timing of Peak Moments	154
Table 31: Calibration data for the dual piezoelectric element force pedals	171
Table 32: Mass, center of mass and moment of inertia calculations	184
Table 33: Displacement of the distal portion of the residual limb	185
Table 34: Different assumptions on how to locate the hip joint center of rotation	192
Table 35: Variable names to calculate joint moments via inverse dynamics	193
Table 36: Uncertainty assigned to the X and Z axes for the JCR location	195
Table 37: Uncertainty assigned to each variable and the rationale	196
Table 38: Uncertainty in shank length and angle based on JCR assumption	197
Table 39: Uncertainty based on knee and hip JCR assumptions	197
Table 40: Uncertainty and sensitivity analysis results for the hip moment	199

## LIST OF FIGURES

	Page
Figure 1: Schematic of the lower limbs	15
Figure 2: Pedal stroke Quadrants	17
Figure 3: Schematic of the lower limb showing representative muscle activity	19
Figure 4: Exemplar Mean Torque	22
Figure 5: Work and force asymmetry in eight TTA cycling	23
Figure 6: Force effectiveness ratio	24
Figure 7: Average EMG of the Gastrocnemius	26
Figure 8: Diagram describing effective prosthetic length for cycling	30
Figure 9: Exemplar data for effective leg length	31
Figure 10: Electromagnetically braked cycle ergometer used	36
Figure 11: Cycling shoes were available in each size	37
Figure 12: Diagram describing effective prosthetic length	39
Figure 13: AFO designed to replicate the mechanics of cycling with an amputation	41
Figure 14: Subject wearing the AFO on the bicycle	42
Figure 15: Diagram showing the two different cleat positions used	43
Figure 16: The plate added to the bottom of the cycling shoe	44
Figure 17: Cycling prostheses used	45
Figure 18: Data collection periods	47
Figure 19: Dual piezoelectric element fore pedals	48
Figure 20: Force pedals adapted with a pedal interface	48
Figure 21: TTA on ergometer	50
Figure 22: Timing of the Gluteus Maximus	60

Figure 23: Timing of the vastus medialis muscle	61
Figure 24: Timing of the long head of the biceps femoris muscle	62
Figure 25: Timing of the rectus femoris muscle	63
Figure 26: Timing of the gastrocnemius muscle	64
Figure 27: Timing for the soleus muscle	65
Figure 28: Timing for the tibialis anterior muscle	66
Figure 29: Crank torque for the dominant limb	75
Figure 30: Work and force pedaling asymmetries	76
Figure 31: Angular motion of the residuum in the prosthesis	77
Figure 32: Hip, knee, and ankle joint moments for the dominant limb	80
Figure 33: Moment at the residuum/prosthesis pseudo joint	81
Figure 34: Moments for the knee joint and the RPP joint	82
Figure 35: Timing of muscle onset, peak and offset	83
Figure 36: Activation of the amputated Rectus Femoris	84
Figure 37: Activation of the amputated Gastrocnemius	84
Figure 38: Schematic of the amputated limb and the prosthesis	86
Figure 39: Quadrants of the crank cycle	87
Figure 40: Group average for muscle activation for the gastrocnemius	89
Figure 41: Diagram showing the two different cleat positions used	100
Figure 42: The plate added to the bottom of the cycling shoes	101
Figure 43: Subject wearing the AFO on the bicycle	102
Figure 44: Diagram showing the location of the AFO center of mass	103
Figure 45: Average joint angle and range of motion	107
Figure 46: Angular motion between the AFO and the shank	108
Figure 47: Movement of the center of rotation throughout the crank cycle	108

Figure 48: Torque about the crank spindle for the conditions tested	110
Figure 49: Joint moments for the control, Bi-CLEAT and Bi-AFO conditions	113
Figure 50: Muscle onset, peak activation and offset	116
Figure 51: Average activity of muscles in the lower limb	117
Figure 52: Muscle activation during the crank cycle	118
Figure 53: AFO design	128
Figure 54: Subject wearing the AFO on the bicycle	129
Figure 55: Diagrams of prosthesis and AFO	130
Figure 56: Angular motion between the AFO and the shank	133
Figure 57: Pedaling asymmetries in the TTA group	134
Figure 58: Torque about the crank spindle	135
Figure 59: Joint moments	137
Figure 60: Muscle onset, peak activation and offset	140
Figure 61: Muscle activation during the crank cycle	141
Figure 62: Average joint angle and range of motion	149
Figure 63: Pedaling asymmetries	150
Figure 64: Change in Work Asymmetry	151
Figure 65: Crank torque	151
Figure 66: Joint moments	155
Figure 67: Electromagnetically braked cycle ergometer used	169
Figure 68: Micro-adjust seatpost clamp adapted to cycle ergometer	169
Figure 69: Dual piezoelectric element fore pedals	171
Figure 70: Force pedals adapted with a pedal interface	172
Figure 71: Aluminum adapter plate between force pedals and pedal interface	173
Figure 72: Adjustable crank arms used for the experiment	173

Figure 73: Cross sectional view of a prosthetic socket	177
Figure 74: The LSM device mounted on a prosthetic socket	179
Figure 75: Backside of the LSM	179
Figure 76: Pin and cuff strap suspensions	181
Figure 77: Diagram showing the location of the bracket	182
Figure 78: Displacement and pedal forces for the pin suspension	185
Figure 79: Dual element piezoelectric force pedals with the pedal interface	190
Figure 80: An example of the output of the Crystal Ball software	198
Figure 81: Relationship between uncertainty in thigh length and CoV	200

## LIST OF SYMBOLS AND ABBREVIATIONS

ACSM	American College of Sports Medicine
AFO	Ankle foot orthosis
AMP-TTA	Amputated limb of the group with a trans-tibial amputation
ANOVA	Analysis of variance
A-P	Anterior/posterior direction
ASIS	Anterior superior iliac spine
BF	Biceps femoris long head muscle
Bi-AFO	Condition using AFOs applied bi-laterally
Bi-CLEAT	Condition using a posterior cycling cleat applied bi-laterally
BNC	Bayonet Neill-Concelman connector
BP	Bone pin
COM	Center of mass
COMAc x	Acceleration of the center of mass about the x-axis
COMAc z	Acceleration of the center of mass about the z-axis
CoV	Coefficient of variation
DC	Direct current
DOM	Dominant limb
DOM-INT	Dominant limb in the Intact group
EMG	Electromyography
FE	Force effectiveness ratio
GAS	Gastrocnemius muscle
GM	Gluteus maximus muscle
GT	Greater trochanter of the femur

HAM	Hamstring group
IL	Iliopsoas muscle
Int-AFO	Limb wearing the AFO in the Intact group
JCR	Joint center of rotation
LSM	Limb/socket motion
LVDT	Linear variable differential transducer
MOI	Moment of inertia
NON-DOM	Non-dominant limb
RF	Rectus femoris muscle
RMC	Random Monte Carlo analysis
ROM	Range of motion
RPP	Residuum/prosthesis pseudo joint
SAP	Shank AFO pseudo joint
SL	Segment length
SND-TTA	Sound limb of the group with trans-tibial amputation
SOL	Soleus muscle
TA	Tibialis anterior muscle
TDC	Top dead center
TTA	Group with a uni-lateral trans-tibial amputation
TTA-CLEAT	Group with trans-tibial amputation and a posterior cleat position
TTA-CONTROL	Group with trans-tibial amputation control condition
TTA-CRANK	Group with trans-tibial amputation and a shorten crank arm
Uni-AFO	Condition when the AFO was applied uni-laterally to the Intact group
VAS	Vasti muscle group
VAS	Vastus medialis muscle

## SUMMARY

Motor control of any movement task involves the integration of neural, muscular and skeletal systems. This integration must occur throughout the sensorimotor system and focus its efforts on controlling the system endpoint, e.g. the foot during locomotion. A person with a uni-lateral trans-tibial amputation has lost the foot, ankle joint, and muscles crossing those joints, hence the residuum becomes the new motor system endpoint. The amputee must now adjust to the additional challenges of utilizing a compromised motor system as well as the challenges of controlling an external device, i.e. prosthesis, through the mechanical interface between the residuum and prosthetic socket.

The obvious physical and physiologic asymmetries between the sound and amputated limbs are also involved in strategies for locomotion involving kinematic and kinetic asymmetries (Winter & Sienko, 1988). These asymmetric locomotor strategies may be driven by several factors related to the amputation and the prosthesis yet there remain many questions as to why the particular locomotor strategies are selected and what factors may be influencing that strategy. Factors influencing a change in locomotor strategy could be related to 1) the central nervous system accounts for the activation-contraction dynamics despite the loss of sensorimotor feedback from the amputated portion of the limb, 2) the altered mechanics of this new human/prosthetic system, or some combination of these factors. Understanding how the human motor system adjusts to the amputation and to the addition of an external mechanical device can provide useful insight into how robust the human control system may be and to adaptations in human motor control.

This research uses a group of individuals with a uni-lateral trans-tibial amputation and a group of intact individuals using an Ankle Foot Orthosis (AFO) performing a

cycling task to understand the “motor adjustments” necessary to utilize an external device for locomotion. Results of these experiments suggest 1) the motor system does account for the activation-contraction dynamics when coordinating muscle activity post amputation, 2) the motor system also changes joint kinetics and muscle activity, 3) these changes are related to control of the interface between the limb and the external device, and 4) the motor system does not alter kinetic asymmetries when kinematic asymmetries are minimized, contrary to a common practice in rehabilitation (Kapp, 2004).

Results suggest that control of the external device, i.e. prosthesis or AFO, via the interface between the limb and the device reflect “motor adjustments” made by the nervous system and may be viewed in the context of tool use. Clinical goals in rehabilitation currently focus on minimizing gait deviations whereas the clinical application of these results suggest these deviations from normal locomotion are motor adjustments necessary to control a tool, i.e. prosthesis, by the motor system. Examining amputee locomotion in the context of tool use changes the clinical paradigm from one designed to minimize deviations to one intended to understand this behavior as related to interface control of the device thereby shifting the focus to improving function of the limb/prosthesis system.

# CHAPTER 1

## INTRODUCTION

Individuals with lower extremity limb loss provide a unique model to investigate how the neuromuscular system responds to the loss of physiological resources in task-specific control. A trans-tibial amputation (TTA) removes the ankle joint and surrounding musculature responsible for power production and sensory feedback during movement control. Individuals with lower limb loss must use their remaining physiological resources in combination with an external device, i.e. a prosthesis, to interact with their environment. The prosthesis is not directly attached to the skeletal system. Therefore, in order to affect the prosthesis, loads must be transferred from the tibia via the soft tissues of the residuum and through the interface between the prosthesis (prosthetic socket). In addition, the residuum is now the end point of the lower limb and sensory information from the receptors in the skin of the residuum are providing feedback to the central nervous system as to the local integrity of the skin as well as interaction of the prosthesis and the environment. This additional mechanical complexity to the limb/prosthesis system as well as the altered sensory feedback coming from the residuum may have implications on motor control.

Reports of persons with TTA have shown a strategy during gait that is seemingly designed to minimize the moment at the knee while increasing the moment at the hip joint compared to the sound limb or intact individuals (Winter & Sienko, 1988, Sanderson & Martin, 1997, Silverman et al., 2008). The vasti, hamstrings, and gluteus maximus demonstrate increased muscular activity during stance (Winter & Sienko, 1988; Sanderson & Martin, 1997; Powers et al., 1998; Fey et al., 2010). Silverman et al. (2008) explained this increased activity as a method to use the hamstrings to transfer energy from the knee joint to the hip joint and to aid in propulsion of the trunk over the prosthesis. These changes could be related to loss of ankle plantarflexors necessary for propulsion (Sanderson & Martin, 1997; Silverman et al., 2008) or to stabilization of the knee and control knee flexion during the loading response in early stance

(Powers et al., 1998). Sanderson & Martin (1997) further suggested these changes may be related to the mechanical properties of the prosthesis or to neural reorganization, e.g. alteration of neural pathways/mechanism, to better control the prosthesis, or to both. The human motor system has demonstrated the ability to quickly adapt to altered task mechanics (Neptune & Herzog, 2000). This could be due to a similar reorganization of neural components, e.g. compensation, capable of producing the change in muscle/joint output necessary to perform the altered task without major neural reorganization. Therefore, it is not clear whether these altered locomotor strategies reflect some neural reorganization or the altered mechanics of the limb/prosthesis system.

The control of movement within the prosthetic socket resulting to contend with the limb/prosthesis system may also provide an explanation as to why TTAs utilize different motor strategies. This idea was proposed by Jaegers et al. (1996) based on muscle activity patterns in the amputated muscles within the prosthetic socket of trans-femoral amputees. However, Jaegers et al. (1996) were not able to measure motion of the limb within the socket, a measurement requisite to making a clear connection between muscle activity and motion between the residuum and the prosthetic socket. Motion at this interface has been reported using radiographic techniques in a quasi-static environment (Erikson & Lemperg 1969; Newton et al., 1988; Lilja et al., 1993; Narita et al., 1997; Soderberg & Roentgen 2003; Brooks 2009). None of these reports however, discussed a possible link between motion and control at this interface. In fact, studies examining the motor control of gait with amputation assume there is no motion between the residuum and prosthesis precluding the investigation of links between strategies developed in the human neuromuscular system and motion at this interface (Winter & Sienko, 1988; Sanderson & Martin, 1997; Powers et al., 1998; Selles et al., 2004; Fey et al., 2010). It seems reasonable then to pursue research to establish a possible link between motion at the interface and motor control and attempt to discern if any differences in motor control between amputee and intact locomotion reflect altered task mechanics. **Therefore, the goal of this research was to better understand motor control with an amputation and changes related to control of an external**

**device using subjects with intact limbs (Intact group) and with trans-tibial amputation (TTA group) during the cycling task.** That is to test the *general hypothesis* that **the control of an external device designed to extend the endpoint of the lower limb, i.e. a prosthesis, will elicit changes in motor strategy.**

This research would be the first to explore the link between the control of the interface between the residuum and the prosthesis and altered locomotor strategies specifically by methods designed to measure the movement of the residuum within the prosthesis during locomotion while measuring muscle activity and joint kinetics. This exploration has not been done before in the literature and this knowledge would provide a deeper understanding of how the human motor system has adjusted to the amputation. This knowledge would also provide useful insight into the robustness of the human control system as well as help direct interventions to aid the population of people living with amputation.

**AIM #1: To examine motor strategies used by persons with intact lower limbs and persons with uni-lateral trans-tibial amputation in the control of a cycling task.**

The effect of cadence on lower limb muscle coordination in persons with a trans-tibial amputation

The rhythmic pattern of movement observed during locomotion is generated by mechanisms within the central nervous system (central pattern generators). This basic output is modified using additional information, e. g. peripheral sensory feedback, to determine the final motor command to the muscle. This final output represents the sum of all of these mechanisms within the central nervous system and may be measured as the temporal aspects of muscle activity. Neptune et al. (1997) used cycling to study muscle coordination with increasing cadence and suggested these central mechanisms would be responsible for the contraction dynamics of the skeletal muscle and would activate the muscle earlier in the crank cycle to maintain timing of crank torque. However, loss of sensorimotor feedback from the amputated

limb, what might be modified feedback coming from the residuum and an altered musculoskeletal system could influence the central nervous system's ability to understand and respond to task demands. The motor system could respond to increasing cadence by increasing the amplitude of muscle activity without shifting the timing of that activity. An increase in the amplitude of muscle activity would be in contrast to changes in muscle output reported previously for intact cyclists.

To understand how any differences in control strategy may be related to differences between intact and TTA groups I tested the groups' response to a perturbation i.e. change in cadence. I tested *Hypothesis 1.1* that **the timing of muscle activation will occur earlier in the crank cycle with increasing cadence despite the loss of physiologic systems associated with amputation** by using intact and TTA groups (nine subjects in each group) pedaling at constant torque (15 Nm) and three different cadences (60, 90, and 120 rpm).

#### Motor control with an amputation during cycling at constant load and cadence

Motor control of locomotion in persons with trans-tibial amputation using a prosthesis should include a strategy to control the loads at the interface between the residuum and the prosthesis. The prosthesis is not directly attached to the skeletal system. Therefore, in order to affect the prosthesis, the tibia via the soft tissues of the residuum must produce a loading pattern at the interface between the prosthesis (prosthetic socket) that is able to effectively control the prosthesis during the task. This strategy should also include feedback from the residuum regarding the interaction of the skin and soft tissues and the prosthetic socket.

Motion of the tibia relative to the prosthetic socket has been reported using radiographic techniques in a quasi-static environment (Erikson & Lemperg 1969; Newton et al., 1988; Lilja et al., 1993; Narita et al., 1997; Soderberg & Roentgen 2003; Brooks 2009). None of these reports discussed a possible link between motion at this interface and the control of the residuum within the prosthesis. In fact, studies examining the motor control of gait with amputation assume there is no motion between the residuum and prosthesis precluding the investigation of links between

strategies developed in the human neuromuscular system and motion at this interface (Winter & Sienko, 1988; Sanderson & Martin, 1997; Powers et al., 1998; Selles et al., 2004; Fey et al., 2010). Control of the prosthesis could be related to how the motor system interprets the sensory information coming from the skin and soft tissue of the residuum as well as the mechanical constraints of the interface. Control of this interface could have implications for locomotion using any prosthesis and recent methods have been developed to begin to measure movement in the socket. during a cycling task.

The cycling task provides a controlled environment in which rhythmic locomotion can be studied (Gregor & Childers, 2011 for review) and motion at the RPP joint may be measured without radiographic techniques (Childers et al., 2011; see Appendix B). Pedaling kinetics has showed greater asymmetry between limbs in pedal forces and work about the crank spindle in TTA compared to Intact cyclists (Childers et al., in press). Childers et al., (in press) suggested these asymmetries may not be entirely related to strength or inertial differences between limbs. Their results suggest there may be other motor strategies utilized by TTA that cannot be understood by examining reaction forces at the foot/pedal interface (Childers et al., in press).

The purpose of this study was to explore motor control in TTA during cycling by analyzing joint kinematics, kinetics, and muscle activation patterns during amputee cycling. A group of nine Intact and nine TTA individuals pedaled at constant torque (15 Nm) and 90 rpm were used to test *Hypothesis 1.2; the neuromuscular system changes absolute muscle output to control a prosthesis via the limb/prosthesis interface.*

AIM #2: To examine the contribution of task mechanics in intact cyclists and use this information to explain changes observed in cyclists with trans-tibial amputation.

### The effect of altered ankle joint mechanics on lower limb output during cycling

The absolute differences noted between intact and TTA during AIM #1 could be related to the mechanics of their altered musculoskeletal system. A person with a uni-lateral trans-tibial amputation has lost the foot, ankle joint, and muscles crossing those joints. In addition, the amputee must now adjust to the additional challenge of controlling an external device, i.e. prosthesis and the motion of the residuum relative to the prosthesis. Therefore the mechanics of locomotion with an amputation is two-fold, 1) these individuals have lost the ability of ankle plantarflexors and dorsiflexors to contribute to locomotion and 2) the mechanics of the task are altered due to the mechanical properties of the prosthesis and the interface between the residuum and the prosthetic socket. The purpose of this chapter was to discern how the ankle joint contributes to the cycling task and develop a method to simulate the mechanics of using prosthesis in cyclists with intact limbs.

Cycling provides a unique research environment that allows for the manipulation of rider position thus providing a method to alter mechanics in an intact cyclist to minimize the contribution from ankle plantarflexors as well as influence the mechanics of the rider/bicycle system via an Ankle Foot Orthosis (AFO). In particular, output from the intact triceps surae may be influenced using two different perturbations. One perturbation is to move the cycling cleat to a more posterior position, bi-laterally, on the cycling shoe. This will reduce the moment necessary to stabilize the ankle and therefore reduce output from the triceps surae (Ericson et. al., 1985, Van Sickle & Hull, 2007, Childers et. al., 2008) without limiting ankle motion.

A second method would be to limit ankle motion, bi-laterally, using an AFO. This device would bypass the ankle joint by suspending the shank section from the pedal via an aluminum frame and a molded plastic interface. The design of the AFO used in the present experiment was modeled after an orthosis used to stabilize and axially unload tibia fractures (Zagorski et al., 1992). An adjustable closure with an anterior/posterior clamshell design used hydrostatic

pressure to suspend the AFO on the shank. The hydrostatic pressure of the soft tissues (e.g., muscle tissue) when the AFO was tightened provided an effective way to transfer loads to the shank in order to bypass loading of the foot. Medial and lateral uprights incorporated into the AFO extended past the subject's ankle and foot and attached to the pedal. This allowed loading of the pedal to occur while bypassing the foot. The 'conical' shape of the tricep surae also allows for axial loading to occur during the power phase of cycling. This type of AFO design is unique because it requires energy to be transferred through the device in order to pedal the bicycle and bypasses the ankle joint.

This type of AFO design also mimics the mechanics of the residuum/prosthesis interface because it requires energy generated at the joints to be transferred to the AFO indirectly via the soft tissue of the shank. The indirect attachment between the tibia and the AFO should allow for motion between the shank and the AFO, a situation similar to that between the residuum and prosthesis.

The use of these two perturbations allow for a spectrum of altered mechanical demands by first limiting the contribution made by the muscles controlling the ankle joint via changing the cleat position and then bypassing the ankle joint and requiring the cyclist to manipulate the pedal via the interface between the AFO and the shank. These perturbations were applied to a group of eight individuals with intact lower limbs cycling at a constant load of 15Nm and at 90 rpm to test *Hypothesis 2.1* that **an external device requiring the user to control the pedal via an interface at the shank and utilized by Intact cyclists will mimic the mechanics of cycling with a prosthesis.**

#### The effect of Interface mechanics between the lower limb and an external device during cycling

Locomotion becomes more complex when the endpoint of the lower limb is no longer the foot and the person must utilize a mechanical device between the distal limb segment and the environment e.g. a person with a uni-lateral amputation using a prosthesis. This distal limb

segment i.e. the residuum, must now interact with the environment via a prosthetic socket and the mechanical properties of the interface as well as the prosthesis to affect control.

Hypotheses 1.2 and 2.1 were tested to understand control of interface mechanics between the lower limb and an external device in both uni-lateral amputees using a prosthesis (Hypothesis 1.2) and intact cyclists using bi-lateral AFOs (Hypothesis 2.1). Results of these experiments demonstrated some evidence to suggest the motor system altered its control strategy to contend with the properties of these devices and the motion between the limb and device. Therefore it is appropriate to compare strategies used by individuals with and without amputation controlling an external device during a cycling task.

A group of eight individuals using an AFO uni-laterally were compared to a group of eight individuals with uni-lateral trans-tibial amputation cycling at a constant torque of 15Nm and 90 rpm to test *hypothesis 2.2* that **individuals with and without amputation will modify the control strategy of proximal joint in order to control an external device on the distal limb segment.**

The effect of minimizing kinematic asymmetries between limbs on kinetic asymmetries in individuals with uni-lateral trans-tibial amputation.

The relationship between asymmetries in limb kinematics, e.g. joint angles and range of motion, and limb kinetics, e.g. ground reaction forces and joint moments and powers, has not been well established. It is common within clinical practice to “optimize” the movements of persons with amputation by adjusting the prosthesis i.e. adjusting the task mechanics, so they gravitate toward symmetrical kinematics (Kapp, 2004). However the notion that kinematic or kinetic symmetry is “optimal” for performance has been questioned by Winter and Sienko (1988) who state that “It is safe to say that any human system with major structural asymmetries in the neuromuscular and skeletal systems cannot be optimal when the gait is symmetrical. Rather, a new *nonsymmetrical* optimal is probably being sought by the amputee within the constraints of the residual limb and the mechanics of the prosthesis.” Therefore a debate exists

between texts used to train clinicians that appear to advocate minimizing kinematic asymmetries (Kapp, 2004) and scientific articles stating kinematic symmetry may not be a goal of the motor system (Winter & Sienko, 1988). This may be because a relationship between kinetic and kinematic symmetry has not been well documented. Childers et al. (2009b) reported data suggesting reduction of kinematic asymmetries in a small group of three TTA cyclists may result in reduction in kinetic asymmetries yet stressed the need for additional research. Research into a relationship between kinetic and kinematic asymmetries would also emphasize the importance of device control because if control of the prosthesis was a goal of the motor system then large kinetic asymmetries should still exist when kinematic symmetry is achieved.

Lower limb kinematics are not symmetrical during amputee cycling because the prosthetic ankle is fixed while the sound ankle extends at the bottom of the pedal stroke and flexes at the top. The intact ankle in the sound limb actively plantarflexes at the bottom of the pedal stroke and dorsiflexes at the top (Pierson-Carey et al., 1997). Prosthetic ankles lack the ability to actively move and thus the amputated side can either compensate by increasing knee range of motion (ROM) and/or by greater movement at the hip joint.

The cycling task provides a method to control lower limb kinematics by altering the geometric constraints between the rider and the bicycle e.g. rider position. Shortening the crank on the amputated side brings the pedal closer at the bottom and further away at the top of the pedal stroke making demands on the affected, i.e. amputated, side knee ROM similar to the intact side while reducing the need for hip joint movement. A computer program was developed and calibrated with experimental data collected on an intact cyclist to simulate the kinematics of a TTA cycling with and without a shortened crank (Childers & Gregor, 2010). Shortening the crank by ~10mm on the amputated side should reduce the geometric asymmetries between the lower limbs of a TTA. Therefore, shortening the crank arm on the amputated side provides a method to reduce kinematic asymmetries and provides a method to test the effect of minimized kinematic asymmetries on kinetic asymmetries.

A group of eight TTA pedaled at constant torque (15 Nm) and 90 rpm with a shortened crank arm on the amputated limb as well as with symmetrical crank arms to test *Hypothesis 2.3*; **symmetrical kinematics do not reduce asymmetries in limb kinetics**. The significance of these results would emphasize the importance of device control in TTA while demonstrate the efficacy of minimizing movement asymmetries in rehabilitation.

### **Significance**

The significance of this work lies in the use of individuals with trans-tibial amputation to understand the robustness of the motor system for locomotion. Amputation of the lower limb is a major alteration to skeletal, muscular and neural systems and this research provides insight into how this altered motor system compensates for these losses. While this not only highlights differences between individuals with and without amputation it also highlights particular strategies maintained by the nervous system after the amputation to emphasize their importance to the motor system.

The first hypothesis addresses this by asking if the motor system still accounts for the activation-contraction dynamics of muscle in persons with amputation. . If both Intact and TTA groups compensate for increased cadence by shifting muscle activity earlier in the crank cycle this would suggest the motor system includes the activation-contraction dynamics of muscle when it selects a strategy for locomotion, i.e. this parameter is robust and important to the system.

The second hypothesis builds on the first by addressing absolute differences between motor strategies between Intact and TTA groups and exploring the causes of those differences, i.e. those specifically related to control of the interface between the residuum and the prosthesis. If these differences were found to be related to controlling the mechanics of the interface between the prosthesis and the residuum it could suggest that, 1) improving the mechanics of the prosthesis or the interface with the residuum may minimize these differences (if they aren't advantageous) e.g. improving prosthetic design would improve outcomes for prosthetic users, 2)

these differences or “deviations” from “normal” are simply adjustments by the motor system to utilize their remaining musculature and the prosthesis for movement or 3) a combination both possible conclusions.

The third hypothesis attempts to understand how muscles controlling the ankle joint aid in performance of a cycling task by removing their ability to contribute first by changing the position of the foot on the pedal and then by cycling with an AFO. This AFO attempts to simulate the mechanics of a prosthesis because it requires the cyclist to pedal via an AFO that attaches to the shank and bypasses the ankle joint. Information gained from this experiment would allow a deeper understanding of 1) how the loss of the ankle joint would affect locomotion and 2) the effect of using an external mechanical device, i.e. the AFO. This would then strengthen conclusions drawn from testing the second hypothesis while demonstrating the robustness of an intact motor system to perturbations in task mechanics.

The fourth hypothesis then compares the Intact group pedaling with an AFO to the TTA group to further understand the effect of using an external device for a locomotor task. Information gathered in this experiment allows for a more complete picture because if the two groups are controlling the device in the same manner than it strengthens conclusions related to control of the prosthesis.

The fifth and final hypothesis builds on all prior results and explores a concept used in clinical practice that minimization of “gait deviations” leads to symmetrical kinematics, yields symmetrical kinetics and improved performance. The significance of these results relates to the efficacy of this clinical practice in rehabilitation. If these results fail to show a link between kinematic and kinetic symmetry then a rehabilitation practice focused on minimizing “gait deviations” is called into question. These “deviations” from “normal” locomotion may be “motor adjustments” necessary to control a prosthesis, by the motor system. Examining amputee locomotion in the context of “motor adjustment” would change the clinical paradigm from one designed to minimize “deviations” to one designed to recognize this behavior as related to

interface control of the device. This would then shift the focus of rehabilitation to improving function of the limb/prosthesis system.

### **Limitations**

This research uses individuals with uni-lateral transtibial amputation because of the difficulty in finding subjects experienced with the cycling task with higher level amputation. This may preclude direct application of these results to prosthetic design specific for individuals with transfemoral amputation yet this research does highlight the need to control the device via the interface. This more general finding does have broad application regarding the use of any external device used by the lower extremity.

This study uses the constrained task of cycling as locomotor task where other rhythmic locomotor task, e.g. walking, includes a swing phase. The constrained nature of cycling may restrict the number of degrees of freedom allowed to the motor system yet there are still more actuators (muscles) than the degrees of freedom. The “redundancy”, or abundancy, in the system allows for an infinite number of possible muscle activation patterns to fulfill the moment requirement at any specific joint during cycling as with any form of locomotion.

The workload was sub-maximal for these subjects. The sub- maximal workload was necessary to minimize fatigue during the number of load conditions needed for the experiment. Sub-maximal testing is different than maximal testing because it allows more freedom for one limb to compensate for the other. Therefore, it is difficult to decipher if one limb was simply unable to perform the task requiring the contralateral limb to compensate or was there some other factor involved that made the task more difficult for the ipsilateral limb thus encouraging the contralateral limb to compensate.

Difficulty in quantifying the reaction forces and skin pressures at the interface between the device also limit this research’s ability to establish a direct cause and effect between limb control and limb movement. Future research may be able to address this limitation through additional instrumentation and computer modeling.

Limitations to the conclusions being drawn from this project are related to limitations in the general methods to analyze motor strategy using inverse dynamics to quantify joint moments

as well as the relationship between muscle activation and their contribution to the joint moment. The error in the calculation of joint moments is subject to the error within the researcher's ability to measure the necessary variables. An uncertainty and sensitivity analysis was performed on the calculation of joint moments based on the equipment available and the results from that analysis were used to improve the method and minimize the effect of measurement error and model assumptions (see Appendix C).

## **CHAPTER 2**

### **BACKGROUND**

#### **Integration of physiological systems for motor control**

Motor control of any task involves integration of neural, muscular and skeletal systems. This includes the appropriate timing of muscle activity in order to manage loads imposed on each joint (Prilutsky, 2000) as well as across joints (Kuo, 2001) and the integration of sensory feedback from the periphery back to the central nervous system helping to shape the motor program (Ting et al., 1998). The strategy utilized for a given task must take into account each muscle's functional role (uni or biarticular) in controlling this task, the properties and training state of the muscle and sensorimotor feedback from the periphery (Gregor et al., 1991) while operating within the geometric constraints of the skeletal system (Kautz & Neptune, 2002).

#### **Trans-tibial Amputation**

Individuals with uni-lateral lower limb loss provide a unique model to study neuromuscular integration because, for example, persons with unilateral trans-tibial amputations (TTA) have lost the structure of the ankle joint itself, the muscles controlling that joint, and the sensory input from the joint and surrounding musculature. These individuals must now adapt to these structural and physiological changes and interact with their environment through a prosthetic limb on one side and an intact limb on the other (Figure 1). Changes that occur after amputation include the sound limb becoming dominate for locomotion (Winter & Sienko, 1988, Silverman et al., 2008, Childers et al., in press), atrophy of the amputated limb with possible hypertrophy of the sound limb (Schmalz et al., 2001), and alteration in movement strategies (Childers et al., 2009b).

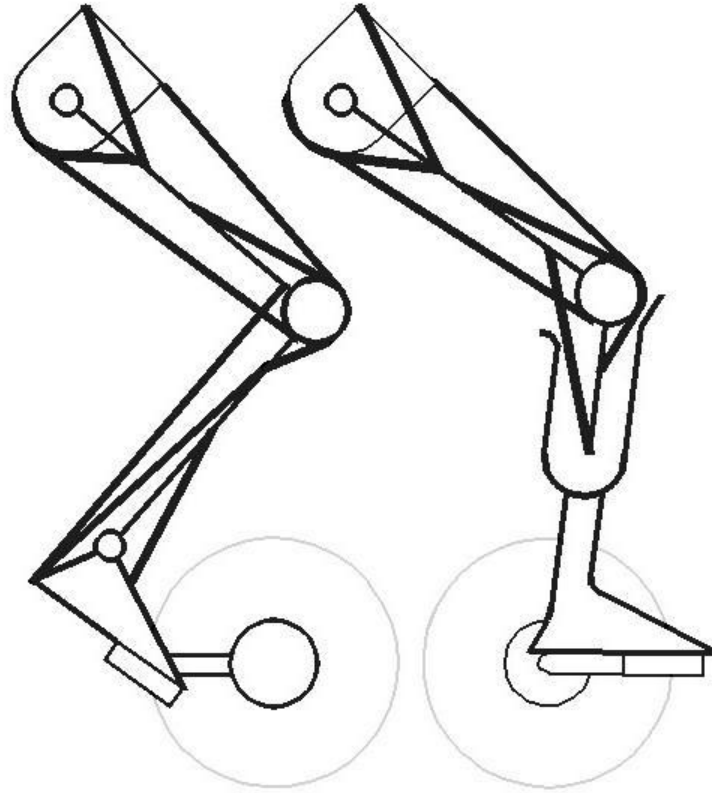


**Figure 1 - Schematic of an intact limb (left) and a limb with a trans-tibial amputation (right) using a prosthesis to demonstrate the mechanical differences between the two. Muscles are represented as thick black lines.**

Reports of TTA during gait have shown a strategy to minimize the moment at the knee while increasing the moment at the hip joint compared to the sound limb or intact individuals (Winter & Sienko, 1988, Sanderson & Martin, 1997, Silverman et al., 2008). The vasti, hamstrings, and gluteus maximus demonstrate increased muscular activity during stance phase (Winter & Sienko, 1988; Sanderson & Martin, 1997; Powers et al., 1998; Fey et al., 2010). Silverman et al. (2008) explained this strategy as a method to use the hamstrings to transfer energy to the hip joint to aid in propulsion of the trunk over the prosthesis. These changes could be related to loss of ankle plantarflexors necessary for propulsion (Sanderson & Martin, 1997; Silverman et al., 2008) or to stabilize the knee and control knee flexion during loading response (Powers et al., 1998). Sanderson & Martin (1997) also suggested these changes could be related

to the mechanical properties of the prosthesis or neural reorganization yet more research is necessary to clarify these effects.

Motion between the residuum and the prosthetic socket has been reported using radiographic techniques in a quasi-static environment (Erikson & Lemperg 1969; Newton et al., 1988; Lilja et al., 1993; Narita et al., 1997; Soderberg & Roentgen 2003; Brooks 2009). Sanders et al. (2006) presented a method to measure movement about the vertical axis during gait. Their results suggest movement about the longitudinal axis could be as high as 40mm during normal walking (Sanders et al., 2006). None of these reports however, discussed a possible link between motion and control at this interface. In fact, studies examining the motor control of gait with amputation assume there is no motion between the residuum and prosthesis precluding the investigation of links between strategies developed in the human neuromuscular system and motion at this interface (Winter & Sienko, 1988; Sanderson & Martin, 1997; Powers et al., 1998; Selles et al., 2004; Fey et al., 2010). This exposes a gap in research that relates motion between the limb and the socket to control of the entire limb/prosthesis system for locomotion.

### **The Cycling Task**

Cycling was chosen as the locomotor task for these experiments because cycling requires effective integration of human neuromuscular control and bicycle systems; thus provides a unique environment for the investigation of motor control. Cycling is a rhythmic task similar to gait yet the cycling task represents a more reduced model compared to walking since the upper body is supported by the saddle minimizing the need to stabilize the torso during propulsion. The rhythmic aspect of cycling may be controlled by similar mechanisms within the spinal cord (Zher, 2007).

The cycling task also provides a well controlled mechanical environment allowing for easy manipulation of the imposed load and cadence to the human system. In addition, the cycling task allows the researcher to control the position of the rider which will influence the range of motion of the joints and thus the operating range of a muscle's force-length and force-

velocity relationships. The mechanics as well as neural control of the cycling task has been well described (Gregor et al., 2011; Gregor & Childers 2011 for a comprehensive review) and provides a solid foundation to continue research using this task.

### **Review of the cycling task**

The cycling task may be broken down into different pedaling quadrants to better visualize the various phases (Figure 2). While each cycle is part of a continuum of demands, understanding the different control requirements during each quadrant and how those requirements are met by coordinated activation of key muscles (Table 1) is crucial.

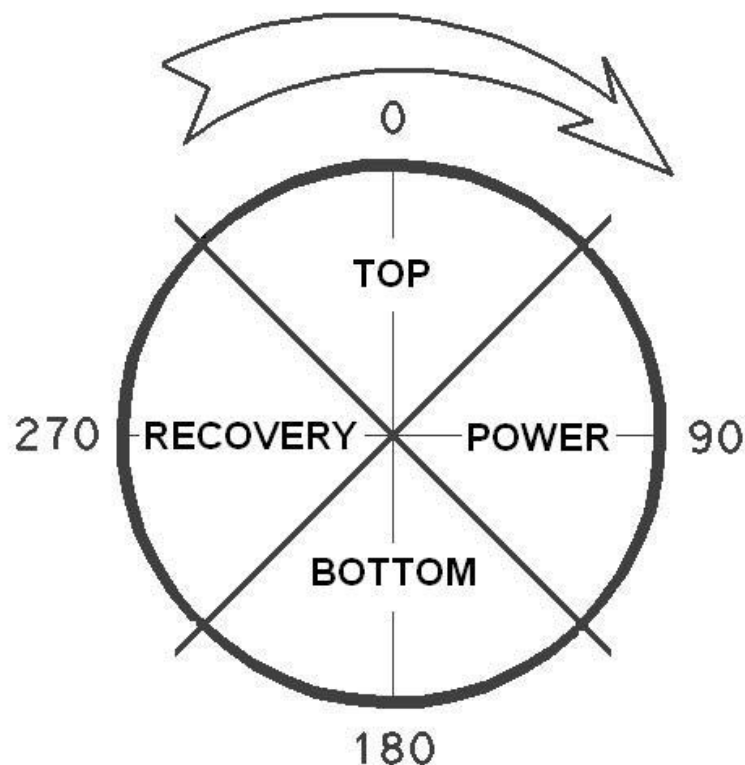


**Figure 2 - Pedal stroke Quadrants. Zero is defined as when the crank is vertical or at top dead center (TDC). The top of the stroke is from 315 to 45 degrees. The power phase is from 45 to 135 degrees. The bottom of the stroke is defined as 135 to 225 degrees. The recovery phase is defined as 225 to 315 degrees.**

**Table 1 - Major lower limb muscles involved in cycling, the motions they produce and their major functions to performance of the cycling task.**

<b>Muscle</b>	<b>Abbreviation in Figure 2</b>	<b>Moment produced by muscle activation</b>	<b>Major function in cycling</b>
<b>Tibialis Anterior</b>	TA	Ankle flexor (dorsiflexor)	Stabilize ankle during bottom and recovery phases
<b>Soleus</b>	SOL	Ankle extensor (plantarflexor)	Stabilize ankle during power phase
<b>Gastrocnemius</b>	GAS	Knee flexor and ankle extensor	Stabilize ankle and direct pedal forces during power and bottom phases
<b>Vasti</b>	VAS	Knee extensor	Major power producing muscle group
<b>Rectus Femoris</b>	RF	Hip flexor and knee extensor	Direct force at the top of the stroke and produce power during power phase
<b>Hamstring Group</b>	HAM	Hip extensor and knee flexor	Direct forces during power and bottom phases
<b>Iliopsoas</b>	IL	Hip flexor	Possibly aids to lift leg during recovery
<b>Gluteus Maximus</b>	GM	Hip extensor	Major power producer

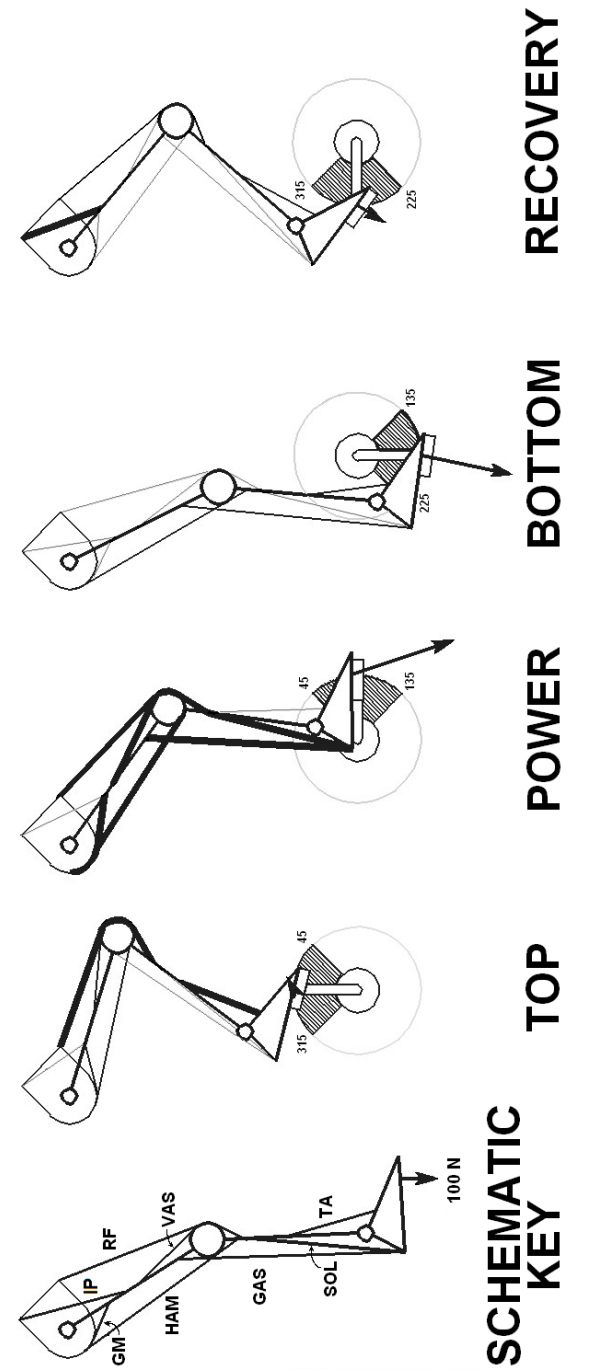


**Figure 3 - Schematic of the lower limb showing representative muscle activity of the lower limb, direction and magnitude of the force at the pedal, and limb positions in the four different quadrants of the pedal stroke. Muscle activity within each quadrant is indicated by the thickness and shade of the lines. Muscles may be very active (thick black), moderately active (thin black) or not active (thin grey). Values for limb orientation, muscle activation and force production are derived from experimental data on an intact cyclist operating at 200 watts and 90 rpm**

### The top of the pedal stroke

The top of the pedal stroke is a transition area and occurs from approximately 315 to 45 degrees relative to 0 degrees or top dead center of the crank (TDC, Figure 2). The pedal is traveling from posterior to anterior while transitioning from moving superiorly to inferiorly. To get through the top of the stroke the leg must direct force forward while preparing for the power phase (Figure 3). Effective application of force to the pedal during this phase is difficult but critical to the transition and development of an effective power phase. The Rectus Femoris (RF), for example, is active trying to flex the hip and extend the knee to direct forces anteriorly. To prepare for the power phase, the Gluteus Maximus (GM) and Vasti (VAS) start to activate just before TDC while the hamstring group (HAM) begins activity to aid in hip extension.

### The Power Phase

The power phase is where the body must produce enough force to overcome the resistance at the pedal as well as to help lift the opposite leg during its recovery phase. During this phase about 90% of the total power is imparted to the bicycle. The GM and VAS are generating most of the force seen at the pedal during this time. The ankle extensors (plantarflexors) activate to stabilize the ankle and allow the energy generated by the larger more proximal muscles to be transferred to the pedal and energize the bicycle.

### The Bottom of the Pedal Stroke

The bottom of the pedal stroke is another transitional region of the pedal cycle. The HAM, Gastrocnemius (GAS) and Tibialis Anterior (TA) are all active in this phase. The TA is active to stabilize the ankle so that tension developed in the GAS may be transferred to the knee joint to assist the HAM with knee flexion (Gregor et al., 1987). In TTA, the ankle is either absent or prosthetically simulated and thus cannot be stabilized by active muscular contraction. Furthermore, the GAS has been surgically changed to a single-joint knee flexor and can only act upon the knee joint concentrically (if at all) to aid in directing forces during this portion of the

pedal cycle. Note - The large downward forces during this phase (Figure 3) are due to the inertia of the heavy limb being redirected from moving inferiorly to a superior direction and are not derived directly from muscular activation. Muscle activation during this phase is needed to redirect this force posteriorly and aid in limb transition (Ting et al., 1999).

### The recovery phase

This phase occurs when the pedal has cleared the bottom and is now ascending back toward TDC. As the name implies, this phase of the crank cycle is intended for recovery of several extensor muscle groups. During this phase, the Vastii show no appreciable activity. The TA and the Iliopsoas (IL) are most active (Ryan & Gregor 1992, Juker et al., 1998) with the TA assuming two functions; the first to stabilize the ankle for force transfer from hip flexor muscles and the second to start dorsiflexing the ankle thereby minimizing hip and knee joint flexion during the top of the stroke. This cannot be accomplished in TTA. Their prosthetic ankle cannot actively dorsiflex through TDC creating the need for accommodation through increased hip and knee flexion for these cyclists. The RF will begin activity during the end of this phase aiding in hip flexion, while preparing for the top of the pedal cycle.

The torque produced by an individual limb during this phase is negative, i.e. energy is being absorbed, (Figure 4) because the forces during this phase are directed inferiorly (Figure 3). From the standpoint of mechanical effectiveness, this phase of power absorption may seem inefficient to the casual observer. However, there is a difference between mechanical effectiveness and metabolic efficiency. Mechanical effectiveness is the ratio between the total force seen at the pedal and the force directed to turn the cranks. In cycling, inertial and gravitational forces of a heavy (~18kg) spinning leg are large and generally directed inferiorly (impeding rotation) during the recovery phase (Kautz & Hull, 1993). The two limbs are coupled by the cranks so that while one limb is in recovery, the other is in its power output phase. In order to generate the same baseline power, the flexor groups of the ascending limb must increase muscular activity 1.1 to 3.4 beyond baseline performance and increase the whole body metabolic

demand by 9% (Mornieux et al., 2008) to overcome these gravitational and inertial forces to pull the foot up faster than it is being “pushed” up by the opposite limb. Attempting to “pull up” and generate positive power during this phase will increase mechanical effectiveness but at a high metabolic cost (Korff et al., 2007) regardless of cycling experience and pedal type (Mornieux et al., 2008). Korff et al. (2007) studied the energy requirements of different pedaling techniques and reported that the cyclist’s “preferred technique” was the one most metabolically efficient, and that consciously altering this technique, e.g. “pulling up”, resulted in a decrease in metabolic efficiency. This was the case even when the cyclists were “pulling up” as they remained unable to generate positive power during this phase. Attempting to “pull up” will certainly reduce the demand on the opposite limb but the costs appear to outweigh any possible benefits available at least to intact cyclists (Mornieux et al., 2008).

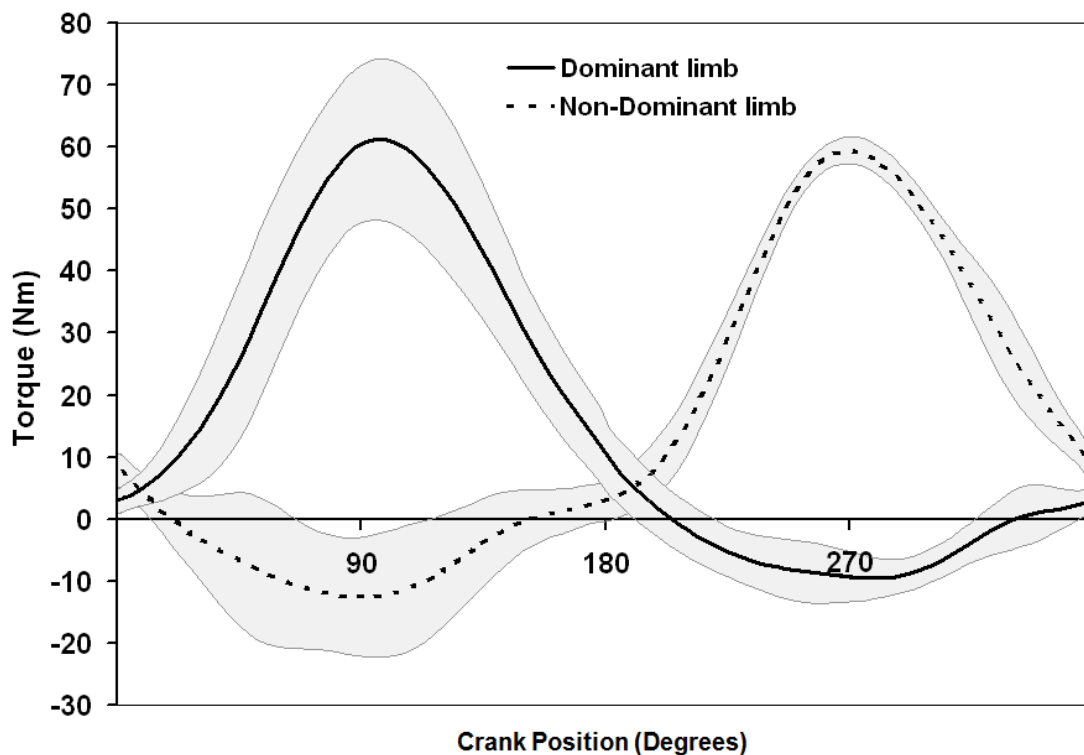


**Figure 4 - Exemplar crank torque (dark line) from nine intact cyclists  $\pm$  1 standard deviation (thin line) developed about the crank spindle during the pedal stroke. Crank zero position defined as when the dominant limb crank is pointed up to illustrate when one leg is generating a large impulse during the power phase, the contralateral limb is in the recovery phase with a negative impulse.**

## Biomechanics of Cycling with a Trans-tibial Amputation

Cycling with a uni-lateral trans-tibial amputation poses significant challenges because this geometrically asymmetrical system is coupled via the bicycle cranks. The geometric asymmetry between limbs contributes to asymmetric work (torque) production seen in cyclists with a uni-lateral TTA (Broker & Gregor, 1996; Childers et al., in press). In one report, in eight TTAs work asymmetry was seven times greater than in a control group of nine intact cyclists (Childers et al., in press) (Figure 5). Work asymmetry occurs when one limb has difficulty producing and/or directing forces appropriately (Sanderson, 1990). This asymmetry appears to be related to multiple factors beyond a strength or mass difference between limbs (Childers et al., in press) and may even represent a change in the motor control strategy used by the body to accomplish this task.

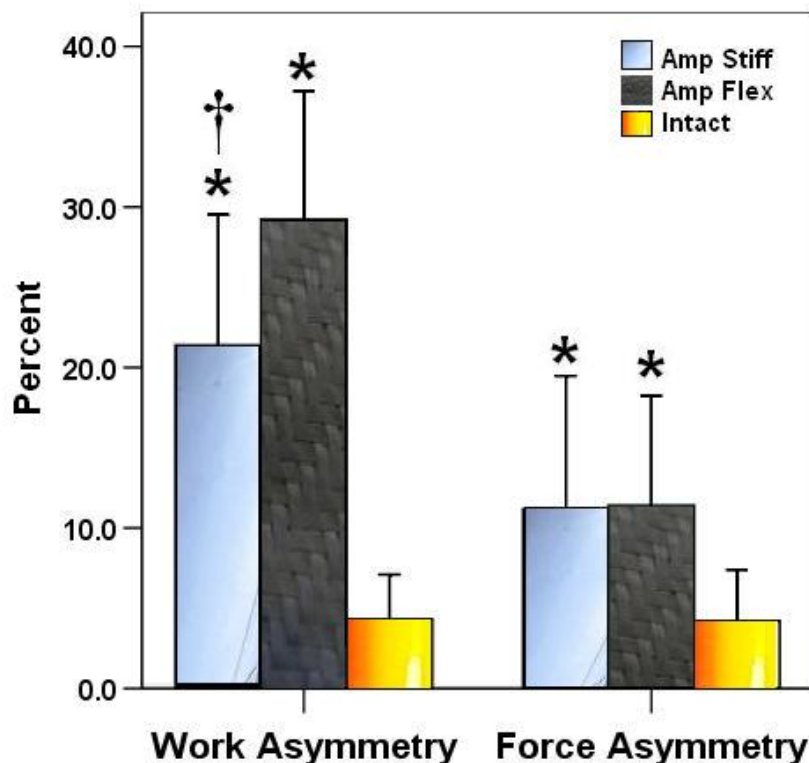


**Figure 5 - Work and force asymmetry in eight TTA cycling with a stiff foot (chrome bars) and a flexible foot (carbon fiber bars) compared to nine intact cyclists (orange bars) during a simulated time trial. † = stat. sig diff. from the FLEX foot condition. \* = stat. sig diff. from the intact group.**

Interestingly, pedaling kinetics, e.g. reaction forces measured at the foot/pedal interface, have been reported in persons with trans-tibial amputation (TTA), and show similar pedaling techniques (measured as force effectiveness and reported by Lafortune & Cavanagh, 1983), were used by TTA and Intact cyclists (Childers & Gregor, in review)(Figure 6). Force Effectiveness (FE) is the ratio between the force component orthogonal to the crank and the resultant force applied to the pedal. In this current investigation FE calculations were used to provide insight into compensations used by the rider after a portion of the neuromuscular system has been removed. These results suggest that despite the greater asymmetry in both pedal forces and work about the crank spindle the combined output of both limbs was equally as effective at directing forces about the crank as observed in intact cyclists. Therefore, pedaling technique, as the combined output of both limbs, is not dependant on an altered musculoskeletal system. This finding suggest measurements of pedaling kinetics may not be an effective method to understand motor strategies in TTAs and future research should concentrate on more local variables, e.g. joint kinetics.

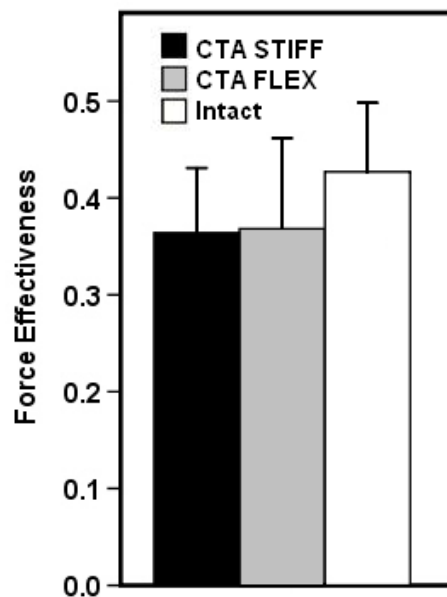


**Figure 6 - Force effectiveness ratio combining both limbs and averaged over the pedal stroke. The Cyclists with Trans-tibial Amputation (TTA) cycling with the stiff foot (black bars), the CTA with the flexible foot (grey bars) and the intact group (white bars).**

## EMG patterns in TTAs

Muscle activation patterns in uni- and bi-articular muscles generally reflect their biomechanical role in movement control (Prilutsky, 2000). Lower limb loss will affect the role played by individual muscles in limb control. The GAS muscle is altered following trans-tibial amputation, i.e. relegated to a uni-articular knee flexor, while the more proximal, non-amputated, muscles retain their anatomical attachments. Pilot work was performed to develop to understand activity patterns in the amputated GAS. Analysis of muscle activation patterns collected using surface electromyography (EMG) in six TTAs revealed that the neuromuscular system shifted activation in three of the six amputated GAS muscles to later in the pedaling cycle (Figure 7). While in all cases the GAS was reattached surgically to the tibia, the other three subjects showed almost no activation. Reasons for this lack of activation could be related to the surgical procedure, signal artifact of the electrode rubbing the socket, nerve damage and/or excessive scarring of the residual limb. This shift in timing appears to be more appropriate for the muscles' new role as a uni-articular knee flexor (Childers et al., 2009a) but will require additional research. Future research should address better methods to minimize signal artifact and include more subjects.

Other changes observed in TTA include 1) increased variability in the activity patterns of bi-articular muscles in the sound and amputated limb compared to intact cyclists and 2) the GAS in the sound limb increased its duration of activity (Childers et al., 2009a). These results help explain the asymmetries observed between the two limbs as prolonged activation of the GAS will help apply more force effectively during the bottom of the pedal stroke, thereby helping the ineffective amputated side through the top of the pedal stroke. The increases in muscle activation variability observed in the bi-articular muscles in TTAs (Childers et al., 2009a) may also reflect difficulty in energy management across multiple joints (Broker & Gregor, 1994), failure of the neuromuscular system to integrate sensorimotor information into the modified neural control system (Ting et al., 1998; Kautz et al., 2002) and/or to control movement within

the prosthesis (Jaegers et al., 1996). Additional research is necessary before these issues can be fully understood.

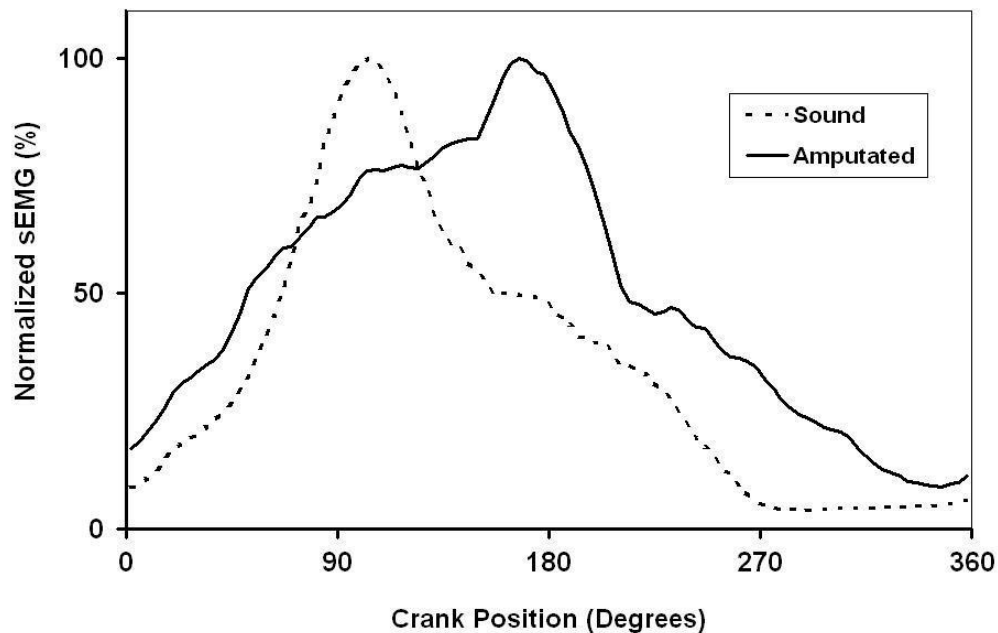


**Figure 7 - Average EMG of the Gastrocnemius (GAS) muscle from the sound (dashed) and amputated (solid) limbs showing a shift in activation to later in the crank cycle for the amputated GAS. The sound limb data was derived from six CTA while the amputated limb data was derived from three CTAs**

### **Summary of Different Adaptation of the Bicycle and Cycling Prosthesis Designs**

#### Bicycle Positioning

How the body interacts with the bicycle is affected by changes in body position (Gregor et al., 2011). The location of the saddle in relation to the crank spindle, the handlebar and the pedals defines the constraints imposed on the neuromuscular system to energize the bicycle. For example, alterations in saddle height will partially determine the functional joint range of motion (ROM), and thereby determine the range of muscle lengths and available contraction velocities (Gregor et al., 2011). Experience gained with TTA athletes suggests that following published guidelines for intact cyclists (Pruitt, 2004) is appropriate when no comorbidities exist.

## The Effect of Crank Shortening

Shortening the crank on the amputated side will help reduce the geometric asymmetries between the two lower limbs of a TTA (Childers & Gregor, 2010)(Table 2). Preliminary work completed in three TTAs to evaluate the effects of shortened cranks showed a reduction in work asymmetry in two TTAs while one TTA showed no change (Table 3). Work asymmetry is the difference in work or torque production at the crank between the two limbs. A reduction in work asymmetry indicates the sound limb had to contribute less work to turn the pedals and the amputee limb contributed more work. Despite the reduction of work asymmetry with the shorter crank in two out of three subjects, no experimental data were taken on limb kinematics thus no conclusions can be drawn as to whether a reduction in knee ROM or hip joint translation occurred as calculated by the computer simulation. More research is necessary to gain a more complete understanding as to the effect of a shortened crank arm.

**Table 2 - Hip and Knee Angles derived from a computer simulation showing changes in limb kinematics by shortening the crank arm 15 mm. Hip angle defined as the included angle between the thigh and horizontal. Knee angle defined as the included angle between thigh and shank segments. The model was calibrated to experimental data of an intact cyclist pedaling at 200 watts and 90 rpm. The amputated limb was simulated by eliminating ankle motion. Hip joint translation was assumed to be similar in all conditions.**

Condition	Hip Angle (Degrees)			Knee Angle (Degrees)		
	Min	Max	ROM	Min	Max	ROM
Sound Limb	14	57	43	65	133	68
Amputated Limb with Symmetrical Crank Arms	10	56	46	64	135	71
Amputated Limb with 15mm Shorter Crank Arm	12	53	41	67	129	63

**Table 3 - Results of pilot work performed on TTA comparing work asymmetry (defined as a percent difference between the contributions of each limb to total work output) with symmetric crank arms and a 15 mm shorter crank arm on the amputated side.**

<b>Subject Number</b>	<b>Work Asymmetry with Symmetrical Crank Arms (%)</b>	<b>Work Asymmetry with 15mm Shorter Crank Arm on the Amputated Side (%)</b>
<b>1</b>	<b>15.0</b>	<b>7.0</b>
<b>2</b>	<b>30.0</b>	<b>20.8</b>
<b>3</b>	<b>20.8</b>	<b>20.8</b>

The Role of the Prosthetic Foot in Cycling

The stiffness of the prosthetic foot influences cycling performance at high intensities (90% max heart rate) but not at low intensities, i.e. more recreational level intensities (70% max heart rate) (Childers et al., in press). Cycling with an intact lower limb requires activation of the triceps surae and tibialis anterior muscles to stabilize the ankle so that energy generated by the knee and hip extensors may be transferred to the pedal (Ryan & Gregor, 1992). While triceps surae and tibialis anterior muscle activation is necessary in walking, for example, for ankle stability, braking and propulsion (Perry, 1992). Prosthetic feet meant for walking are designed to mimic the ankle/foot complex, i.e. allowing it to compress and store energy at initial contact then decompress and release that energy at toe off. Forces and the timing of those forces are different between walking and cycling however, requiring a prosthetic foot be designed to meet the specific demands of cycling.

In cycling, the compressive forces used to store energy in a prosthetic foot are derived from muscular sources being used to turn the crank during the power phase. Then at the bottom of the stroke, these vertical forces are removed to allow the foot to decompress and release energy. The problem with a flexible prosthetic foot is that it requires muscular forces to compress it during the power phase thus removing energy that should be transferred to the cranks. The foot decompresses during the bottom of the pedal stroke. The forces during this

phase are directed ineffectively to produce torque. (Figure 3) shows limb orientation as well as the scaled magnitude and direction of typical forces at the foot/pedal interface during the power phase (when the foot is being compressed) and the bottom of the pedal stroke. The use of a flexible prosthetic foot results in energy removed from the crank cycle and not returned in an effective manner.

The energy removed from the crank by the flexible prosthetic foot requires compensation from the sound limb to increase its output in order to meet task demands. The result is an increase in pedaling asymmetry (Figure 5). Further, I have found that the increases in work asymmetry are only apparent at higher cycling intensities. Cycling at lower intensity requires lower normal forces which in turn may not be sufficient to compress the prosthetic foot to create a noticeable asymmetry.

#### Anterior – Posterior Cleat Placement and Effective Prosthetic Length

Anterior-Posterior (A-P) placement of the cleat does not affect metabolic efficiency in intact cyclists (van Sickle & Hull, 2007) or TTA (Murray, 2003) but will affect muscle activation of the GAS, SOL and TA in intact cyclists (Childers & Gregor, 2008). Mean activation of these muscles was minimized when the cycling cleat was placed under the medial longitudinal arch of the foot (Childers & Gregor, 2008).

In TTA the A-P location of the cleat will determine the overall socket flexion/extension angle as well as determine the effective prosthetic length. The effective prosthetic length in cycling is different than walking. In walking, the effective length is the distance from the knee center to the bottom of the heel while in cycling, the end point is the pedal spindle and not the heel. Therefore, effective prosthetic length for cycling should be measured from the knee center to the centerline of the cycling cleat (Figure 8). Furthermore, the effective prosthetic length should be set similar to the sound limb to minimize geometric asymmetries. However, the sound limb ankle can actively move thus constantly changing this length throughout the pedal cycle (Figure 9). The same computer model used to analyze crank arm lengths (Childers & Gregor,

2010) was used to analyze the kinematics of effective prosthetic length changes. A compromise was made so that if the effective prosthetic length was similar to the sound limb when the ankle was in the neutral position, kinematic asymmetries were minimized. These results however, should be used with caution as there is currently no experimental data to determine the effect of A-P placement of the cycling cleat or the complex interaction between A-P placement and effective prosthetic length.

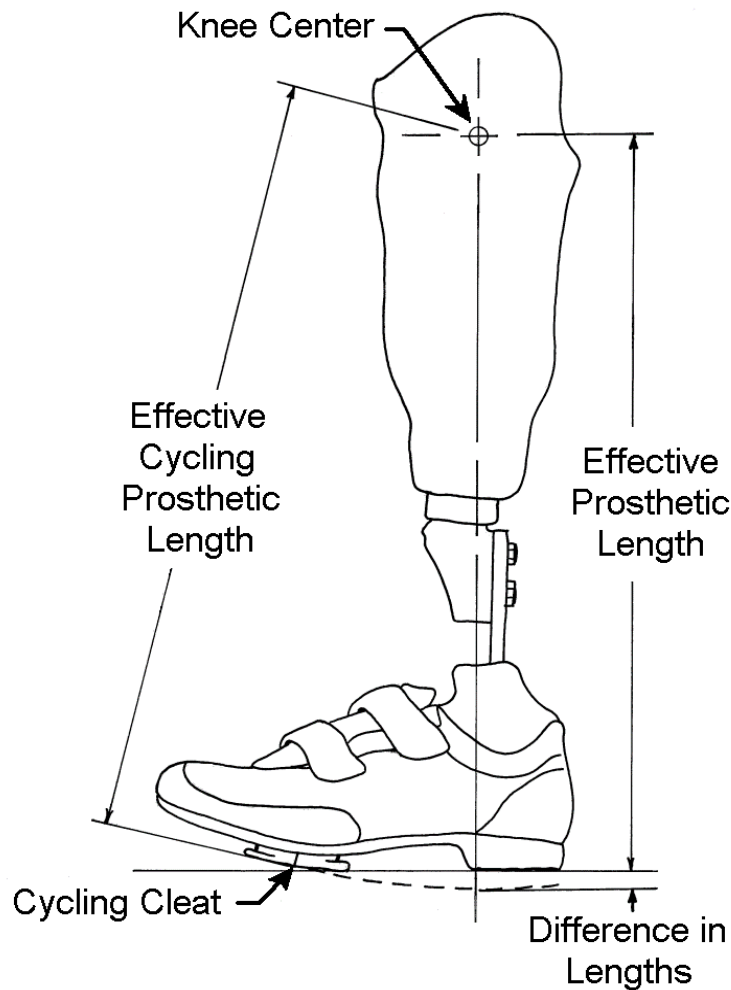


**Figure 8- Diagram describing the difference in effective prosthetic length for cycling and walking. Effective prosthetic length in cycling is from the knee center to the cycling cleat. Effective prosthetic length should be matched to the sound limb. For example, if the cleat on the sound limb is positioned at the 1st metatarsal head yet the cleat on the prosthesis is positioned posteriorly then the prosthesis should be lengthened to minimize geometric asymmetries.**

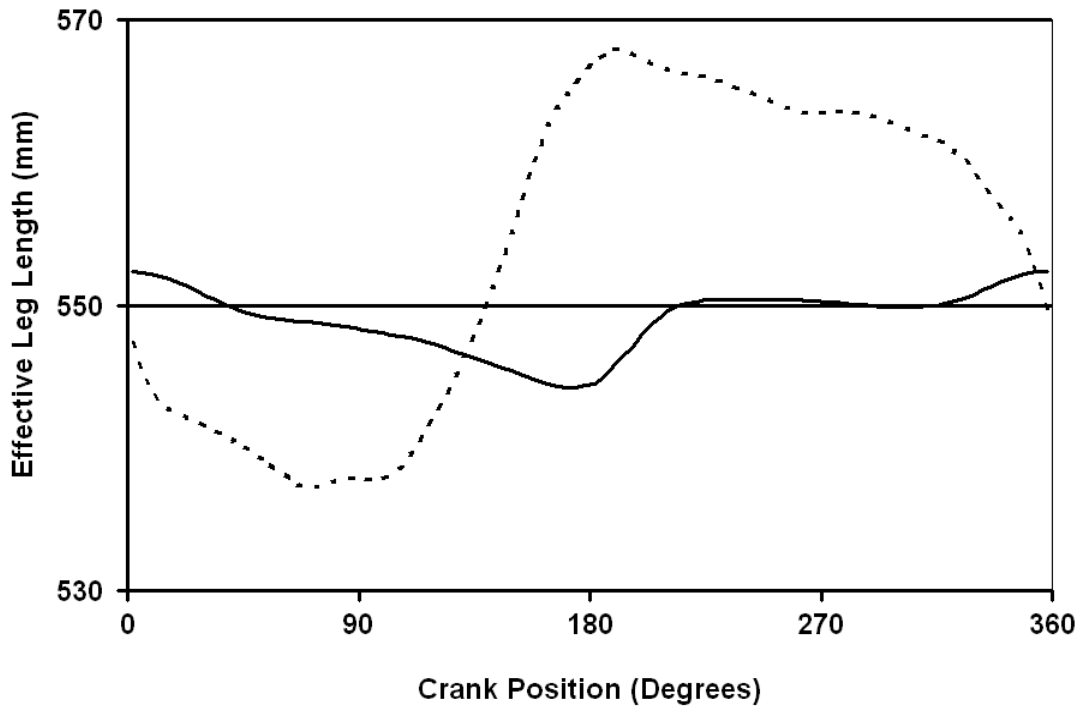


**Figure 9 – Exemplar data for effective leg length during the crank cycle of the sound limb (dashed line) and a prosthesis (solid line) using a flexible dynamic response type prosthetic foot. The horizontal line at 550mm represents the effective leg length of the sound limb when the ankle is in the neutral position for this particular TTA. Cleat location for both limbs is approximately the 1st metatarsal head. Effective leg length in cycling is measured from knee joint center to the center of the cycling cleat. Increases in effective leg length indicate the ankle is extending. Note - Although the prosthetic foot allows movement, is not similar to the sound limb in both amplitude and phase. Therefore allowing ankle motion in the prosthetic foot will not replicate the motion of the sound limb during cycling. Data derived from a TTA subject operating a 350 watts and 125 rpm during a simulated time trial.**

## **CHAPTER 3**

### **METHODS**

#### **Subject Information**

Two main groups of subjects volunteered for these studies. A group of nine persons with trans-tibial amputation that used cycling for recreation (TTA group) and a group of nine intact subjects that used cycling for recreation (Intact group). The Intact group was matched to the TTA group based on the following criteria (in order of importance); cycling discipline, self reported hours of cycling per week, body mass, height, age, and gender. This matching was performed to ensure 1) similar motor skill (regarding cycling) across the intact and TTA groups and 2) similar inertial properties of their limbs. The order of importance were derived from data presented Chapman et. al. (2007) and Broker (2003) regarding differences in cycling disciplines and Zatsiorsky et al. (1990) regarding inertial properties. Inclusion criteria are listed in Table 4. The inclusion criteria were based on health screening protocols to ensure the subjects were capable of performing the task while minimizing the risk of a cardiac event during testing (ACSM, 2006). Exclusion criteria for all groups included anyone with cardiovascular disease, diabetes, peripheral vascular disease or anything that would limit the person's ability to exercise. Anthropometrics, cycling discipline and experience are listed in Tables 5 & 6 for the TTA and Intact groups, respectfully.

**Table 4 - Inclusion Criteria**

INCLUSION CRITERIA FOR AMPUTEE GROUP	INCLUSION CRITERIA FOR INTACT GROUP
Uni-lateral transtibial amputation secondary to trauma or cancer	Some cycling experience
Greater than 1 yr post surgery	Perform cardiovascular exercise >6 hr per week
Cycling experience after having the amputation	Between 18 – 44 years of for men or 18 – 54 years old for women
Perform cardiovascular exercise >6 hr per week	Body mass index less than 30
Between 18 – 44 years of for men or 18 – 54 years old for women	No secondary neuromuscular conditions
Body mass index less than 30	
No secondary neuromuscular conditions	

**Table 5 - Volunteer Information for the TTA group. Abbreviations are as follows; DISC = Discipline, EXP = Experience, EXERC = Exercise, HT = Height, AMP = Amputation, yrs = years, hrs/wk = hours per week, kg = kilograms, m = meters, Tri. = Triathlete, Rec. = Recreational cyclists, and M = Male**

SUBJECT		CYCLING			AEROBIC EXERC	MASS	HT	AGE	YRS. SINCE AMP	SEX
#	CODE	DISC	(hrs/wk)	(yrs)	(hrs/wk)	kg	m	yrs.		
1	DP	Tri.	6	4	20	73.5	1.85	27	7	M
2	WP	Rec.	4	9	14	97.1	1.78	40	9	M
3	SE	Tri.	8	8	24	109.7	1.98	38	8	M
4	JR	Rec.	4	32	14	76.6	1.75	44	32	M
5	JN	Tri.	6	1	16	84.9	1.83	28	1.5	M
6	SB	Rec.	2	1	6	78.5	1.73	29	7	M
7	JG	Tri.	6	1.5	22	77.5	1.83	44	18	M
8	CT	Rec.	2	1.5	9	60.5	1.91	19	1.5	M
9	JM	Rec.	4	6	8	96.2	1.83	38	32	M
Mean			4.7	7.1	14.8	83.8	1.83	34.1	12.9	
Std. Dev.			2.0	9.8	6.4	14.9	0.08	8.7	11.9	

**Table 6 - Volunteer Information for the Intact group. Subject number for the TTA group corresponds to the appropriate match in the intact group. Abbreviations are as follows; DISC = Discipline, EXP = Experience, EXERC = Exercise, HT = Height, AMP = Amputation, yrs = years, hrs/wk = hours per week, kg = kilograms, m = meters, Tri. = Triathlete, Rec. = Recreational cyclists, and M = Male**

SUBJECT		CYCLING			AEROBIC EXERC	MASS	HT	AGE	SEX
#	CODE	DISC	(hrs/wk)	(yrs)	(hrs/wk)	kg	m	yrs.	
1	SA	Tri.	6	3	18	72.7	1.83	25	M
2	AW	Rec.	10	2.5	10	76.9	1.85	41	M
3	JO	Tri.	10	6	24	86.1	1.85	36	M
4	MS	Rec.	6	4	6	85.1	1.83	35	M
5	ML	Tri.	8	4	14	85.5	1.79	43	M
6	TG	Rec.	3	7	6	75.4	1.77	24	M
7	SK	Tri.	6	38	14	90	1.85	43	M
8	MH	Rec.	2	4	15	64.5	1.73	22	M
9	LW	Rec.	4	14	10	105.1	1.87	43	M
Mean			6.1	9.2	13	82.4	1.82	34.7	
Std. Dev.			2.8	11.4	5.8	11.7	0.05	8.8	

All volunteers were recruited via local prosthetic clinics and/or through personal contacts within the local cycling community. All volunteers read and signed an informed consent form approved by the Institutional Review Board for the Georgia Institute of Technology before participating.

### **Experiment Protocol**

The subjects pedaled a stationary electromagnetically braked ergometer (Figure 10) (Excaliber Sport, Lode BV, Groningen, Netherlands) adapted with custom fabricated pedal/crank system. The pedal/crank system allowed for changes in crank arm length and consisted of dual piezoelectric element force pedals (Broker & Gregor 1990) adapted with a commercial “clipless” pedal system (see Appendix A for a detailed description). The saddle height of the stationary cycle was initially set to 98% leg length and then fine adjustments ( $\pm 1$  cm) were made for comfort (Childers et. al., 2009c) and the crank arm length set to 172mm unless noted otherwise (see Aim #2). The saddle height during the initial setup is defined as the distance from the pedal when the crank is furthest away from the saddle to the top of the saddle at the widest point. To verify the saddle height was held constant relative to leg length during the experiment and after adjustment for comfort, the saddle height was calculated using the motion system as the maximum distance from the hip joint center to the pedal spindle and then normalized to leg length. The handlebar reach, drop, and seat tube angle was adjusted to the subject’s position as measured from their primary bicycle or (if their bicycle was unavailable) the position was adjusted based on established bicycle positioning protocol (Pruit 2004).



**Figure 10 - Electromagnetically braked cycle ergometer used.**

The cycling shoe (Bontrager Race Mountain, Trek bicycle corp., Madison, WI) was sized to the subject's foot and the pedal interface (Shimano SPD MTN, Shimano inc., Osaka, Japan) was controlled across all subjects (Figure 11). This pedal interface allows a total of eight degrees of foot axial rotation relative to the pedal ( $\pm 4$  degrees from neutral) but will not allow translation in any other direction between the foot and pedal. Subjects received feedback about their cycling cadence via a tachometer mounted on the cycle ergometer.



**Figure 11 - Cycling shoes were available in each size to control for the shoe and pedal interface.**

### **Experimental Conditions**

The experimental conditions for each group are outlined in Table 7. The TTA and Intact group represent the two main groups for these experiments and provide the basis for this study. The load and cadence for all conditions involving altered mechanics were kept at 15Nm and 90 rpm (~150 watts). All experimental conditions are described below.

**Table 7 - Outline of Load/Cadence Conditions for all groups. The abbreviated labels for each condition are in parentheses.**

TTA GROUP	INTACT GROUP
15Nm @ 60 rpm (60)	15Nm @ 60 rpm (60)
15Nm @ 90 rpm (90)	15Nm @ 90 rpm (90)
15Nm @ 120 rpm (120)	15Nm @ 120 rpm (120)
15Nm @ 90 rpm w/ shortened crank arm (TTA-CRANK)	
15Nm @ 90 rpm w/ uni-lateral posterior cleat position (TTA-CLEAT)	15Nm @ 90 rpm w/ uni-lateral AFO (Uni-AFO)
	15Nm @ 90 rpm w/ bi-lateral AFO (Bi-AFO)
	15Nm @ 90 rpm w/ bi-lateral posterior cleat position (Bi-CLEAT)

### 60, 90, and 120 rpm Conditions

The TTA and Intact group both cycled at a constant torque of 15 Nm and at 60 (~95 watts), 90 (~150 watts), and 120 rpm (~190 watts) (referred to as the 60, 90, and 120 conditions respectfully). Historically, cadence has been tested at constant power (Ansley & Cangle, 2009 for review) yet power equals the multiplication of pedaling torque and cadence. Thus when power was held constant and cadence increases; torque decreases. Recent literature has challenged the historic use of constant power to test the effect of cadence (Gardner et. al., 2007). These authors contended that by holding power constant, two important variables are being tested simultaneously and testing of cadence should be performed at constant torque. In addition, pilot work with two intact cyclists demonstrated lower kinetic and kinematic variability when torque was held constant vs. power.

### TTA-CRANK condition

The TTA group pedaled at 15Nm and 90 rpm with the crank arm shortened 10mm on the amputated side. Shortening the crank on the amputated side was performed to reduce the geometric asymmetries between the two lower limbs of a TTA. The intact ankle in the sound limb actively plantarflexes at the bottom of the pedal stroke and dorsiflexes at the top (Pierson-Carey CD et al., 1997). The total movement of the cycling cleat is approximately 20mm given normal ankle movement and typical cleat location relative to the ankle joint (Childers et. al., 2009b). Therefore, shortening the crank on the amputated side brings the pedal closer at the bottom and further away at the top of the stroke to compensate for the lack of motion of the prosthetic foot and decreasing kinematic asymmetries between the sound and amputated limbs.

### TTA-CLEAT condition

The TTA group pedaled at 15Nm and 90 rpm with the cycling cleat moved posteriorly on the prosthetic foot approximately 40% distance between the standard cleat location and the prosthetic ankle. This position was based on pilot work performed on intact cyclists

demonstrating a minimization of triceps surae activity near this point (Childers & Gregor, 2008) as well as reports of similar cleat positions for cycling prostheses (Gailey & Harsch, 2009) The prosthesis was lengthened to maintain a constant effective cycling prosthetic length (Childers et al., 2009b). Effective cycling prosthetic length for cycling was measured from the knee center to the centerline of the cycling cleat (Figure 12).

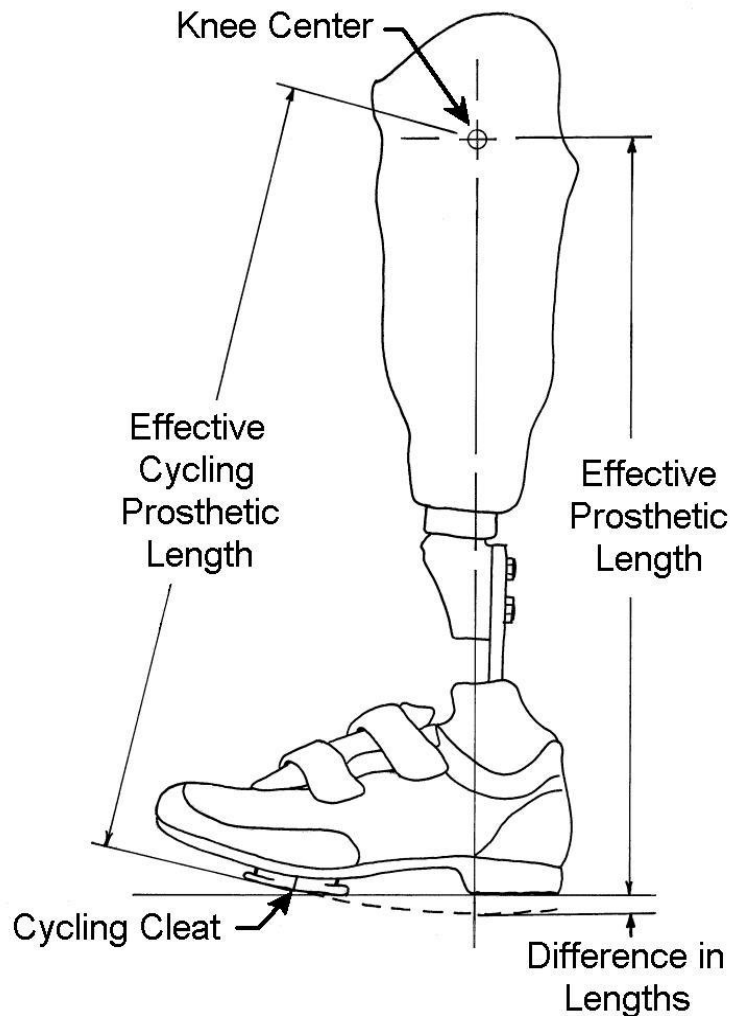


**Figure 12 - Diagram describing the difference in effective prosthetic length for cycling and walking. Effective prosthetic length in cycling is from the knee center to the cycling cleat. Effective prosthetic length should be matched to the sound limb. For example, if the cleat on the sound limb is positioned at the 1<sup>st</sup> metatarsal head yet the cleat on the prosthesis is positioned posteriorly then the prosthesis should be lengthened to minimize geometric asymmetries.**

### Uni-AFO and Bi-AFO conditions

The Intact group pedaled at 15Nm and 90 rpm wearing a custom fabricated Ankle Foot Orthosis (AFO) (Figure 13) either uni-laterally (Uni-AFO condition) on the subject's non-dominant limb or bi-laterally (Bi-AFO condition). The AFO condition was designed to simulate the mechanics of cycling with prosthesis with an intact cyclist. The AFO consisted of an anterior and a posterior thermoplastic shell and shaped to conform to a human shank. The anterior shell was lined with 3mm pelite foam to provide padding over the tibia. The anterior aspect of the anterior shell was ribbed to increase longitudinal stiffness while 25mm slits were cut perpendicular to the longitudinal centerline of the anterior shell and equally spaced 30mm apart to allow the anterior shell to better conform to the shank when the straps were tightened. The proximal trimlines of the AFO were approximately at or just distal to the tibial tubercle. The distal trimline was approximately 2 cm distal to the malleoli (Figure 14). A frame fabricated from 20 X 6mm 6061-T651 aluminum section extended distally from the posterior shell to an aluminum plate. The proximal end of the aluminum frame was attached via four countersunk machine screws to an aluminum plate fabricated into the posterior shell of the AFO. The aluminum frame was formed to provide adequate clearance for a reflective marker placed on the apex of the lateral malleolus. The cycling cleat was mounted to the plate of 38 X 5 X 75mm 6061-T651 aluminum. A series of M4 X 0.7 tapped holes were placed in the aluminum plate that allowed the cycling cleat to be moved in the anterior/posterior direction in 10mm increments.



**Figure 13 - AFO design to replicate the mechanics of cycling with an amputation in a cyclist with intact limbs.**

The cleat location was underneath the longitudinal arch of the subject's foot. In order to maintain the same effective leg length (Figure 12) as when the cleat was placed at the first metatarsal head, the plate was approximately 3 cm plantar to the plantar aspect of the foot (in a neutral position). This allowed the subjects to relax their shank and the foot to plantarflex into a comfortable position. The metatarsal pads of the forefoot would generally touch the anterior end

of the cleat plate. A piece of adhesive tape was then wrapped around the foot to minimize foot movement due to the inertial forces of pedaling (Figure 14). The design of this AFO required to the user to control the pedal via the interface between the shank and the shell of the AFO similar to the interface between the residual limb and the prosthetic socket in TTA.



**Figure 14 - Subject wearing the AFO on the bicycle to demonstrate the cleat position as well as the relaxed position of the foot. Adhesive tape was used to minimize movement of the forefoot due to inertial forces during pedaling. An additional reflective marker was added to calculated ankle joint kinematics.**

### Bi-CLEAT condition

The Intact group pedaled at 15Nm and 90 rpm with the cycling cleat placed at 40% the distance between the ankle joint and the standard cleat position bi-laterally (Bi-CLEAT condition) (Figure 15). Each pair of cycling shoes was modified to allow a plate to be screwed into the bottom of the shoe. The plate moved the cleat posteriorly and inferiorly in order to maintain a constant effective leg length (Figure 16).

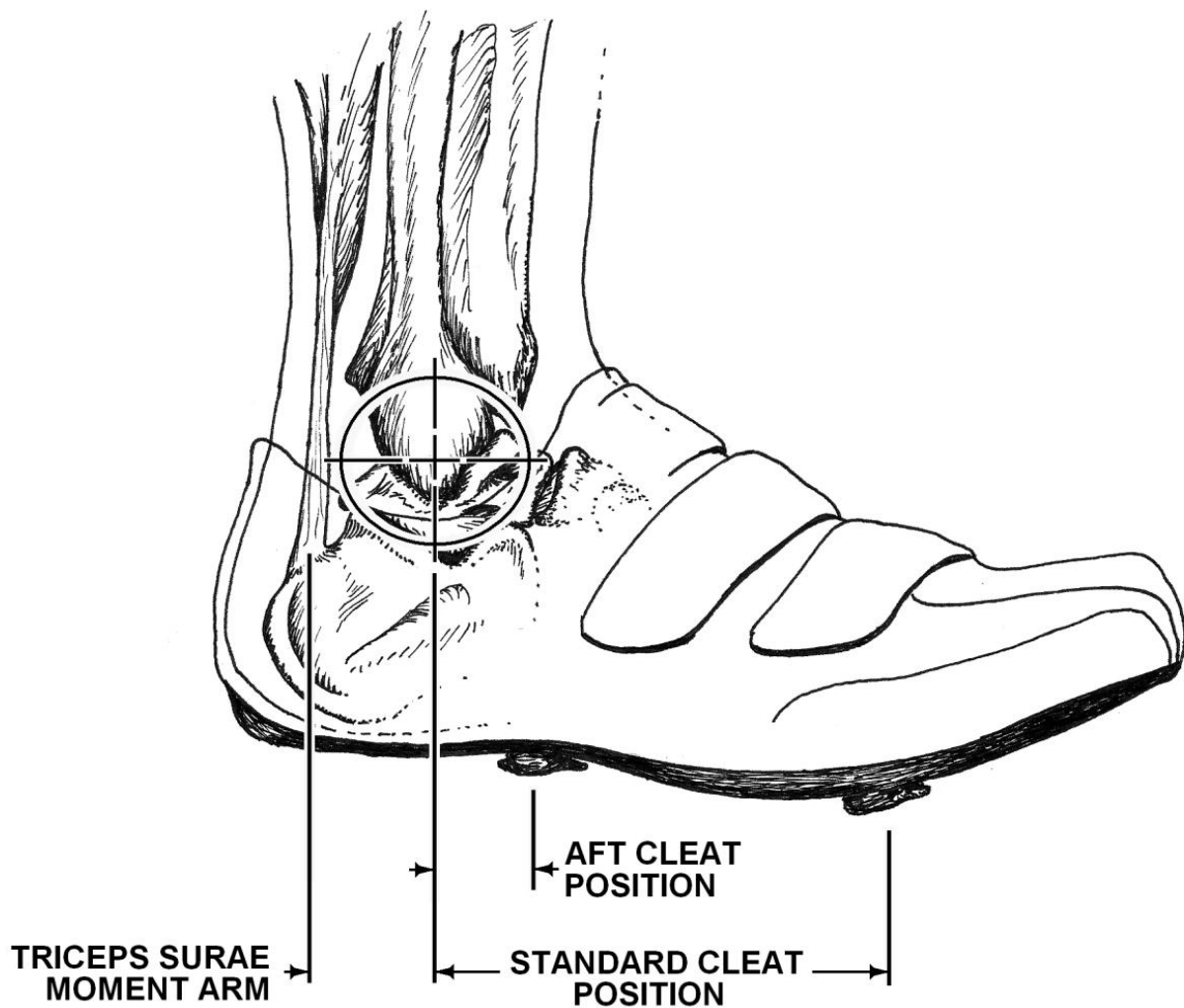


**Figure 15 - Diagram showing the two different cleat positions used and the effect on the moment arm at the ankle joint.**



**Figure 16 - The plate added to the bottom of the cycling shoes to allow a posterior cleat position. The plate also offset the cleat inferiorly to maintain a similar effective leg length.**

### **Cycling Prosthesis**

The stiffness, e.g. prosthetic foot, and alignment, e.g. geometric relationship of the socket relative to the pedal, of the prosthesis (Figure 17) were similar across all subjects for the TTA group. The prosthetic foot was plate of aluminum shown to minimize pedaling asymmetries in prior research (Childers et al., in press). The design of the prosthetic socket was held constant for each subject by duplicating the subject's prosthetic socket with an electromagnetic shape capturing device (TracerCAD, Ohio Willow Wood co. inc., Columbus OH) and a thermoplastic prosthetic socket produced by a central fabrication facility (PDI, Dayton OH). A portion of the lateral wall of the prosthetic socket was removed, allowing for the placement of a knee center marker. In addition, the prosthetic socket incorporated a pocket in the posterior portion to allow room for EMG electrodes over the amputated gastrocnemius muscle. Prosthetic suspension was controlled across subjects and included a silicon liner with mechanical pin type suspension (X-PSH-PLUS, PDI, Dayton OH). This type of prosthetic suspension attached the distal end of the

residual limb to the base of the prosthetic socket via a pin and lock device, effectively creating a pseudo joint. The prosthetic foot was a very stiff 10mm thick plate of aluminum. The cycling cleat was mounted in the approximate location of the 1st metatarsal head in the sagittal plane and the center of the foot in the frontal plane for five out of the six conditions tested. The sixth TTA condition (Figure 17) involved the cycling cleat being moved posteriorly to 40% the distance between the ankle joint and the standard cleat location. Effective cycling prosthetic length (distance between the knee center and pedal spindle) was maintained across all six conditions in accordance with recommendations reported previously (Childers et. al. 2009b). The socket alignment relative to the foot was transferred from the subject's personal prosthesis. This prosthetic design was similar to the STIFF foot condition shown to minimize pedaling asymmetries (Childers et al., in press).



**Figure 17 - Cycling prostheses used incorporated a pin suspension, a stiff prosthetic foot, a "pocket" in the posterior wall for EMG electrodes and removal of the lateral superior portion for the knee marker. The left panel (clear socket) shows the design when the cleat was in the standard position. The right panel (black socket) shows the cleat location for the TTA-CLEAT condition.**

## **Data Collection Protocol**

The subjects were given a 5-10 minute warm up period at 75 watts and self selected cadence. The subject's predicted maximal heart rate was determined  $(220 - \text{age})$  (ACSM 2006). A heart rate monitor (CS400, Polar Electro OY, Kempele, Finland) was worn during all trials to verify the workload was submaximal to minimize the effect of fatigue.

### **Determination of limb dominance within the Intact group**

The Intact group cycled at 15Nm and 90 rpm for approximately two minutes prior to application of EMG electrodes in order to determine limb dominance. Pedal force and pedal position (see section "Data Reduction" for more detail) were recorded for 10 seconds during the final minute of cycling at 15Nm and 90rpm. The data were reduced via custom reduction software (Matlab 2010b) (see section "Data Reduction" for more detail) to calculate the torque produced by the right and left limbs. The dominant limb was defined as the limb that produced the most torque. The dominant (DOM) and non-dominant (NON-DOM) limbs were recorded and used to determine placement of EMG electrodes. The Uni-AFO condition was applied to the subject's non-dominant limb.

### **Data Collection**

The order of conditions was randomized. Data were collected 30 seconds after the subjects achieved steady state cadence (Figure 18). Data collection occurred twice for 30 seconds each for each load. Data collection periods were separated by ~10 seconds. The second data collection period was used for data analysis unless a technical error prevented data reduction in which case the first data collection period was used for analysis. Heart rate was recorded immediately following the second collection period.

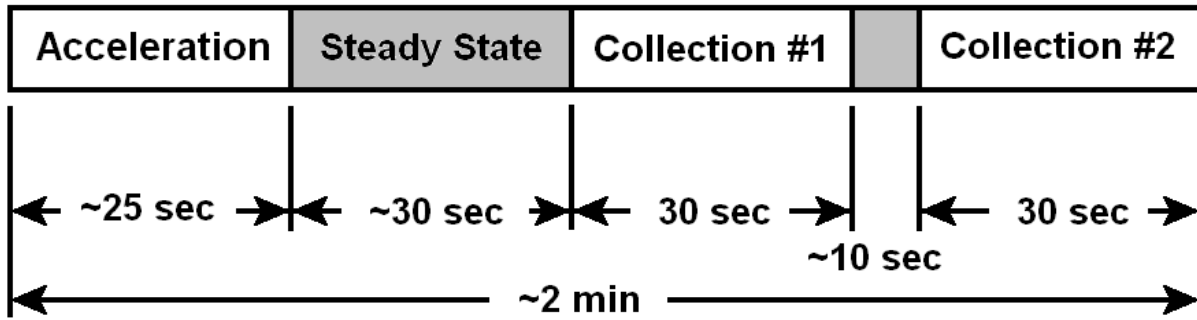


**Figure 18 - Data collection periods starting when the subject initiated pedaling. The ~10 second interval between collections was needed to reset the software for a subsequent trial. Data collection #1 served as a backup in case the second collection experienced technical issues.**

### Kinetic Data Collection

Pedal reaction forces were recorded via piezoelectric element transducers mounted at the foot/pedal interface (Figure 19) (See Appendix A for a detailed description). The pedals were adapted with a commercially available pedal interface system (Figure 20) (Wheeler et. al., 1992). Data were recorded at 300 Hz for 10 seconds using Peak Motus software (Vicon Motion Systems, Oxford, UK).

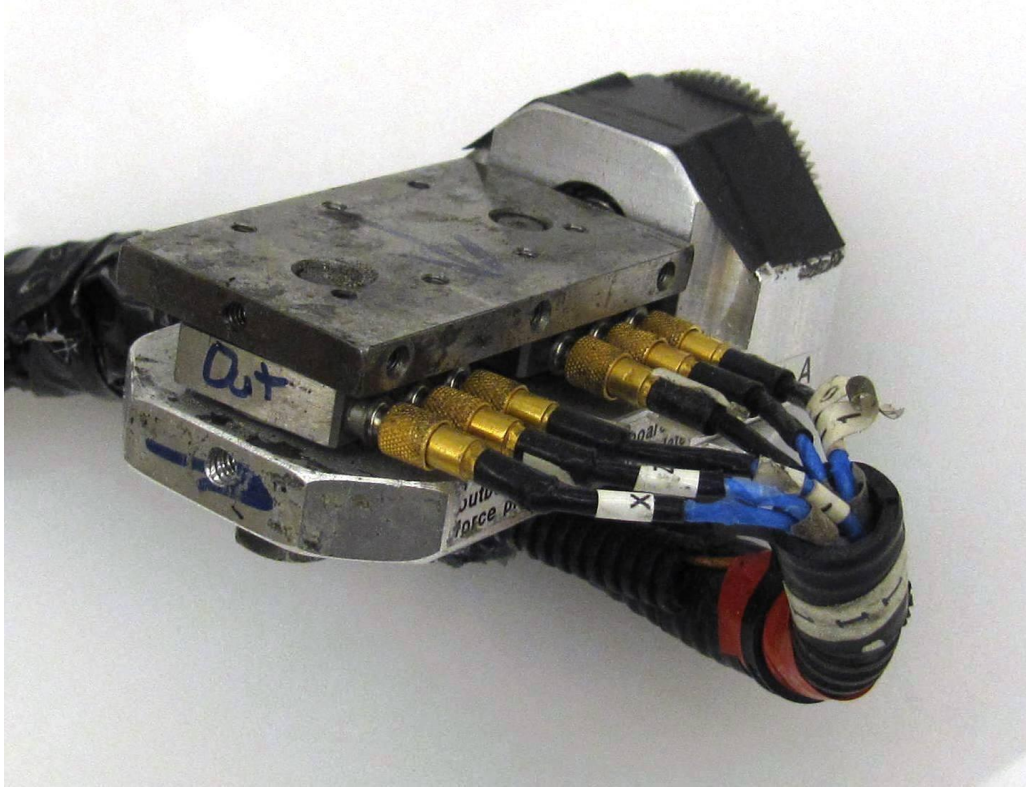


**Figure 19 - Dual piezoelectric element fore pedals**

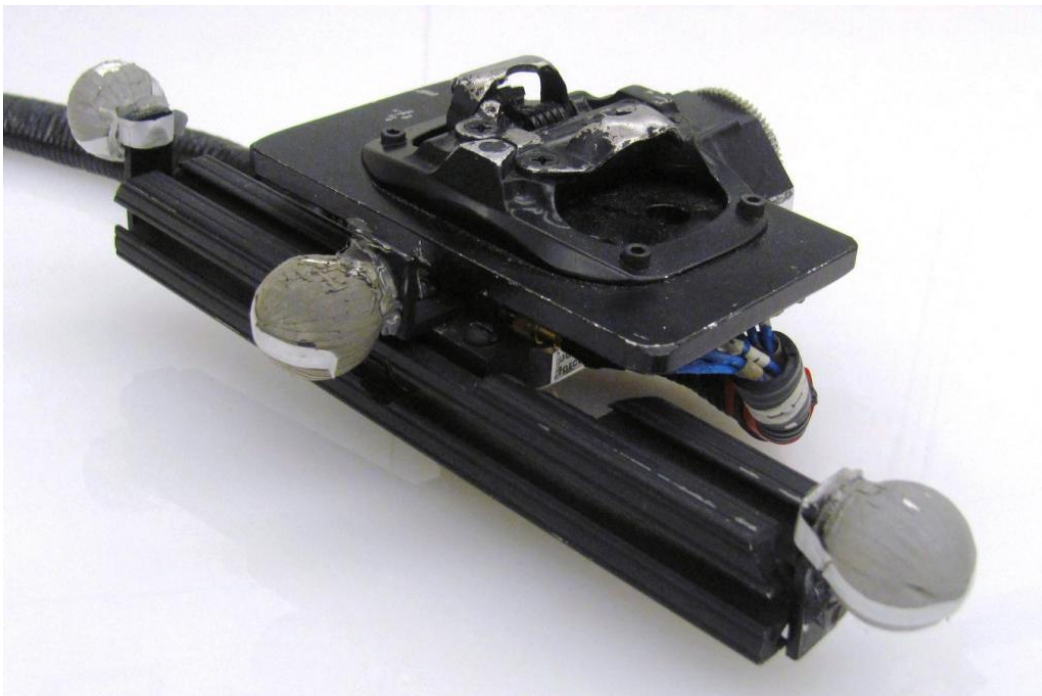


**Figure 20 - Force pedals adapted with a pedal interface that allows the user to lock into the pedals during cycling. A bracket was added to hold reflective markers necessary to calculate pedal angle.**

## Kinematic Data Collection

Kinematic data were collected for 10 seconds at 60 Hz using a motion capture system (Peak Performance Technology Inc.) and digitized using Peak Performance software. An electronic pulse synchronized force, EMG and video records. Reflective markers mounted on a bracket affixed to the pedal body were used to calculate pedal angle (Figure 20). Crank angle was determined using a gear driven continuous turn potentiometer. Nine markers were placed on the subject over the sacrum as well as bilaterally over the greater trochanter of the femur, anterior superior iliac spine (ASIS), lateral epicondyle of the femur, and lateral malleolus. Markers on the heel and 2<sup>nd</sup> metatarsal joint were not needed when the foot was fixed to the pedal at a known angle, i.e. foot angle was calculated from pedal angle. The Intact group had additional markers placed over the 2<sup>nd</sup> metatarsal joint during the AFO conditions. The amputee group had an additional marker placed at the residual limb/prosthesis joint (Figure 21). This allowed for calculation of the angular displacement between the residual limb in the prosthesis. This marker placement assumed that the distal end of the residual limb did not move relative to the inferior portion of the prosthetic socket. Measurement of the motion between distal portion of the residual limb and the prosthetic socket indicated this motion was less than 5mm and would have a minimal effect on the calculation of joint moments (Appendix B). A static calibration trial was performed when the subject initially mounted the ergometer. The subject was asked to be still with the crank parallel to the ground for 10 seconds while data were collected. This information was used later to calculate the center of hip joint rotation based on the ASIS marker.

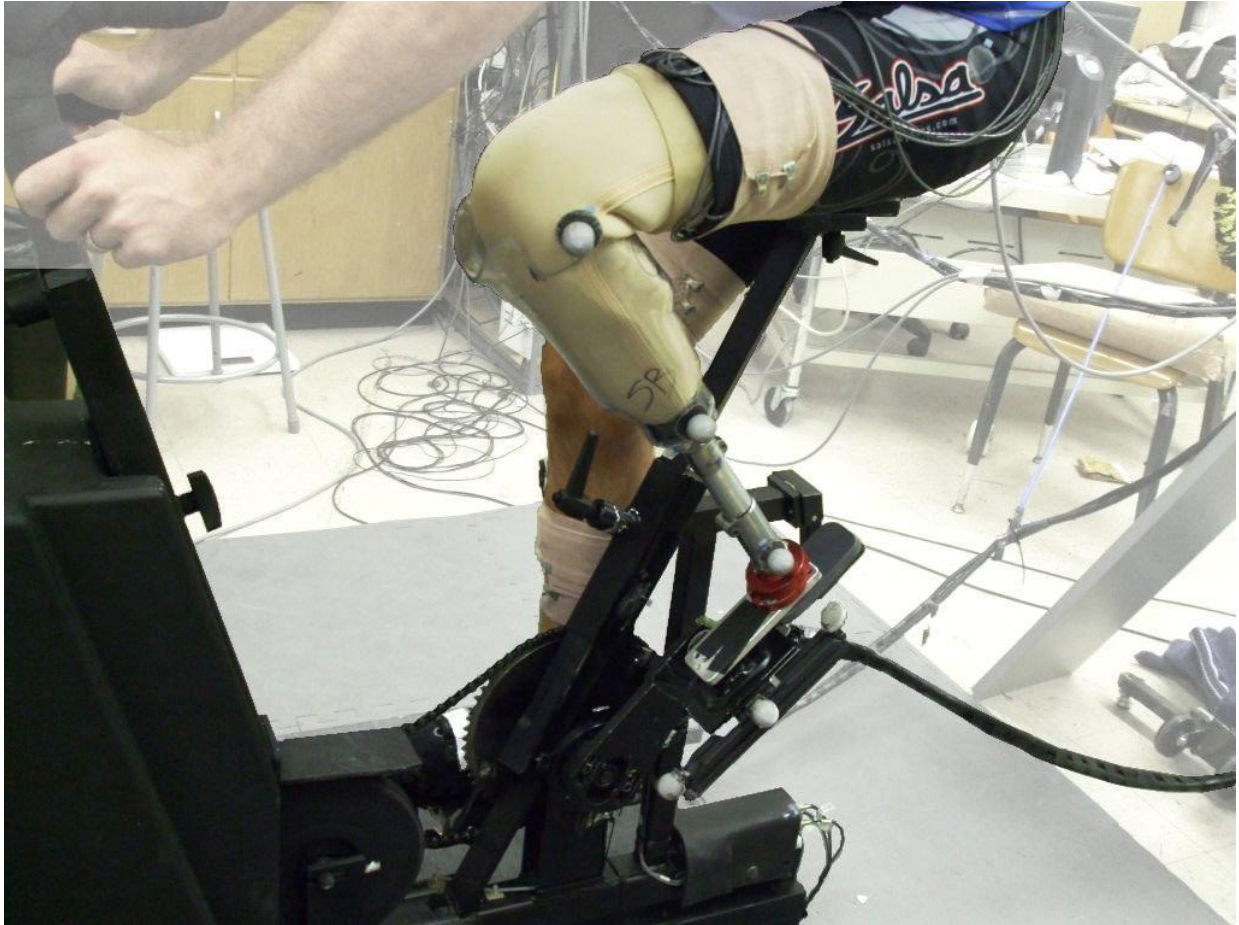


**Figure 21 - TTA on ergometer showing marker placed on the prosthesis over the 'pseudo-joint' where the pin meets the lock. Removal of the lateral superior wall of the prosthesis also facilitated placement of the knee marker.**

#### Surface Electromyography Data Collection

Surface electromyography (EMG) was recorded for 30 seconds using a 12-channel system (Myosystem 1400L, Noraxon USA Inc., Scottsdale AZ) (see Appendix A for a detailed description) at 1000 Hz, pre-amplified, bandpass filtered within the Myosystem 1400L system (3db at 8 and 550 Hz),. Table 8 describes electrode placements for both groups. The electrodes and wires were wrapped with elastic bandage to prevent motion artifact during cycling.

**Table 8 - Electrode placement for the following muscles; Gluteus Maximus (GM), Rectus Femoris (RF), Biceps Femoris Long Head (BFL), Vastus Medialis (VM), Gastrocnemius (GAS), Soleus (SOL), and Tibialis Anterior (TA). Limbs within the group are abbreviated as the dominant (DOM) and non-dominant (NON-DOM) limbs in the intact group as well as the sound and amputated (Amp) limb in the TTA group.**

CH #	INTACT GROUP	TTA GROUP
1	DOM GM (Aim #1) or NON-DOM TA (Aim #2)	Sound GM
2	DOM RF	Sound RF
3	DOM BFL	Sound BFL
4	DOM VM	Sound VM
5	DOM GAS	Sound GAS
6	DOM SOL	Sound SOL
7	DOM TA	Sound TA
8	NON-DOM RF	Amp GM
9	NON-DOM BFL	Amp RF
10	NON-DOM VM	Amp BFL
11	NON-DOM GAS	Amp VM
12	NON-DOM SOL	Amp GAS

### Data Reduction

Kinetic, kinematic and EMG data were processed in custom written matlab software (Matlab 2010b). The kinetic data were digitally filtered using a fourth-order zero-lag Butterworth filter with a 15 Hz cutoff frequency. The kinematic coordinate data were smoothed using a quadratic spline (matlab function csaps,  $p = 0.01$ ). The kinetic and kinematic data of eight complete crank cycles were time normalized to 100 data points and averaged together.

The crank position potentiometer outputs a change in voltage (related to crank position) for 340 degrees. The missing 20 degrees was recorded by a second gear driven potentiometer. The two signals were spliced together digitally using a computer program (Matlab 2010b) to form one continuous line for all 360 degrees of the crank cycle.

The ankle joint center of rotation was calculated based on equations from Vaughan et. al. (1999). The knee joint center of rotation were calculated based on data presented by Smidt (1973) that related actual knee joint center to the lateral epicondyle of the femur. The static calibration trial was used to relate the greater trochanter of the femur to the ASIS and sacrum

markers. The hip joint center of rotation was based on a static trial. The subject would have markers placed over the greater trochanter, the sacrum and the ASIS. The subject would then sit quietly on the bicycle for 10 seconds while kinematic data was recorded. The position of the greater trochanter during the static trial was considered the hip joint center in the sagittal plane. The position of the greater trochanter was calculated relative to the sacrum and ASIS markers. This method was shown to be more accurate representation of the true hip joint center by Neptune & Hull (1995) and verified in Appendix C.

Limb segment center of mass, mass and moment of inertia were calculated from regression equations from Zatsiorsky et. al. (1990). Properties of the residual limb and prosthesis were calculated using methods outlined by Goldberg et. al. (2008). Joint moments were calculated using equations in inverse dynamics for the sagittal plane (Broker & Gregor, 1994).

Surface EMG data were digitally band-pass filtered (Butterworth digital, fourth order, zero-lag, 20 – 500Hz) to attenuate high frequency and low frequency (motion artifact) noise. The data were then rectified and low-pass filtered (Butterworth digital, fourth order, zero-lag, 10Hz cutoff). Twenty consecutive pedal cycles were each normalized to 100 data points, averaged and then normalized to the peak magnitude for each respective muscle from the 15Nm and 90 rpm load condition

The amount of muscle activation was calculated by integrating the EMG linear envelope for each muscle. Muscle onset, offset and peak magnitude were determined via computer program. Muscle onset and offset were determined by setting a threshold of 20% maximum activation (Baum & Li, 2003). In addition, the onset and offset calculated by the computer program were graphed with the linear envelope and visually inspected to verify timing.

## **Statistical Analysis**

Statistical analyses varied depending on the hypothesis being tested. The specific analysis performed is provided in the respective chapter. Statistical significance was set at  $p \leq 0.05$  for all tests.

## CHAPTER 4

# THE EFFECT OF CADENCE ON LOWER LIMB MUSCLE COORDINATION IN PERSONS WITH A TRANS-TIBIAL AMPUTATION

### Introduction

Output of central neural control mechanisms generating rhythmic patterns determine the phasic onset and offset of muscle activity in the lower limb during reciprocal locomotion (Rossignol, 1996). These central mechanisms incorporate a strategy to coordinate muscle activity across joints based on expected task demands (Raasch et al., 1997) and utilize peripheral feedback to update and/or modify output (Nichols 2002). The final output of these mechanisms may be measured as the temporal aspects of muscle activity. The timing of this phasic activity during cycling provides a window into the control strategy used by the nervous system (Prilutsky, 2000). Analyzing how phasic activity in muscle output e.g. electromyography, responds to limb cadence offers an opportunity to study the control strategy used for locomotor control (Sarre & Lepers, 2005).

Neptune et al. (1997) used cycling to study muscle coordination with increasing cadence and proposed the “activation-contraction dynamics hypothesis” suggesting these central mechanisms would be responsible for the excitation and contraction dynamics of the skeletal muscle and would activate the muscle earlier in the crank cycle to maintain timing of crank torque. The observations reported by Neptune et al. (1997) have been supported by other studies (Baum & Li, 2003; Sarre & Lepers, 2005; Bieuzen et al., 2007) yet little is known if this control strategy would also account for the activation-contraction dynamics in a compromised motor system.

A trans-tibial amputation represents a major alteration to the human system because it removes the foot, ankle joint, a portion of the leg, the muscles that control the ankle/foot complex and sensorimotor feedback from these muscles. Loss of sensorimotor feedback from

the amputated limb in combination with altered feedback coming from the residuum and an altered musculoskeletal system could alter the central nervous system's ability to understand and respond to task demands. The motor system could respond to increasing cadence by increasing the amplitude of muscle activity without shifting the timing of that activity. An increase in the amplitude of muscle activity would be in contrast to activation-contraction dynamics demonstrated in intact cyclists and highlights the need for research on this subject.

Understanding how robust the control system is after a major alteration to the musculoskeletal system adds to our basic knowledge of motor system performance while enabling a better interpretation of experimental data.

The purpose of this research was to determine if muscle activation in persons with Trans-tibial Amputation (TTA) would respond in a way similar to Intact cyclists with increasing limb speed (cadence) and test the general hypothesis that The timing of muscle activation will occur earlier in the crank cycle with increasing cadence despite the loss of physiologic systems associated with amputation. Specific hypotheses addressed include; 1) muscle onset and peak activation will occur earlier as cadence increases; and 2) change in EMG timing will be similar in both the Intact and TTA groups.

## **Methods**

In-depth discussions of the general methods are presented in Chapter 3 and are briefly summarized here to restate what methods are specific to this hypothesis.

### **Subjects and load conditions**

A group of nine persons with trans-tibial amputation (TTA) and a group of nine intact subjects (Intact) volunteered for this study. Both groups used cycling for recreation. The subjects pedaled at a constant torque of 15Nm and at cadences of 60, 90, and 120 rpm (~90, ~150, and ~190 watts respectfully). Torque was held constant in the present experiments in contrast to previous reports where the effects of cadence on muscle timing were tested at

constant power (Ansley & Cangle, 2009 for review). Recent reports have indicated that more consistent results may be obtained holding constant torque when testing for the effects of changes in cadence (Gardner et. al., 2007). Pilot work was performed prior to these experiments at both constant torque and constant power in three subjects demonstrating lower within subject variability when torque was held constant and providing the rationale behind the use of constant torque.

Pedaling kinetics (Broker & Gregor 1990), limb kinematics (Peak Performance, Vicon Motion Systems, Oxford, UK) and surface EMG (Myosystem 1400L, Noraxon USA Inc., Scottsdale AZ) were used to address these two hypotheses. The dominant limb in the Intact group (DOM-INT) was used to compare to the sound (SND-TTA) and amputated limbs (AMP-TTA).

Timing variables were related to peak crank torque as Sarre & Lepers (2007) suggested relating the timing of muscle activation to peak crank torque when cadence is not constant would better reflect the control strategy of the nervous system as opposed to relating timing to the kinematic position of the crank arm.

Muscle onset, offset and peak magnitude were determined using Matlab software. This software would output timing based on a threshold of 20% of peak magnitude (Baum & Li, 2003). Because this method would occasionally output more timing marks than necessary, each of the 648 datasets were visually inspected and verified.

Some muscles are known for “double bursting” i.e. two peaks have been reported for the tibialis anterior, biceps femoris long head, gastrocnemius and rectus femoris (Ryan & Gregor 1992). When this occurred, the onset of the first peak was considered onset of the muscle and the offset of the second peak was considered the offset of the muscle.

## **Statistical Analysis**

A repeated measures ANOVA with a Bonerferroni Post-Hoc test was used to determine significance ( $p < 0.05$ ) across cadence within each group for muscle onset, peak and muscle

offset. A trend analysis was performed to determine overall trends in the variables tested. A significant trend toward earlier activity with increasing cadence was considered to exist whether the trend was linear or non-linear. A one-way ANOVA with a Tukey post-hoc test was used to determine if the change in timing between 60 – 90 rpm as well as 90 – 120 rpm was different across DOM-INT, SND-TTA, and AMP-TTA limbs.

## Results

### Pedaling Kinetics

Peak torque relative to top dead center (TDC) was the same for the 60 and 90 rpm conditions whereas peak torque in the 120 rpm condition was significantly greater than in the 60 and 90 rpm conditions (Table 9).

**Table 9 – Timing of Peak Torque in degrees past TDC  $\pm$  1 standard deviation. † = stat. sig diff. from 60 rpm. ✦ = stat. sig diff. from 90 rpm.**

Group	60 rpm	90 rpm	120 rpm
Dominant Limb, Intact Group	95 $\pm$ 7.4	96 $\pm$ 8.4	114 $\pm$ 16 ✦ †
Sound Limb, TTA Group	98 $\pm$ 5.24	99 $\pm$ 9.4	124 $\pm$ 17 ✦ †
Amputated Limb, TTA Group	106 $\pm$ 8.4	104 $\pm$ 19.8	129 $\pm$ 15 ✦ †

### Muscle Activation

The gluteus maximus muscle (GM) demonstrated significant shifts and a trend in the onset, offset and peak activation toward earlier activation with increased cadence in all limbs (Figure 22).

The vastus medialis muscle (VM) demonstrated significant shifts and trends in the onset, offset and peak activation toward earlier activation with increasing cadence in the Intact group

and in the sound limb (Figure 23). The amputated limb showed significant shifts and trends in the onset and peak activity.

The long head of the biceps femoris muscle (BF) demonstrated significant shifts and trends in only the onset and peak activation in all limbs but no shift or trend was noted in the offset (Figure 24). The earlier onset without a difference in offset also resulted in significant increases in burst duration as cadence increased in all limbs (Figure 24).

Activation in the rectus femoris muscle (RF) was similar to the BF showing significant shifts and trends in only the onset and peak activation in all limbs. No shift or trend was observed in the offset (Figure 25).

The gastrocnemius muscle showed significant trends in the onset, offset, and peak activation in all limbs yet only significant shifts in the DOM limb of the Intact group and Sound limb for onset and peak activation (Figure 26). Technical problems recording EMG within a prosthetic socket resulted in the loss of 3 datasets in the amputated gastrocnemius muscle. Group averages and statistics were performed on the remaining six datasets whereas the other two limbs (DOM-INT and SND-TTA) represent all nine subjects in each group. The GAS muscle also demonstrated significant increases in burst duration in the SND-TTA and AMP-TTA limbs (Figure 26).

The soleus (SOL) demonstrated significant shifts and trend in the onset, and peak activation in all limbs yet no trend was observed in the offset despite a significant shift in the sound limb between 60 and 120 rpm (Figure 27).

Data for the tibialis anterior (TA) demonstrated high variability and showed a significant shift in only the Intact group for the onset and peak activation. Significant trends in both limbs for the onset and peak were observed (Figure 28). There were no significant shifts or trends noted in the offset.

There were 76 significant shifts noted out of 171 (44%) comparisons made for shifts muscle onset, offset and peak EMG. There were 50 significant trends detected out of 57 (88%)

possible trends analyzed and in all cases these trends point toward muscle activity occurring earlier in the pedaling cycle as cadence increased.

Differences in timing between each cadence were compared across the DOM-INT, SND-TTA, and AMP-TTA limbs to verify when timing occurred earlier with increasing cadence. The relative shifts were similar across limbs. Of the 102 comparisons made between limbs, only two variables showed significant differences across limbs. The shift in peak activation in the BFL muscle going from 90 – 120 rpm was different between the DOM-INT and AMP-TTA. There was a significant difference in the shift in the SOL muscle onset from 90 – 120 rpm between the DOM-INT and SND-TTA. In both these variables, muscle timing still occurred earlier as cadence increased but not the same relative amount.

### Timing of Gluteus Maximus

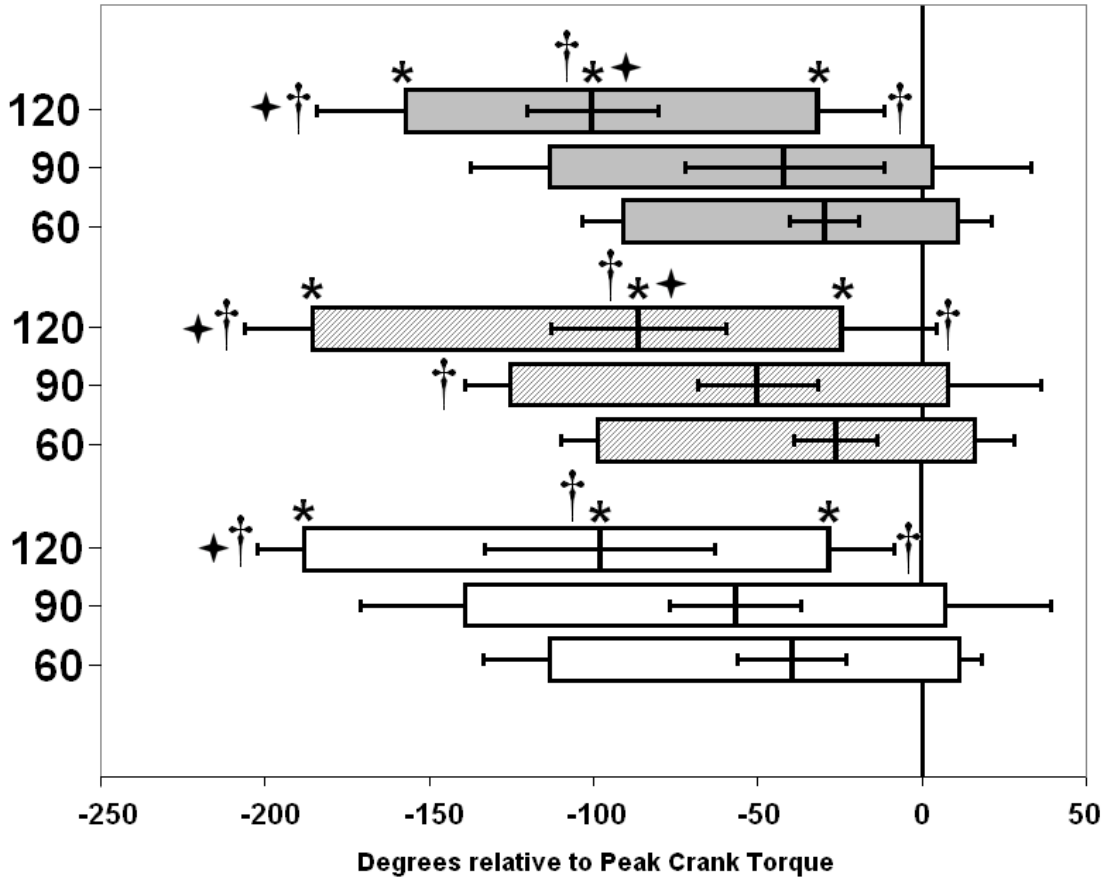


**Figure 22 - Timing of the Gluteus Maximus for the Dominant limb in the Intact group (grey), the Sound limb in TTA (grey striped), and the amputated limb in TTA (white). Peak activation indicated by the vertical line within the bar. Error bars indicate  $\pm 1$  standard deviation.**

‡ = stat. sig diff. from 60 rpm.

† = stat. sig diff. from 90 rpm.

\* = stat. sig. trend toward earlier activation with increasing rpm.

### Timing of Vastus Medialis

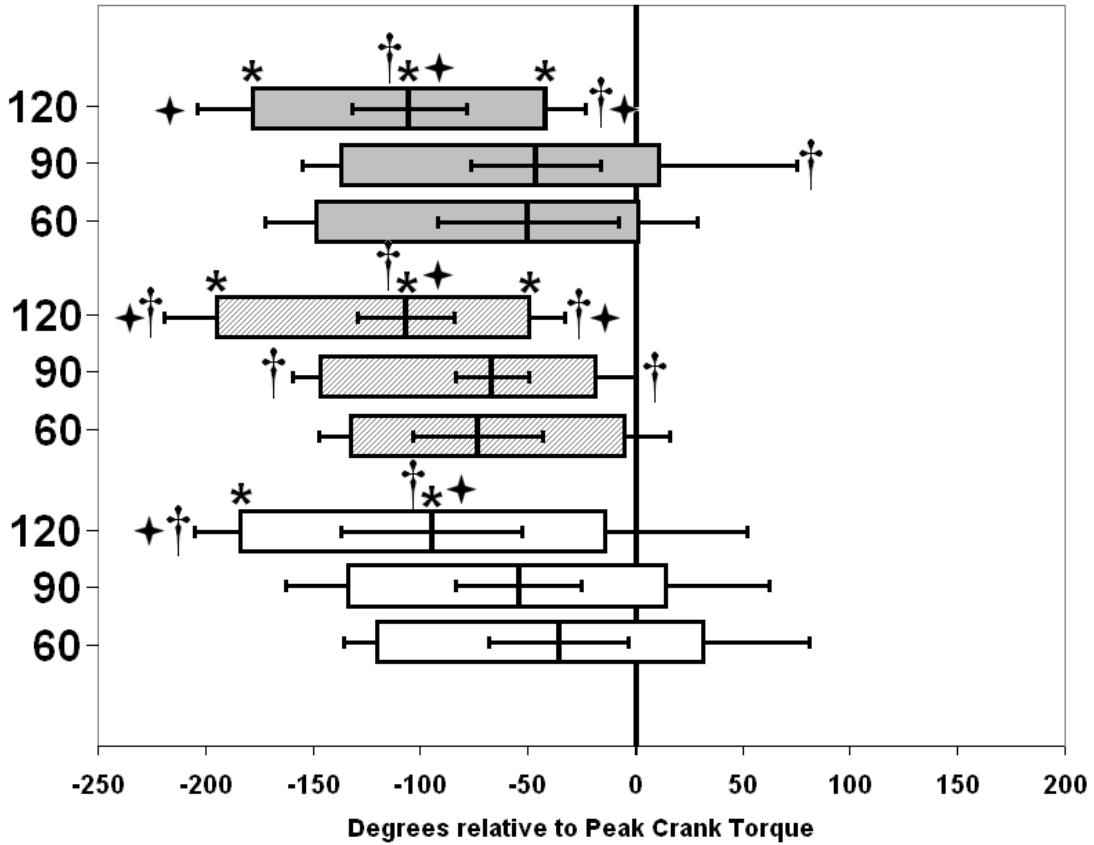


**Figure 23 – Timing of the vastus medialis muscle for the Dominant limb in the Intact group (grey), the Sound limb in TTA (grey striped), and the amputated limb in TTA (white). Peak activation indicated by the vertical line within the bar. Error bars indicate  $\pm 1$  standard deviation.**

- † = stat. sig diff. from 60 rpm.
- ‡ = stat. sig diff. from 90 rpm.
- \* = stat. sig. trend toward earlier activation with increasing rpm.

### Timing of Biceps Femoris Long Head

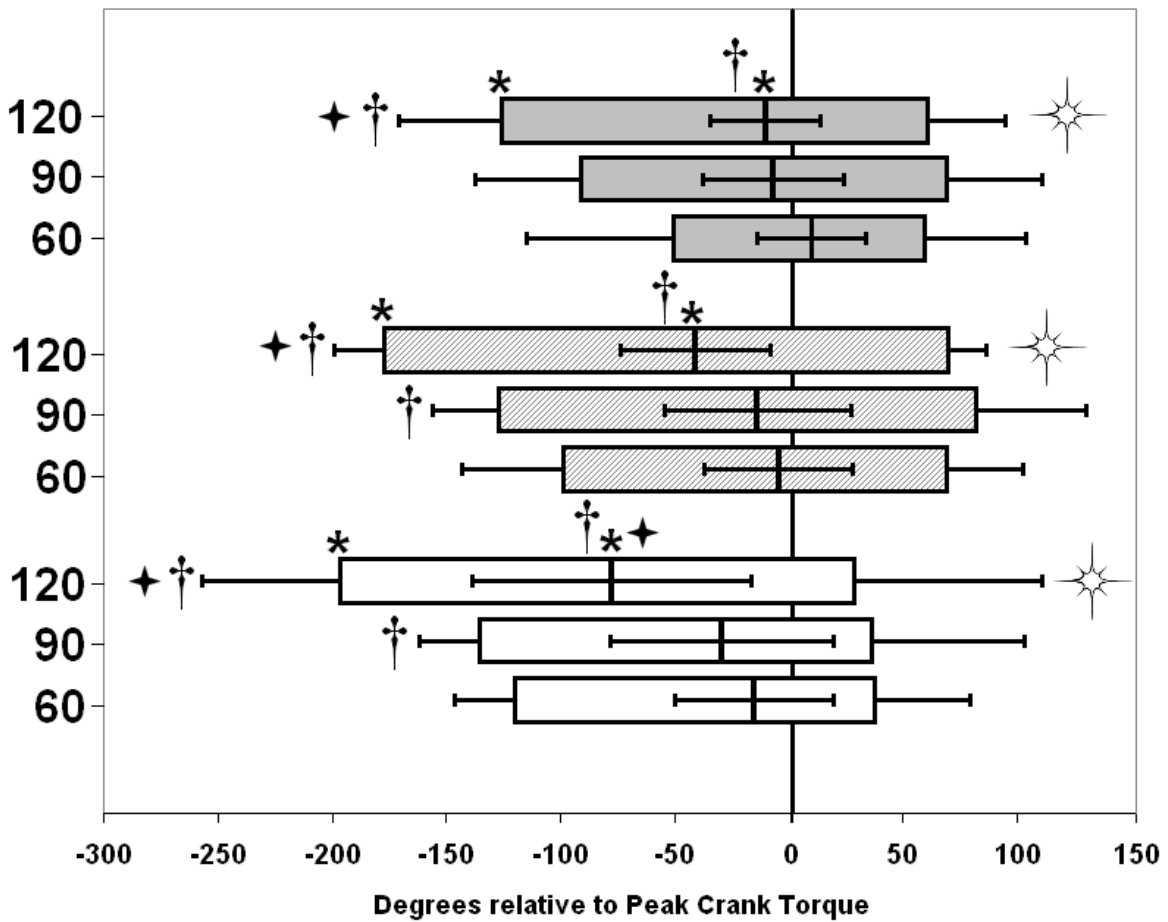
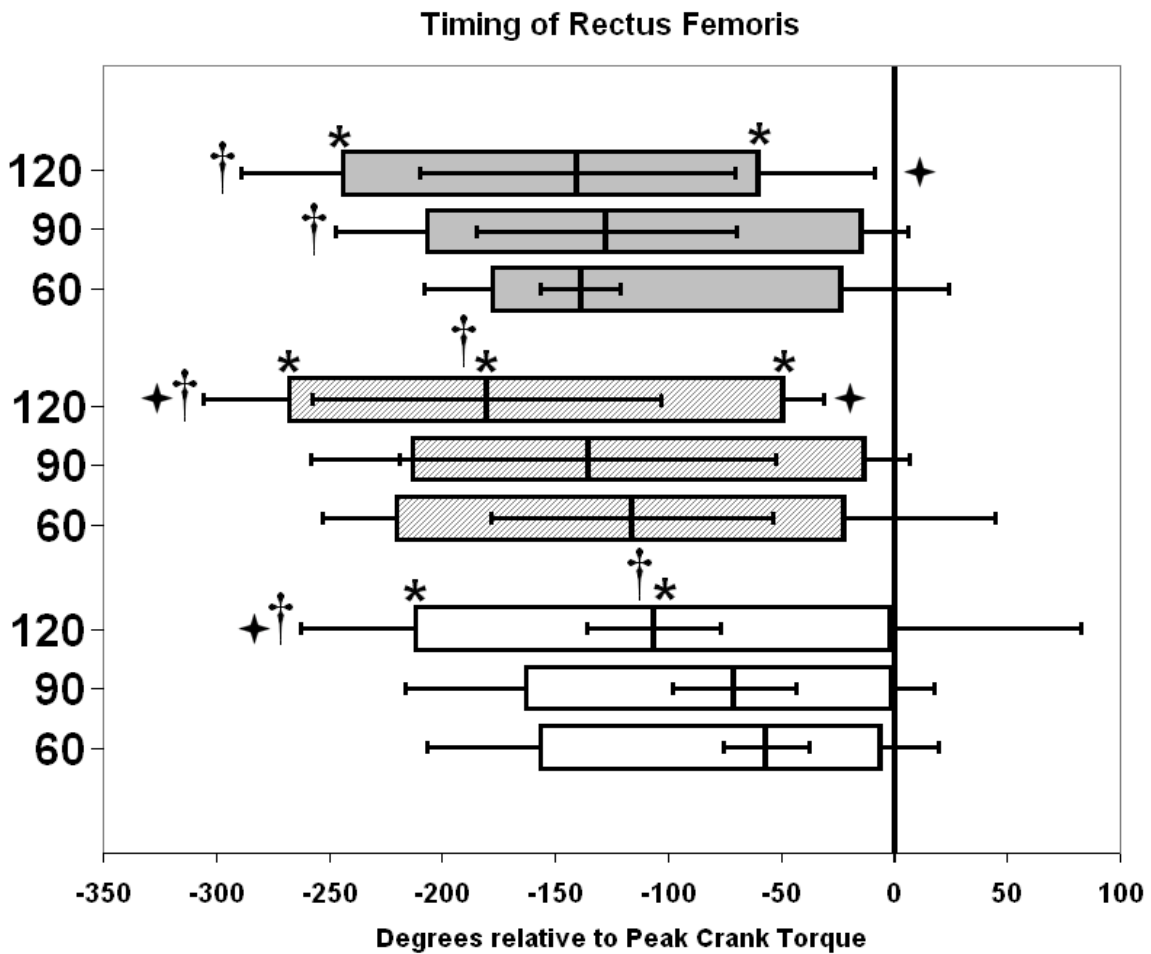


Figure 24 - Timing of the long head of the biceps femoris muscle for the Dominant limb in the Intact group (grey), the Sound limb in TTA (grey striped), and the amputated limb in TTA (white). Peak activation indicated by the vertical line within the bar. Error bars indicate  $\pm 1$  standard deviation.

- † = stat. sig diff. from 60 rpm.
- ‡ = stat. sig diff. from 90 rpm.
- \* = stat. sig. trend toward earlier activation with increasing rpm.
- ✦ = stat. sig. diff. from the 60 rpm condition regarding burst duration.



**Figure 25 - Timing of the rectus femoris muscle for the Dominant limb in the Intact group (grey), the Sound limb in TTA (grey striped), and the amputated limb in TTA (white). Peak activation indicated by the vertical line within the bar. Error bars indicate  $\pm 1$  standard deviation.**

- † = stat. sig diff. from 60 rpm.
- ‡ = stat. sig diff. from 90 rpm.
- \* = stat. sig. trend toward earlier activation with increasing rpm.

### Timing of Gastrocnemius

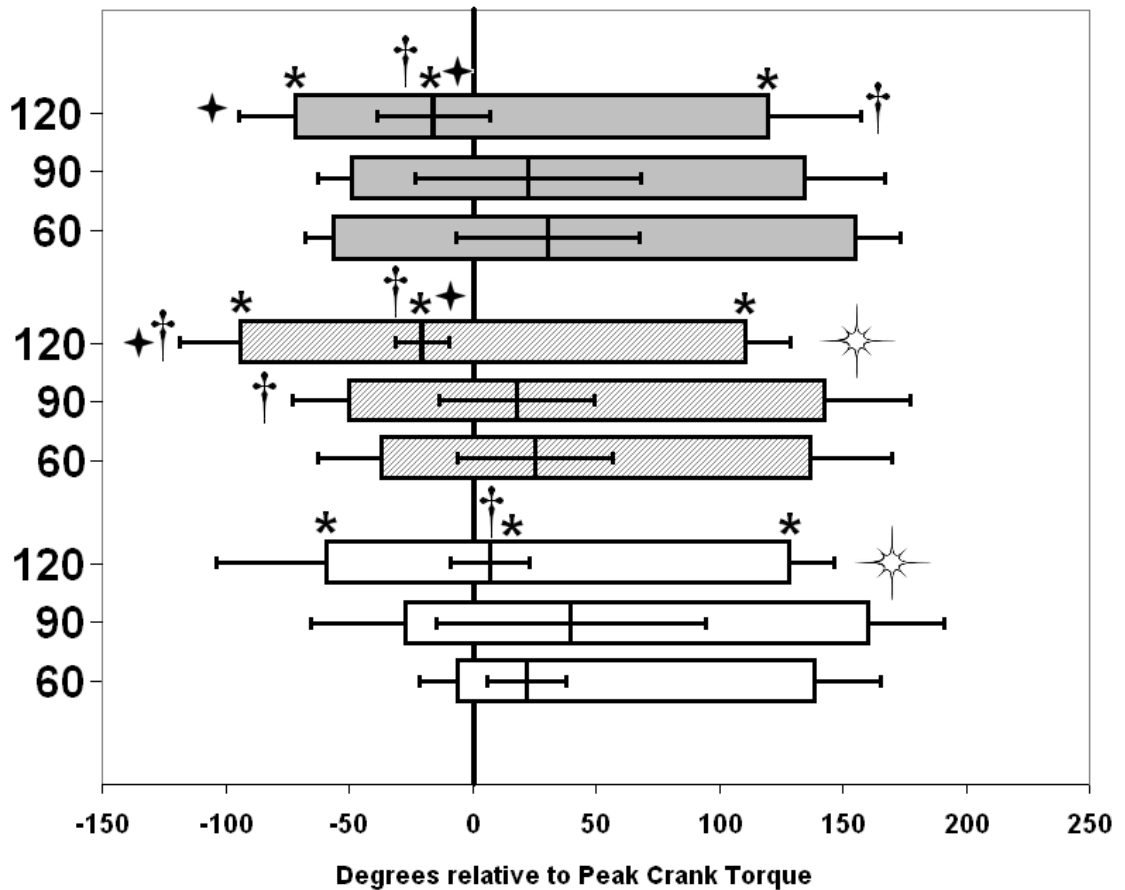


Figure 26 - Timing of the gastrocnemius muscle for the Dominant limb in the Intact group (grey), the Sound limb in TTA (grey striped), and the amputated limb in TTA (white). Peak activation indicated by the vertical line within the bar. Error bars indicate  $\pm 1$  standard deviation.

† = stat. sig. diff. from 60 rpm.

‡ = stat. sig. diff. from 90 rpm.

\* = stat. sig. trend toward earlier activation with increasing rpm.

✨ = stat. sig. diff. from the 60 rpm condition regarding burst duration.

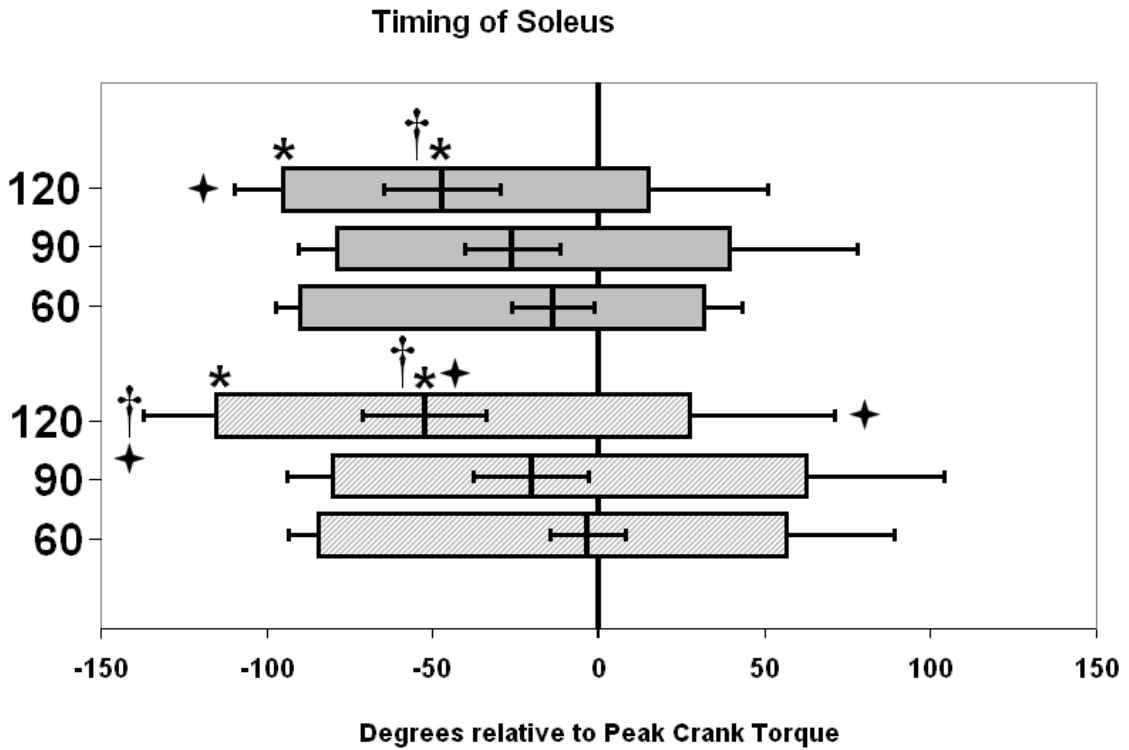


**Figure 27 - Timing for the soleus muscle for the Dominant limb in the Intact group (grey) and the Sound limb in TTA (grey striped). Peak activation indicated by the vertical line within the bar. Error bars indicate  $\pm 1$  standard deviation.**

† = stat. sig diff. from 60 rpm.

‡ = stat. sig diff. from 90 rpm.

\* = stat. sig. trend toward earlier activation with increasing rpm.

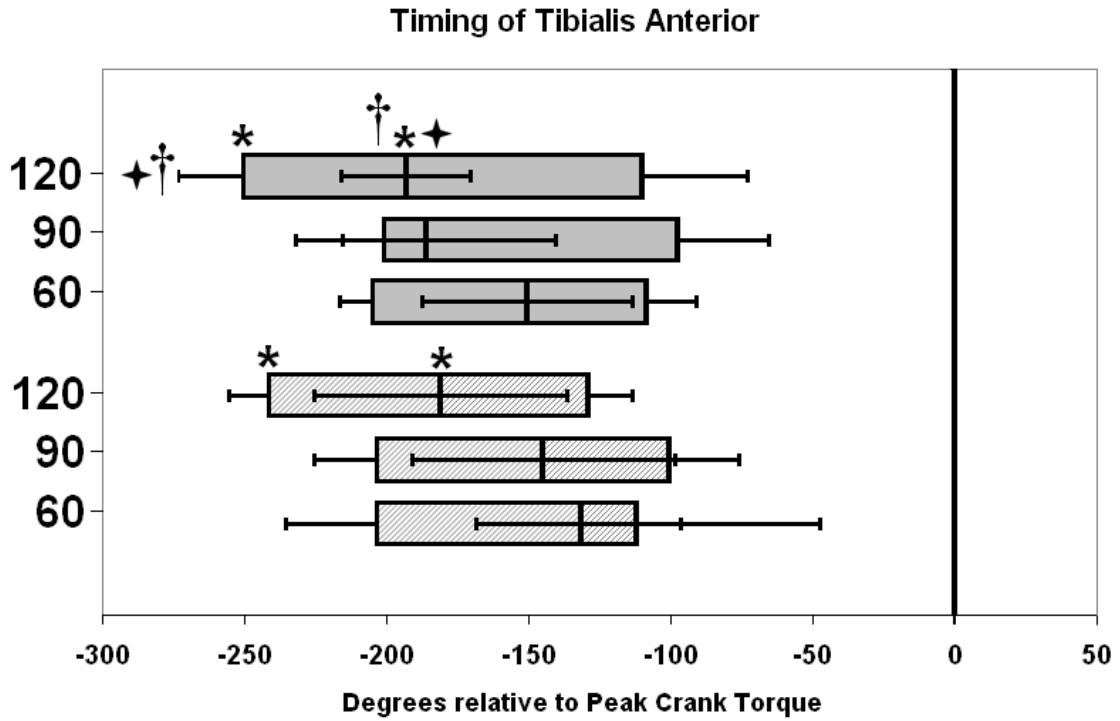


**Figure 28 - Timing for the tibialis anterior muscle for the Dominant limb in the Intact group (grey) and the Sound limb in TTA (grey striped). Peak activation indicated by the vertical line within the bar. Error bars indicate  $\pm 1$  standard deviation.**

- † = stat. sig diff. from 60 rpm.
- ‡ = stat. sig diff. from 90 rpm.
- \* = stat. sig. trend toward earlier activation with increasing rpm.

## Discussion

The most significant finding from this study was that the central control strategy, accounting for the contraction dynamics of the skeletal muscle, was robust and maintained in persons with amputation. This finding is supported by results indicating there were significant trends in 88% of the timing variables tested as well as significant shifts detected in muscle timing indicating earlier activation with increased cadence. These shifts were the same in 98% of the comparisons made between the Intact and TTA groups indicating both groups utilized a similar control strategy responding to changes in cadence, i.e. limb speed.

Neptune et al. (1997) proposed the “activation-contraction dynamics hypothesis” suggesting the central nervous system would account for the dynamics of contraction and excitation in muscle to compensate for increasing limb speed. This hypothesis was investigated further to include timing of muscle activity in relation to peak crank torque (Sarre & Lepers, 2007; Bieuzen et al., 2007) and similar results were reported. Our results also support these earlier findings in that DOM-INT muscle activity demonstrated significant shifts in activation 46% of the time and demonstrated significant trends toward earlier activation 86% of the time.

Timing variables were related to peak crank torque in a manner similar to current reports (Bieuzen et al., 2007) whereas earlier reports presented muscle timing relative to the top of the pedal stroke (Neptune et al., 1997; Baum & Li, 2003; Sarre & Lepers, 2005). Sarre & Lepers (2007) reported timing of peak crank torque was not constant as cadence increased as was assumed in earlier reports (Neptune et al., 1997; Baum & Li, 2003; Sarre & Lepers, 2005). Peak crank torque occurs later in the crank cycle as cadence increases (Sarre & Lepers, 2007). Therefore, Sarre & Lepers (2007) suggested relating the timing of muscle activation to peak crank torque when cadence is not

constant would better reflect the control strategy of the nervous system as was done for this experiment.

Significant shifts in muscle onset and peak in the GM, VM, BF, RF, GAS (except AMP-TTA), SOL and TA (DOM-INT only) were found. Similar shifts have been reported previously for proximal muscles (GM, VM, BF) (Neptune et al., 1997; Baum & Li, 2003; Sarre & Lepers, 2005; Bieuzen et al., 2007) but not in more distal muscles (GAS, SOL, TA) (Neptune et al., 1997; Baum & Li, 2003). Differences observed between proximal and distal muscles may be related to the method of relating timing to peak crank torque vs. TDC of the crank cycle. The ankle joint serves primarily in an energy transfer role in cycling (Broker & Gregor 1994) and it would therefore seem reasonable that the activation of muscles controlling this joint would be related to peak crank torque as used in this study. The method of relating timing to peak torque allowed for these real differences in muscle timing in the SOL, GAS and TA to be detected.

The GAS in the amputated limb did not demonstrate significant shifts in timing as often as did the DOM-INT and SND-TTA. The GAS in the amputated limb has been altered from a bi-articular knee flexor-ankle extensor to a uni-articular knee flexor. In addition to a change in biomechanical function, the amputated GAS has been shown to be involved in control of the limb/prosthesis interface and not in direct control of an ankle joint (see Chapter 4). The altered function of the amputated GAS may explain, in part, why fewer significant shifts in timing were detected. Despite the lack of significant shifts in timing, the amputated GAS did have a significant trend toward earlier activation in onset, peak and offset as cadence increased indicating the motor system still accounted for the activation-contraction dynamics of this muscle.

There was no significant effect of cadence regarding timing of muscle offset in the BF and RF muscles. Previous reports suggest these muscles are involved in managing energy across joints and therefore can adjust activity in order to better perform this role (Prilutsky 2000). In this context, delaying muscle offset may be a strategy used

to manage the demands of this task at different cadences e.g. increase in power or inertial forces. The offset of muscle activity can be affected by sensorimotor input in the BF and RF (Kautz et al., 2002) and timing of these muscles are often modified based on task demands (Rouffet et al., 2009). Limitations in the current dataset preclude any conclusion as to why offset in the BF and RF muscles did not vary with cadence yet highlight the need for future research. An important observation specific to our hypotheses is that the offset in the BF and RF is the same in the DOM-INT, SND-TTA and AMP-TTA limbs indicating the motor system in both groups utilized a similar strategy.

The focus of this research was to determine if the cyclists with a trans-tibial amputation maintained the same relative phasic relationships across cadence as cyclists with intact lower limbs. The motor system could have responded to increasing cadence by increasing the amplitude of muscle activity without shifting the timing of that activity. However, the TTA group did maintain the same phasic relationships in muscle activity as the Intact group indicating the motor system was able to adapt to the losses associated with an amputation. These results support the “activation-contraction dynamics hypothesis” proposed by Neptune et al. (1997) in that even a compromised motor system accounts for these properties of muscle, Furthermore, these results expand on Neptune et al. (1997) demonstrating the muscles controlling the ankle joint account for activation-contraction dynamics when considering timing relative to a physiological output of the motor system (peak crank torque) and not relative to crank kinematics as proposed by Sarre & Lepers (2007).

In conclusion, the control strategy of both cyclists with amputation and with intact lower limb includes accounting for the activation-contraction dynamics of the muscles involved in locomotion. This new understanding of the robustness of the control strategy adds to our basic knowledge of motor system performance while highlighting areas for future research.

# **CHAPTER 5**

## **MOTOR CONTROL WITH AN AMPUTATION DURING CYCLING AT CONSTANT LOAD AND CADENCE**

### **Introduction**

Motor control of any movement task involves the integration of neural, muscular and skeletal systems. This integration must occur throughout the sensorimotor system and focus its efforts on a loadsharing process to control the system endpoint, e.g. the foot during locomotion. A person that has acquired a trans-tibial amputation has lost the ankle joint, surrounding musculature, connective tissue and the gastrocnemius muscle (GAS) has been surgically altered from a bi-articular knee flexor/ankle extensor to a single-joint knee flexor. The limb portion removed during the amputation has been replaced with a prosthesis that will have certain mechanical properties matched to some extent to the mass, moment of inertia and the stiffness of the original limb. The amputee must now adjust to the additional challenges of utilizing a compromised motor system as well as the challenges of controlling a prosthesis through the mechanical interface between the residuum and prosthetic socket. Understanding how the human motor system adjusts to the loss due to amputation and to the addition of an external mechanical device (prosthesis) can provide useful insight into the robustness of the human control system and to compensations and adaptations in human motor control.

The prosthetic socket provides the interface between the residual limb and the prosthesis. Motion does occur between the residuum and the socket as loads are transferred to the prosthesis. Motion at this interface has been reported using radiographic techniques in a quasi-static environment (Erikson & Lemperg 1969; Newton et al., 1988; Lilja et al., 1993; Narita et al., 1997; Soderberg & Roentgen 2003; Brooks 2009) and in a more dynamic environment during gait (Sanders et al., 2006) but only

about one axis. None of these reports however, discussed a possible link between motion at this interface and the control of the *residuum/prosthesis pseudo joint* (RPP). In fact, studies examining the motor control of gait with amputation assume there is no motion between the residuum and prosthesis precluding the investigation of links between strategies developed in the human neuromuscular system and motion at this pseudo joint (Winter & Sienko 1988; Sanderson & Martin, 1997; Powers et al., 1998; Selles et al., 2004; Fey et al., 2010). Recently, Childers et al. (Appendix B) presented a technique to measure movement at the RPP joint and the inclusion of this information in studies of amputee cycling.

The cycling task provides a controlled environment in which rhythmic locomotion can be studied (Gregor & Childers, 2011 for review). Pedaling kinetics have been reported in persons with trans-tibial amputation (TTA) indicating similar pedaling techniques were used by TTA and Intact cyclists (Childers & Gregor, in review). These results suggest that despite the demonstration of similar techniques the TTA group showed greater asymmetry in both pedal forces and work about the crank spindle (Childers et al., in press). Childers et al., (in press) suggested this increase in sound limb output may not be entirely related to strength or inertial differences between limbs but rather suggest there may be other motor strategies utilized by TTA that cannot be understood by pedaling kinetics alone. This study explores these issues by analyzing joint kinematics, kinetics, and muscle activation patterns during amputee cycling to test a general hypothesis; the neuromuscular system changes absolute muscle output to account for the loss of a limb segment.

The purpose of this experiment was to determine the motor strategy used by TTA versus Intact cyclists pedaling against a constant load at constant cadence. The specific hypotheses tested include; 1) the motor system will alter muscle activation patterns to control the RPP joint and utilize the prosthesis for task performance; 2) the motor system will utilize the amputated GAS as a uni-articular knee flexor and shift peak activation to

later in the pedaling cycle; and 3) the sound limb will demonstrate greater knee extensor moment and increase limb output relative to the dominant limb in the Intact group.

## **Methods**

In-depth discussions of the general methods are presented in Chapter 3 and are briefly summarized here to summarize the methods specific to this hypothesis.

### **Subjects and load conditions**

A group of nine persons with trans-tibial amputation (TTA) and a group of nine intact subjects (Intact) were recruited for this study (see Chapter 3; Methods). Subjects in both groups used cycling for recreation. The subjects pedaled at a constant torque of 15Nm and a constant cadence of 90 rpm (~150 watts). Pedaling kinetics (Broker & Gregor 1990), limb kinematics (Peak Performance, Vicon Motion Systems, Oxford, UK) and surface electromyography (EMG) (Myosystem 1400L, Noraxon USA Inc., Scottsdale AZ) were used to calculate the measures selected to address this hypothesis (Table 10). The dominant limb in the Intact group (DOM-INT) was compared to the sound (SND-TTA) and amputated (AMP-TTA) limbs in the TTA group.

**Table 10 - Variables quantified to answer Hypothesis 1.2**

Quantified Variables for Analysis of Hypothesis 1.2
Work Asymmetry between both limbs
Force Asymmetry between both limbs
Timing of maximum and minimum peak crank torque
Mean Joint Extension and Flexion Moment per limb and per joint
Timing of maximum and minimum joint moment per limb for ankle, knee and hip
Angular movement of the residuum relative to the prosthesis
Muscle Onset relative to TDC
Muscle Offset relative to TDC
Peak muscle activation relative to TDC

## Statistical Analysis

Statistical significance was set at  $p \leq 0.05$ . Independent T-tests were used to analyze anthropometric variables and load condition variables between the Intact and TTA group to verify that the two groups performed at a similar workload and cadence. A one way ANOVA was used to compare joint moments, pedal forces, joint kinematics and EMG data (see General Methods) between the DOM-INT, the AMP-TTA, and the SND-TTA. If statistical significance occurred with the one-way ANOVA, a Tukey post-hoc test was used to determine significance between groups.

## Results

### Subjects and load conditions

There were no significant differences between anthropometric data or cycling experience (Tables 5 & 6 in Chapter 3), resistance, cadence or saddle height (Table 11) between groups. The combination of the residual limb and prosthesis had significantly less mass and moment of inertia about the knee compared to the sound and intact limbs (Table 12). The center of mass (COM) location for the residuum plus prosthesis was similar to the shank of the sound and intact limbs (Table 12). The average length of the residual limb was  $20.9 \pm 3.8$  cm. Note; the RPP joint is located at the distal end of the residual limb, thus the COM location of just the prosthetic device is approximately 11.4 cm distal to the RPP joint (Table 12).

**Table 11 - Pedaling resistance and cadence calculated via the force pedals indicating these factors were held constant between groups.**

Group	Resistance (Nm)	Cadence (rpm)	Saddle Height normalized to Leg Length (%)
TTA	$15.1 \pm 2.9$	$91.4 \pm 1.4$	$104.3 \pm 2.2$
Intact	$14.9 \pm 1.8$	$91.2 \pm 0.9$	$104.4 \pm 2.3$

**Table 12 - Mass, center of mass and moment of inertia calculations for the lower limb. Center of mass location was measured along a line going from the proximal to distal joint center. Mass, COM location and MOI calculations for the foot include the cycling shoe. Note, the residuum/prosthesis pseudo joint was located  $20.9 \pm 3.8$  cm distal to the knee joint. \* = stat. sig diff. from amputated limb**

	Mass (kg)	Center of mass location (cm)	Moment of Inertia (kg cm <sup>2</sup> )	Joint center used for COM and MOI
Intact Group Foot	$1.8 \pm 0.3$ *	$11 \pm 0.5$ *	$93 \pm 16$ *	Ankle
Sound Limb Foot	$1.7 \pm 0.5$ *	$11 \pm 0.8$ *	$86 \pm 40$ *	Ankle
Prosthetic Foot	$0.72 \pm 0$	$2 \pm 0$	$138 \pm 0$	Distal Pyramid attachment
Intact Group Shank	$3.9 \pm 0.4$ *	$18.9 \pm 1.3$	$720 \pm 170$ *	Knee
Sound Limb Shank	$3.7 \pm 0.8$ *	$18.8 \pm 1.2$	$660 \pm 210$ *	Knee
Prosthesis + Residual Limb	$3.1 \pm .34$	$18.6 \pm 1.9$	$360 \pm 94$	Knee
Residual Limb	$1.9 \pm 0.4$	$9.2 \pm 1.5$	$84 \pm 40$	Knee
Prosthesis	$1.25 \pm 0.2$	$32.3 \pm 4.5$	$270 \pm 71$	Knee
Intact Group Thigh	$11.8 \pm 2.2$	$16.6 \pm 0.3$	$1550 \pm 310$	Hip
Sound Limb Thigh	$11.2 \pm 1.9$	$16.8 \pm 0.9$	$1510 \pm 340$	Hip
Amputated Limb Thigh	$10.5 \pm 2.6$	$16.8 \pm 0.9$	$1550 \pm 0.3$	Hip

## Pedaling Kinetics

The SND-TTA limb produced the greatest torque about the crank spindle (Figure 29) followed by the DOM-INT and the AMP-TTA limb. The amputated limb displayed significantly less mean positive torque than the DOM-INT limb and the SND-TTA as well as less mean negative torque than the DOM-INT (Table 13). The TTA group pedaled with greater work and force asymmetries than the Intact group (Figure 30).

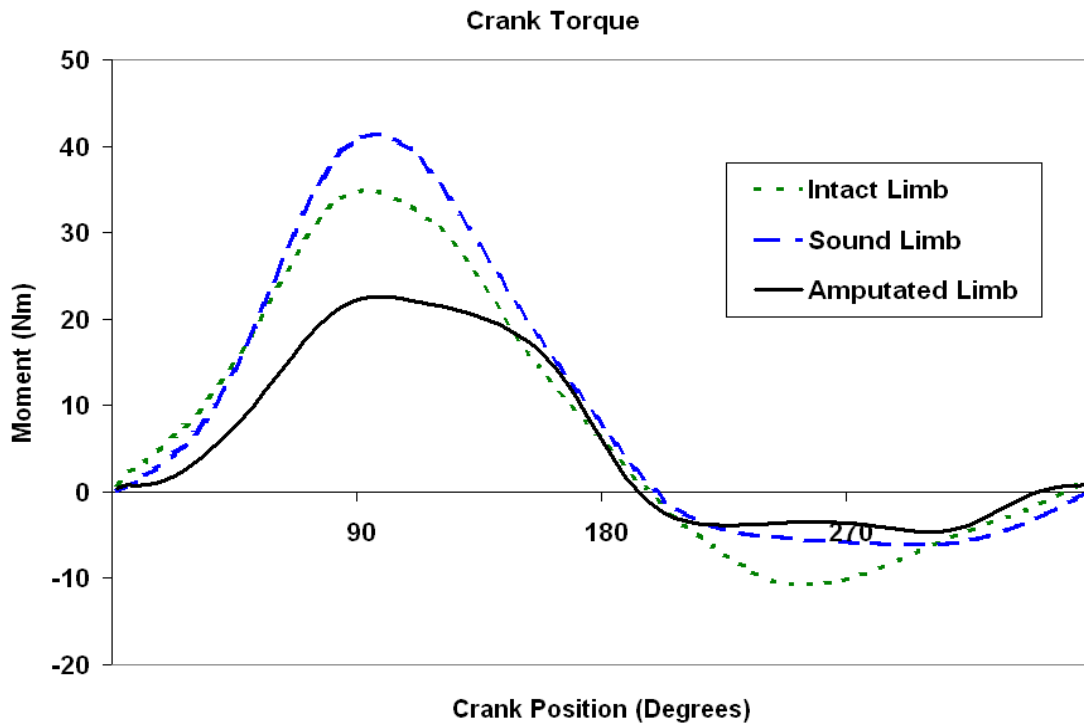


**Figure 29 - Crank torque for the dominant limb in the intact group (green, small dashes), the Sound limb of the TTA group (blue, large dashes) and the amputated limb in the TTA group (black, solid).**

**Table 13 – Magnitude and timing of Peak Torque. \* = stat. sig diff. from amputated limb**

	Average Positive Torque (Nm)	Average Negative Torque (Nm)	Timing of Peak Torque (degrees)
Intact Group, Dominant Limb	18 ± 4.3 *	12.4 ± 7.7 *	96 ± 8.4
Amputee Group, Sound Limb	20 ± 4.8 *	7.2 ± 1.8	104 ± 20
Amputee Group, Amputated Limb	11.9 ± 1.4	5.4 ± 1.9	99 ± 9.4

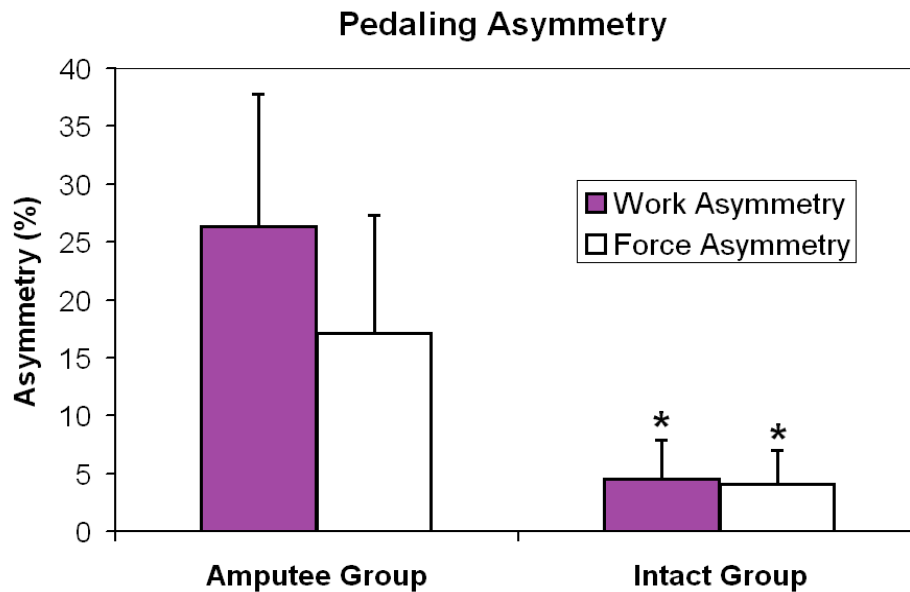


**Figure 30 – Work and force pedaling asymmetries for the amputee group and intact group. \* = stat. sig diff. from the Amputee group.**

### Residual limb kinematics

The relative motion between the residual limb and the socket of the prosthesis (Figure 31) was  $4.8 \pm 1.8$  degrees. The residuum was parallel to a line drawn through the geometric center of the socket of the prosthesis at the bottom of the pedal stroke after which the residuum would rotate posteriorly relative to the prosthesis through the top of the pedal stroke (Figure 31).

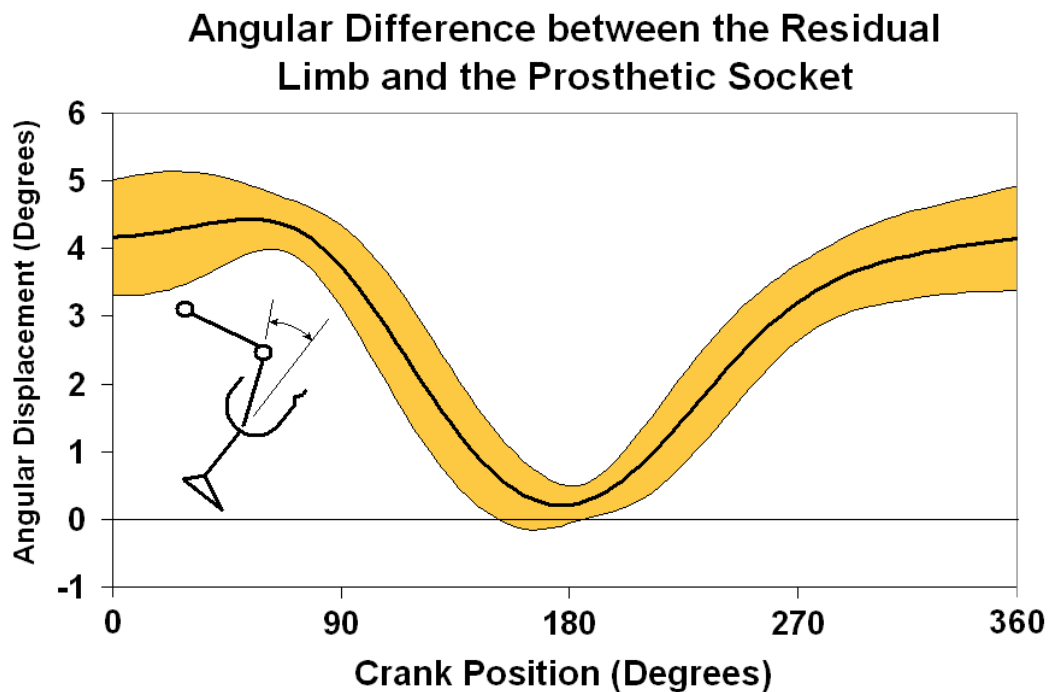


**Figure 31 - Angular motion of the residuum in the prosthesis. The shaded region represents  $\pm 1$  standard deviation. Zero indicates a parallel alignment between the residuum and an axis through the distal end of the prosthesis.**

### Joint Kinetics

The hip, knee and ankle joint moments demonstrated differences between limbs (Figure 32). The hip moment in the amputee group (AMP-TTA) showed less extension between 90 and 270 degrees than the DOM-INT and SND-TTA. The average (Table 14) and peak (Table 16) knee extension moment increased from the AMP-TTA to the DOM-INT to the SND-TTA limb. The amputated limb demonstrated a reduced average knee flexion moment from 180 to 270 degrees compared to DOM-INT (Figure 32) and the ankle moment in AMP-TTA was lower during the first 180 degrees and the peak moment shifted later in the cycle (Figure 32) when compared to DOM-INT and SND-TTA.

The joint moment data were then separated into flexion and extension components as well as the timing of peak moments. The average (Table 14) and peak (Table 16) ankle extensor moment was smaller and the peak occurred later in the cycle (Table 15) for the amputated limb. In addition, the amputated limb demonstrated a

decreased average knee extensor moment compared to SND-TTA and DOM-INT (Table 14). The average knee flexor moment in the DOM-INT was significantly greater than the sound limb and the amputated limb (Table 14). The timing of the minimum hip extensor moment occurred earlier in the crank cycle for the amputated limb when compared to the DOM-INT (Table 15). There were no significant differences regarding the point in the crank cycle where the knee joint moment turned from extensor to flexor, i.e. at  $105 \pm 14^\circ$  for the DOM-INT,  $123 \pm 18^\circ$  for the SND-TTA, and  $116 \pm 21^\circ$  for the AMP-TTA.

The prosthetic suspension system used created a Residuum/Prosthesis Pseudo joint (RPP) located at the intersection point between distal residuum and the inferior aspect of the prosthetic socket (see Chapter 3; Methods). An extension moment at this joint would tend to rotate the proximal end of the residuum anteriorly relative to the prosthetic socket centerline. The moment at this joint (Figure 33) demonstrated an extension moment during the first 90 degrees of the crank cycle. The moment became flexor at the bottom of the crank cycle then progressed toward zero through recovery but stayed generally flexor (Figure 33). The RPP joint moment displays lower magnitudes compared to the knee joint moment calculated in the other limbs (Figure 34).

**Table 14 – Average Joint Moment.** † = stat. sig diff. from the sound limb. ✦ = stat. sig diff. from the dominant limb of the intact group

	Average Ankle Extensor Moment (Nm)	Average Knee Extensor Moment (Nm)	Average Knee Flexor Moment (Nm)	Average Hip Extensor Moment (Nm)
Intact Group, Dominant Limb	$19.2 \pm 5.3$	$12.7 \pm 5.9$	$20.1 \pm 3.3$ †	$42.7 \pm 12$
Amputee Group, Sound Limb	$20.0 \pm 5.7$	$15.4 \pm 4.5$	$17.4 \pm 5.0$	$43.8 \pm 9.9$
Amputee Group, Amputated Limb	$13.3 \pm 2.3$ ✦ †	$8.4 \pm 5.0$ †	$14.0 \pm 3.9$ ✦	$37.4 \pm 10.0$

**Table 15 – Timing of Peak Moments.** † = stat. sig diff. from the sound limb. ✦ = stat. sig diff. from the dominant limb of the intact group

	Timing of Peak Ankle Extensor Moment (degrees)	Timing of Peak Knee Extensor Moment (degrees)	Timing of Peak Knee Flexor Moment (degrees)	Timing of Peak Hip Extensor Moment (degrees)	Timing of Minimum Hip Extensor Moment (degrees)
Intact Group, Dominant Limb	131 ± 26	70 ± 14	171 ± 11	141 ± 17	318 ± 74
Amputee Group, Sound Limb	134 ± 33	77 ± 15	174 ± 13	148 ± 44	285 ± 64
Amputee Group, Amputated Limb	165 ± 11 ✦ †	72 ± 23	171 ± 8	127 ± 63	246 ± 17 ✦

**Table 16 – Magnitude of Peak Moments.** † = stat. sig diff. from the sound limb. ✦ = stat. sig diff. from the dominant limb of the intact group

	Peak Ankle Extensor Moment (Nm)	Peak Knee Extensor Moment (Nm)	Peak Knee Flexor Moment (Nm)	Peak Hip Extensor Moment (Nm)
Intact Group, Dominant Limb	<b>39 ± 9.0</b>	<b>23 ± 11</b>	<b>41 ± 8.9</b>	<b>76 ± 19</b>
Amputee Group, Sound Limb	<b>47 ± 12</b>	<b>29 ± 9.3</b>	<b>39 ± 8.7</b>	<b>89 ± 19</b>
Amputee Group, Amputated Limb	<b>33 ± 9 †</b>	<b>15 ± 11 †</b>	<b>35 ± 10</b>	<b>71 ± 22</b>

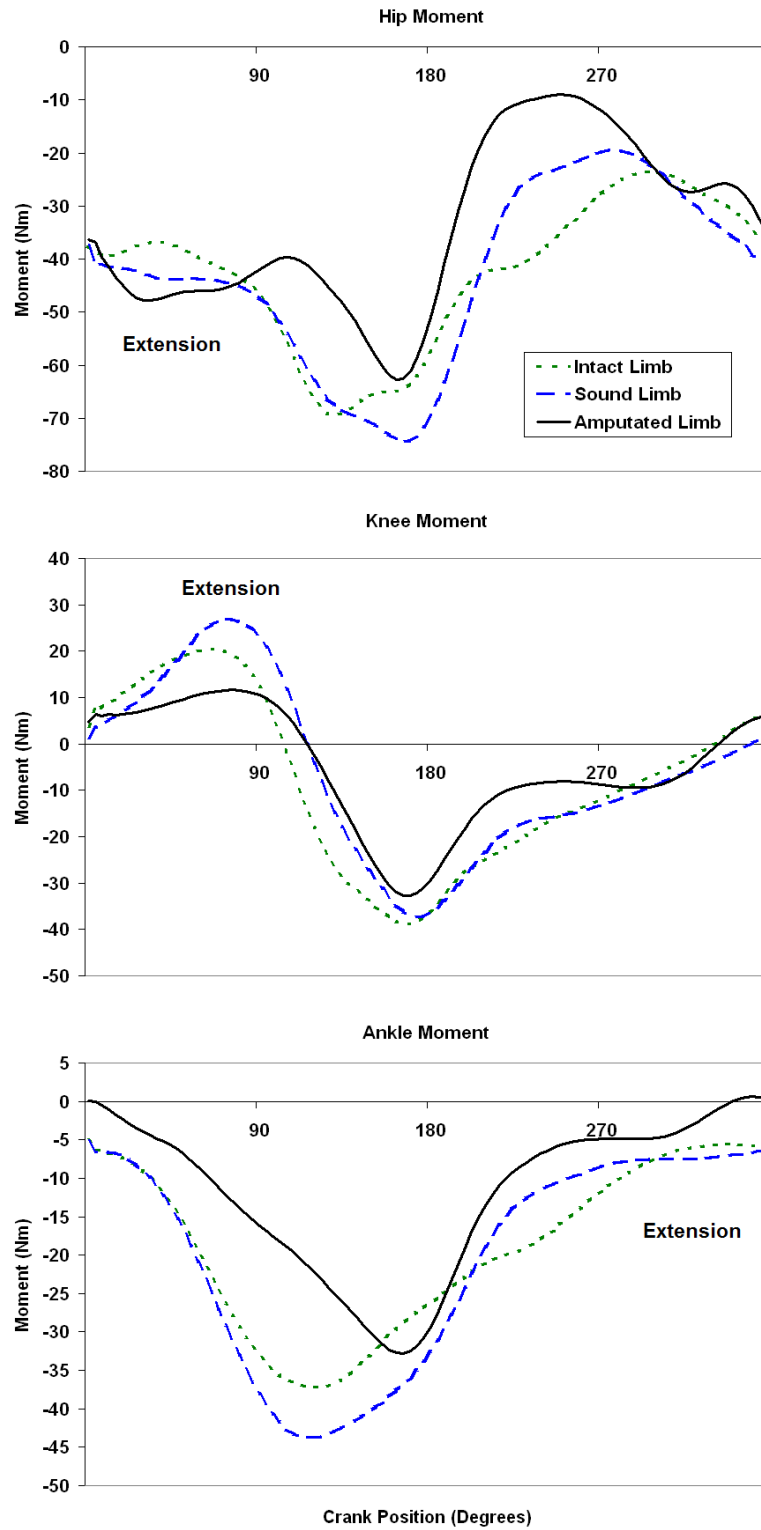


**Figure 32 - Hip, knee, and ankle joint moments for the dominant limb in the intact group (green, small dashes), the Sound limb of the TTA group (blue, large dashes) and the amputated limb in the TTA group (black, solid).**

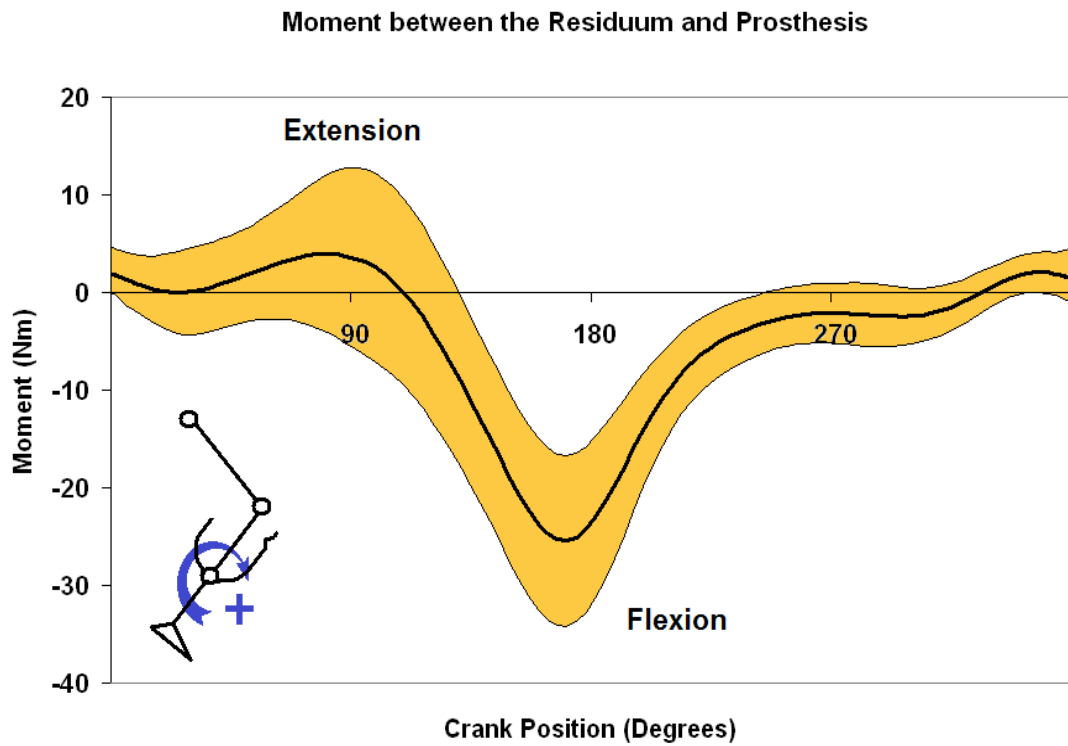


**Figure 33 - Moment at the residuum/prosthesis pseudo-joint. Positive numbers represent an extension moment. An extension moment would tend to rotate the proximal end of the residuum toward the anterior portion of the prosthetic socket.**

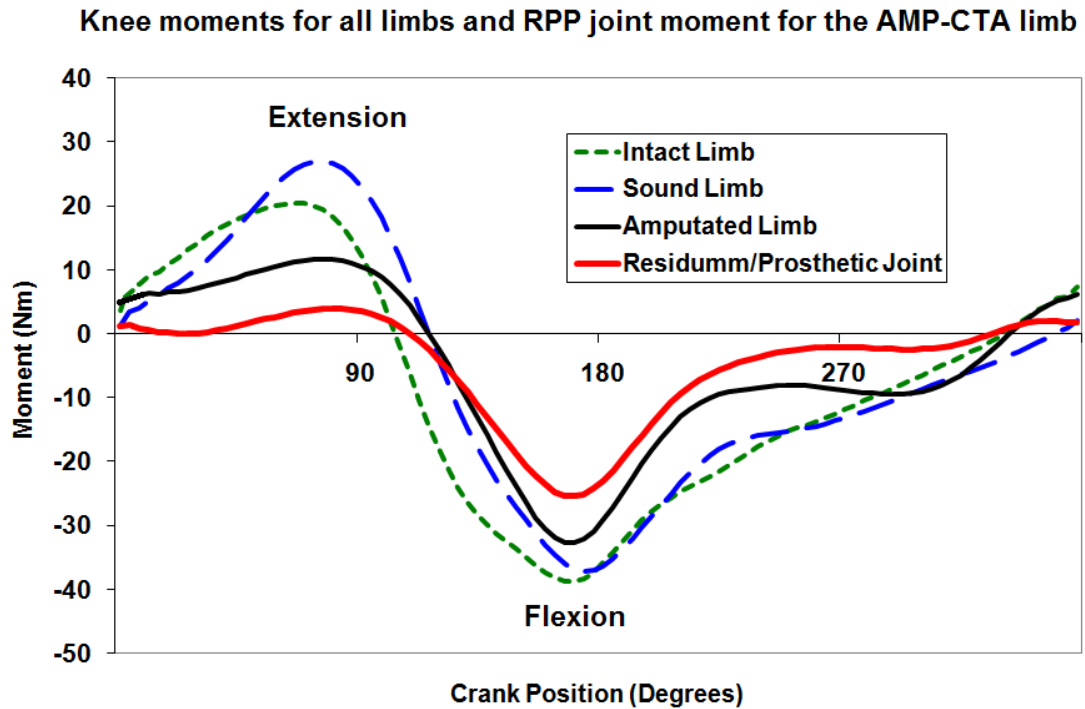


**Figure 34 - Moments for the knee joint and the RPP joint overlaid for comparison**

### **Muscle Activation**

Muscle timing, i.e. onset, offset and peak EMG (Figure 35), demonstrated no significant differences when comparing the SND-TTA to DOM-INT. There were however, notable differences in timing within the amputated limb. The rectus femoris (RF) demonstrated a significant shift toward later onset, peak and offset in AMP-TTA compared to DOM-INT (Figure 35).

The typical bimodal activation demonstrated in the DOM-INT was not present in the RF in the amputated limb (Figure 36). The gastrocnemius (GAS) in the amputated limb also demonstrated a significant shift in peak activation toward later in the crank cycle. Similar to the RF, the typical bimodal activation curve for the GAS was replaced with a single peak of activity at (average degrees in the pedaling cycle) (Figure 37).

Technical difficulty leading to large signal artifact in EMG samples taken with electrodes

within the prosthetic socket resulted in the loss of 3 datasets for the amputated GAS. The remaining six datasets were used for this analysis.

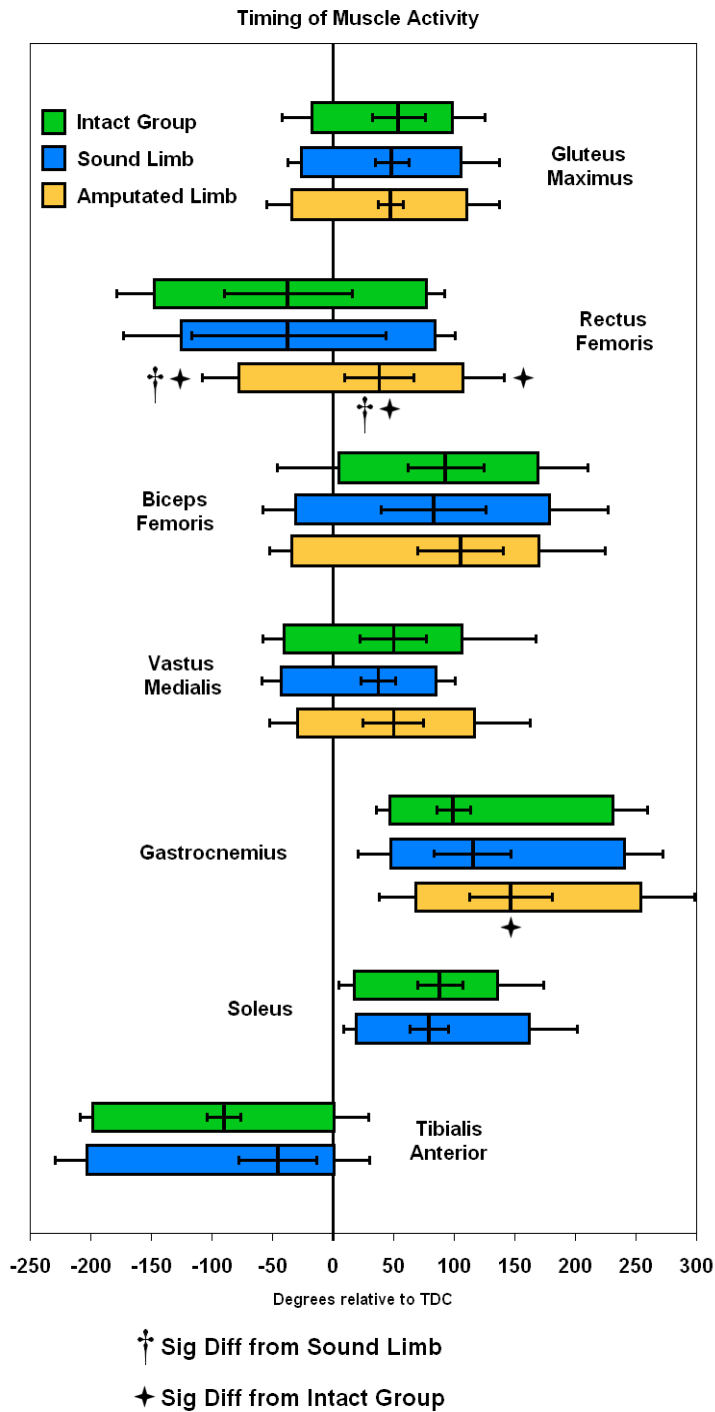


**Figure 35 - Timing of muscle onset, peak and offset. Error bars indicate  $\pm 1$  standard deviation from the mean. Technical difficulty resulted in only 6 complete datasets for the amputated gastrocnemius.**

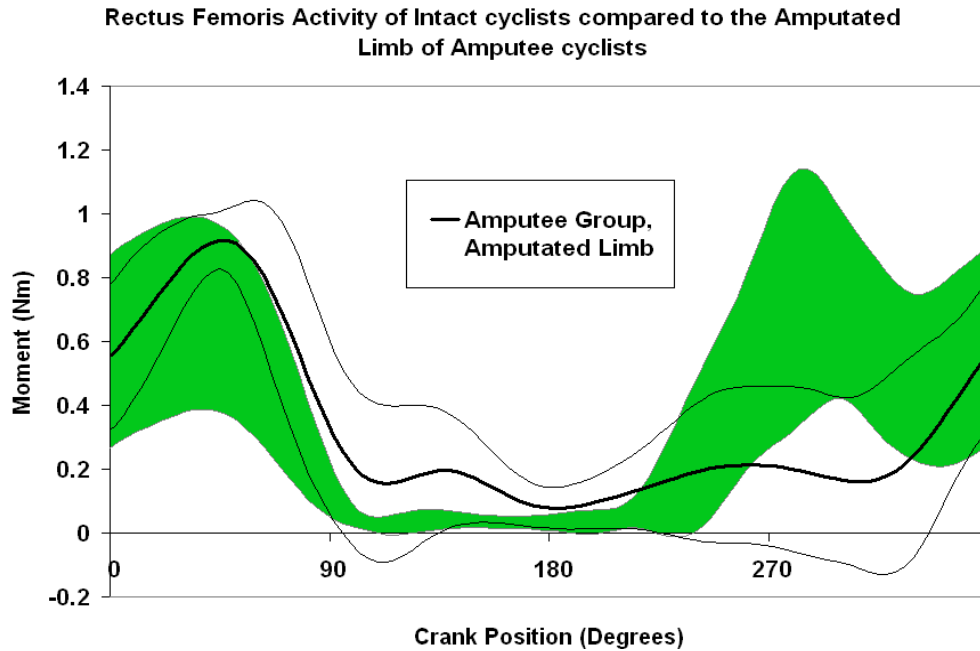


**Figure 36 - Activation of the amputated Rectus Femoris  $\pm 1$  standard deviation (Black line) compared to the activation of the same muscle in the Intact group (green shaded region).**

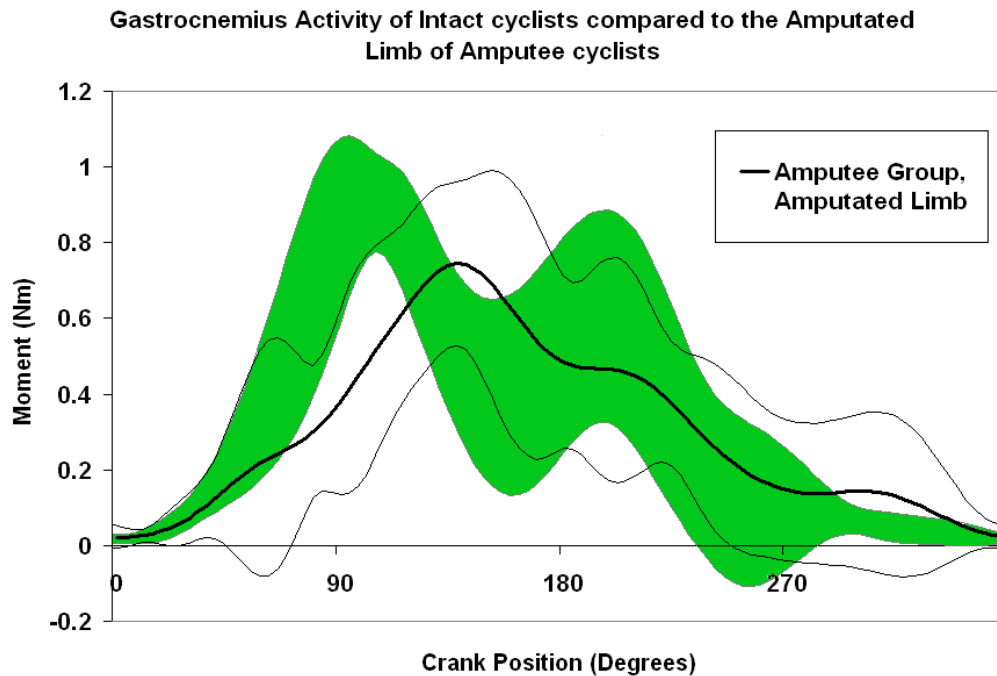


**Figure 37 - Activation of the amputated Gastrocnemius  $\pm 1$  standard deviation (Black line) compared to the activation of the same muscle in the Intact group (green shaded region). Technical difficulty resulted in six datasets for the amputated GAS**

## **Summary of Results**

Data from limb kinematics, pedaling kinetics, and muscle activation are summarized in Figure 38 with the limb pictured in different pedaling quadrants (Figure 39) to provide a more integrated picture of the mechanics and control of the limb/prosthesis system during the pedal cycle. The inertial properties of the prosthesis as well as gravitational effects may influence control of this device because the center of mass is located below the RPP joint (Table 12). Inertial and gravitational forces acting on residual limb due to the displacement of the prosthesis were calculated and displayed (Figure 38) to help the reader better visualize those effects at the residuum/prosthetic interface.

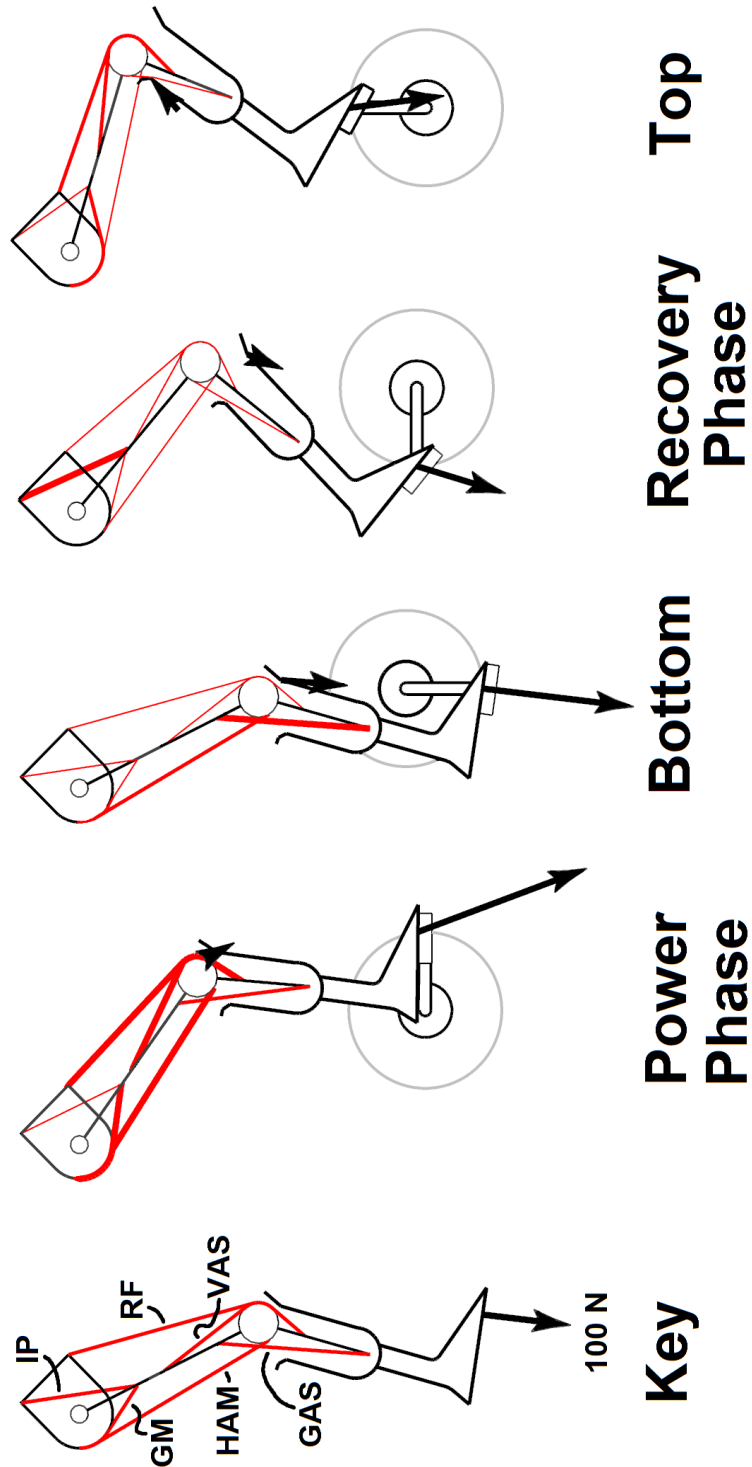


**Figure 38 - Schematic of the amputated limb and the prosthesis through the crank cycle. Force vectors indicate forces at the foot/pedal interface as well as the inertial/gravitational forces being applied by the prosthesis to the residuum and acting at the brim of the socket. Muscle activity is represented by line thickness. Activity for the iliopsoas muscle is assumed based on joint moments as well as Juker et al., 1998.**

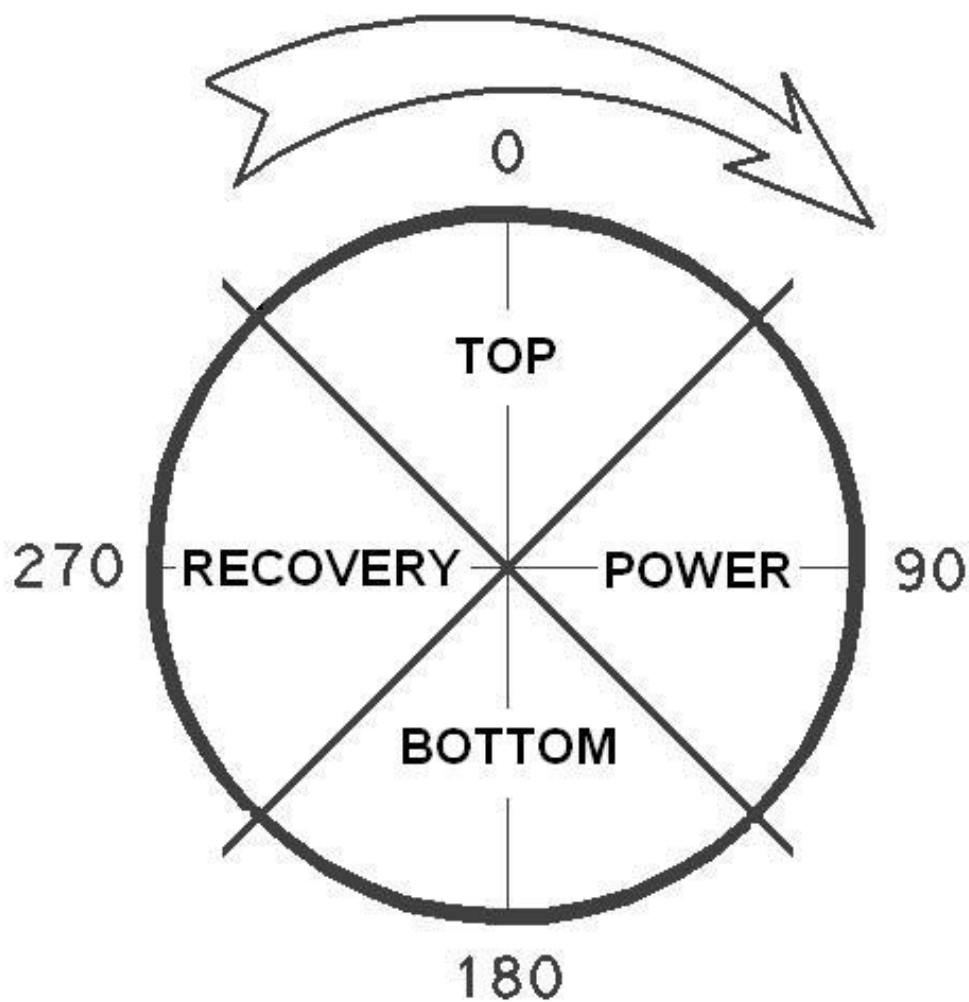


**Figure 39 - Quadrants of the crank cycle are defined as the top of the pedal stroke (315 - 45 degrees), the power phase (45 - 135), the bottom of the pedal stroke (135 - 225), and the recovery phase (225 - 315).**

## **Discussion**

The most significant findings show muscle activity patterns from the rectus femoris (RF) and gastrocnemius (GAS) were altered in the amputated limb. The muscle activity patterns from the SND-TTA as well as the gluteus maximus (GM), long head of the biceps femoris (BF) and the vastus medialis (VM) in AMP-TTA were not different than the DOM-INT. The altered activity in the RF and GAS will be discussed after the quality of the dataset and patterns of sound limb output are presented.

### **Quality of Dataset**

The TTA group in this study demonstrated greater work and force asymmetry than the intact group and these results are similar to data reported previously (Broker & Gregor, 1996; Childers et al., in press) indicating these subjects were representative of a larger population. Both groups pedaled at the same workload, maintained the same cadence, and pedaled with a similar saddle height normalized to leg length indicating the differences noted in joint and pedal kinetics and muscle activity are not related to the above mentioned variables. The pedaling kinetics, limb kinematics, joint moments and muscle activation for DOM-INT and SND-TTA are similar to other published reports (Gregor et al., 1985; Ryan & Gregor 1992,) and seem to be typical for steady-state cycling.

Six of the nine datasets for the GAS muscle in the AMP-TTA limb were acceptable for analysis. Recording EMG within a prosthetic socket is a difficult technical undertaking (Jaegers et al., 1996; Hong & Mun, 2005; Childers et al., 2009a; Klodd et al., 2011). Noise artifact related to movement of the electrodes relative to the hard prosthetic socket accounted for two of the lost three datasets whereas the third subject demonstrated GAS activity off the bicycle yet no activity during cycling. Noise artifact is a common technical challenge associated with EMG recording within a prosthetic socket (Childers

et al., 2009a; Klodd et al., 2011) and resulted in the loss of 8 out of 12 datasets during pilot work for this experiment. The number of lost datasets was reduced in this experiment through fabrication of a prosthetic socket with extra space for the EMG electrodes as well as a better filtering technique (see Chapter 3; Methods) to attenuate movement artifact. The four datasets from pilot experiments and the six datasets from this experiment were combined (Figure 40) and demonstrated nearly identical activation patterns indicating the six datasets used for the amputated GAS in this experiment are a sufficient representation of this muscle's activity.

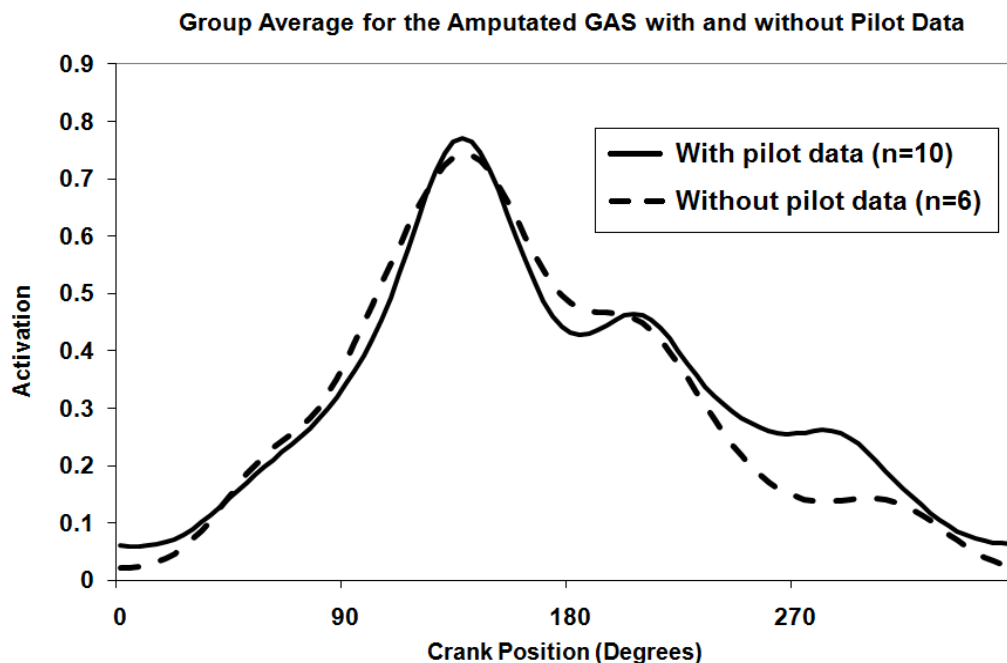


**Figure 40 -- Group average for muscle activation of the amputated gastrocnemius muscle of the six datasets used for this experiment (solid line) and the combination of experimental and pilot datasets (dashed line).**

### The Sound Limb

There were no significant differences in the timing of muscle activation between SND-TTA and DOM-INT ( $p < 0.05$ , Figure 25). The SND-TTA demonstrated a significantly lower average knee flexor moment (Table 14), a trend toward a lower hip extensor moment compared to DOM-INT during the recovery phase (Figure 32) and less

average negative pedal torque (Figure 29 & Table 13). In addition the sound limb showed a trend toward more positive crank torque (Figure 29) and greater peak and average knee extensor moment (Figure 32). Collectively, these data suggest the sound limb increased its output through knee extensors during the power phase and hip flexors during the recovery phase.

### **The Amputated Limb**

Peak activation for the GAS in the amputated limb shifted, significantly, to later in the crank cycle (Figure 37). A trans-tibial amputation surgically alters the gastrocnemius from a bi-articular knee flexor/ankle extensor to a uni-articular knee flexor. And, as a uni-articular knee flexor, activation of the GAS muscle will affect the knee flexor moment as well as how the residual limb transfers load through the prosthetic socket and onto the pedal. Van Ingen Shenau (1989) demonstrated the relationship between muscle activation, the muscle's functional role and the moment at the respective joint and suggested peak activation of a muscle is correlated with the peak joint moment that muscle would control allowing for a ~90ms electromechanical delay. Peak activation of the amputated GAS occurred approximately 67 ms before the peak knee flexor moment allowing for an electromechanical delay suggested by Van Ingen Shenau (1989), i.e one appropriate for a uni-articular knee flexor. In addition, the GAS activation pattern followed a pattern similar to the one predicted for the short head of the biceps femoris (Neptune & Hull 1998) which is also a uni-articular knee flexor. The correlation of the peak activation of the amputated GAS with peak knee joint moment as well as the significant difference from the unaltered GAS in the DOM-INT limb suggest the motor system recognized the uni-articular nature of this muscle and altered its activation to reflect its new biomechanical role.

An alternate explanation for the altered GAS activity in the AMP-TTA limb may be developed from ideas proposed by Kuo (2001) stating muscle activity should be taken

in the context of whole system performance and not performance about a particular joint or joints. The power phase of cycling includes a large hip and knee extensor moment (Figure 32) as well as activity in the GM, BF and VM (Figure 35). Forces generated by these muscles must be transferred down the kinematic chain via the residuum, through the limb/socket interface, the prosthesis and onto the pedal. A prosthetic socket is designed to appropriately secure the residuum to the prosthesis and provide effective transfer of energy into the prosthesis while minimizing pressure on the skin of the residuum when the residuum is parallel with the prosthesis (Kristinsson, 1993).

Activation of the GAS as well as the BF would counteract knee joint extensors and attempt to move the residual limb parallel with the prosthetic socket reducing discomfort and enhancing force transmission during the power phase (Figure 38). The orientation of the residuum in the prosthesis is flexed during the power phase but starts moving into a more parallel orientation within the prosthesis as the crank moves toward the bottom of the pedal stroke (Figure 38) during periods of BF and GAS activity. Therefore, it is possible this muscle activity is used to control the interface between the residuum and prosthesis which would benefit system performance while utilizing the amputated GAS in accordance with its new biomechanical function.

The residuum begins to flex again in the prosthetic socket as GAS activity decreases during the recovery phase (Figures 37 & 38). The recovery phase, as defined in Figure 40, is associated with little muscle activity (Figure 35 & 38). In addition, the mechanical coupling between the two limbs through the crank allows the contralateral limb (in its power phase) to drive the pedal upward into the ascending ipsilateral limb. Therefore, forces produced within the limb are related to the mechanical constraints imposed by the dynamics of the joints and limb segments as well as the inertial forces of those segments (Kautz & Hull, 1993). The path of the knee joint during the recovery phase follows a trajectory set by the location of the hip joint and the length of the femur that is more horizontal than vertical whereas the trajectory of the pedal in this region is

more vertical than horizontal (Figure 38). Meanwhile, inertial forces related to the prosthesis being translated vertically are acting to flex the RPP joint (Figure 38). These forces act to rotate the prosthesis clockwise about pedal spindle (Figure 38) while the amputated limb is ascending creating the flexor moment that persists at the RPP joint (Figure 33) and leads to the movement of the residuum within the prosthetic socket toward RPP joint flexion (Figure 38).

The knee and hip joint moments in the amputated limb are reduced (less flexor) compared to SND-TTA and DOM-INT (Figure 32) during the recovery phase. A reduction of the hip extension moment during this phase would serve to lower forces resisting the upward motion of the pedal and prosthesis thus slowing flexion between the residuum and the prosthesis. The reduction of the hip joint extensor moment during this phase is likely due to activity of the iliopsoas (IP) muscle. The hip joint is extended during this phase placing the IP in the suitable biomechanical position to affect the hip joint moment, it has been reported to be active during this region in intact cyclists (Juker et al., 1998) and no other major muscles are active during this phase (Figure 35).

Alternatively, the amputated GAS could stay active during this region to help further flex the knee and minimize movement of the residuum in the prosthesis. Delayed offset in the amputated GAS did occur in two TTA datasets yet the movement of the residuum in the prosthesis was similar to the group average. This may be because the knee is flexed during recovery placing this muscle at a disadvantage to produce force. The amputated GAS may not be able to produce enough force given its shorter length to overcome the geometric constraints and inertial forces responsible for flexion of the RPP joint. Therefore, in order to minimize residuum movement in the prosthesis, the IP would have the advantage to reduce the hip extensor moment thereby helping to pull the knee anteriorly and control the RPP joint. This scenario is consistent with ideas proposed by Kuo (2001) in which activation of a muscle at one joint may be utilized to control joints not crossed by the active muscle.

The top of the pedal stroke is a region associated with discomfort in TTAs because the residuum/prosthetic pseudo joint (RPP) is flexed in the socket increasing pressure between the posterior wall and posterior aspect of the knee as well as the anterior/distal portion of the tibia (Childers et al., 2009c). Excessive flexion of the RPP joint would place mechanical loads on the skin of the residuum. These loads on the skin will provide cutaneous sensory feedback to the central nervous system. The TTAs used for this experiment were all active and experienced prosthetic users, meaning they have experience at recognizing skin loading that could lead to skin breakdown, i.e. they understand the importance of minimizing excessive pressures on the skin of the residuum because skin breakdown would impede their daily activity while given time to heal. Therefore, mechanical loading of the skin and soft tissue in the residuum becomes an additional criterion for task performance and an important variable to consider when discussing the top of the pedal stroke.

The top of the pedal stroke is a transition region also associated with activation of the RF muscle in order to aid in hip flexion and knee extension while directing forces more anteriorly in preparation for the power phase (Ting et al., 1999). The DOM-INT and SND-TTA demonstrated activation of the RF (Figure 35) similar to other reports (Ryan & Gregor 1992; Ting et al., 1999) whereas the RF in the amputated limb had a delayed onset, peak and offset (Figures 35 & 36). The RPP joint is flexed as the amputated limb progressed through the top of the pedal stroke (Figure 38) placing it in a position of increased discomfort (Childers et al., 2009b) and sub-optimal energy transfer (Kristinsson, 1993). RF activation through the top of the pedal stroke would increase pressure about the posterior aspect of the knee as well as the anterior distal portion of the tibia (Figure 38) thus it would not be advantageous to activate the muscle during this phase. This may explain why RF activity is delayed until after the prosthesis progresses through the top of the pedal stroke and the limb enters the power phase. This delayed activity may also be responsible for the reduced knee extensor moment early in the crank

cycle (Figure 32) and this reduced output in the amputated limb may explain increased sound limb output to compensate.

The altered muscle coordination demonstrated directly in the RF and GAS and presumed in the IP in combination with the recorded movement of the residuum within the prosthesis suggests a motor system involved in the control of the limb/socket interface as well as task performance. The residuum represents the endpoint of the motor system and in order to control the pedal, the system must control the interface between the limb and the prosthesis as well as the mechanical/inertial properties of the prosthesis.

This concept of interface control has been demonstrated in the upper extremity regarding the use of tools (Arbib et al., 2009; Mizelle et al., in press). During tool use, muscle activation has been altered by the size and shape of the interface (Dong et al., 2007), the number of degrees of freedom allowed to the endpoint (Kornecki et al., 2001; Laursen et al., 2003; Fischer et al., 2009), the orientation of the hand relative to the endpoint (Fischer et al., 2009), when the inertial properties of the tool are greater than the limb controlling the tool (Kornecki et al., 2001) and this altered activation can be explained by the need to control the tool interface as well as the endpoint (Kornecki et al., 2001; Laursen et al., 2003; Dong et al., 2007; Fischer et al., 2009). Similar to upper extremity tool use, the interface between the distal limb segment (residuum) and the tool (prosthesis) must be controlled to compensate for the mechanical and inertial properties of the prosthesis in performing a locomotor task. The results of this experiment demonstrate control of the residuum/prosthesis interface by the motor system in response to the additional DOF provided by the RPP joint as well as the mechanics of the interface and inertial properties of the prosthesis. Therefore, I propose the prosthesis should be considered in the context of tool use.

To summarize, these results demonstrate that the motor system of TTAs did alter muscle activation to utilize the prosthesis to perform a cycling task. Specifically, the GAS and RF muscles demonstrated shifts in the timing of muscle activity. In addition,

the IP presumably altered its output to aid in control of the residuum/prosthesis interface. The sound limb compensated primarily by increasing limb output while maintaining similar timing of muscle activity. The altered muscle activity patterns are best explained as the motor system adapting to the inertial properties as well as the mechanics of the residuum/prosthesis interface to control the prosthesis. In addition, I propose the prosthesis should be viewed in the context of tool use in that the residuum is the end-effector of the motor system and the prosthesis is the tool to extend that end-effector to the environment, i.e. the bicycle.

Understanding the prosthesis as a tool may help to explain the differences in motor control between an intact limb and a limb/prosthesis system. The need to change muscle activation and hence joint moments to control the prosthesis relates to clinical goals associated with minimizing “gait deviations” because these “deviations” refer to a deviation from “normal” gait, e.g. gait with intact limbs. The limb/prosthesis system represents a new “normal” for these individuals and this research suggests what has historically been viewed as a “deviation” is simply a “motor adjustment” necessary to complete the task. In this context, a motor adjustment isn’t necessarily “bad”. Instead the clinician may now view the performance of the limb/prosthesis as a whole system and understand the performance of the proximal joints will related to the amputee’s ability to utilize the prosthesis (tool). The clinician may then decide the cost or benefit to a given adjustment and alter the design or rehabilitation program accordingly instead of treating a motor adjustment as a “deviation”.

Understanding these “motor adjustments” as necessary to control the tool, e.g. prosthesis, may allow for advancements in prosthetic socket technology. For example, an engineer could now predict the motor adjustment based on a particular prosthetic socket interface design, the tissue properties of the residuum, the mechanical properties of the prosthesis, and the mechanical requirements of the task. This could be taken one step further once an engineer/scientist can predict the motor adjustment; the prosthesis design

could then be optimized to manipulate how the motor system would adjust to a prosthesis. Similar to how one may improve the ergonomics of a screwdriver handle, one may improve the design of the socket in ways that would better allow the motor system to utilize this tool.

# **CHAPTER 6**

## **THE EFFECT OF ALTERED MECHANICS ON LOWER LIMB OUTPUT DURING CYCLING**

### **Introduction**

The mechanical constraints imposed by the skeletal system on muscle function in combination with the physiological properties of the muscles and a neural control system will determine how muscle activation is coordinated. This involves muscle contraction to generate the mechanical energy at individual joints and the transfer of energy to the distal limb segment to meet the mechanical requirements of a locomotor task. Therefore, altering the mechanics of a task will influence muscle coordination and joint kinetics.

Cycling provides a unique research environment that allows for the manipulation of rider position, thus influencing the mechanics of the rider/bicycle system and output of muscles within the lower limb. In particular, output from the intact triceps surae may be influenced using two different perturbations. One perturbation is to move the cycling cleat to a more posterior position, bi-laterally, on the cycling shoe (Bi-CLEAT). This will reduce the moment necessary to stabilize the ankle and therefore reduce output from the triceps surae (Ericson et. al., 1985, Van Sickle & Hull, 2007, Childers & Gregor, 2008) without limiting ankle motion.

A second method would be to limit ankle motion, bi-laterally, using an Ankle Foot Orthosis (Bi-AFO). This device bypasses the ankle joint by suspending the shank section from the pedal via an aluminum frame and a molded plastic interface. This type of AFO design is unique because it requires energy to be transferred through the device in order to pedal the bicycle bypassing the ankle joint. In order to effect reaction forces at the foot/pedal interface, energy generated proximally must be transmitted through the soft tissue of the shank and into the AFO. Tissue deformation in combination with

movement of the shank within the AFO should result in an energy loss in the transfer of energy from the anatomical joint to the device. A strategy to perform this task with an external device should include a method to contend with the mechanics of the interface as well as energy losses associated with structures between the skeleton and the AFO.

The use of these two perturbations allow for a spectrum of altered mechanical demands by first limiting the contribution made by the muscles controlling the ankle joint via changing the cleat position (Bi-CLEAT) and then bypassing the ankle joint and requiring the cyclist to manipulate the pedal via the interface between the AFO and the shank (Bi-AFO).

The purpose of this research was to examine the contribution of altered task mechanics in intact cyclists by 1) changing the position of the foot relative to the pedal and 2) replicating the interface mechanics of a trans-tibial prosthesis using a custom fabricated AFO to test the general hypothesis; **an external device requiring the user to control the pedal via an interface at the shank and utilized by Intact cyclists will mimic the mechanics of cycling with a prosthesis.** Specific hypotheses addressed include; 1) muscle activity in the triceps surae will decrease in the Bi-CLEAT and Bi-AFO conditions; 2) kinetic output of the knee joint will increase at the top and bottom of the pedal stroke to aid in limb transition in the Bi-CLEAT and Bi-AFO conditions; and 3) the increase in knee joint output will be greatest in the Bi-AFO condition.

## Methods

In-depth discussions of the general methods are presented in Chapter 3 and are briefly summarized here to re-iterate what methods are specific to this hypothesis.

### Subjects and load conditions

A group of eight male recreational cyclists with intact lower limbs ( $82.0 \pm 12.5$  kg,  $1.82 \pm 0.05$  m,  $33.6 \pm 8.8$  yrs) were recruited for this study. The subjects pedaled at a

constant torque of 15Nm at 90 rpm (~150 watts). Pedaling kinetics (Broker & Gregor 1990), limb kinematics (Peak Performance, Vicon Motion Systems, Oxford, UK) and surface EMG (Myosystem 1400L, Noraxon USA Inc., Scottsdale AZ) were used to address the specific hypotheses. Surface EMG was collected bi-laterally on the rectus femoris (RF), vastus medialis (VM), long head of the biceps femoris (BF), gastrocnemius (GAS), soleus (SOL) and the tibialis anterior (TA).

Muscle onset, offset and peak EMG magnitude were determined via Matlab software. This software outputs timing parameters, e.g. onset of activity, based on a threshold of 20% of peak magnitude (Baum & Li, 2003). This method would occasionally output more timing marks than necessary. Therefore each of the 288 datasets were visually inspected and verified.

Some muscles are known for “double bursting” (Ryan & Gregor 1992). Two peaks have been reported for the tibialis anterior, biceps femoris long head, gastrocnemius and rectus femoris muscles. When this occurred, the onset of the first peak was considered onset of the muscle and offset of the second peak was considered the offset of the muscle.

### **Bi-CLEAT condition**

The cycling cleat was placed bi-laterally at 30% the distance between the ankle joint and the standard cleat position (Figure 41) (Bi-CLEAT). The distance is similar to a position that minimized tricep surae muscle activity (Childers & Gregor 2008) and this position was similar to the location of the cycling cleat relative to the ankle joint in the AFO condition. The cycling shoes were modified to allow a plate to be screwed into the bottom of the shoe. The plate moved the cleat posteriorly and inferiorly (Figure 42) in order to maintain a constant effective leg length similar to the AFO condition (see Chapter 3; Methods).

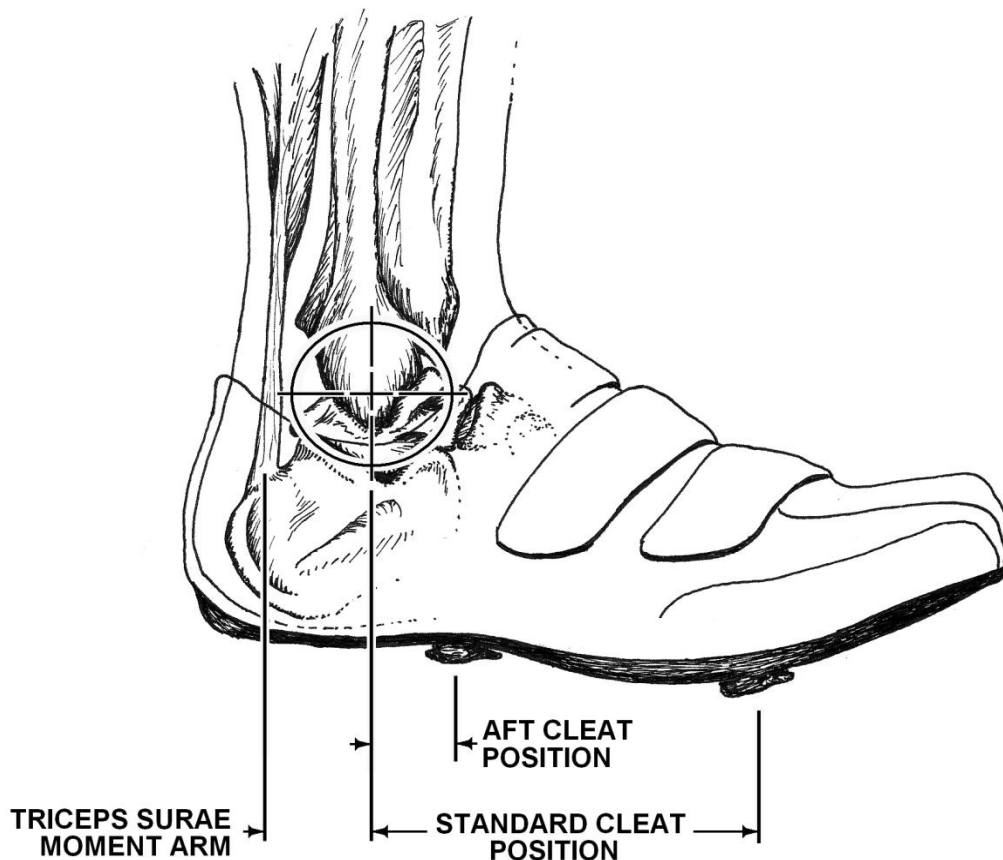


**Figure 41 - Diagram showing the two different cleat positions used for the control condition (standard position) and the Bi-CLEAT condition (aft position) and the effect on the moment arm at the ankle joint.**



**Figure 42 - The plate added to the bottom of the cycling shoes to allow a posterior cleat position. The plate also offset the cleat inferiorly to maintain a similar effective leg length.**

### **Bi-AFO condition**

An Ankle Foot Orthosis (AFO) (Figure 43) was designed and fabricated to simulate the interface mechanics of a prosthesis with an intact cyclist. The AFO consisted of an anterior and a posterior thermoplastic shell and shaped to conform to a human shank. An aluminum frame extended distally from the posterior shell to an aluminum plate. The cycling cleat was mounted to the aluminum plate.

The cleat location was underneath the longitudinal arch of the subject's foot. In order to maintain the same effective leg length (Figure 43) as when the cleat was placed at the first metatarsal head, the plate was approximately 3 cm lower than the bottom of the foot (in a neutral position). This allowed the subject to relax and allow the foot to plantarflex into a comfortable position. A piece of adhesive tape was then wrapped

around the foot to minimize foot movement due to the inertial forces of pedaling (Figure 43). The design of this AFO required the user to control the pedal via the interface between the shank and the shell of the AFO similar to the interface between the residual limb and the prosthetic socket.

The mass, center of mass (COM) location and moment of inertia (MOI) of the different limb segments distal to the knee joint were calculated to improve the calculation of joint moments (Table 17). The COM and MOI of the AFO was recalculated for the knee joint for each subject because of limb length differences between subjects. The COM of the AFO was proximal to the ankle joint (Figure 44).



**Figure 43 - Subject wearing the AFO on the bicycle to demonstrate the cleat position as well as the relaxed position of the foot. Adhesive tape was used to minimize movement of the forefoot due to inertial forces during pedaling. An additional reflective marker was added to calculate ankle joint kinematics. Note- the visible gap between the bottom of the foot and the AFO in the contralateral limb.**

**Table 17 - Mass, center of mass location and moment of inertia calculations for the lower limb. Center of mass is measured along a line going from the proximal to distal joint center.**

	Mass (kg)	Center of mass location (cm)	Moment of Inertia (kg cm <sup>2</sup> )	Joint center used for COM and MOI
Shank + Foot	$5.7 \pm 0.5$	$30.5 \pm .02$	$725 \pm 170$	Knee
AFO	0.80	14.7	71	Top of the device
Shank + Foot + AFO	$6.5 \pm 0.52$	$28.6 \pm 1.6$	$796 \pm 170$	Knee

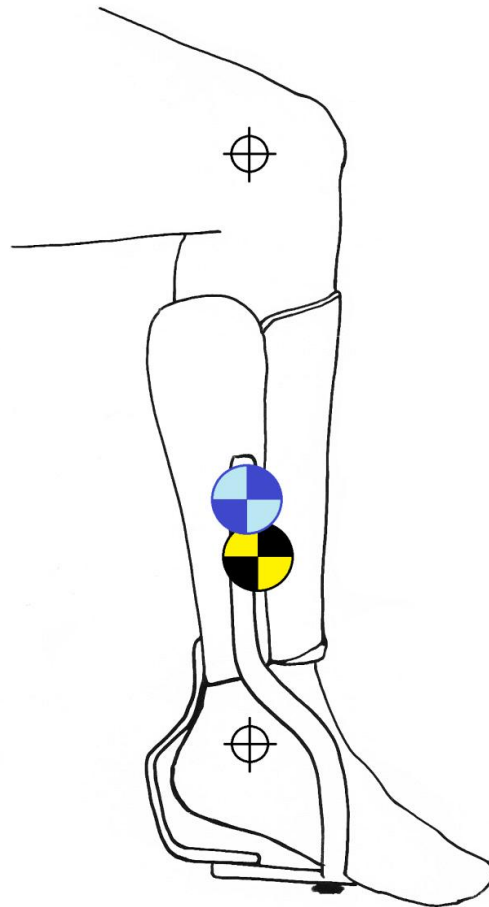


**Figure 44 - Diagram showing the location of the AFO center of mass (light and dark blue circle) and the shank + foot section center of mass (yellow and black circle).**

## Statistical Analysis

Paired T-tests were used to evaluate differences between the dominant and non-dominant limbs within each condition. If no difference existed, it would be considered appropriate to combine data from the dominant and non-dominant limb to create a composite limb effectively doubling the number of limbs per condition for the analysis.

A repeated measures ANOVA with a Bonerferroni Post-Hoc was used to test significance ( $p < 0.05$ ) across the three conditions (control, Bi-CLEAT, and Bi-AFO) for muscle onset, peak and offset.

## Results

### Between Limb Differences

Pedaling asymmetries did not vary significantly between conditions (Table 18). In addition, there were no significant differences between the dominant and non-dominant limbs within each condition in all variables tested for timing and magnitude in joint kinetics, pedal kinetics, limb kinematics, and muscle activity. **Therefore, data for the dominant and non-dominant limbs were combined into one larger dataset.** The group averages presented includes data from all 16 limbs tested (8 subjects X 2 limbs).

**Table 18 – Pedaling asymmetries in work and force about the crank spindle expressed as a percent difference between limb and represents the group average of eight subjects  $\pm$  1 standard deviation.**

Condition	Work Asymmetry (%)	Force Asymmetry (%)
Control	4.8 $\pm$ 3.5	3.6 $\pm$ 2.8
Bi-CLEAT	9.2 $\pm$ 4.8	3.2 $\pm$ 3.0
Bi-AFO	5.5 $\pm$ 4.7	4.2 $\pm$ 2.4

## **Limb Kinematics**

The location of the cycling cleat relative to the ankle joint was calculated to verify the location was held constant across the Bi-CLEAT and Bi-AFO conditions (Table 19). The distance between the knee center and the spindle center (effective limb length) when the ankle was in a neutral position was held constant in all conditions. Holding this constant alters the geometric relationship between joints by making the knee joint more extended yet should hold knee joint range of motion (ROM) constant across conditions with a minimal effect on the hip joint predicted using a limb kinematic model (Childers et al., 2010). The knee joint was more extended in the Bi-CLEAT and Bi-AFO conditions compared to the control condition and were more extended compared to the Bi-CLEAT and Bi-AFO conditions (Figure 45). However, there were no significant differences between conditions in knee joint ROM. The hip joint was significantly more flexed in the Bi-AFO condition compared to controls but not between the Bi-AFO and Bi-CLEAT conditions (Figure 45). The hip joint did demonstrate increasing ROM from the control to the Bi-CLEAT and Bi-AFO conditions. The foot was allowed to relax in a plantarflexed alignment during the Bi-AFO condition and was reflected by a significantly greater average ankle angle compared to the control and Bi-CLEAT conditions (Figure 45). The motion of the foot was restricted in the Bi-AFO condition and this was supported by a significantly smaller ROM compared to either the control or Bi-CLEAT conditions (Figure 45). The ankle joint maintained a similar alignment and ROM between the control and AFO conditions (Figure 45).

Angular motion between the shank and the AFO was calculated based on marker location data (Figure 46) and had an average ROM of  $6.6 \pm 1.3^\circ$ . The shank was parallel to the AFO centerline at the bottom of the pedal stroke and angled relative to the AFO at the top of the pedal stroke so that the knee joint was in a more extended position (Figure 46). The movement of the center of rotation of the shank section relative to the AFO was larger than the movement of the ankle joint (Figure 47). The instantaneous center of

rotation did move for the ankle joint and the shank section within the AFO the movement yet this movement is small (note scale in Figure 47). The average center of rotation of the shank section was ~1.2 cm distal to the ankle joint. The average center of rotation of the shank section relative to the AFO is the equivalent to having the pseudo joint between these two segments.

**Table 19 – Cleat location as a percentage of the distance between the ankle joint center and the standard cleat position measured parallel to the pedal surface. Data represents the group average of 16 limbs  $\pm$  1 standard deviation.**

Condition	Cleat Location (% relative to control)
Bi-CLEAT	$30 \pm 5.2$
Bi-AFO	$36 \pm 10$

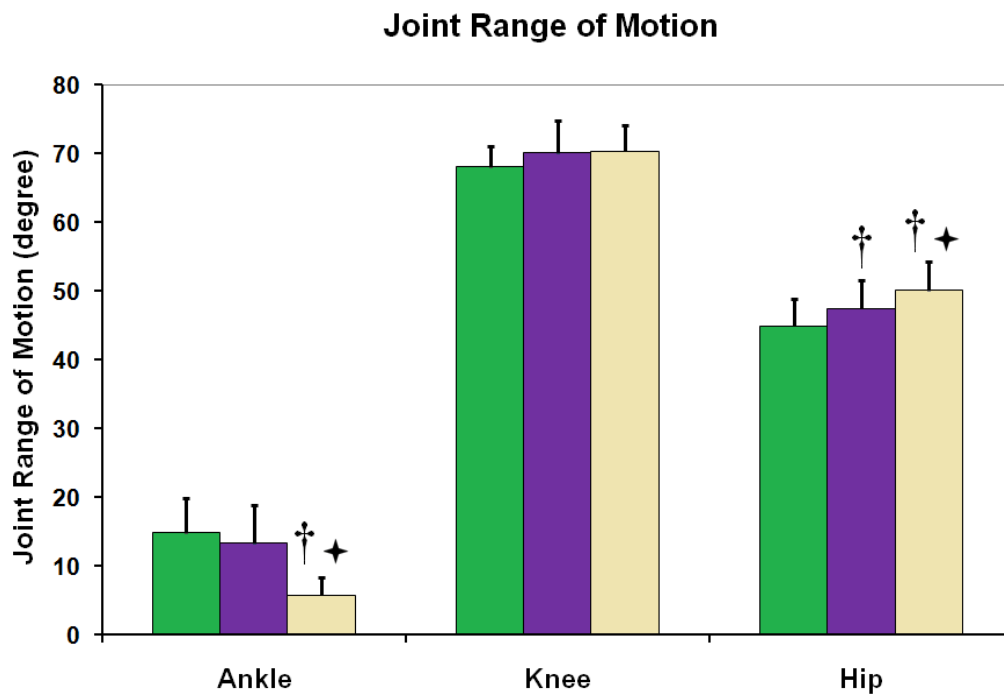
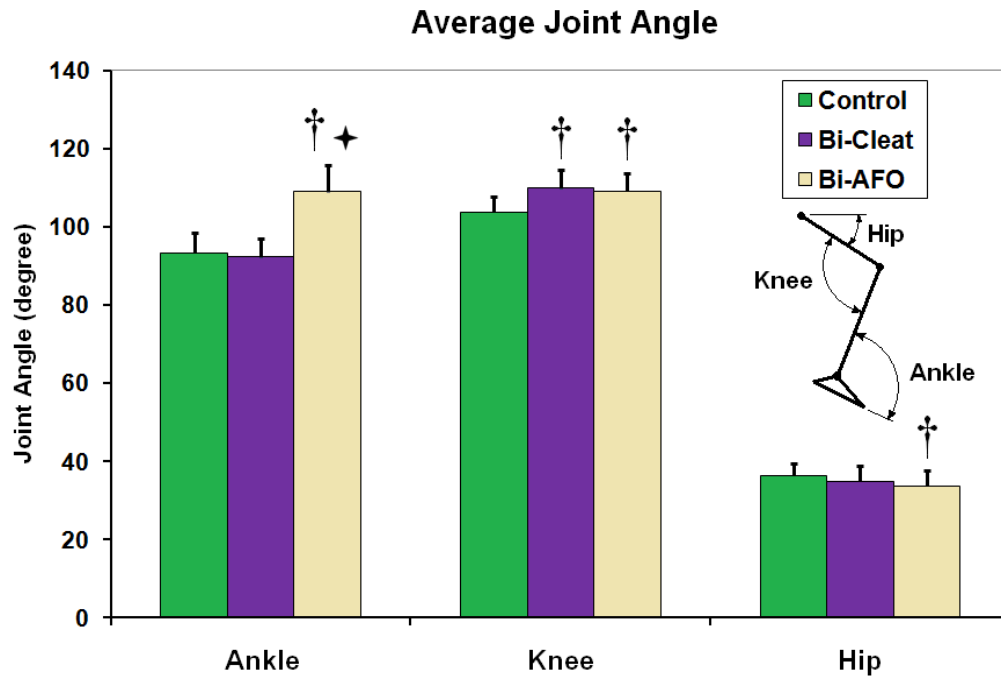
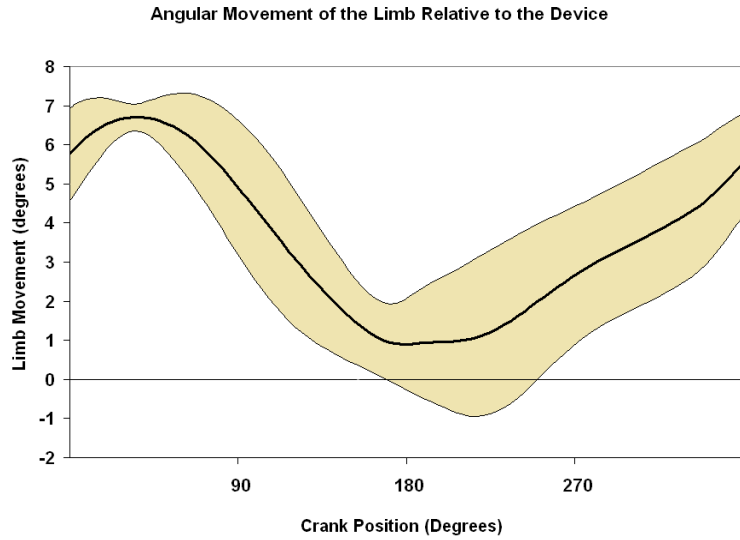
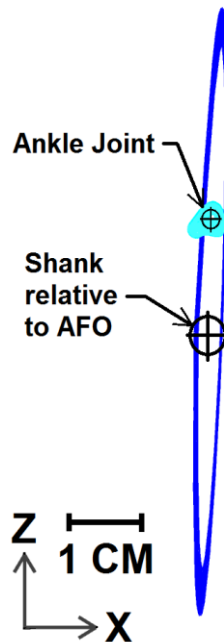


Figure 45 - Average joint angle and range of motion. † = stat. sig diff. from the control condition. ✦ = stat. sig diff. from Bi-CLEAT condition.



**Figure 46 - Angular motion between the AFO and the shank. Data represents the group average of 16 limbs  $\pm$  1 standard deviation.**



**Figure 47 - Movement of the center of rotation throughout the crank cycle of the shank section (blue) and the ankle joint (cyan) relative to the AFO. The shaded region represents  $\pm$  1 standard deviation of the mean. The average center of rotation for the shank section and the ankle joint is displayed as a cross-hair and the shank section is effectively pivoting within the AFO approximately 1.2 cm distal to the ankle joint. The proximal-distal movement of the ankle joint relative to the AFO provides a good approximation of “pistoning” within the device and was  $\sim$ 4 mm**

## Pedaling Kinetics

Peak torque magnitude was significantly less in the Bi-AFO condition compared to control and Bi-CLEAT conditions (Table 20). Timing relative to top dead center (TDC) demonstrated no significant differences between conditions (Table 20). The Bi-CLEAT and Bi-AFO conditions demonstrated similar crank torque profiles including an increase in torque at the bottom of the pedal stroke and greater average negative torque during the recovery phase compared to the control condition (Figure 48). The Bi-AFO condition also demonstrated greater average crank torque through the top of the pedal stroke compared to the Bi-CLEAT and control conditions (Figure 48).

**Table 20 – Timing of Peak Torque in degrees past TDC  $\pm$  1 standard deviation. † = stat. sig diff. from the control condition. ✦ = stat. sig diff. from Bi-CLEAT condition.**

Condition	Peak Torque (Nm)	Timing of Peak Torque (degrees)
Control	37 $\pm$ 6.6	95 $\pm$ 8.2
Bi-CLEAT	38 $\pm$ 7.4	85 $\pm$ 11
Bi-AFO	33 $\pm$ 4.8 ✦ †	89 $\pm$ 7.4

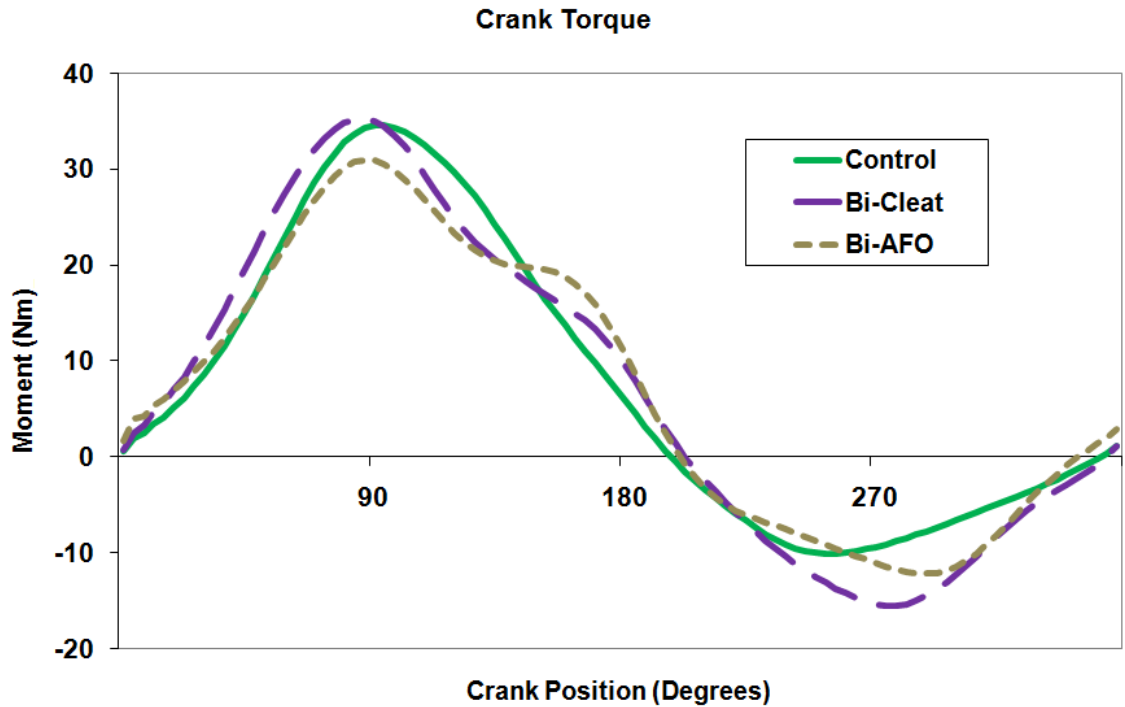


**Figure 48 - Torque about the crank spindle for the conditions tested.**

### **Joint Kinetics**

The hip, knee and ankle joint moments showed marked differences, in particular at the ankle and hip early in the pedaling cycle, between conditions (Figure 50). In particular, the Bi-CLEAT condition demonstrated a greater hip extension moment in the first 180° of crank rotation while the Bi-AFO showed a large reduction in the hip extension moment compared to the control condition (Figure 49). The average hip extensor moment was greatest in the Bi-CLEAT condition with no significant differences noted between control and Bi-AFO conditions (Table 21). However, the peak hip extension moment was greater (Table 22) and occurred later (Table 23) in the Bi-CLEAT and Bi-AFO conditions compared to control.

The average (Table 21) and peak (Table 22) knee extensor moment was significantly higher in the Bi-AFO compared to the Bi-CLEAT and control conditions. The peak flexor moment in the Bi-CLEAT and Bi-AFO conditions were significantly greater than control (Table 6) and occurred later in the pedaling cycle (Table 23).

The average ankle extensor moment increased from the Bi-AFO to the Bi-CLEAT and control condition (Table 21). The peak moment occurred progressively later from the Bi-CLEAT to the control to the Bi-AFO (Table 23).

**Table 21 – Average Joint Moment.** † = stat. sig diff. from the control condition. ✦ = stat. sig diff. from Bi-CLEAT condition.

Condition	Average Ankle Extensor Moment (Nm)	Average Knee Extensor Moment (Nm)	Average Knee Flexor Moment (Nm)	Average Hip Extensor Moment (Nm)
Control	19.5 ± 5.2	13.2 ± 5.3	20.4 ± 3.4	42.7 ± 12
Bi-CLEAT	14.5 ± 3.7 †	12.8 ± 5.1	21.7 ± 3.4	51.2 ± 14.5 †
Bi-AFO	7 ± 2.2 ✦ †	27.0 ± 7.7 ✦ †	23.2 ± 6.1 †	38.8 ± 9.4 ✦

**Table 22 – Magnitude of Peak Moments. † = stat. sig diff. from the control condition. ★ = stat. sig diff. from Bi-CLEAT condition.**

Condition	Peak Ankle Extensor Moment (Nm)	Peak Knee Extensor Moment (Nm)	Peak Knee Flexor Moment (Nm)	Peak Hip Extensor Moment (Nm)
Control	39 ± 9.3	24 ± 9.8	42 ± 9.6	76 ± 21
Bi-CLEAT	26 ± 5.5 †	22 ± 7.4	56 ± 10 †	90 ± 30 †
Bi-AFO	19 ± 5.6 ★	48 ± 14 ★ †	62 ± 16 †	96 ± 30 †

**Table 23 – Timing of Peak Moments. † = stat. sig diff. from the control condition. ★ = stat. sig diff. from Bi-CLEAT condition.**

Condition	Timing of Peak Ankle Extensor Moment (degrees)	Timing of Peak Knee Extensor Moment (degrees)	Timing of Peak Knee Flexor Moment (degrees)	Timing of Peak Hip Extensor Moment (degrees)
Control	129 ± 30	69 ± 16	170 ± 10	147 ± 20
Bi-CLEAT	96 ± 31 †	65 ± 15 †	171 ± 13	173 ± 15 †
Bi-AFO	176 ± 13 ★ †	70 ± 11 ★	171 ± 12	174 ± 10 †

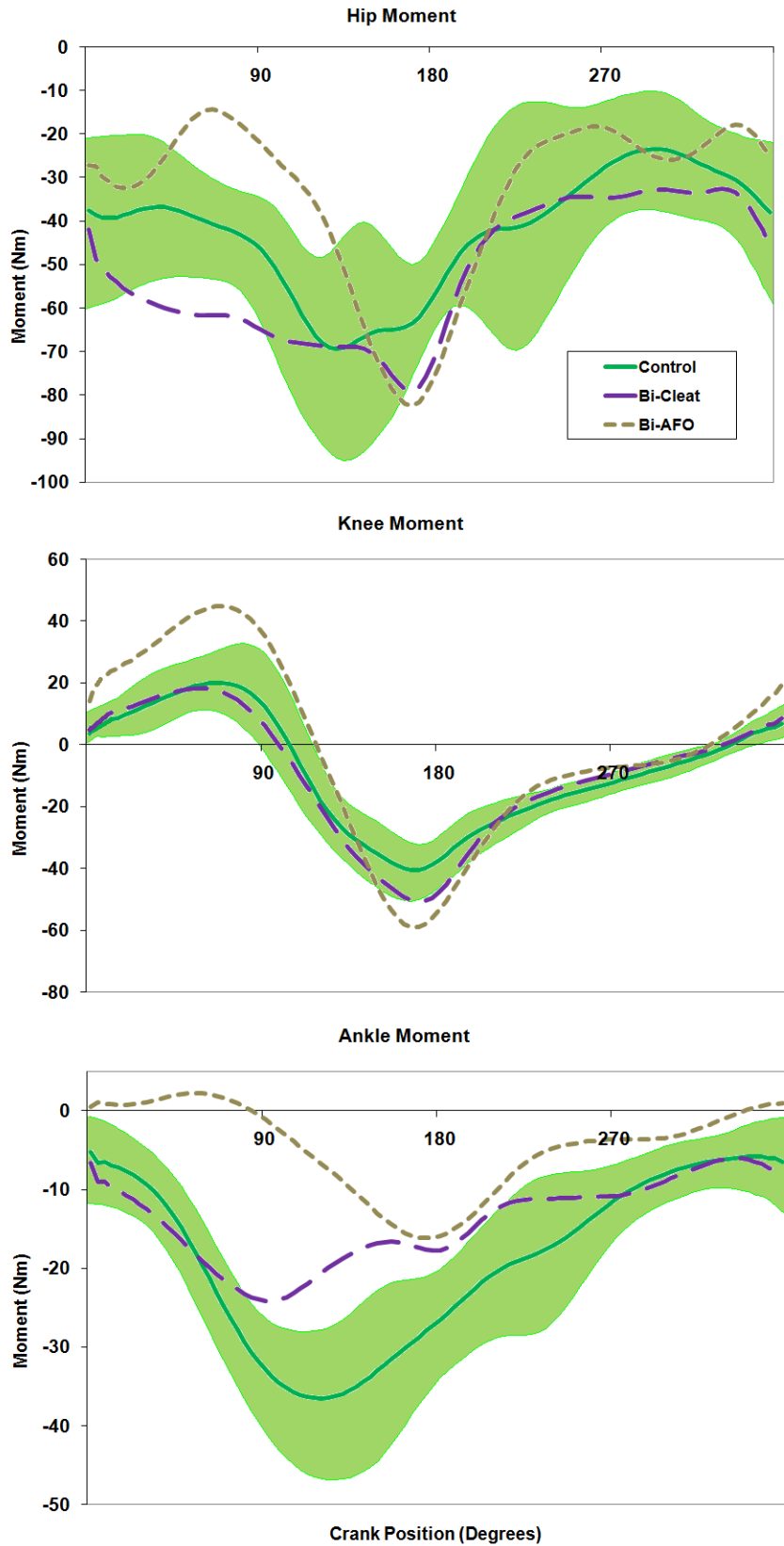


Figure 49 - Joint moments for the control, Bi-CLEAT and Bi-AFO conditions

## **Muscle Activation**

The Bi-CLEAT and Bi-AFO conditions generally displayed similar trends in all muscles except the TA (described later). Activation in the rectus femoris muscle (RF) did not show any significant shifts in timing of onset, peak activation and offset and no changes in burst duration (Figure 50) and average EMG activity (Figure 51). Activity of the RF was attenuated from ~250 – 330° of crank rotation in the Bi-AFO and Bi-CLEAT conditions compared to control (Figure 50).

The long head of the biceps femoris muscle (BF) demonstrated significant shifts in the onset of activity during the Bi-AFO condition compared to control (Figure 51). The onset of the BF during the Bi-CLEAT demonstrated a shift to earlier in the crank cycle yet the higher variability in these data precluded achieving any statistical significance. The burst duration of the BF was significantly greater than control in both Bi-CLEAT and Bi-AFO conditions (Figure 50). The BF during the Bi-CLEAT and Bi-AFO demonstrated a trend to later offset yet did not achieve statistical significance (Figure 50). BF peak activation was lower in the Bi-CLEAT and Bi-AFO conditions (Figure 50). The combination of increased burst duration and lower peak kept the average activation the same in Bi-CLEAT and Bi-AFO conditions relative to the control (Figure 51).

Activation in the vastus medialis muscle (VM) did not show any significant shifts in timing of onset, peak activation and offset and no changes in burst duration (Figure 50) and average activity (Figure 51). Activity of the VM during the Bi-AFO condition demonstrated prolonged activity after 90° of crank rotation (Figure 51) yet this did not produce statistical significance in the offset (Figure 50) due to variability across subjects.

The gastrocnemius (GAS) muscle showed significant reduction in activity in the Bi-CLEAT and Bi-AFO conditions compared to control (Figure 51) and muscle onset

was delayed (Figure 50). The bi-modal activation pattern was maintained across all conditions yet the first peak was significantly attenuated in the Bi-CLEAT and Bi-AFO conditions (Figure 50). The reduction of the first peak resulted in both peaks being of similar magnitude increasing the number of times the second peak would be selected as the peak vs. the first peak. Therefore, neither the first nor the second peak was consistently the highest resulting in increased variability in peak GAS timing (Figure 50) when the group mean was computed. The timing of peak GAS activity displayed in Figure 50 is a result of the averaging of these two separate and distinct peaks and not necessarily a real change in muscle timing.

The soleus (SOL) muscle showed significant reduction in activity in the Bi-CLEAT and Bi-AFO conditions compared to control (Figure 51) and muscle onset was delayed (Figure 50).

The tibialis anterior (TA) muscle activity was significantly increased in the Bi-CLEAT compared to control (Figure 51) with no differences in timing (Figure 50). The second peak in TA activity was attenuated in the Bi-AFO condition compared to control and Bi-CLEAT conditions (Figure 50).

**Timing of Muscle Activity  
Control, Bi-Cleat and Bi-AFO Conditions**

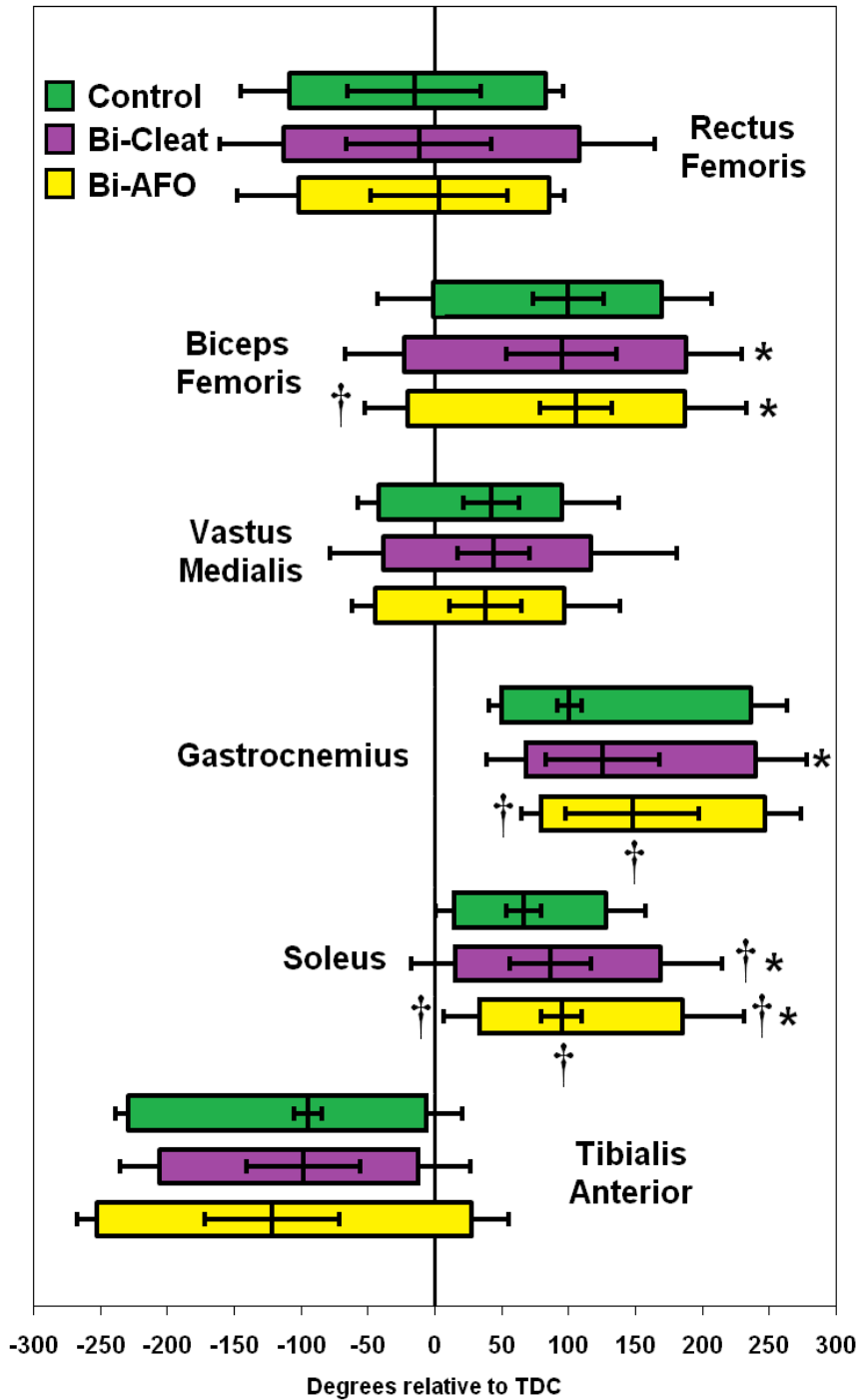


**Figure 50 - Muscle onset, peak activation and offset for the conditions tested. † = stat. sig diff. from the control condition. \* = stat. sig diff. from the control condition regarding burst duration.**

### Muscle Activity in the Lower Limb

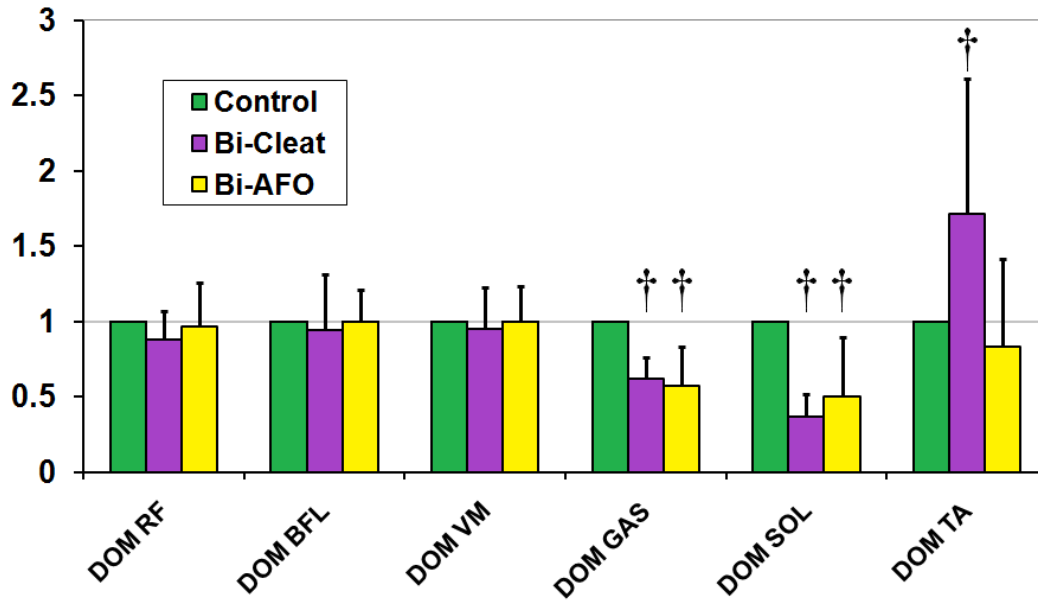


Figure 51 - Average activity of muscles in the lower limb relative to the control condition. † indicates significant difference from the control condition.

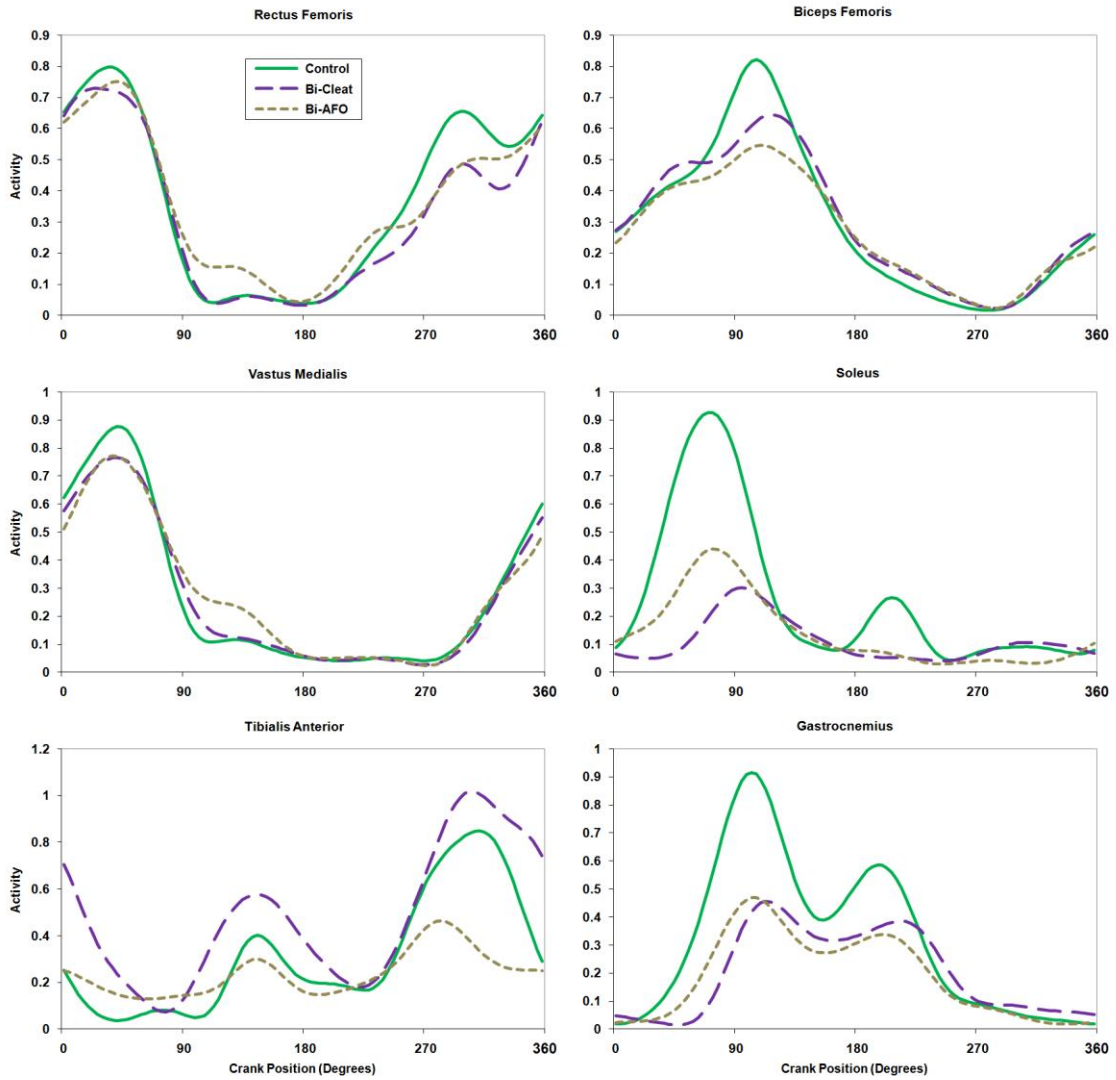


Figure 52 - Muscle activation during the crank cycle.

## Discussion

### Bi-Cleat Condition

The most significant finding from these experiments was the changes made utilizing more of a hip strategy, i.e. increased hip extensor moments, in response to changes in cleat position. This shift to a hip based strategy was related to significant decreases in muscle activation in the SOL and GAS muscles (Figures 51 & 52) during the Bi-CLEAT condition compared to the control condition. Similar reductions in SOL and GAS activity have been reported previously (Ericson et al., 1985; van Sickle & Hull, 2007; Childers & Gregor, 2008). The ankle joint serves primarily in an energy transfer capacity in cycling and muscle activity in SOL and GAS is related to stabilizing the ankle joint and contributing to the ankle extensor moment during propulsion (Gregor et al., 1991). The moment arm between the ankle joint and the pedal spindle was reduced during the Bi-CLEAT condition (Figure 41), reducing the ankle extensor moment required for stabilization (Figure 49) and reducing the need for SOL and GAS activity. Likewise, TA activity is necessary at the top of the pedal stroke to resist ankle extension and allow for the iliopsoas and rectus femoris to redirect forces superiorly and anteriorly (Ting et al., 1999). The TA contributes to the ankle moment and as the cleat moves from the standard location to the Bi-CLEAT location, the TA moment arm is reduced. The TA must then increase activity in order to have an equal affect on the net ankle joint moment during the Bi-CLEAT condition. This increase in activity is shown in these data (Figures 51 & 52) and reported previously (Childers & Gregor, 2008).

The hip extensor moment increased for the Bi-CLEAT condition (Figure 49) and the BF increased in burst duration (Figure 50). The increase in BF burst duration would serve to transfer energy for a longer period of time toward the hip joint (Gregor et al., 1985) and explain, in part, the increased the hip extension moment during the first 90° of

crank rotation. The increase in BF duration would also serve to increase the knee flexor moment from 90 – 180° (Gregor et al., 1985) and increase crank torque through the bottom of the pedal stroke; an outcome observed in these data (Figures 48). A posterior cleat position effectively neutralizes the ankle joint's ability to contribute to cycling thus reducing the behavior of this limb/bicycle system to a four-bar linkage which can be effectively driven by the hip joint and is suggested as an explanation as to why a hip based strategy was used by the motor system. The primary responsibility of muscles crossing the ankle joint is to stabilize the ankle (Gregor et al., 1991). The use of the Bi-CLEAT condition, i.e. the mechanics of the Bi-CLEAT intervention, did not interfere with this function, yet the ankle has been shown to contribute to propulsion of the crank (Broker & Gregor 1994) and the GAS has been described as important for accelerating the limb through the bottom of the pedal stroke (Neptune et al., 2000). These responsibilities may have been compromised by the change in cleat position and this would require other joints to compensate, e.g. the hip joint. However, precisely why, this hip-based strategy was used versus, for example, increasing knee extensor moment, to overcome the challenges imposed by the mechanics of the Bi-CLEAT condition cannot be determined with these data but may provide a basis to understand control strategies in future research.

### **Bi-AFO Condition**

The most significant finding from these experiments using an AFO is that the joints in the lower extremity, collectively, seem to change their behavior to use the external device to overcome the resistance at the crank. For example, the Bi-AFO condition demonstrated very different knee and ankle moment profiles during the first 180° of crank rotation (Figure 49). This type of AFO design required energy to be transferred through the device in order to pedal the bicycle and bypasses the ankle joint. In order to affect force at the pedal, energy generated via the interaction of muscle

activation and the skeleton must be transmitted through the soft tissue of the shank and into the AFO. Some the energy generated at the joints via muscle contraction will be lost to tissue deformation as energy must be transmitted through these tissues before it enters the AFO and eventually effects the pedal. Therefore, the increase in knee joint moment was necessary to 1) contend with energetic losses associated with energy transfer through the soft tissue of the shank, and 2) control the shank/AFO interface and increase the effective force through the top of the pedal stroke.

The ankle moment was close to zero during the power phase. The ankle joint is located close to the instant center of rotation of the shank relative to the AFO thus making it, in effect, the shank/AFO pseudo joint (SAP). The SAP is not enclosed by the AFO interface and thus a moment at this joint cannot directly influence forces developed at the pedal. An ankle flexor/extensor moment would not benefit performance because the ankle joint is suspended in the AFO and does not influence force at the pedal.

Manipulation of the shank within the interface is another control parameter necessary for tool use. The shank moved within the AFO (Figure 46) and the average center of rotation (COR) was just distal to the ankle joint center (Figure 47). The shank relative to the AFO is flexed through the top of the pedal stroke and starts to extend (become more parallel with the AFO) after  $\sim 45^\circ$  of crank rotation (Figure 46). The hip moment also demonstrates a reduction in magnitude during this time (Figure 49). The shank/crank alignment during this region of the pedal stroke is generally parallel and is a common “region of difficulty” for cyclists with trans-femoral amputations (unpublished observations). A hip extension moment during this phase tends to increase forces about the longitudinal axis of the shank (normal to the pedal surface) and decrease the effective force about the crank resulting in a reduction in propulsion. Reducing the hip moment in combination with an extensor moment about the knee joint would help the limb transition through the top and into the power phase while allowing the shank to extend relative to the AFO. Therefore, reduction in magnitude of the hip extensor moment in the power

phase would benefit task performance by aiding propulsion at the pedal and controlling motion between the shank and the AFO.

The BF muscle demonstrated increased burst duration during the Bi-AFO condition (Figure 50). This increase in BF did not correspond with an increase in hip extensor moment as seen in the Bi-CLEAT condition; however, the BF has additional responsibilities in the Bi-AFO condition because it is able to effect control of the shank within the AFO. The increased burst duration in the BF could be related to controlling the AFO interface by increasing the knee flexor moment at the bottom of the pedal stroke (Figure 49) and aid in the shank becoming more parallel with the AFO (Figure 46).

The hip moment demonstrates trend toward a reduction in the extensor moment from  $\sim 200 - 270^\circ$  (Figure 49). A reduction in the magnitude of the hip extension moment during this phase would serve to lower forces resisting the upward motion of the pedal and AFO thus slowing flexion between the shank and the AFO. The reduction of the hip joint extensor moment during this phase is likely due to activity of the iliopsoas (IP) muscle. The hip joint is extended during this phase placing the IP in the suitable biomechanical position to affect the hip joint moment, it has been reported to be active during this region in intact cyclists (Juker et al., 1998).

This concept of interface control as demonstrated in the Bi-AFO condition has been demonstrated in the upper extremity regarding the use of tools (Arbib et al., 2009; Mizelle et al., in press). Similar to upper extremity tool use, the interface between the shank and the tool (AFO) must be controlled to perform this locomotor task. The results of this experiment demonstrate control of the shank/AFO interface by the motor system is unrelated to cleat placement. In particular, the motor system altered output at the knee and ankle joint. Previous research has focused on changes in muscle activity in the upper extremity (Kornecki et al., 2001; Laursen et al., 2003; Dong et al., 2007; Fischer et al., 2009). This research builds on earlier work and demonstrates the motor system has altered the strategy of joint moments to produce torque about the crank spindle similar to

the Bi-CLEAT and control conditions (Figure 48). Future research should be necessary to model the how energy is dissipated through the soft tissues, demonstrate how the AFO is being energized via the combination of joint moments presented here, and how this relates to task performance. This information may also improve orthosis design because it allows one to predict how the system may respond due to the interface mechanics, similar to how interface design affects the performance of tool use in the upper extremity.

In conclusion, these results demonstrate changes in joint kinetics and muscle activity in response to altered cleat placement (Bi-CLEAT condition) and an altered mechanical interface (Bi-AFO). The center of rotation for the AFO was near the ankle joint, the limb movement within the interface demonstrated similarities to use of a prosthesis in an amputee indicating the device may be a reasonable method to simulate the mechanics of cycling with a prosthesis. The additional changes in knee and ankle joint and pedaling kinetics associated with the AFO indicate the need to control the shank/AFO interface as well as the endpoint. Similar to the use of a handtool, the motor system must manipulate the kinetics of the joints controlling the interface required for successful task performance. Therefore, the use of an external device placed on the lower extremity could be looked at in the same context as tool use in the upper extremity. Future research should focus on modeling how energy may be transmitted from the musculoskeletal system via the soft tissues in the limb and into the AFO. Additional research would be useful to compare cycling with a uni-lateral AFO to cycling with a trans-tibial amputation because the mechanical constraints of the AFO appear to offer a reasonable simulation of the limb/prosthesis mechanics.

## **CHAPTER 7**

# **THE EFFECT OF INTERFACE MECHANICS BETWEEN THE LOWER LIMB AND AN EXTERNAL DEVICE DURING CYCLING**

### **Introduction**

Locomotion is a complex motor task requiring integration of physiological systems in combination with the mechanics of the environment. Locomotion becomes more complex when the distal limb segment is no longer the foot and the person must utilize a mechanical device, e.g. a tool, between the distal limb segment and the environment e.g. a person with a uni-lateral amputation using a prosthesis. The distal limb segment i.e. residuum must now interact with the environment via a prosthetic socket and the mechanical properties of the interface as well as the prosthesis will affect motor control.

Previous research utilized cycling as the locomotor model to understand control of interface mechanics between the lower limb and an external device in both uni-lateral amputees using a prosthesis (see Chapter 2) and intact cyclists using bi-lateral Ankle Foot Orthoses (AFO) (see Chapter 6). The AFO was developed and tested (see Chapter 6) to simulate the mechanics of a cyclist with an amputation utilizing a prosthesis for locomotion by requiring the user to manipulate the pedal via an interface on the shank. The AFO simulates the mechanics of a cyclist with an amputation utilizing a prosthesis for locomotion by requiring the user to manipulate the pedal via an interface on the shank. The AFO may not fully simulate the interface mechanics of amputee cycling because the AFO interface is between the ankle and knee joints, the center of mass of the AFO is proximal to the ankle joint (Figure 44) and this allows the shank to generate a force couple about a distance proximal and distal to the COM whereas the residuum ends proximal to the center of rotation of the residuum/prosthesis joint (Table 12).

This AFO was previously applied bi-laterally to better understand the motor system's response to the mechanics of this new limb/device system (see Chapter 6). Results of these experiments indicated changes in motor control in order to 1) control the motion of the limb within the interface and 2) to manipulate joint moments external to the device in order to generate a torque profile about the crank spindle required for task performance.

These results indicate the use of an external device can be viewed in the context of tool use similar to how the upper extremity uses a screwdriver. The distal limb segment must control the orientation of limb segment at the interface as well as generate the mechanical energy within the screwdriver to perform the task at the tool's endpoint. However, it is still unclear if the mechanics of these "lower limb tools" are responsible for the changes demonstrated in individuals with trans-tibial amputation (TTA). Therefore, it is appropriate to compare TTA and individuals with intact lower limbs cycling with an AFO applied uni-laterally.

The purpose of this research was to investigate the strategies used by TTA and intact cyclists using an external device, uni-laterally, during a cycling task to better understand if control of the interface and the device can explain differences between TTA and intact cycling. The general hypothesis addressed was **individuals with and without amputation will modify the control strategy of proximal joints in order to control an external device on the distal limb segment.**

## Methods

In-depth discussions of the general methods are presented in Chapter 3 and are briefly summarized here to re-iterate what methods are specific to this hypothesis.

### Subjects and load conditions

A group of eight male recreational cyclists with uni-lateral trans-tibial amputation (TTA) ( $81.3 \pm 16.1$  kg,  $1.84 \pm 0.09$  m,  $33.7 \pm 10.0$  yrs) and a group of eight male

recreational cyclists with intact lower limbs ( $82.0 \pm 12.5$  kg,  $1.82 \pm 0.05$  m,  $33.6 \pm 8.8$  yrs) were recruited for this study (see Chapter 3; Methods). The subjects pedaled at a constant torque of 15Nm at 90 rpm (~150 watts). The prosthesis used by the TTA group had the cycling cleat placed ~40% of the distance between where the 1<sup>st</sup> metatarsal head and ankle joint used to be (TTA-CLEAT condition). The Intact group pedaled wearing an Ankle Foot Orthosis (AFO) uni-laterally, placed on the subject's non-dominant cycling limb. Limb dominance was determined by which limb produced the greatest torque about the crank spindle and tested prior to the beginning of the experiment. The Intact group used a custom fabricated AFO with the cycling cleat placed in a similar location (Int-AFO condition) and is explained in more detail later in this section. Pedaling kinetics (Broker & Gregor 1990), limb kinematics (Peak Performance, Vicon Motion Systems, Oxford, UK) and surface EMG (Myosystem 1400L, Noraxon USA Inc., Scottsdale AZ) were used to address the hypotheses. Surface EMG was collected bi-laterally on the rectus femoris (RF), vastus medialis (VM), long head of the biceps femoris (BF), gastrocnemius (GAS), soleus (SOL) and the tibialis anterior (TA) with the exception of the TTA group in which SOL and TA EMG could not be collected on the amputated limb.

Onset of muscle activity, offset and peak magnitude of EMG were determined via Matlab software. This software would output timing based on a threshold of 20% of peak magnitude (Baum & Li, 2003). This method would occasionally output more timing marks than necessary. Therefore each of the 184 datasets were visually inspected and verified.

### **Determination of limb dominance within the Intact group**

The Intact group cycled at 15Nm and 90 rpm for approximately two minutes prior to application of EMG electrodes in order to determine limb dominance. Pedal force and pedal position were recorded for 10 seconds during the final minute of cycling. The data

were reduced to calculate the torque produced by the right and left limbs. The dominant limb was defined as the limb that produced the most torque. The dominant (DOM) and non-dominant limbs were recorded and used to determine placement of EMG electrodes. The AFO was applied to the subject's non-dominant limb.

### **Uni-AFO condition**

An Ankle Foot Orthosis (AFO) (Figure 53) was designed and fabricated to simulate the interface mechanics of a prosthesis with an intact cyclist. The AFO consisted of an anterior and posterior thermoplastic shell and shaped to conform to a human shank. An aluminum frame extended distally from the posterior shell to an aluminum plate. The cycling cleat was mounted to the aluminum plate.



**Figure 53 - AFO design to replicate the mechanics of cycling with an amputation in a cyclist with intact limbs.**

The cleat location was underneath the longitudinal arch of the subject's foot. In order to maintain the same effective leg length (Figure 53) as when the cleat was placed at the first metatarsal head, the plate was approximately 3 cm plantar to the plantar aspect of the foot (in a neutral position). This allowed the subject to relax and allow the foot to plantarflex into a comfortable position. A piece of adhesive tape was then wrapped around the foot to minimize foot movement due to the inertial forces of pedaling (Figure 54). The design of this AFO required the user to control the pedal via the interface between the shank and the shell of the AFO similar to the interface between the residual limb and the prosthetic socket. The proximal trimlines of the AFO were approximately at or just distal to the tibial tubercle. The distal trimline was approximately 2 cm distal to the malleoli (Figure 55). A frame fabricated from 20 X 6mm 6061-T651 aluminum section extended distally from the posterior shell to an aluminum plate.



**Figure 54 - Subject wearing the AFO on the bicycle to demonstrate the cleat position as well as the relaxed position of the foot. Adhesive tape was used to minimize movement of the forefoot due to inertial forces during pedaling. An additional reflective marker was added to calculate ankle joint kinematics. Note- this figure was taken during the Bi-AFO condition used in Chapter 6, the AFO was applied uni-laterally to address the hypotheses in this Chapter.**

### **TTA-CLEAT Condition**

The TTA group pedaled at 15Nm and 90 rpm with the cycling cleat moved posteriorly on the prosthetic foot approximately 40% of the distance between the standard cleat location and the prosthetic ankle (Figure 55). This position was based on pilot work performed on intact cyclists demonstrating a minimization of triceps surae activity near this point (Childers & Gregor, 2008) as well as reports of similar cleat positions for cycling prostheses (Gailey & Harsch, 2009). The prosthesis was lengthened to maintain a constant effective cycling prosthetic length (Childers et. al., 2009b).

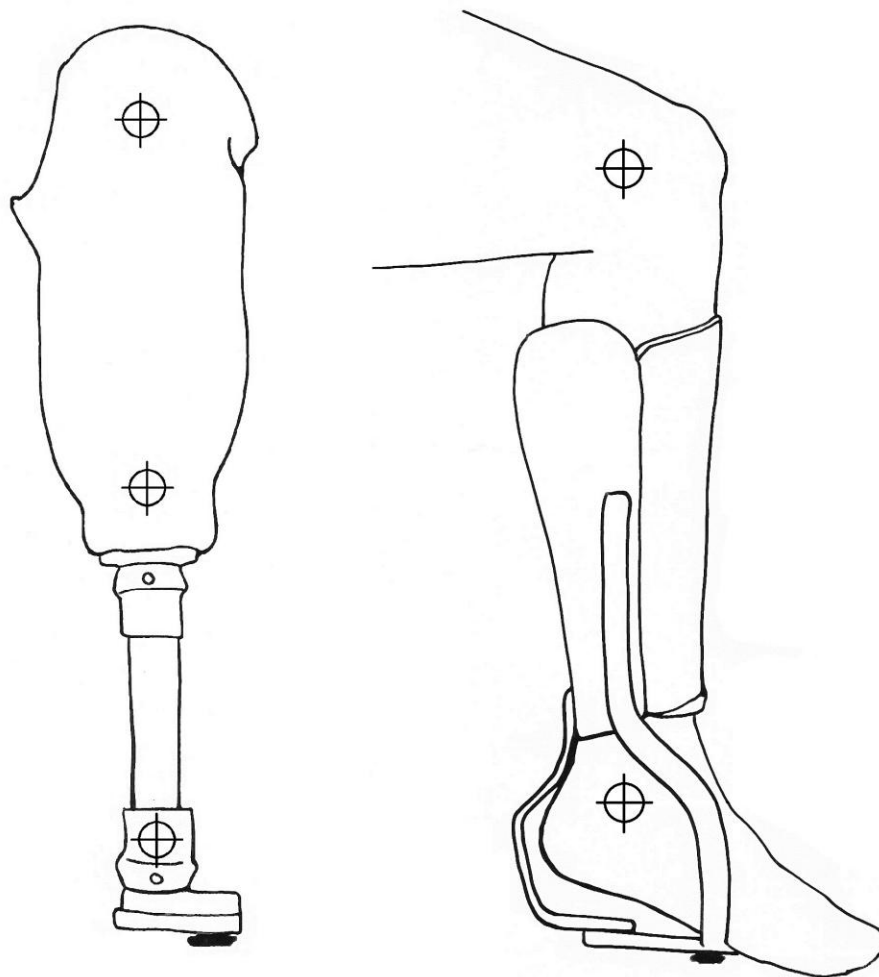


**Figure 55 - Diagrams of both the prosthesis with posterior cleat position and the AFO applied to a lower limb.**

## **Statistical Analysis**

Paired T-tests were used to evaluate differences between the dominant (sound) and non-dominant (amputated) limbs within each group. Independent T-tests were used to evaluate differences between the sound limb in the TTA group and the dominant limb in the Intact group as well as test between the amputated limb in the TTA group and the non-dominant limb (wearing the AFO) in the Intact group. A statistically significant difference existed if  $p \leq 0.05$ .

## **Results**

### **Limb Kinematics**

The location of the cycling cleat relative to the ankle joint was calculated to verify the location was held constant on the prosthesis and AFO (Table 24). The experiment was designed to maintain effective limb length in the prosthesis and AFO. This would alter the geometric relationship between joints by making the knee joint more extended yet should hold knee joint range of motion (ROM) constant within a group (between the dominant and non-dominant limbs). Knee joint ROM was similar between limbs within the Intact or TTA group but the Intact group demonstrated larger knee joint ROM when compared to the TTA group (Table 26). No differences were observed in the average hip joint angle (Table 25). The amputated limb did move through a larger range of hip joint motion, ROM, than did the sound limb within the TTA group (Table 26).

The foot in the Non-DOM limb was allowed to relax in a plantarflexed alignment while using the AFO and was reflected as a significantly greater average ankle angle compared to the DOM limb (Table 25). The motion of the foot was restricted in the AFO and this is reflected in the kinematic data as significantly less ROM compared to the DOM limb (Table 26). The ankle joint of the prosthesis was fixed and this constraint was reflected in a lower ROM compared to the sound limb (Table 26).

Angular motion between the shank and the AFO as well as the residuum and the prosthesis were calculated based on marker displacement (Figure 56) with an average ROM of  $7.7 \pm 5.5^\circ$ . The shank was parallel with the AFO centerline at the bottom of the pedal stroke and angled relative to the AFO so that the knee joint was more extended at the top of the pedal stroke (Figure 55). The ROM between the residuum and prosthesis was  $5.41 \pm 3.1^\circ$  and was not significantly different from the ROM between the shank and AFO.

**Table 24 – Cleat location as a percentage of the distance between the ankle joint center and the standard cleat position measured parallel to the pedal surface.**

Group, Limb	Cleat Location (% relative to control)
TTA-CLEAT, AMP Limb	$40 \pm 18$
Intact, AFO Limb	$40 \pm 8$

**Table 25 – Average Joint Angle.** † = stat. sig diff. from the sound limb. ★ = stat. sig diff. from AFO applied limb.

Group, Limb	Average Ankle Angle (°)	Average Knee Angle (°)	Average Hip Angle (°)
TTA, Sound Limb	$94 \pm 5.2$	$99 \pm 6.2$	$34 \pm 7.3$
TTA-CLEAT, AMP Limb	$96 \pm 2.3$ ★	$109 \pm 6.7$ ★ †	$34 \pm 5.8$
Intact, DOM Limb	$93 \pm 8.1$ ★	$106 \pm 5.0$	$37 \pm 4.0$
Intact, AFO Limb	$106 \pm 3.3$	$111 \pm 5.9$	$36 \pm 3.3$

**Table 26 – Joint Range of Motion.** † = stat. sig diff. from the sound limb. ✦ = stat. sig diff. from AFO applied limb.

Group, Limb	Average Ankle ROM (°)	Average Knee ROM (°)	Average Hip ROM (°)
TTA, Sound Limb	11 ± 4.2	63 ± 3.0	42 ± 3.8
TTA-CLEAT, AMP Limb	2 ± 1.6 ✦ †	64 ± 4.0 ✦	46 ± 2.9 ✦ †
Intact, DOM Limb	12 ± 5.6 ✦	67 ± 2.5 ✦ †	46 ± 4.7
Intact, AFO Limb	5 ± 1.8	69 ± 3.0	47 ± 5.3

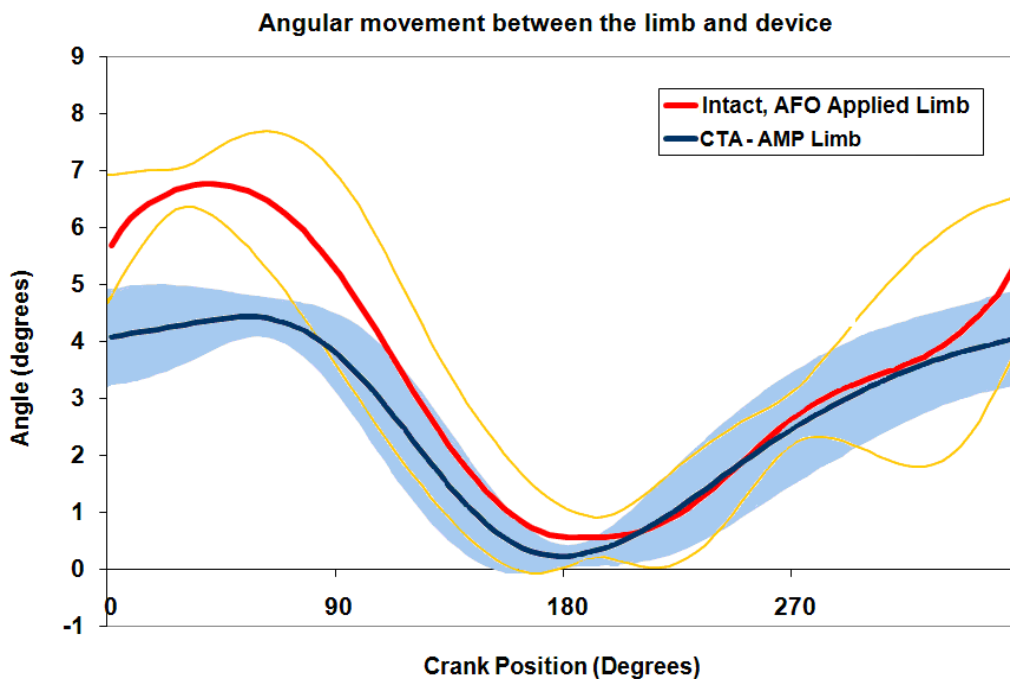


**Figure 56 - Angular motion between the AFO and the shank (Red line) as well as residuum and prosthesis (Blue line). Data represents the group average ± 1 standard deviation.**

### Pedaling Kinetics

Pedaling asymmetries did not differ between the TTA group pedaling with posterior cleat position (TTA-CLEAT) and the Intact group pedaling with an AFO on their non-dominant limb (Int-AFO) (Figure 57). However, it should be noted that work and force asymmetries were greater than normal cycling without an AFO of ~4% for work and force asymmetry (see Chapter 5). Therefore, the work and force asymmetries demonstrated by the Intact group were ~5 times and ~2 times (respectfully) greater than normal.

No significant differences were observed between limbs or groups regarding the timing of peak torque relative to top dead center (TDC) (Table 27). Significant differences in Peak Torque were observed between limbs within the TTA and Intact groups (Table 27). The Intact group produced more crank torque through the top of the pedal stroke in both limbs (Figure 58). The AFO applied limb showed greater negative torque during the recovery phase whereas the other three limbs demonstrated similar torque profiles (Figure 58).

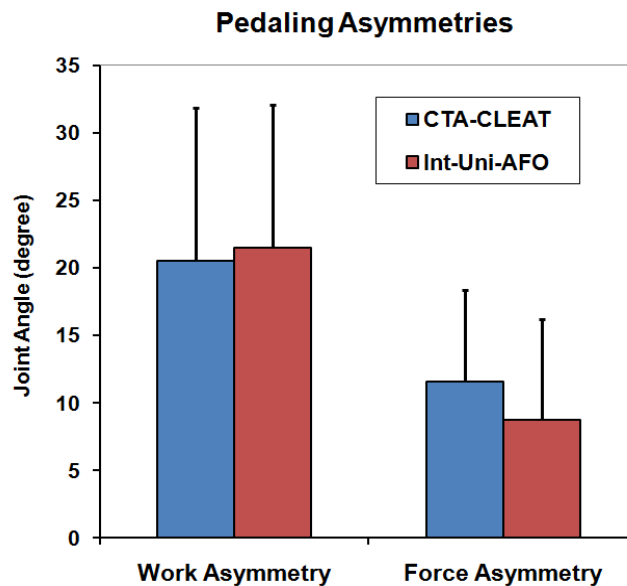


**Figure 57 - Pedaling asymmetries in the TTA group cycling with the posterior cleat position (blue) and the Intact group pedaling with the AFO on the non-dominant limb (red).**

**Table 27 – Mean torque and Timing of peak torque in degrees past TDC  $\pm$  1 standard deviation. † = stat. sig diff. from the sound limb. ✦ = stat. sig diff. from AFO applied limb.**

Group, Limb	Mean Torque (Nm)	Peak Torque (Nm)	Timing of Peak Torque (degrees)
TTA, Sound Limb	8.4 $\pm$ 2.5	37 $\pm$ 9	102 $\pm$ 12
TTA-CLEAT, AMP Limb	6.1 $\pm$ 0.5 †	29 $\pm$ 4.2 †	106 $\pm$ 21
Intact, DOM Limb	9.5 $\pm$ 3.2 ✦	45 $\pm$ 7.7 ✦	96 $\pm$ 5.1
Intact, AFO Limb	6.3 $\pm$ 2.2	33 $\pm$ 7.7	98 $\pm$ 29

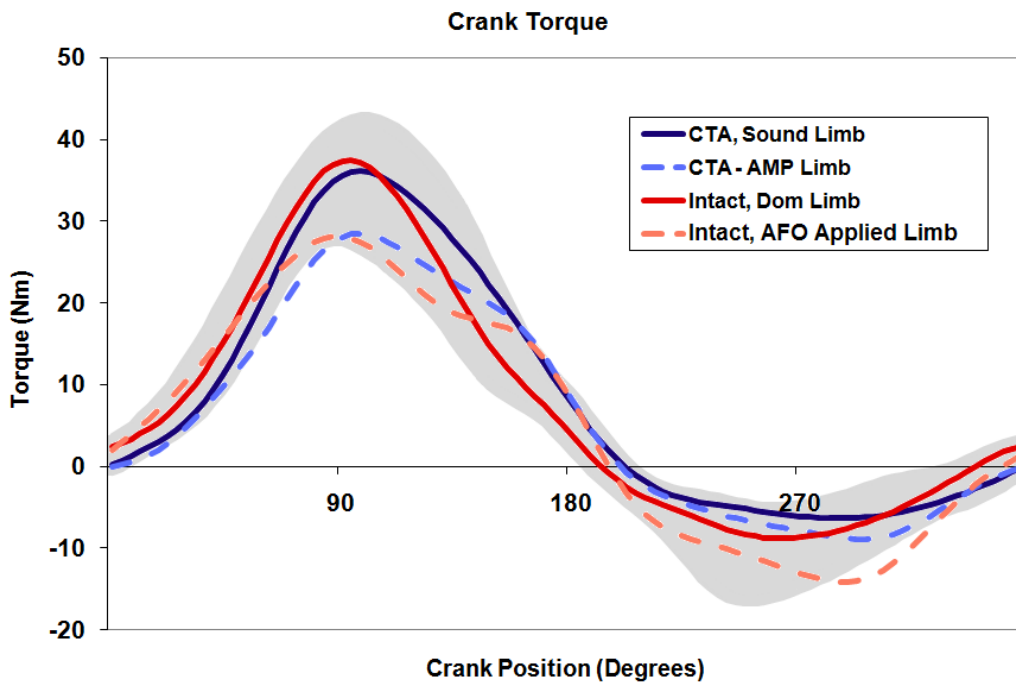


**Figure 58 - Torque about the crank spindle for the sound limb (dark blue solid line), the amputated limb (light blue dashed line) of the TTA group, the dominant limb (red solid line) and the AFO applied (orange dashed line). The grey shaded region is  $\pm$  1 standard deviation during normal intact cycling and is included here to provide a baseline for comparison (data from Chapter 6).**

## **Joint Kinetics**

The amputated limb demonstrated a greater hip extensor moment compared to the AFO applied limb as well as the sound and Int-DOM limbs during the first 180° of crank rotation (Figure 58). The AFO applied limb demonstrated a reduction in a hip extensor moment compared to the other three limbs during the same period whereas all four limbs demonstrated similar moment patterns during the final 180° of crank rotation (Figure 59).

The moment at the knee joint was greatest in the AFO applied limb (Figure 59). The knee joint moment in the amputated limb demonstrated a reduced extensor component compared to the other three limbs (Figure 59).

The moments at the residuum/prosthesis pseudo (RPP) joint and shank/AFO pseudo (SAP) joint, i.e. the ankle joint in the AFO applied limb, both demonstrated an extensor component during the beginning of the pedal stroke and a flexor component at the bottom of the pedal stroke (Figure 60). The peak magnitudes for both extensor and flexor moments were greater in the amputated limb yet the profile shapes were similar for both limbs (Figure 60).

The ankle joint in the AFO applied limb demonstrated the lowest magnitude followed by the ankle joint on the amputated limb where as the ankle moments in the sound and Int-DOM were similar in magnitude and profiles (Figure 59).

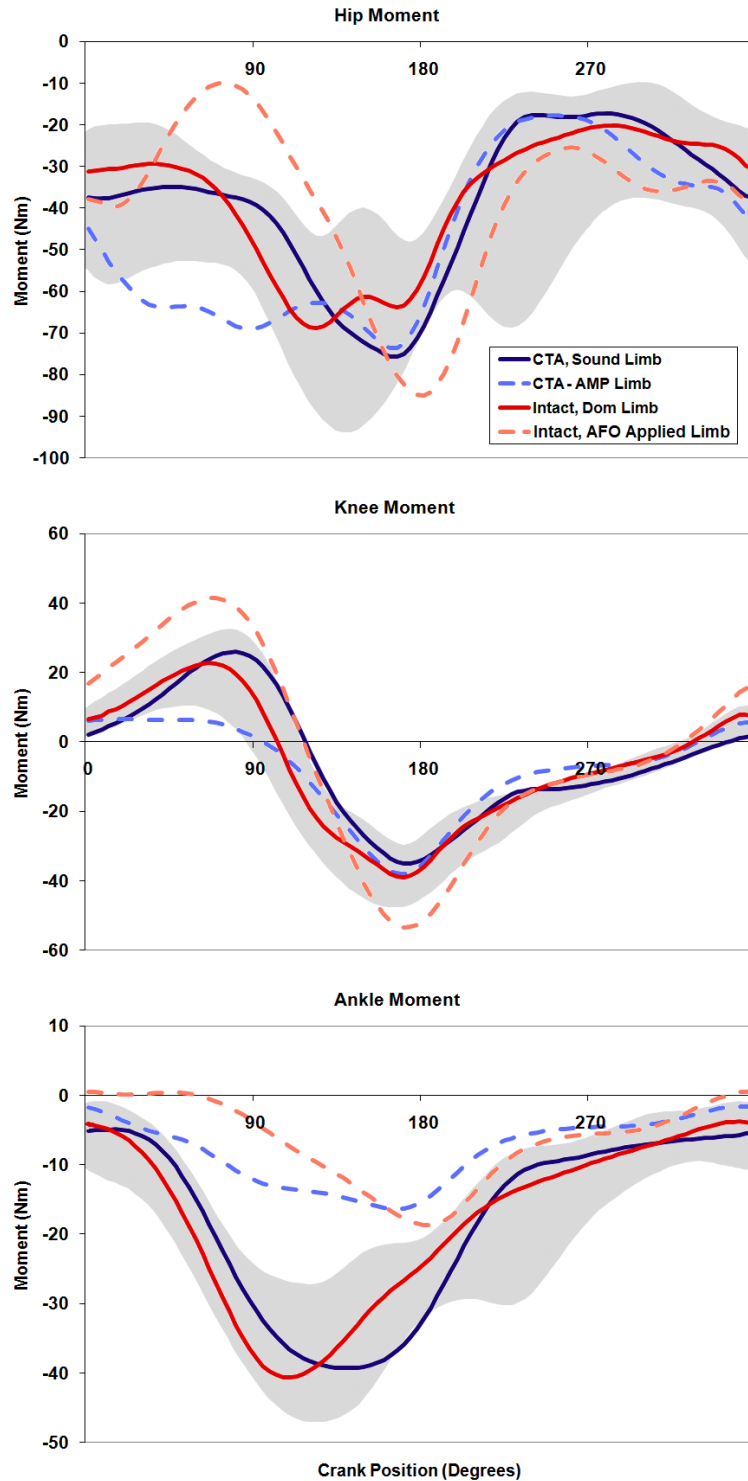


**Figure 59 - Joint moments for the sound limb (dark blue solid line), the amputated limb (light blue dashed line) of the TTA group, the dominant limb (red solid line) and the AFO applied (orange dashed line). The grey shaded region is  $\pm 1$  standard deviation during normal intact cycling and is included here to provide a baseline for comparison (data from Chapter 6).**

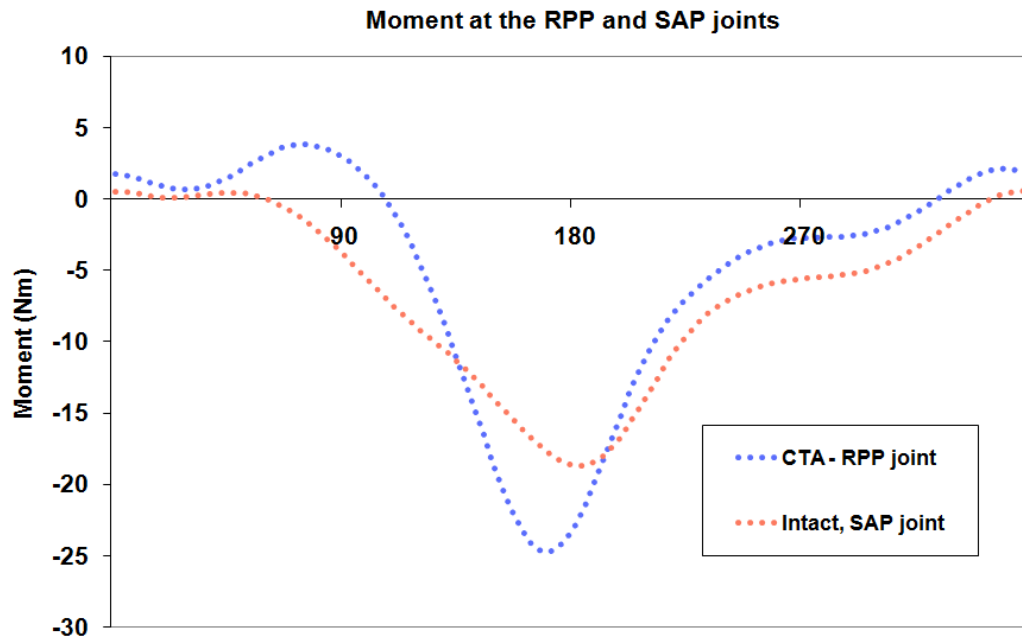


**Figure 60 - Moment at the residuum/prosthesis pseudo (RPP) joint and shank/AFO pseudo (SAP) joint, i.e. the ankle joint in the AFO applied limb.**

### **Muscle Activation**

Activation of the rectus femoris muscle (RF) in the amputated limb showed a significant shift to later in the crank cycle (Figure 61) compared to the sound limb and is similar to data reported earlier (see Chapter 5). The typical bi-modal activation pattern of the RF was also absent in the amputated limb similar to data reported earlier (Figure 62) (see Chapter 5). The RF in the AFO applied limb demonstrated a shorter burst duration than the Int-DOM limb (Figure 62).

The long head of the biceps femoris muscle (BF) demonstrated significant increases in burst duration in the AFO applied limb when compared to the contralateral limbs (Figure 61). BF offset also shifted significantly to later in the AFO applied limb when compared to the Int-DOM and the amputated limb (Figure 61). The BF also showed a reduction in activation in the Int-DOM compared to the AFO applied limb (Figure 62).

The onset of vastus medialis muscle (VM) in the AFO applied limb showed a significant earlier activation compared to the Int-DOM limb (Figure 61). VM activity in the other limb showed no significant shifts in timing of onset, peak activation, offset and burst duration (Figure 62).

Peak activity of the amputated gastrocnemius (GAS) muscle showed a trend toward later activation as reported earlier (see Chapter 5) (Figure 62). GAS activity in the other limbs did not show any significant shifts in timing of onset, peak activation, offset and burst duration (Figure 61).

The soleus (SOL) muscle showed a reduction in activity in the AFO applied limb compared to Int-DOM (Figure 61).

The tibialis anterior (TA) onset occurred earlier in the Intact group compared to the sound limb in the TTA group and a significant increase in burst duration (Figure 61).

Timing of Muscle Activity for the CTA-CLEAT and INT-Uni-AFO Conditions

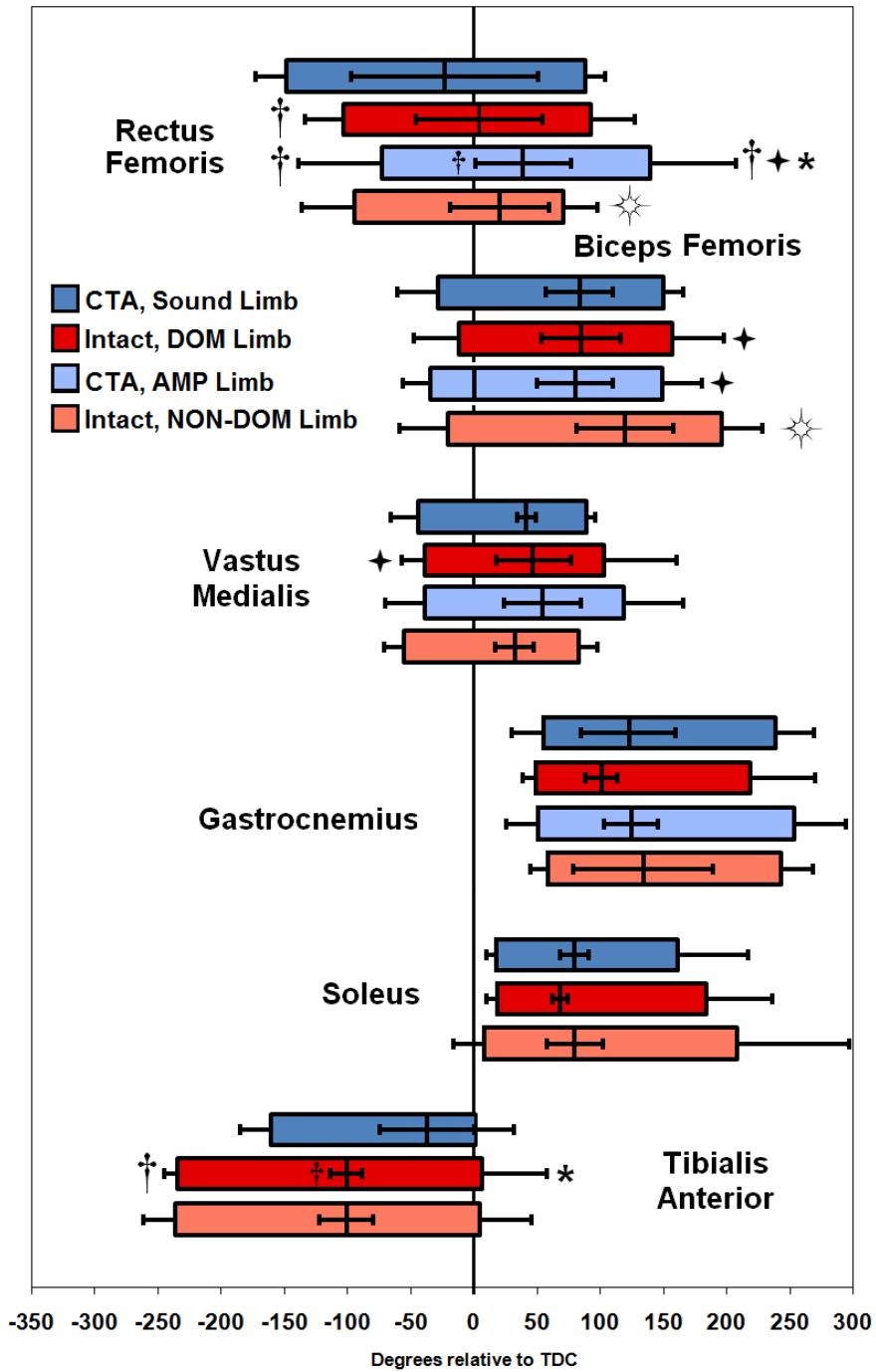
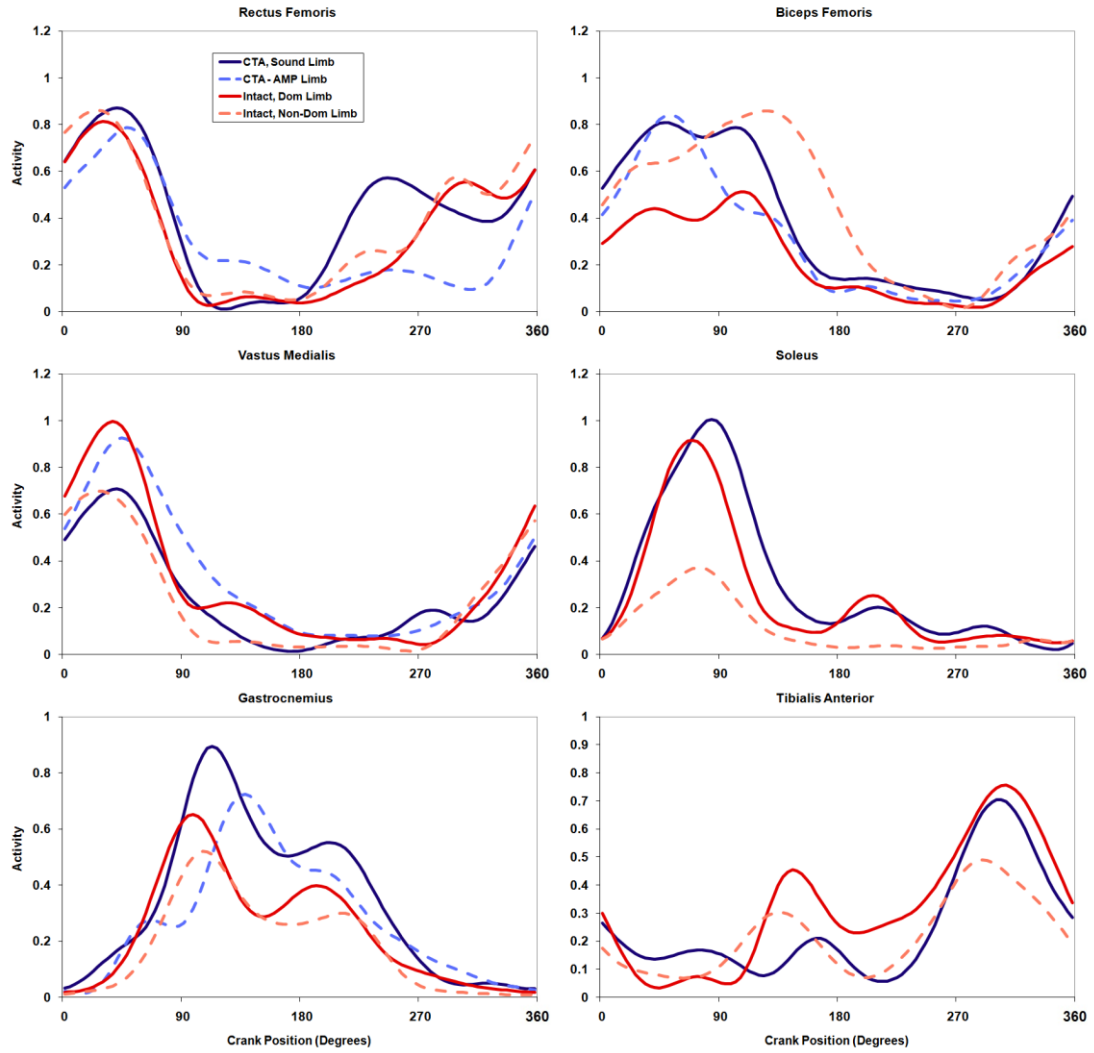


Figure 61 - Muscle onset, peak activation and offset for the conditions tested. † = stat. sig diff. from the sound limb. ✦ = stat. sig diff. from AFO applied limb (Non-DOM). \* = stat. sig diff. from the sound limb regarding burst duration. ✨ = stat. sig. diff. from the Int-DOM regarding burst duration.



**Figure 62 - Muscle activation during the crank cycle.**

## Discussion

The most significant finding from these experiments was that both groups utilized seemingly different external devices in a similar manner by altering joint output in proximal joints (Figure 59) yet maintaining similar output about the crank in both average crank torque (Table 27) and torque profile (Figure 58) in the limbs using a device. This concept of interface control was demonstrated in the lower extremity in both TTA (see Chapter 5) and intact cyclists (see Chapter 6) as well as in the upper extremity regarding the use of tools (Arbib et al., 2009; Mizelle et al., in press). The unique finding here is that both the TTA and intact cyclists utilized the external device by manipulation of the moments at joints within the control of the motor system to produce very similar output about the crank.

The combination of moments in proximal joints as well as muscle activity was different between the TTA and Intact groups. Peak knee joint extensor and flexor moments were larger in the AFO applied limb compared to the knee joint in the amputated limb (Figure 59). However, the trimlines of the prosthesis were higher (more proximal) than the trimlines of the AFO (Figure 55). This increased distance would require increased output at the knee joint in excess of what was necessary at the interface for task performance (Figure 59). The more distal trimline of the AFO may also explain the reduction in the hip extension moment between  $\sim 30 - 100^\circ$  (Figure 59). A reduction in the hip extension moment would aid in limb transition and control movement of the shank within the AFO (see Chapter 6). The longer distance between knee joint and the AFO trimline would also require a greater change in more proximal joint moments in order to affect control of the interface as seen in these data.

In contrast to the Intact group, the TTA group increased the hip extensor moment and decreased the knee extensor moment (Figure 59). The rectus femoris also displayed late onset, offset and a shift in peak activation reducing the ability to generate a knee

extension moment while reducing a hip extension moment. Meanwhile, biceps femoris activity remained unchanged which would transfer additional energy from the knee joint back to the hip joint further contributing to an increase in hip extension. In addition, a reduction in the knee extensor moment with a corresponding increase in hip extensor moment has been a documented strategy in amputee gait (Winter & Sienko, 1988; Sanderson & Martin, 1997; Silverman et al., 2008). This more hip-based strategy may reflect a strategy learned in gait and carried over into other forms of rhythmic locomotion, i.e. cycling.

The RPP and SAP joint moments demonstrated similarities in profiles yet the RPP moment demonstrated a greater extensor moment around 90° and a larger peak flexor moment. This could be because of the mechanical difference between these two limb/device systems. The residuum is completely enclosed by the prosthetic socket and mechanically coupled via a pin/shuttle lock suspension whereas the distal trimline of the AFO is proximal to the ankle joint. The connectivity provided by the pin suspension between the residuum and prosthesis may allow the motor system more control over the RPP moment and keep the moment in extension longer to help move reduce the angle between the residuum and prosthesis (as described in Chapter 5).

The ankle moment was reduced in the amputated limb compared to the sound or Int-DOM limb. The moment arm, e.g. the longitudinal centerline of the prosthesis and the cycling cleat, was approximately 40% of the distance in the sound limb and this in itself would reduce the moment calculated at the ankle joint (see Chapter 6). In addition, ankle moment is related to crank torque and this is also reduced for the amputated limb. Therefore the reduction in ankle moment demonstrated in the amputated limb is related to the cleat position used as well as the reduction in limb output.

Drawing comparisons between the moment calculated at the ankle joint in the AFO applied limb is difficult because the ankle joint is distal to the interface and does not provide a pathway for the limb to effect pedal forces. The moment within the distal

frame of the AFO would be a better indicator of energy going into the pedal. Loads in the AFO frame were not measured but one can infer these loads are similar to what is being transferred via the prosthesis because the crank torque profiles were similar. The generation of crank torque represents the “business end” of performing the cycling task and the average torque generated at the crank was not statistically different between the amputated limb and the AFO applied limb (Table 27).

Asymmetries in force magnitude between limbs (force asymmetry) was ~9% in the Intact group, more than double what the same group of cyclist performed without an AFO (Figure 57 & Figure 30 in Chapter 6). The Intact group also demonstrated asymmetries in work production at the crank approximately five times greater than without an AFO (Figure 57 & Figure 30 in Chapter 6). The presence of these increased asymmetries indicates the AFO applied limb was delivering less force to the pedal, yet the extensor moment in the AFO applied limb was much greater than the sound or Int-DOM limbs. In order to affect output at the pedal, energy must be transferred into the interface via the soft tissues of the shank. Deformation of the soft tissue as well as movement of the shank relative to the AFO would consume energy before being delivered to the AFO interface, thus reducing the amount of force applied at the pedal for the same knee extensor moment.

Another contributor to the reduced output in the limbs with an external device may be related to altered sensory information from the ipsilateral limb. The amputated limb is missing the ankle/foot complex including sensory information related to pressure on the plantar surface of the foot as well as force and length dependant feedback from the amputated muscles. Force dependant feedback from the sensors in the remaining proximal portion of the amputated GAS could have remained intact. Distribution of force and length sensors throughout and intact GAS are now known hence, while some length and force-dependent information can still be obtained from the remaining portion of the GAS, exact knowledge of how many sensors remain is unknown. The design of the AFO

removes the ankle/foot complex from contributing to the crank cycle and the plantar surface of the foot is not touching the pedal, perhaps reducing force-dependent sensory information from these structures. In addition to these losses, the motor system is also receiving information about the mechanical loading in the skin of the residuum and shank within the AFO. These loads on the skin would provide cutaneous sensory feedback to the central nervous system. This altered mechanical loading of the skin and soft tissue in the residuum/shank becomes an additional criterion for the motor system to consider while performing this task.

In conclusion, these results suggest the motor systems of both groups used an external device altered joint output in proximal joints to maintain similar output at the crank. The Intact group used a control strategy that increased knee joint output while reduced hip joint output. The TTA group used a control strategy that decreased knee joint output while increasing hip joint output. The design of the AFO had trimlines that did not encompass the entire limb segment meaning the knee joint had to increase output to have a similar effect at the interface. Despite these differences in proximal joints between the two groups, both groups generated a similar amount of torque about the crank spindle which represents the summation of all control processes necessary to perform the cycling task. The above mentioned normal work and force asymmetries could be due to energetic losses between the skeletal system and the interface via the soft tissues in the limb segment and/or related to altered sensory feedback from the distal portion of the limb and the skin at the device interface. Future research may concentrate on understanding the energetic loss at the interface to better understand its effect on performance. This understanding could then spur new developments in the design of prosthetic and orthotic interfaces that could change shape throughout the gait cycle to compress and “pre-load” soft tissues prior to the need to transfer loads through them. This would reduce the extra energetic demand placed on user while providing a more stable device for locomotion.

# CHAPTER 8

## SYMMETRICAL KINEMATICS DOES NOT MEAN SYMMETRICAL KINETICS IN CYCLISTS WITH TRANSTIBIAL AMPUTATION

### Introduction

The complex task of human locomotion involves integration of the neuromuscular and musculoskeletal systems taking into account the underlining morphology of the individual, the environment, and specific task demands in order to move the body in a stable and controlled manner. Symmetry in human locomotion is often assumed but asymmetry appears to be the more apparent outcome, even in the absence of pathology (Sadeghi et al., 2000 for review).

Reports indicate a person with a uni-lateral trans-tibial amputation can successfully perform locomotor tasks with considerable motor asymmetries (Winter & Sienko, 1988; Silverman et al., 2008; Childers et al., in press). Yet, it is common within clinical practice to “optimize” the movements of persons with amputation by adjusting the prosthesis i.e. adjusting the task mechanics, so they gravitate toward symmetrical kinematics and presumably more symmetrical joint kinetics (Kapp, 2004). However the notion that kinematic or kinetic symmetry is “optimal” for performance has been questioned by Winter and Sienko (1988) who state that “It is safe to say that any human system with major structural asymmetries in the neuromuscular and musculoskeletal systems cannot be optimal when the gait is symmetrical. Rather, a new *nonsymmetrical* optimal is probably being sought by the amputee within the constraints of his residual limb and the mechanics of his prosthesis.” Therefore, the controversy surrounding the relationship between kinetic and kinematics warrants additional exploration.

The cycling task provides a method to control lower limb kinematics by altering the geometric constraints between the rider and the bicycle e.g. rider position. Lower limb kinematics are not symmetrical during amputee cycling for example, because the prosthetic ankle is fixed while the sound ankle extends at the bottom of the pedal stroke and flexes at the top. This lack of ankle motion in the amputated limb leads to greater knee and hip flexion and extension to complete the crank cycle. Normal range of motion for an intact ankle joint is about twenty degrees (Heil, et. al., 1997) as it extends (plantarflexes) at the bottom of the pedal stroke and flexes (dorsiflexes) as the top of the pedal stroke. Limiting ankle motion on one limb e.g. a prosthesis, alters the mechanics of cycling by increasing the range of motion of the hip and knee joints to compensate for the loss of ankle motion.

Shortening the crank arm on the impaired limb is a method to adjust the geometry of the bicycle to minimize asymmetries in limb kinematics and has been shown to reduce kinetic asymmetries at the pedal in a limited number of cyclists with trans-tibial amputation (TTA) (Childers et. al., 2009b). Shortening the crank arm on the amputated side provides a method to alter the geometric constraints of the bicycle rider system in order to test the hypothesis that symmetrical kinematics will reduce asymmetries in limb output.

## **Methods**

In-depth discussions of the general methods are presented in Chapter 3 and are briefly summarized here to re-iterate what methods are specific to this hypothesis.

### **Subjects and load conditions**

A group of eight male recreational cyclists with uni-lateral trans-tibial amputation (TTA) ( $81.3 \pm 16.1$  kg,  $1.84 \pm 0.09$  m,  $33.7 \pm 10.0$  yrs) were recruited for this study. Pedaling kinetics (Broker & Gregor 1990) and limb kinematics (Peak Performance,

Vicon Motion Systems, Oxford, UK) were used to answer the hypothesis. The subjects pedaled at a constant torque of 15Nm at 90 rpm (~150 watts) with 173mm crank arms as a control condition (TTA-Control). The TTA subjects also pedaled at 15Nm and 90 rpm with the crank arm shortened 10mm on the amputated side (163mm) (TTA-CRANK).

### **Statistical Analysis**

Paired T-tests were used to evaluate differences in the sound and amputated limbs between the TTA-Control and TTA-CRANK conditions. A statistically significant difference would be noted if  $p < 0.05$ .

## **Results**

### **Limb Kinematics**

Significant differences were observed in the average knee angle and hip ROM between the sound and amputated limbs in the TTA-Control condition indicating these subjects were kinematically asymmetrical before altering crank arm length (Figure 63). The TTA-CRANK condition significantly reduced the knee and hip ROM in the amputated limb compared to control (Figure 63) as predicted using a limb kinematic model (Childers et al., 2010 *Ipsilateral*). There were no significant differences between the sound and amputated limb within the TTA-CRANK condition indicating the shortened crank arm did minimize kinematic asymmetry (Figure 63). There were no statistically significant differences noted in sound limb ankle, knee, and hip kinematics between TTA-Control and TTA-CRANK conditions.

The ROM between the residuum and the prosthesis was  $4.5 \pm 2.0^\circ$  for TTA-Control and  $4.7 \pm 2.0^\circ$  for the TTA-CRANK condition and were not significantly different.

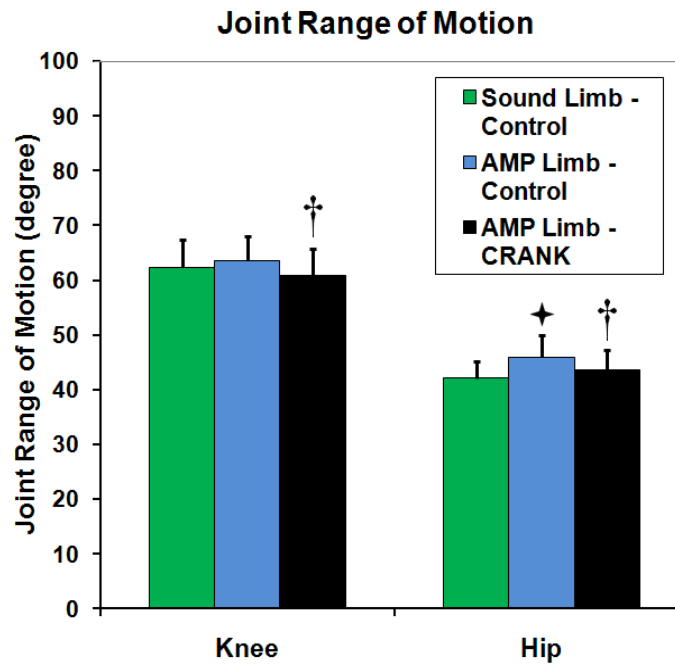
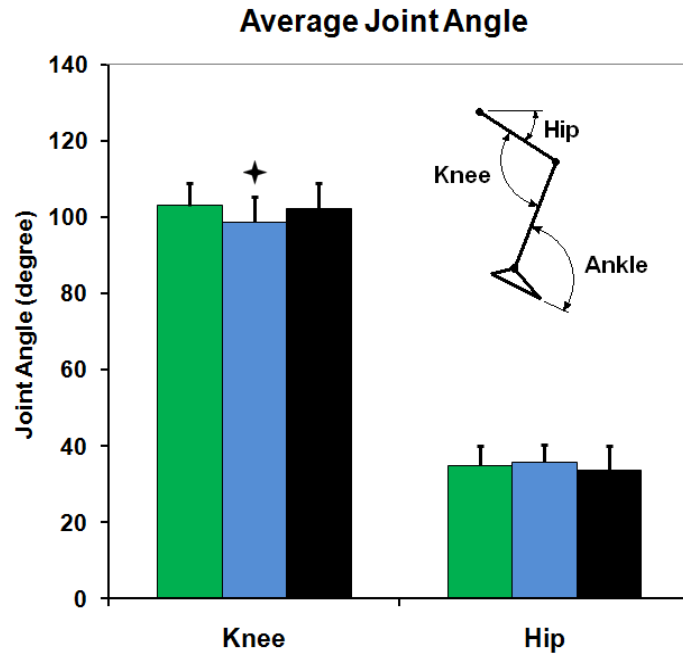


**Figure 63 - Average joint angle and range of motion for the knee and hip joint. Information for the sound limb during the CRANK condition is not shown for clarity because there were no differences in sound limb kinematics between control and CRANK conditions. † = stat. sig diff. from the control condition within limb. ★ = stat. sig diff. from the sound limb within a condition.**

## Pedaling Kinetics

Pedaling asymmetries were not significantly different between TTA-Control and TTA-CRANK conditions (Figure 64). Work asymmetry was reduced in four subjects when utilizing the shortened crank but was greater in the other four subjects (Figure 65). The differences in work asymmetry between conditions were small within subjects (Figure 65). Crank torque production was similar in the amputated limb between conditions (Figure 66).

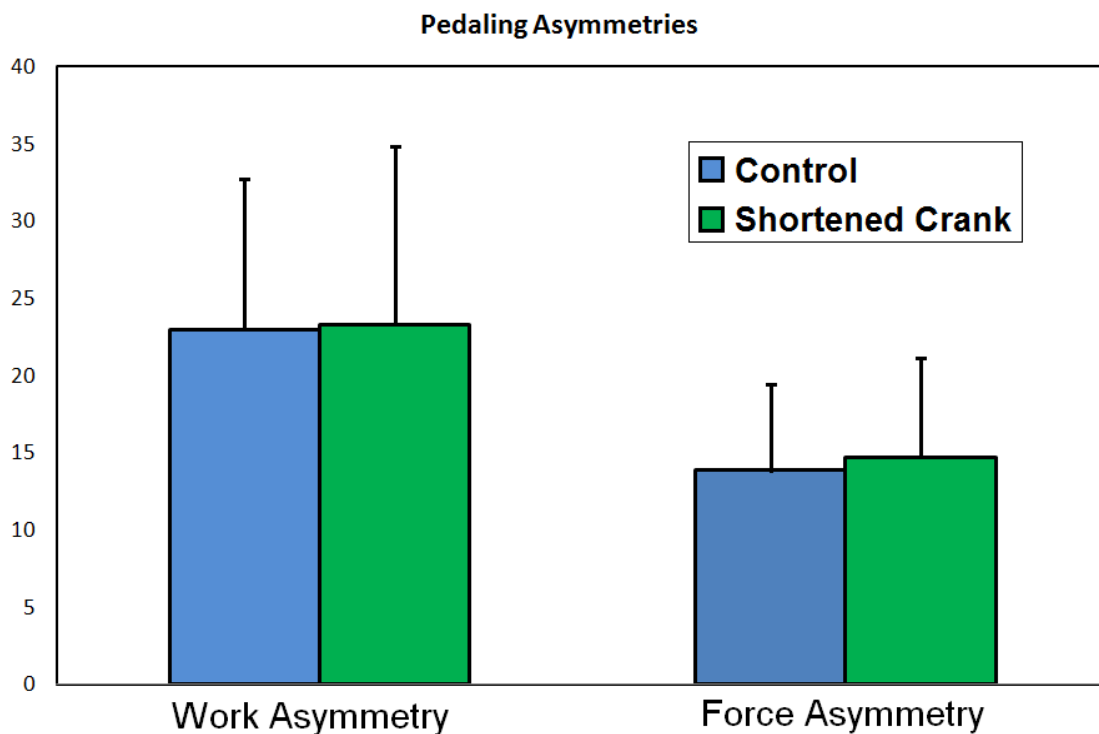


**Figure 64 - Pedaling asymmetries regarding work produced about the crank spindle as well as force produced at the pedal. There were no significant differences in pedaling asymmetries.**

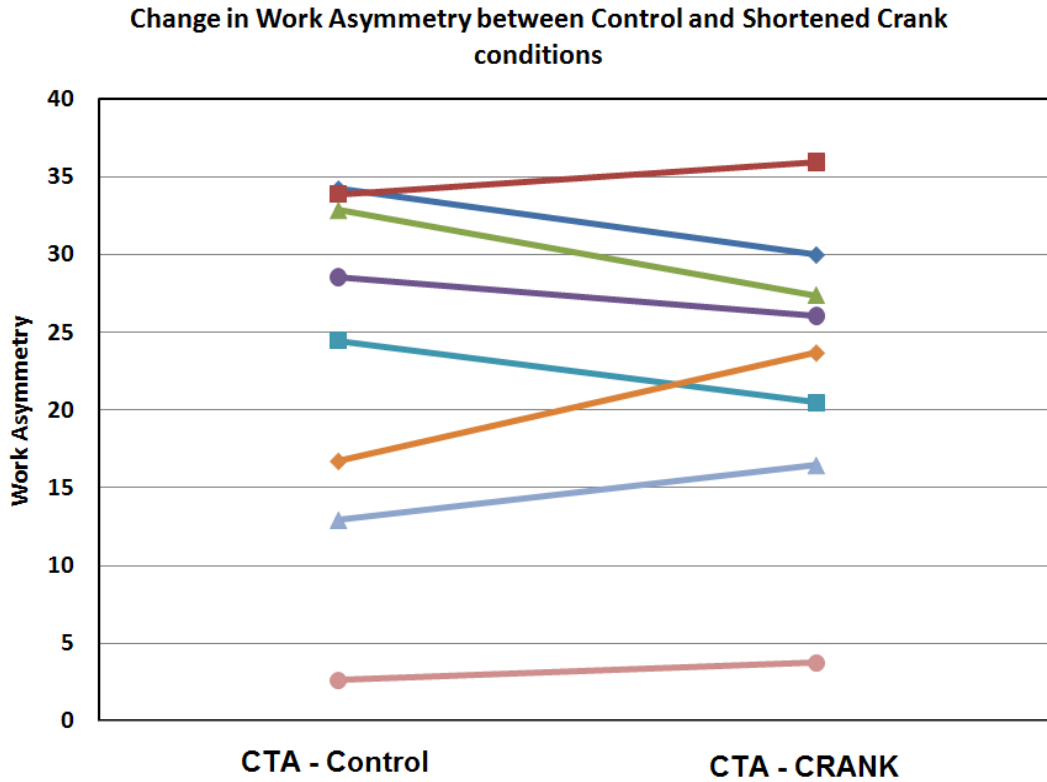


**Figure 65 - Change in Work Asymmetry between conditions demonstrating four subjects decreased and four subjects increased asymmetry with a shortened crank. Each line represents data for an individual subject.**

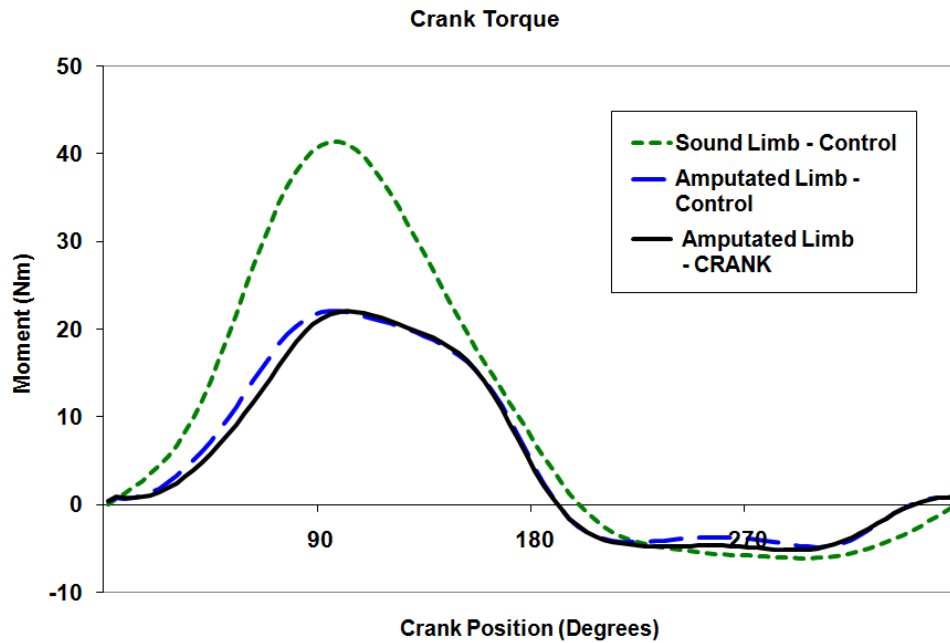


**Figure 66 - Crank torque for the Sound limb during the control condition (green dashed), the amputated limb during control (blue dashed), and the amputated limb during the CRANK condition (black solid).**

## **Joint Kinetics**

The average (Table 28), peak magnitude (Table 29), and timing of the peak (Table 30) hip extensor moment did not show any significant differences between the TTA-Control and TTA-CRANK conditions yet did demonstrate a trend toward increasing hip extension moment in the TTA-CRANK condition during the power phase (Figure 70).

The knee joint moment demonstrated significant asymmetry between limbs during both TTA-Control and TTA-CRANK conditions regarding the average (Table 28) and the peak (Table 29) extension moment but not in the flexor moment. The average and peak knee joint extensor moment was significantly reduced from the TTA-Control to the TTA-CRANK condition (Tables 28 & 29). This reduction in knee extensor moment occurred in all eight subjects regardless of whether the individual subject demonstrated a change in work asymmetry at the crank. There were no significant differences between limbs or across conditions regarding the timing of peak knee joint moments (Table 30).

The ankle joint demonstrated significant asymmetry between limbs during both TTA-Control and TTA-CRANK conditions regarding the average (Table 28) and the peak (Table 29) extension moment and showed no changes comparing across conditions.

**Table 28 – Average Joint Moment.** † = stat. sig diff. from the control condition within limb. ✦ = stat. sig diff. from the sound limb within a condition.

Limb and Condition	Average Ankle Extensor Moment (Nm)	Average Knee Extensor Moment (Nm)	Average Knee Flexor Moment (Nm)	Average Hip Extensor Moment (Nm)
Sound Limb/ TTA-Control	19 ± 3.5	16 ± 5.5	17 ± 4.5	39 ± 6.5
Sound Limb/ TTA-CRANK	18 ± 4.3	17 ± 5.3	18 ± 4.6	41 ± 8.0
Amputated Limb/ TTA-Control	13 ± 2.5 ✦	9.9 ± 4.0 ✦	15 ± 3.4	35 ± 8.2
Amputated Limb/ TTA-CRANK	13 ± 3.2 ✦	7.4 ± 3.9 ✦ †	15 ± 3.7	38 ± 9.2

**Table 29 – Magnitude of Peak Moments.** † = stat. sig diff. from the control condition within limb. ✦ = stat. sig diff. from the sound limb within a condition.

Limb and Condition	Peak Ankle Extensor Moment (Nm)	Peak Knee Extensor Moment (Nm)	Peak Knee Flexor Moment (Nm)	Peak Hip Extensor Moment (Nm)
Sound Limb/ TTA-Control	45 ± 11	33 ± 13	37 ± 10	82 ± 20
Sound Limb/ TTA-CRANK	43 ± 9.9	32 ± 11	40 ± 10	88 ± 24
Amputated Limb/ TTA-Control	34 ± 8.8 ✦	18 ± 7.2 ✦	35 ± 11	69 ± 23
Amputated Limb/ TTA-CRANK	34 ± 11 ✦	14 ± 8.0 ✦ †	35 ± 12	76 ± 26

**Table 30 – Timing of Peak Moments. † = stat. sig diff. from the control condition.  
 ★ = stat. sig diff. from Bi-CLEAT condition.**

Limb and Condition	Timing of Peak Ankle Extensor Moment (degrees)	Timing of Peak Knee Extensor Moment (degrees)	Timing of Peak Knee Flexor Moment (degrees)	Timing of Peak Hip Extensor Moment (degrees)
Sound Limb/ TTA-Control	152 ± 28	81 ± 14	177 ± 16	168 ± 17
Sound Limb/ TTA-CRANK	148 ± 25	82 ± 11	178 ± 13	168 ± 13
Amputated Limb/ TTA-Control	168 ± 6.5	64 ± 37	173 ± 7	169 ± 1.9
Amputated Limb/ TTA-CRANK	167 ± 4.7	71 ± 25	172 ± 7	165 ± 6.8

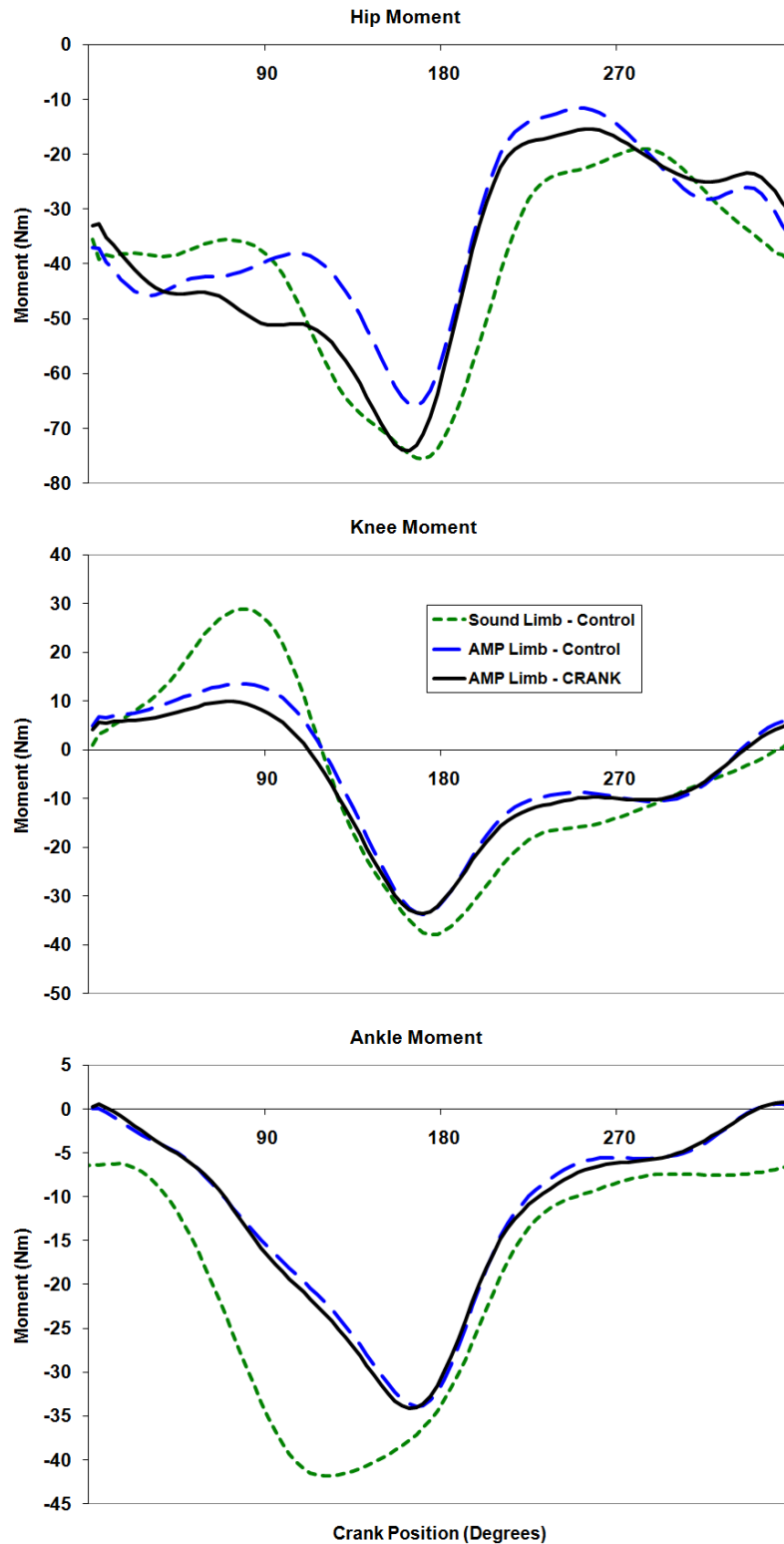


**Figure 67 - Joint moments for the Sound limb during the control condition (green dashed), the amputated limb during control (blue dashed), and the amputated limb during the CRANK condition (black solid).**

## Discussion

The most significant finding was that utilization of a shortened crank arm on the amputated limb to offset the almost complete lack of motion in the prosthetic ankle did minimize kinematic asymmetries but had no significant effect on pedaling asymmetries. The shortened crank did reduce the knee extensor moment in the amputated limb.

Work asymmetry and crank torque were not affected by use of a shortened crank arm suggesting the amputated limb imparted an equal amount of energy into the bicycle in both conditions. The combination of joint moments used to deliver the energy to the crank did differ between conditions in that the peak and average knee extensor moment was reduced in the TTA-CRANK condition. This reduction in the knee extensor moment was associated with an increase in the hip extensor moment (Figure 67) although this increase did not achieve statistical significance. This combination of changes in joint moments may be necessary in order to maintain torque output with a shortened crank arm. A shortened crank arm would require an increase in force normal to the crank arm during the power phase (45 - 135°). A method to increase force during this region given the orientation of the limbs (see Figure 31, Chapter 4) would be to increase the hip extensor moment and decrease the knee extensor moment (Gregor et al., 1985). Therefore, this change in joint kinetics represents the manner in which the subjects adapted to the altered mechanics of a shortened crank arm and not related to kinematic changes in the limb.

A common goal in clinical practice is to minimize kinematic asymmetries in the belief this will also minimize kinetic asymmetries (Kapp, 2004). Scientific researchers have been challenging this idea for some time (Winter & Sienko, 1988). Our results demonstrate a shortened crank arm on the amputated limb will minimize kinematic asymmetries. Despite the minimization of kinematic asymmetries, these subjects still pedaled with significant kinetic asymmetries indicating a limited relationship between

kinematic and kinetic asymmetries as indicated in earlier reports (Winter & Sienko, 1988).

Cycling is a constrained motor task in which limb kinematics may be manipulated by changing the position of the rider. Walking is a less constrained form of locomotion including a phase when the foot is not in contact with the ground. This allows the prosthetic user to vary step length and timing as documented in previous research (Sanderson & Martin, 1997). Prosthetic users also demonstrate asymmetries in ground reaction forces and joint kinetics (Sanderson & Martin, 1997; Silverman et al., 2008) and these asymmetries have been suggested as an underlying factor in the higher prevalence of osteoarthritis in the sound limb of TTA (Norvell et al., 2005). This research uses a constrained task because it allowed the researcher to minimize kinematic asymmetries without providing any sort of visual feedback that would add a confounding variable by involving additional supraspinal control (Dingwell et al., 1996). Regardless of the constrained or unconstrained nature of these two forms of locomotion, kinematic and kinetic asymmetries have been documented in both and this research demonstrated these kinetic asymmetries did not change when limb motion was symmetrical.

In conclusion, these results indicate kinetic symmetry may not be the goal of the motor system in persons with uni-lateral trans-tibial amputation in the presence of kinematic symmetry. Task performance appears to be an important goal of the motor system and not task symmetry. A person with amputation must perform a locomotor task within the asymmetrical constraints their remaining limbs allow in combination with a prosthesis. In this scenario, the human system will make motor adjustments within the remaining limbs in order to utilize the mechanical properties of the prosthesis and contend with the interface between the residuum and the prosthesis. Taken together, a better goal during rehabilitation would be to enable the person to perform a functional task, e.g. locomotion, with the understanding there will be motor adjustments rather than simply setting the rehabilitation goal toward symmetrical kinematic output.

## CHAPTER 9

### SUMMARY, CLINICAL APPLICATION AND DIRECTION FOR FUTURE RESEARCH

#### Summary of Findings

The goal of this project was understand differences in motor control strategies between individuals with a uni-lateral trans-tibial amputation and individuals with intact lower limbs and determine if those changes were related to utilization of the prosthesis for locomotion. Cycling was used as the locomotor task because it provides a controlled environment in which rhythmic locomotion can be studied (Gregor & Childers, 2011). A group of individuals with a uni-lateral trans-tibial amputation and a group of intact individuals using an Ankle Foot Orthosis (AFO) performed a cycling task to understand the “motor adjustments” necessary to utilize an external device for locomotion.

The first experiment used a group of nine Intact and nine TTAs pedaling at a constant torque (15 Nm) and three different cadences (60, 90, and 120 rpm). The purpose was to understand how differences between intact and TTA groups relate to a possible shift in a control strategy to account for muscle activation-contraction dynamics. This control strategy could have been altered by loss of sensorimotor feedback from the amputated limb in combination with altered feedback coming from the residuum and an altered musculoskeletal system. The motor system could have responded to increasing cadence by increasing the amplitude of muscle activity without shifting the timing of that activity. *Hypothesis 1.1* was tested stating **the timing of muscle activation will occur earlier in the crank cycle with increasing cadence despite the loss of physiologic systems associated with amputation.** Timing of muscle activity was calculated relative to peak crank torque and results showed timing would shift earlier in the crank cycle as cadence increased. These results were consistent with the “Activation-contraction

dynamics hypothesis” proposed by Neptune et al. (1997) and suggest that the motor systems in both cyclists with amputation and with intact lower limb includes accounting for the activation-contraction dynamics of the muscles involved in locomotion.

Limitations in this method preclude a way to quantify exactly how sensory feedback was altered or how it could of played a role in this control strategy.

The second experiment explored motor control in TTAs during cycling by analyzing joint kinematics, kinetics, and muscle activation patterns during amputee cycling . A group of nine Intact and nine TTA individuals pedaled at constant torque (15 Nm) and 90 rpm and tested *Hypothesis 1.2; the neuromuscular system changes absolute muscle output to control a prosthesis via the limb/prosthesis interface.* Results demonstrated the GAS and RF muscles demonstrated shifts in the timing of muscle activity. The shift in GAS activity was explained as the motor system using this muscle in accordance with its post-amputation biomechanical function (uni-articular knee flexor). The altered muscle activity patterns were best explained as the motor system adapting to the inertial properties as well as the mechanics of the residuum/prosthesis interface to control the prosthesis. In addition, I proposed the prosthesis should be viewed in the context of tool use in that the residuum is the end-effector of the motor system and the prosthesis is the tool to extend that end-effector to the environment, i.e. the bicycle. A limitation to this work was the lack of pressure measurement from within the prosthetic socket that would help link movement in the limb to pressure imposed on the skin and thus a control strategy based on this information yet this research does highlight the need to future work in this area.

The third experiment built on the second and further explored the concept of tool use by having a group of eight intact individuals pedal first with a posterior cleat position (Bi-CLEAT condition) to understand what would happen if the contribution of ankle plantarflexors were minimized. Then the same group pedaled with an AFO designed to replicate the mechanics of pedaling with an amputation/prosthesis (Bi-AFO condition).

The experiment tested *Hypothesis 2.1* that **an external device requiring the user to control the pedal via an interface at the shank and utilized by Intact cyclists will mimic the mechanics of cycling with a prosthesis.** Results showed the Bi-CLEAT condition reduced ankle plantarflexor activity and the subjects compensated by increasing duration in the BF muscle and increasing the hip extensor moment. The Bi-AFO condition elicited a different response from the Bi-CLEAT condition in that the hip and ankle extensor moments decreased while the knee extensor moment increased. The changes noted in the Bi-AFO condition were not due to lack of ankle plantarflexors but were necessary to control the interface and frame of the AFO needed to perform the task. These results suggests the motor system manipulated moments at other joints in order to produce torque about the crank spindle necessary for task performance and is indicative of tool use by the motor system. Limitation in this research stems from the difficulty in quantifying the forces at the shank/AFO interface, the forces within the AFO and estimation of tissue deformation. Future research may address these limitations to better link the changes of proximal joints to control of the device and quantifying the energetic losses due to tissue deformation.

The fourth experiment combined knowledge gained in the second and third experiments to understand if an external device used by an intact motor system would be utilized in a similar manner to a TTA using a prosthesis. This strengthens the conclusions drawn in the second experiment that the changes observed in muscle activity and joint kinetics were related to control of the limb/device interface. A group of eight TTA was compared to eight intact individuals cycling with an AFO applied uni-laterally. The cleat on the prosthesis and the AFO were both placed posterior to the standard location in order to maintain the mechanics of the task across the two groups. Both groups pedaled at a constant torque of 15Nm and 90 rpm and tested *hypothesis 2.2* that **individuals with and without amputation will modify the control strategy of proximal joint in order to control an external device on the distal limb segment.**

Results suggest the motor systems of both groups used an external device altered joint output in proximal joints to maintain similar output at the crank. The Intact group used a control strategy that increased knee joint output while reduced hip joint output. The TTA group used a control strategy that decreased knee joint output while increasing hip joint output. The design of the AFO had trimlines that did not encompass the entire limb segment meaning the knee joint had to increase output to have a similar effect about the interface. Despite these differences in proximal joints between the two groups, both groups generated a similar amount of torque about the crank spindle which represents the summation of all control processes necessary to perform the cycling task. The above normal work and force asymmetries could be due to energetic losses between the skeletal system and the interface via the soft tissues in the limb segment and/or related to altered sensory feedback from the distal portion of the limb and the skin at the device interface. These results further demonstrate the differences noted between TTA and individuals during normal cycling are likely due to “motor adjustments” necessary to control the prosthetic device. Future research should concentrate on understanding the energetic loss at the interface to better understand its effect on performance.

The fifth and final experiment explores a controversy between clinical practice and scientific literature over the influence of kinematic symmetry on the kinetic asymmetries demonstrated in uni-lateral amputees during locomotion. A group of eight TTA pedaled at constant torque (15 Nm) and 90 rpm with a shortened crank arm on the amputated limb and with symmetrical crank arms and tested *Hypothesis 2.3*; **symmetrical kinematics do not reduce asymmetries in limb kinetics**. Results indicate kinematic measures between the sound and amputated limbs were not statistically different with the shortened crank indicating these subjects pedaled with kinematic symmetry. However, asymmetries in pedaling kinetics did not change between conditions. In fact, the knee extensor moment decreased with a corresponding increase in the hip extensor moment in the amputated limb compared to the control condition and the

sound limb with the crank arm was shortened indicating some kinetic variables may increase asymmetry with a decrease in kinematic asymmetry. Results indicated kinetic symmetry was not sought by the motor system in persons with uni-lateral trans-tibial amputation in the presence of kinematic symmetry. Therefore, task performance appeared to be the more important goal of the motor system than task symmetry.

## **Clinical Application**

### **A New Clinical Paradigm**

This work suggests control of the external device, i.e. prosthesis or AFO, via the interface between the limb and the device represents “motor adjustments” utilized by the motor system and may be viewed in the context of tool use. Clinical goals in rehabilitation currently focus on minimizing “gait deviations” whereas the clinical application of these results suggest these “deviations” from “normal” locomotion are “motor adjustments” necessary to control a tool, i.e. prosthesis, by the motor system. Examining amputee locomotion in the context of tool use changes the clinical paradigm from one to minimize “deviations” to understanding this behavior is related to interface control of the device thereby shifting the focus to improving function of the limb/prosthesis system. This work does not suggest that “motor adjustments” or “good” or “bad” for task performance but does explain how they may arise and this knowledge may then empower the clinician when designing a rehabilitation strategy.

### **Improved Prosthetic Socket Design**

Improved design of prosthetic sockets is another clinical application of this work based on understanding that these motor adjustments are related to interface control. A prosthetic socket designed to change its shape or stiffness properties during the gait cycle could minimize movement of the residuum within the socket while easing control of the interface. This “dynamic socket” would be able to enhance the control of the interface.

For example, the socket could actively deform to “pre-load” the soft tissues of the residuum and prevent extension of the RPP joint prior to initial contact and ease the transition to midstance. The magnitude and timing of socket deformation could also be modulated based on gait speed and terrain being negotiated by the user. This type of “actively controlled dynamic” socket would not eliminate movement within the prosthetic socket but would enhance control of the device because the device would expend energy to compress the soft tissue and allow better energy transfer between the skeleton and the device. In addition to potentially reducing energetic demand on the prosthetic user a prosthetic socket that could “pre-load” would enhance stability and power transfer. Although it is not known if existing technology has the capacity to deform and modulate the shape of a prosthetic socket, if one did want to design such a device, the importance of interface control highlighted in this work provides a basis for specifying the design requirements of such a prosthetic socket as well as predict how this socket could be used by an individual with an amputation.

### **Improved Cycling Specific Prostheses**

This body of research also provides information to design prostheses specific to cycling. The prosthetic foot should be as stiff as possible to allow the greatest energy transfer from the residuum to the pedal (Childers et al., in press). The position of the cycling cleat in the sagittal plane remains open to debate. As the cleat was moved to the posterior position, the knee extensor moment decreased while the hip extensor moment increased (see Chapters 5 & 7). These data do not necessarily show a cleat position that would elicit better performance, simply a different strategy with similar output at the pedal. Therefore, I recommend cleat position to be determined via other criteria like patient comfort. Cleat placement does provide a method to redistribute the workload across different groups of muscle thus allowing the clinician to bias toward better trained muscles or alleviate the loads on injured muscles. The height of the posterior wall of the

prosthetic socket is another design criterion that is constantly questioned (Childers et al., 2009b) and one highlighted by this research. The rectus femoris altered its activity to help manage the mechanical constraint imposed by the prosthetic socket through the top of the pedal stroke. Although it would seem reasonable to lower the posterior wall to reduce pressure between the socket and the residuum, we have also presented data suggesting reducing the posterior wall may not help. Flexion between the residuum and the socket begins during the recovery phase and a lower posterior wall would allow for more motion to occur during this phase that would then have the residuum in a more flexed position at the top of the pedal stroke. Therefore, there is a compromise between the height of the posterior wall and control through the top of the pedal stroke. In addition, the location of the cycling cleat would change the overall orientation of the prosthesis at the top of the pedal stroke (knee would be more extended) and this would also influence the orientation of the residuum and the prosthesis. Therefore there are at least three factors that influence the design of just one aspect of the prosthetic socket. A computer simulation that allows for motion between the residuum and prosthesis could help find the optimal point across these three variables and guide future experimental research in this area. At present, my opinion is to trim the posterior wall to allow  $\sim 120^\circ$  ROM of the knee joint and provide a generous radius at the trimline.

### **Conclusion and Direction for Future Research**

In conclusion, this body of work suggests 1) the motor system does account for the activation-contraction dynamics when coordinating muscle activity post amputation, 2) it changes joint kinetics and muscle activity to compensate for the loss of physiological systems as well as use of a prosthetic device, 3) these differences in motor control between intact and TTA are related to control of the interface between the limb and the external device, and 4) the motor system does not alter kinetic asymmetries when

kinematic asymmetries are minimized, contrary to a common goal of current rehabilitation plans (Kapp, 2004).

The motor systems in both TTAs utilizing a prosthesis and Intact cyclists utilizing the AFO demonstrated changes in joint moments and muscle activity related to control of the motion of the limb within the device as well as to generate moments within the device necessary for task performance. This concept of interface control has been reported in the upper extremity regarding the use of tools (Arbib et al., 2009; Mizelle et al., in press). Similar to upper extremity tool use, the interface between the distal limb segment (shank or residuum) and the tool (AFO or prosthesis) must be controlled to perform a locomotor task. For example, to use a screwdriver the motor system understands a moment about the longitudinal axis of the screwdriver is necessary to drive a screw. The motor system will then activate and coordinate muscle activity across joints in the upper extremity to produce a combination of forces between the fingers (motor endpoint) and the screwdriver handle (the interface) to generate the moment requirements within the screwdriver necessary for task performance (drive a screw). Similar to tool use in the upper extremity, use of an external device on the lower limb should be viewed in the context of tool use.

Examining TTA locomotion within the context of tool use may enable a better understanding of motor behavior within this population. For example, during gait, the knee moment remains flexor or near zero in the amputated limb during initial contact and through midstance; this corresponds to a reported increase in the hip extensor moment (Winter & Sienko, 1988; Sanderson & Martin, 1997; Powers et al., 1998; Silverman et al., 2008). The vasti, hamstrings, and gluteus maximus demonstrate increased muscular activity during this phase (Winter & Sienko, 1988; Sanderson & Martin, 1997; Powers et al., 1998; Fey et al., 2010). Silverman et al. (2008) explained this strategy as a method to use the hamstrings to transfer energy to the hip joint to aid in propulsion of the trunk over the prosthesis. Examining this behavior within the context of tool use we may be able to

explain why this hip strategy would be desirable as opposed to the generation of a knee extensor moment during this portion of the gait cycle similar to normal gait. In order to use the prosthesis for propulsion, the motor system must also control the residuum within the prosthesis. Although no experimental data exist describing the angular movement of the residuum within the prosthetic socket during gait, one may surmise the pendulum effects of the prosthesis on the limb during swing would position the residuum in an extended position relative to the residuum/prosthesis pseudo (RPP) joint. Initial contact with the ground would pivot the prosthesis forward and then flex the RPP joint. A flexed RPP joint would drive the distal tibia into the anterior wall of the prosthesis while driving the posterior aspect of the knee into the posterior wall of the prosthetic socket, a position that is uncomfortable and inefficient for energy transfer (Kristinsson, 1993). A flexor moment at the knee would be necessary to counteract this movement and move the residuum back toward RPP extension. A knee flexor moment at initial contact has been described in the amputated limb (Sanderson & Martin, 1997). Therefore, the motor adjustment necessary to control the residuum within the prosthesis while aiding in forward propulsion would be to co-activate the vasti and hamstrings and transfer energy back toward the hip joint. However, there have been no studies that have quantified angular movement of the residuum relative to the prosthesis during gait thus making a connection between movement at the RPP joint and motor control difficult without additional research. The methods used during this study were able to quantify angular movement of the RPP joint during a cycling task and these methods could be applied to gait and provide the basis for the proposed future research.

Specific experiments to continue this work includes using TTA fitted with osseointegrated prostheses in order to remove the influence of soft tissue compression and difficulty manipulating the residuum within a prosthetic socket. This would allow a method to examine the effect of interface control. If the change in RF activity was due to control of the residuum/prosthetic interface, then its activity in osseointegrated prosthetic

users should be similar to intact individuals. The use of osteointegrated prosthetic users would also reduce the degrees of freedom (DOF) of the human bicycle system. The normal human/bicycle system can be modeled as a five bar linkage with 2 DOF. The human/prosthesis/bicycle system can also be modeled as a five bar linkage because the DOF of RPP joint replaces the ankle joint. An osseointegrated prosthetic cyclist would not have a RPP joint, thus only 1 DOF. The consequences this may have for motor control would be interesting and provide insight as to the role of mechanics on motor control.

This work also highlights the need for better understanding residuum/prosthesis behavior. There is limited understanding as to the penalty associated to energetic losses between the skeleton and the device via deformation of soft tissues. Research to understand this factor either through computer modeling or additional instrumentation of the external device would provide a more direct link between an altered locomotor strategy and device control. Specific experimental conditions to quantify these energy losses could be cycling at maximal effort to reduce the ability of the sound limb to compensate and/or one legged cycling with and without an external device or even with a split crank system (Ting et al., 1998)

## **APPENDIX A**

### **DESCRIPTION OF INSTRUMENTATION**

#### **Cycle Ergometer**

The subjects pedaled a stationary electromagnetically braked ergometer (Figure 69) (Excaliber Sport, Lode BV, Groningen, NL). The ergometer allowed for saddle height and fore-aft adjustment as well as handlebar height and fore-aft adjustment to adapt the ergometer to the each subject's preferred cycling position. The ergometer was programmed to hold constant power and would adjust the load based on the subject's cadence. Subject cadence was displayed via a tachometer mounted in front of the handlebar. The ergometer utilized a standard road bike "drop" handlebar and non-functional brake hoods were added to the handlebar to better simulate a road bike. A higher quality seat post clamp (LH Thomson co., Macon, GA) was incorporated due to repeated failure of the OEM seat post clamp as well as allow for fine tune adjustment of saddle angle (Figure 68). A moderately padded, leather wrapped saddle (Pure V, WTB USA, Mill Valley, CA) designed for mountain bike racing was consistently found to be the most comfortable saddle during pilot work and thus used for the duration of the experiments.



**Figure 68 - Electromagnetically braked cycle ergometer used.**



**Figure 69 - Micro-adjust seatpost clamp adapted to cycle ergometer.**

### **Dual Piezoelectric Element Force Pedal and Crank System**

Pedal reaction forces were recorded via dual piezoelectric element transducers mounted at the foot/pedal interface (Figure 70)(Broker & Gregor, 1990). These pedals used two Kistler type 9251 piezoelectric load cells. The signals were amplified using Kistler Dual control type 5010 amplifiers. The signal conversion for the pedal normal direction was 100 N/V and 40 N/V for the shear direction. The signal from the amplifiers would start to drift if left in a static condition. The error related to signal drift would exceed 1% if the amplifiers experienced a static load for more than 3 minutes. To minimize the effect of signal drift, the amplifiers were left in the reset mode when the subject was not cycling. The amplifiers were turned to operate while the subject was on the bicycle but were not touching the pedals. The subject was instructed to immediately clip into the pedals and start cycling. If the subject stopped pedaling for more than 2 minutes, the reset process was repeated. The pedals were statically calibrated by securing the pedal in a machinist vise and leveling the pedal. Then the amplifiers were set to operate and a load was slowly applied by stacking four ~5kg masses. The actual mass of each calibration weight was determined to the second decimal place using a calibrated scale. The load applied (~180N) was then determined by multiplying the known mass by gravity. Data were recorded at 300 Hz and the force calculated from the pedals was compared to the load applied. If a discrepancy existed, the sensitivity of the amplifiers was adjusted and the load application/removal was repeated. This process continued for each axis until changing the sensitivities of the amplifiers did not produce a change in error greater than 2% and the test could be repeated 3 times. The sensitivities and measurement error for each axis are shown in Table 31. Crank position was recorded using a gear driven continuous turn potentiometer (see section titled “Kinematic data collection”).

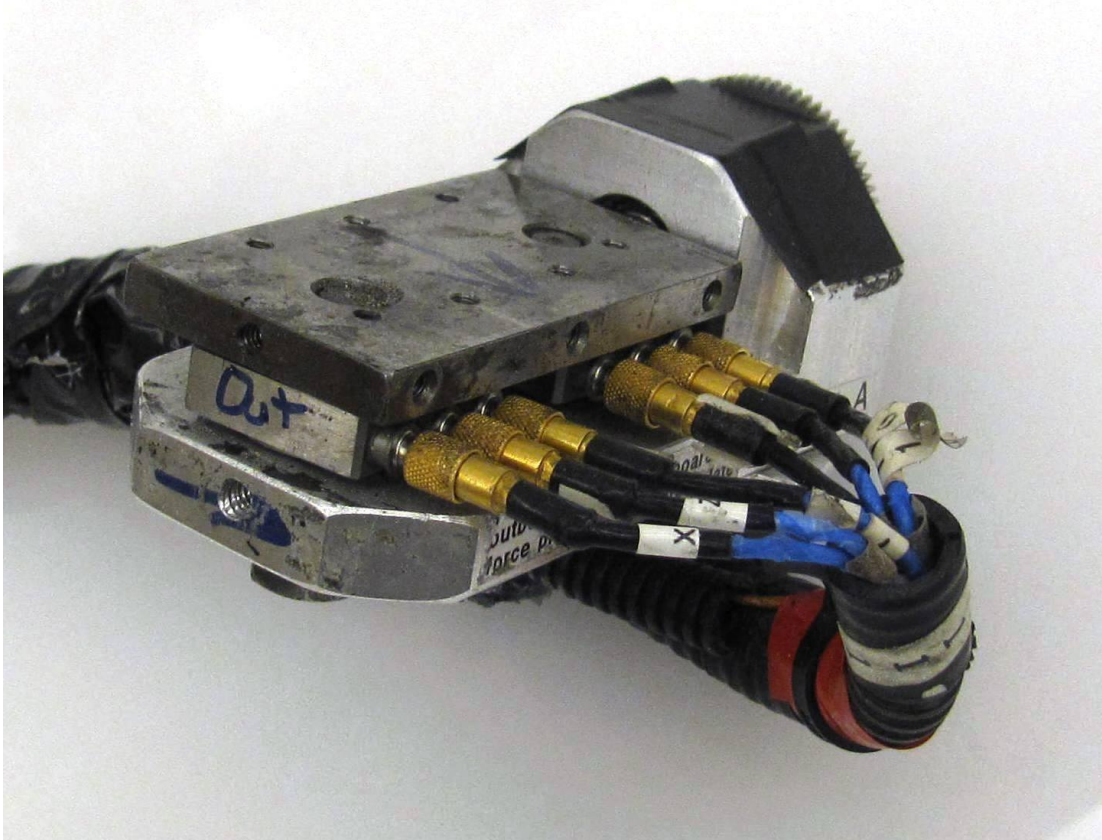


**Figure 70 - Dual piezoelectric element fore pedals**

**Table 31 - Calibration data for the dual piezoelectric element force pedals**

	Normal Direction		Shear Direction	
	Sensitivity (V/Cu)	Error in Calibration (%)	Sensitivity (V/Cu)	Error in Calibration (%)
Right Pedal	3.65	1.30	7.61	0.75
Left Pedal	3.62	1.30	7.62	0.73

The pedals were adapted for commercially available “clipless” pedal system (Shimano SPD, Shimano inc., Osaka, Japan) (Figure 71) and involved the following procedures. First, the pedal spindles and bearing were removed from the SPD pedals.

Next, the pedal bodies were setup in a vertical milling machine and as much material as possible were removed from on the medial and inferior region. An aluminum (6061-T6) adapter plate was machined and added between the SPD interfaces and the piezoelectric force pedals due to differences in bolt patterns necessary to mount the two interfaces (Figure 72). The resulting pedal system achieved a “stack height” (distance between the pedal spindle centerline and the cleat interface about the superior/inferior axis) to within 0.8 cm of the original SPD pedal body (Figure 72). Hull & Gonzalez (1990) tested “stack heights” of up to 4 cm and their results show a minimal effect on pedal forces and joint moments when stack height changed less than 1 cm.

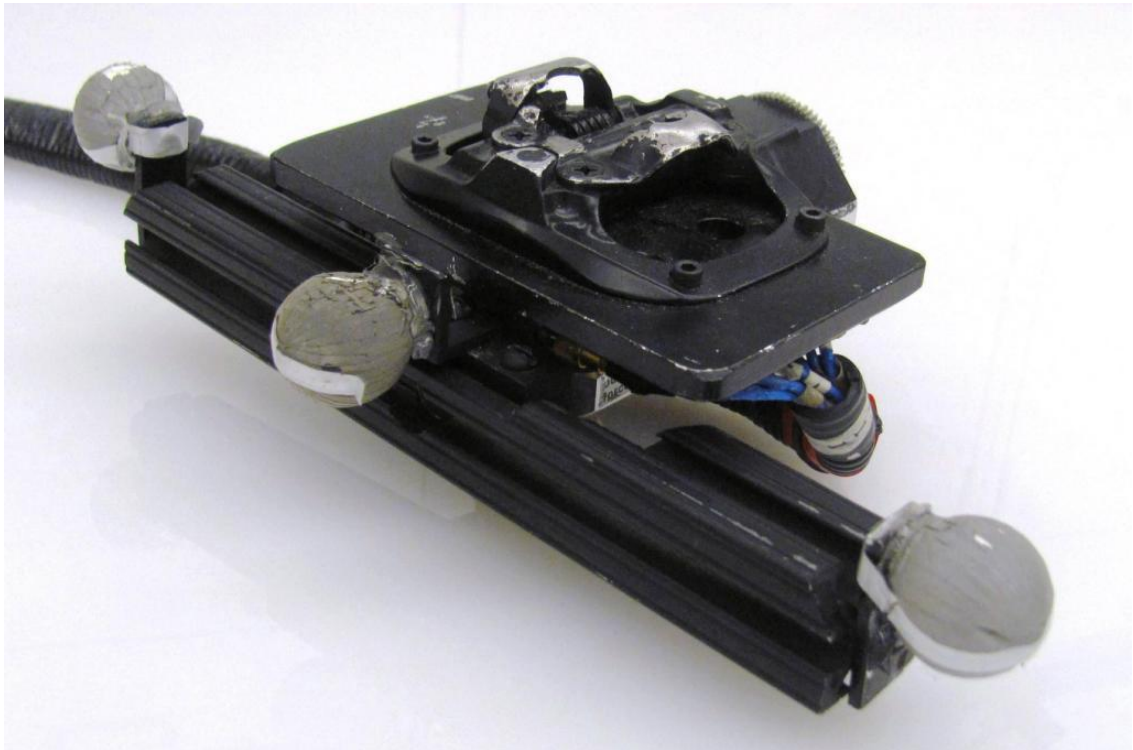


**Figure 71 - Force pedals adapted with a pedal interface that allows the user to lock into the pedals during cycling. A bracket was added to hold reflective markers necessary to calculate pedal angle.**

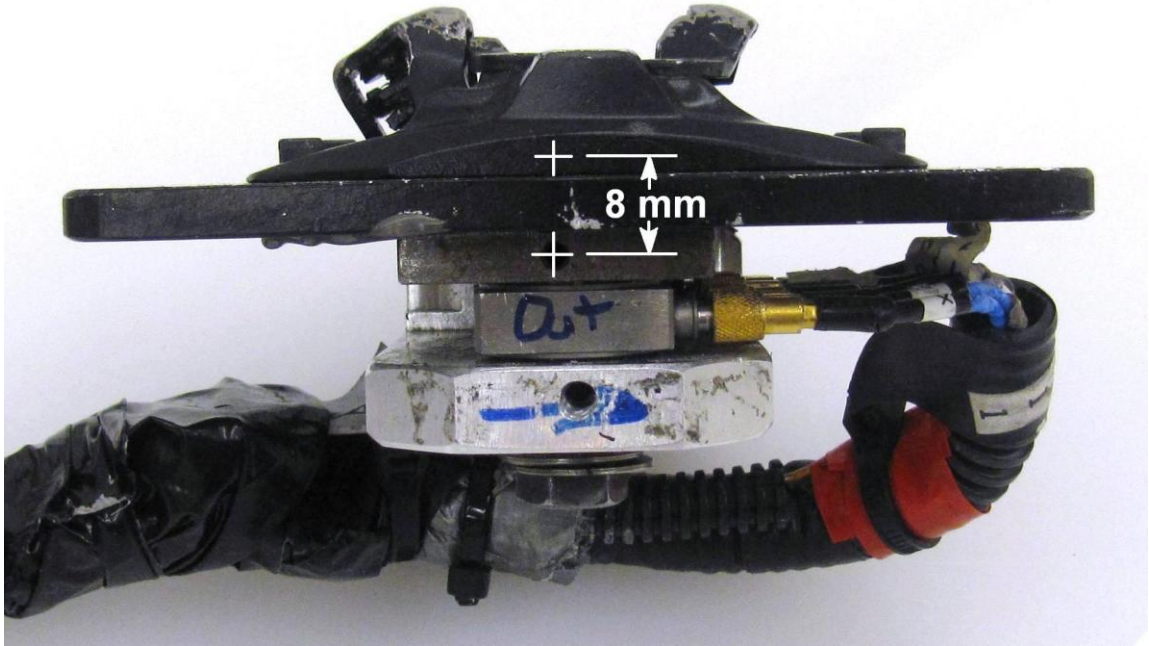


**Figure 72 – Aluminum adapter plate between force pedals and pedal interface. Note - offset of the original pedal spindle from the commercially available pedal interface to the pedal spindle of the force pedal is 8mm.**

The crank arms (Figure 73) were custom machined from billets of 6061-T6 aluminum and specialized to this pedal system. The crank arms consisted of two pieces; a crank hub and the crank arm.



**Figure 73 - Adjustable crank arms used for the experiment.**

The crank hub were machined to fit a standard 130mm bolt circle road chain rings (not needed for this experiment) and a gear on the left side crank hub was added to drive the potentiometer necessary to calculate crank position. Two bosses were machined in the lateral face of the crank hub as well as a bolt pattern that mated with the crank arm. The crank arm was slotted to fit the crank hub bosses such that 1) it aligned the crank arm relative to the crank hub and kept the crank arm 180 degrees out of phase and 2) it allows the researcher to alter crank arm length by loosening two recessed socket head cap screws, sliding the crank arm relative to the crank hub and then retightening the screws. The resulting crank hub/arm system allowed for crank arm lengths between 162 – 185mm. In addition, the crank arms were machined to offset the pedal bodies toward the longitudinal axis of the cycle ergometer. This was necessary because the design of the piezoelectric force pedal bodies offset the center of the pedal laterally and would increase pedal width if this was not accounted for. Pedal width is the distance between the longitudinal axis of the cycle ergometer and the center of the cleat interface about the medial/lateral axis commonly known (incorrectly) as “Q-factor” in popular cycling literature. The combination of the medial offset incorporated in the crank arm design as well as the machining and positioning of the SPD interfaces relative to the piezoelectric force pedal achieved a pedal width within the manufacturing specifications of a conventional road bicycle.

### **Kinematic Instrumentation**

Kinematic data was collected using a six camera infrared Peak Performance motion capture system (Vicon Motion Systems, Oxford, UK). This system was calibrated to within  $\pm 1.2$  mm. An electronic pulse was used to synchronize force, EMG and video records. Reflective markers mounted on a bracket affixed to the pedal body will be used to calculate pedal angle (Figure 71). Crank angle was determined using a gear driven continuous turn potentiometer mounted on the left crank. The potentiometer

outputs a change in voltage (related to crank position) for 340 degrees. The missing 20 degrees was recorded by a second gear driven potentiometer. The two signals were spliced together digitally using a matlab program to form one continuous line for all 360 degrees of the crank cycle. Kinematic and kinetic data were recorded and digitized using Peak Motus software (Vicon Motion Systems, Oxford, UK).

### **Surface Electromyography Instrumentation**

Surface electromyography (EMG) was collected using a 12-channel system (Myosystem 1400L, Noraxon USA Inc., Scottsdale AZ). Bi-polar electrodes spaced 2 cm apart (Noraxon Dual Electrodes #272, Noraxon USA Inc., Scottsdale AZ) were utilized with lead wires that included pre-amplifiers 2-3cm from the electrode site (Pre-Amp Lead Wire #242, Noraxon USA Inc., Scottsdale AZ). EMG data were recorded with crank potentiometer data synchronized to kinetic and kinematic data via an electronic pulse using the MyoReserach XP Master Edition software (Noraxon USA Inc., Scottsdale AZ).

## **APPENDIX B**

# **MEASUREMENT OF MOTION BETWEEN THE RESIDUAL LIMB AND THE PROSTHETIC SOCKET DURING CYCLING**

### **Introduction**

Movement between the residual limb and the prosthetic socket (pistoning) is important to understand when evaluating control of the prosthesis during activities of daily living. Excessive movement, for example, has been correlated with a decrease in prosthetic user comfort (Newton et. al., 1988). Traditional kinetic models to formally evaluate human movement, e.g. the use of inverse dynamics to calculate joint moments, do not take into account movement between the limb and socket making results from these models suspect in obtaining valid laboratory data. Thus, measurement of pistoning is important for clinical outcomes as well as studies in the biomechanics of prosthetic users.

Methods used to evaluate pistoning are generally limited to a radiographic approach (Erikson & Lemperg 1969, Newton et al., 1988, Lilja et al., 1993, Narita et al., 1997, Kahle 2002, Soderberg & Roentgen 2003, Brooks 2009, Woods et al., 2011). Radiographic methods have several limitations including 1) subjects are exposed to radiation, 2) equipment is expensive, and 3) tasks performed are either static or ones where motion is limited. In an effort to measure motion of the limb within a prosthetic socket without radiation Convery & Murray (2000) reported a method using ultrasound to in a transfemoral amputee during gait. Use of ultrasound systems to capture movement between the limb and socket is also cost prohibitive and requires tedious data reduction practices. Sanders et al. (2006) presented a compact, light-weight, low cost and non-contact photo-electric sensor that measured movement about the vertical axis during gait. Their results suggest pistoning could be as high as 40mm during normal walking Sanders

et al., 2006). A major limitation to this method was the sensor's limitation to measure movement about one axis. The distal end of the residual limb is curved and if the limb translated about the anterior/posterior direction, the curvature would be read as additional movement about the superior/inferior axis (Figure 74). As a result, Sanders et al. (2006), recommended measurement systems should measure about multiple axes to improve accuracy.

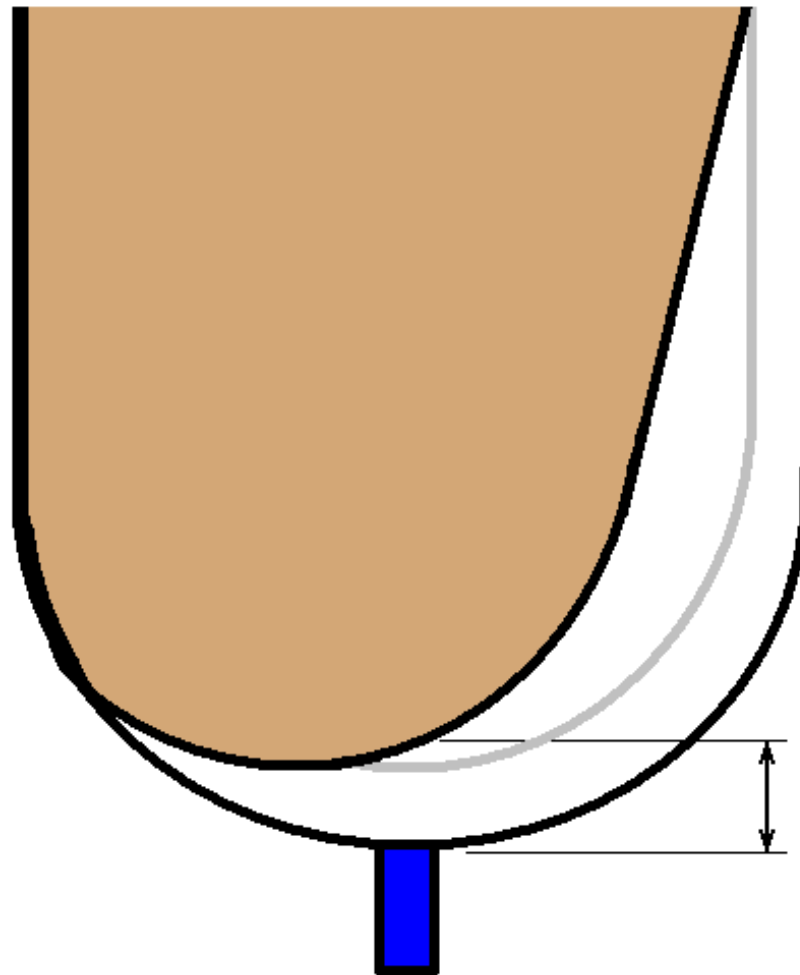


**Figure 74 – Cross sectional view of a prosthetic socket (black outline) showing how the residual limb (brown) could translate from its original position (grey outline) and be erroneously measured by the photo-electric sensor (blue) as an increase in limb pistoning.**

The purpose of this investigation was to develop and test a system to measure pistoning in the sagittal plane (2-D) without exposing the subject to radiation, used during a dynamic task, and built at low-cost. Cycling was chosen as the dynamic task in the evaluation of this system because the mechanical conditions can be better controlled than during activities such as locomotion i.e. output can be better monitored and controlled, postural control is easier to monitor, and task demands are presented more consistently. Two types of suspension design (cuff strap and pin) were tested to evaluate if limb movement would be altered by changes in location of prosthesis suspension on the limb. The pin suspension method would constrain movement of the distal end of the residual limb in the prosthesis while the cuff strap would constrain the proximal end of the residual limb.

Our general hypotheses include 1) movement of the distal portion of the residual limb relative to the prosthetic socket will have a minimal effect on joint moments calculated in the sagittal plane and 2) the cuff strap suspension design will have more distal end motion than the pin suspension design.

## **Method**

### **Development of the Limb/Socket Measurement Device**

The limb/socket measurement device (LSM) consists of an aluminum frame attached to the lateral side of the prosthetic socket (Figure 75). Two linear variable differential transformers (LVDT) with a measurement range of 100mm were aligned 90 degrees apart and attached to the frame. The LVDTs were wired into a common 5V DC source with signal output sent using BNC connectors (Figure 76).



**Figure 75 - The LSM device mounted on a prosthetic socket.**

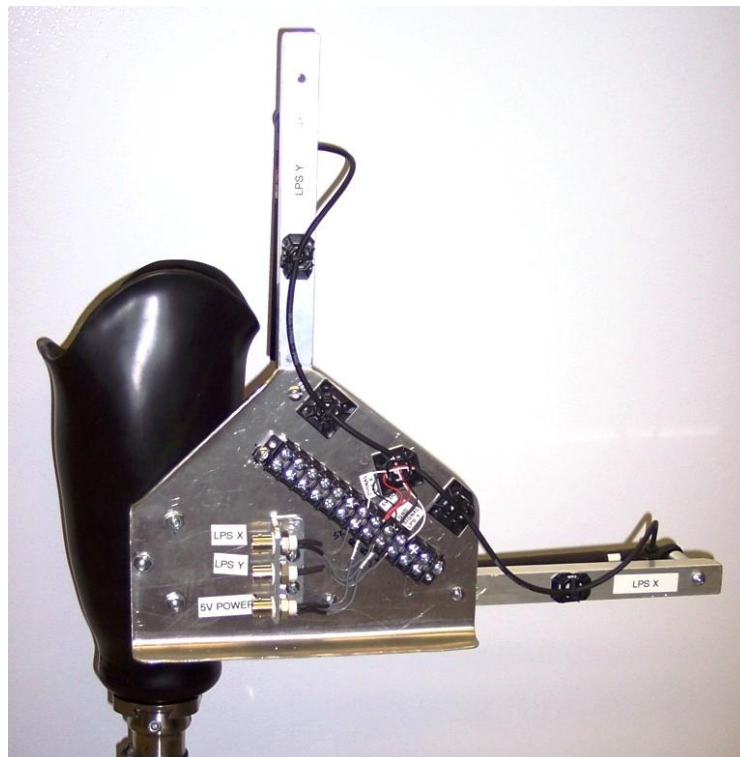


**Figure 76 - Backside of the LSM showing BNC connections for signal and device power. Note: two edges of the baseplate have been rolled to increase stiffness.**

The relationship between output voltage and length of each LVDT was determined by securing one end onto a table and the other to the spindle of a vertical milling machine with digital readout accurate to within 0.001 mm. The table was moved in 25 mm increments and the voltage recorded. The relationship between output voltage and length of the LVDT was determined using linear regression.

The LVDTs were then mounted into the LSM frame. The distance between the two endpoints of the LVDTs on the frame were measured with a digital caliper. The opposite ends of the LVDTs were attached via a machine screw to the LSM frame. The location of the floating endpoint could then be calculated relative to the frame by calculating the intersection point of two radii (those radii being the length of the LVDTs based on output voltage).

The LSM was calibrated by clamping it to the table of the milling machine and attaching the two floating endpoints of the LVDTs to the spindle. The table of the milling machine was moved in known amounts in both X and Y directions and was checked against the calculated coordinates from the LSM.

### **Experimental Protocol to test LSM**

Two subjects with uni-lateral transtibial amputation secondary to trauma (31 +/- 11 yrs, 82 +/- 15 kg) volunteered to participate in the study. Both subjects were experienced cyclists. Each subject provided separate written consent to participate in the experimental protocol approved by the Georgia Institute of Technology's Institutional Review Board.

Subjects pedaled on a stationary electromagnetically braked cycle ergometer (Excaliber Sport, Lode BV, Groningen, NL), adjusted to the subjects preferred position and adapted with piezoelectric element force pedals (Broker & Gregor, 1990). Crank angle was determined using a gear driven continuous turn potentiometer. Crank vertical or top dead center was defined as the beginning of the pedal stroke. The force pedals

were adapted with an interface (Shimano SPD road, Shimano inc., Osaka, Japan) allowing for a total of eight degrees of foot axial rotation relative to the pedal ( $\pm 4$  degrees from neutral) but would not allow translation in any other direction between the foot and pedal. Subjects received feedback on their cycling cadence via a tachometer mounted on the cycle ergometer.

The mechanical properties of the prosthesis were controlled for both subjects by having a thermoplastic prosthetic socket fabricated similar to the prosthesis used for cycling by each individual. The prosthetic socket had a hole cut into the anterior/distal portion to allow for attachment of the LSM device. The prosthetic foot was a stiff 10mm thick plate of aluminum with the cycling cleat mounted in the approximate location of the 1<sup>st</sup> metatarsal head in the sagittal plane and the approximate center of the foot in the frontal plane. The socket alignment relative to the foot was transferred from the subject's personal prosthesis via an Otto-Bock laser posture device (Otto Bock Healthcare, Duderstadt, Germany). This prosthetic design is similar to the STIFF foot condition shown to minimize pedaling asymmetries (Childers et al. in press).



**Figure 77 - Pin (left panel) and cuff strap (right panel) suspensions**

Two prosthetic suspension systems consisting of a mechanical pin/lock system (X-PSH-PLUS, PDI, Dayton OH) and a cuff strap were used in this testing (PTB cuff suspension strap, Trulife USA, Poulsbo, WA) (Figure 77). The pin suspension system

would constrain movement of the distal end of the residual limb in the prosthesis while the cuff strap system would constrain the proximal end of the residual limb. All prosthetic modifications were performed by a licensed prosthetist, including the alignment of the cuff strap.

The LSM device was aligned with the longitudinal and orthogonal axes of the prosthetic socket. The longitudinal axis of the socket was a line made through the center of the socket in the transverse plane at the level of the patella tendon and through the center of the prosthetic lock. The frame was attached to the prosthetic socket via three countersunk machine screws recessed into the lateral wall of the socket. The recessed, yet exposed, heads of the machine screws were covered with Teflon tape to smooth the inner wall of the prosthetic socket.

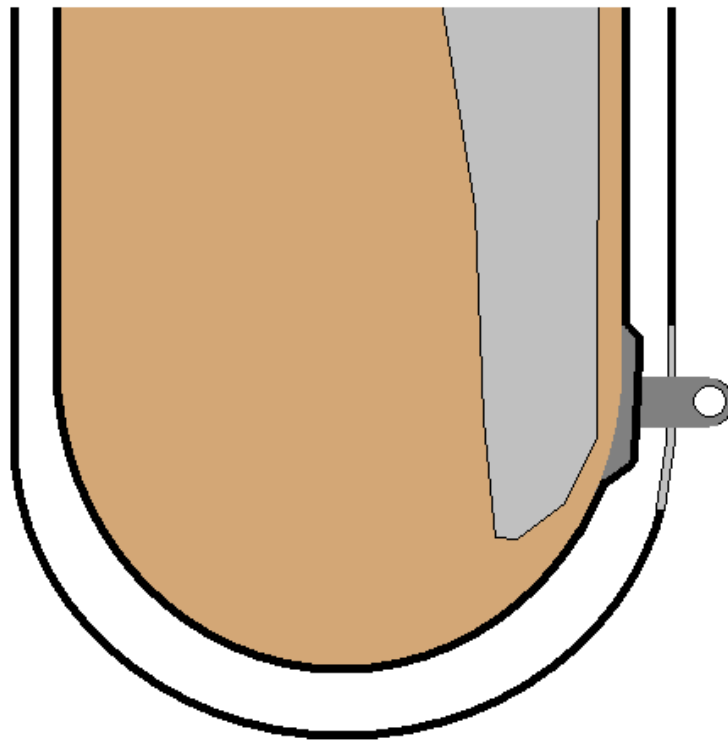


**Figure 78 - Diagram showing the location of the bracket. The bracket was taped to the skin over the distal tibia (grey) and then held in place by the silicone liner. A hole was cut into the anterior/distal portion of the socket to allow room for the bracket. The LVDTs of the LSM were connected to the bracket.**

The subject wore a small metal bracket adhered to the skin over the distal tibia that protruded through a slit cut into a prosthetic liner (Figure 78). The liner around the slit was then wrapped in sealer tape to prevent movement of the liner relative to the bracket. The opposite ends of each LVDT were connected to the bracket. Pistoning of the residual limb was calculated via the intersection of two radii. Movement was calculated relative to the minimum detected within the pedal stroke over the five pedal strokes averaged together.

The mass, center of mass, and moment of inertia for the prosthesis (with and without the LSM) and the subject's residual limb were calculated using methods outlined by Goldberg et. al. (2008). The mass, center of mass, and moment of inertia for the subject's lower limb were calculated using published regression equations (Zatsiorsky et al., 1990).

The order of suspension type was randomized. Subjects pedaled for two minutes at 150 watts with data collected at 300Hz for 10 seconds within the final 30 seconds of the two minute time of cycling at a constant cadence. Data were selected for five consecutive crank cycles, each cycle was isolated and normalized to 100 data points (% cycle), with a mean of the five cycles calculated for each variable, and finally the data were reduced into crank forces and limb/socket motion.

## **Results**

The system as calibrated using vertical milling machine had an accuracy of +/- 0.2mm within an area of 25 X 25mm.

The mass and moment of inertia was greater for the prosthesis, residual limb and LSM combination compared to the combination of just the prosthesis and residual limb (Table 32). These values were still smaller compared to the sound limb (Table 32).

**Table 32 - Mass, center of mass and moment of inertia calculations for the lower limb.**

	Mass (kg)	Center Of Mass (cm)	Moment of Inertia (kg cm <sup>2</sup> )
Prosthesis without LSM	1.3 ± 0.07	36.1 ± 6.8	320 ± 17
Prosthesis + LSM	2.5 ± 0.06	23.9 ± 1.1	463 ± 59
Residual Limb	2.0 ± 0.3	8.4 ± 0.37	79 ± 22
Prosthesis + Residual Limb	3.3 ± 0.22	19.0 ± 1.4	398 ± 38
Prosthesis + Residual Limb + LSM	4.5 ± 0.23	17.0 ± 0.21	524 ± 62
Shank + Foot of the Sound Limb	5.1 ± 0.25	28.1 ± 3.1	677 ± 19

During cycles in which pedal force magnitudes were within (X%, SD) movement of the distal residual limb throughout the crank cycle was qualitatively similar between the pin (Figure 79) and cuff (not shown to save space) suspension conditions.

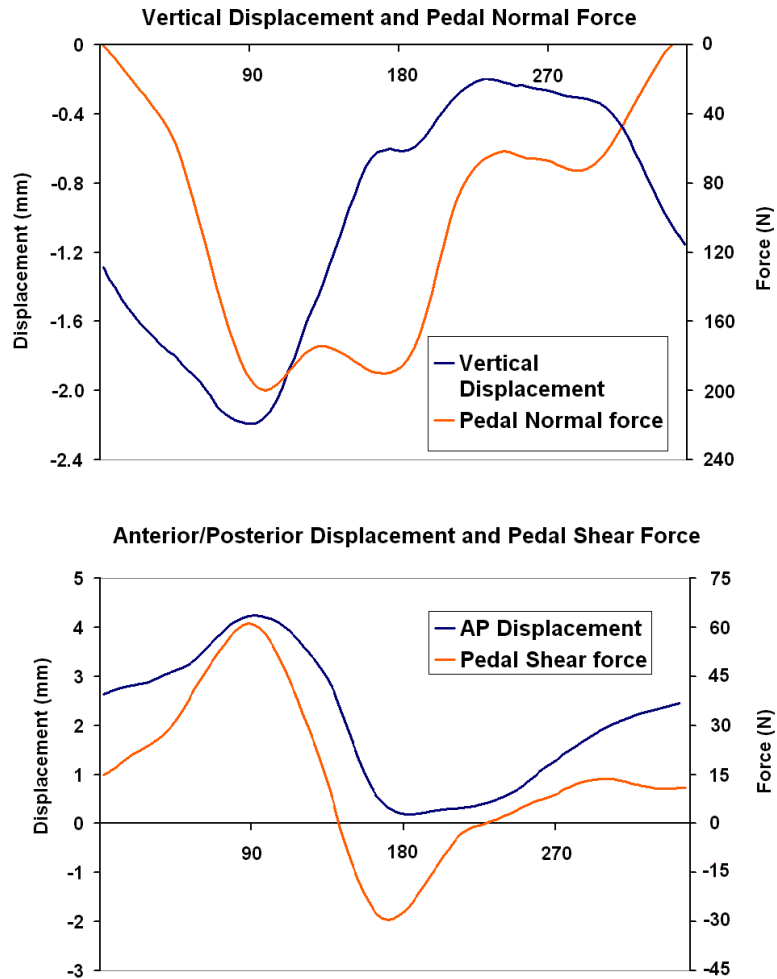


**Figure 79 - Displacement (left axis) and pedal forces (right axis) for the pin suspension. Cuff suspension displayed similar curves and is not shown to save space.**

The pin suspension produced less displacement in the superior/inferior direction (Table 33). Suspension type had no effect on the magnitude of displacement in the anterior/posterior direction.

**Table 33 - Displacement of the distal portion of the residual limb relative to the prosthetic socket.**

	Ant./Post. Movement (mm)	Sup./Inf. Movement (mm)
Pin Suspension	4.3 ± 0.7	2.0 ± 0.6
Cuff suspension	4.2 ± 1.9	4.4 ± 3.1

## Discussion

A device to measure motion between the distal end of a residual limb and a prosthetic socket was developed and evaluated. The resolution of the LSM device was greater than the measured displacements indicating the system could provide accurate measurements of the motion between the limb and the socket. In addition, the device was inexpensive, simple to manufacture and the data could be reduced using readily available software.

Movement of the distal portion of the residual limb relative to the prosthetic socket was less than 5mm in either direction regardless of suspension design. This motion is very small compared to ~ 40mm of superior/inferior (SI) motion recorded during gait (Sanders et al., 2006). The motion generally increased and decreased with pedal forces suggesting movement of the distal limb within the socket may be related to load. The pin suspension displayed a trend toward less SI motion which seems to support, in part, our 2nd hypothesis but more data are needed to more fully explain these results.

The effect of motion between the distal end of the residual limb and the prosthetic socket will have a minimal effect on the calculation of joint moments during cycling. The relatively small amount of movement recorded is similar to the accuracy of a typical multi-camera motion capture system (Cappozzo et al., 1994). In addition, an uncertainty and sensitivity analysis demonstrated the uncertainty in the calculation of joint moments is related mostly to pedal forces as long as error in the calculation of joint centers is below 13mm (see Appendix C).

The added mass of the LSM device did increase the moment of inertia but did not appreciably change the center of mass compared to a prosthesis without an LSM. The mechanical properties of the prosthesis and LSM were still less than the subject's intact limb. The potential interaction effect of inertia on the measured motion cannot be

determined with the limited data collected and are recommended as an area for future research.

This device was designed to measure gross movement of the residual limb within the prosthetic socket while radiographic based methods are able to measure the displacement of the tibia relative to the socket (Brooks 2008, Woods et al., 2011). The movement of the skin/liner relative to the tibia was shown to be ~2.5mm (Wood et al., 2011). This movement of the skin relative to the tibia would, in effect, increase the displacements measured by the LSM to ~6mm. However, this increase in displacement would still be below the displacements that would have an effect on the calculation of joint moments (Appendix C).

The position of the knee joint relative to the prosthetic socket was not measured with the LSM. Anterior/posterior translational movement of the knee relative to the prosthetic socket was noticed visually during data collection and is a common complaint among cyclists with amputation (Childers et al., 2009b). Therefore, it may be more appropriate to concentrate on knee motion relative to the prosthetic socket for future work and treat the intersection of the distal end of the residual limb and the prosthetic socket as a pseudo-joint.

### **Conclusion**

The LSM device could measure limb pistoning with high resolution in two dimensions and produced consistent results during a dynamic task. The device could measure differences between two different prosthetic suspension systems but these differences were very small. The relatively small amount of movement measured during cycling is within the typical error allowed for motion capture systems thus would not increase error associated with joint moment calculation. Future research should address movement of the knee center within the prosthetic socket and use the LSM to measure pistoning during gait.

## **APPENDIX C**

# **UNCERTIANTY AND SENSITIVITY ANALYSIS FOR THE CALCULATION OF INVERSE DYNAMICS DURING CYCLING**

### **Introduction**

The process to calculate joint moments via inverse dynamics involves combining data derived experimentally and a kinematic model (Broker & Gregor 1994). The experimentally derived data has error (and thus uncertainty) associated with the measurement. The kinematic model used includes assumptions that involve uncertainty and may have an effect on the derivation of joint moments. Uncertainty analysis offers a useful method to understand how the uncertainty in the measurement affects uncertainty in the calculated output. This can be followed with a sensitivity analysis to quantify how model input variables contribute to uncertainty in model output. A Monte Carlo simulation method can perform this analysis by assigning a probabilistic distribution to each model parameter to calculate uncertainty in model output.

Random Monte Carlo (RMC) simulation is a technique that uses random numbers generated from a probability density function as the input variables into the mathematical model. For example, if you take a thousand measurements of the same variable, the measured values could follow a normal distribution curve with a standard deviation (or probability density function). The simulation then runs the mathematical model over several hundred thousand iterations using input values that fall within the defined probability density function and records each output. These outputs are combined to form an output probability density function. The output probability density function provides information on the most common output as well as the uncertainty associated with calculating that output. The uncertainty can be measured as the standard deviation

of the output function or, if the means vary between conditions, the coefficient of variation.

The purpose of this experiment was to; 1) use the uncertainty associated with each measurement as well as the uncertainty regarding assumptions within the kinematic model to investigate the effect of different kinematic models, 2) investigate the effect of different kinematic models on the calculation of joint moments during cycling, 3) examine the relationship between error in kinematic model and error in the joint moment calculation, and 4) determine the contribution of uncertainty in the input variables to the uncertainty in the moment calculation (sensitivity analysis).

### **Method**

The general method was to 1) perform an uncertainty analysis to understand how different methods to calculate joint center of rotation (JCR) in the sagittal plane would effect the calculation of limb segment length and angles. Then use the predicted uncertainty in limb segment length and angles based on different JCRs and the uncertainties in measurement to understand the uncertainty in the calculation of ankle, knee and hip joint moments. Finally perform sensitivity analyses to understand how uncertainties in each variable contribute to uncertainty in the joint moment calculation.

### **Experimental Data**

The experimental data used for this analysis were collected on one, well trained, male cyclist (75kg, 1.83m, 32 y/o). The subject provided written informed consent. The consent forms and experimental protocol was approved by the Georgia Institute of Technology's Internal Review Board.

The subject pedaled at 150 watts and 90 rpm on an electromagnetically braked stationary cycle ergometer (Excaliber Sport, Lode BV, Groningen, NL) adjusted to the subject's preferred road cycling position. The ergometer was adapted with dual

piezoelectric element force pedals (Broker & Gregor, 1990). Data were recorded after two minutes of steady state pedaling at 300 Hz for 10 seconds using Peak Motus software (Vicon Motion Systems, Oxford, UK).

Kinematic data was collected with the kinetic data at 60 Hz using a motion capture system (Peak Performance Technology Inc.) and digitized using Peak Performance software. An electronic pulse synchronized force and video records. Reflective markers mounted on a bracket affixed to the pedal body were used to calculate pedal angle (Figure 80). Crank angle was determined using a gear driven continuous turn potentiometer. Crank vertical or top dead center was defined as the beginning of the pedal stroke. Nine markers were placed on the subject over the sacrum (midway between the two PSIS) as well as bilaterally over the greater trochanter of the femur, ASIS, lateral epicondyle of the femur, and lateral malleolus.

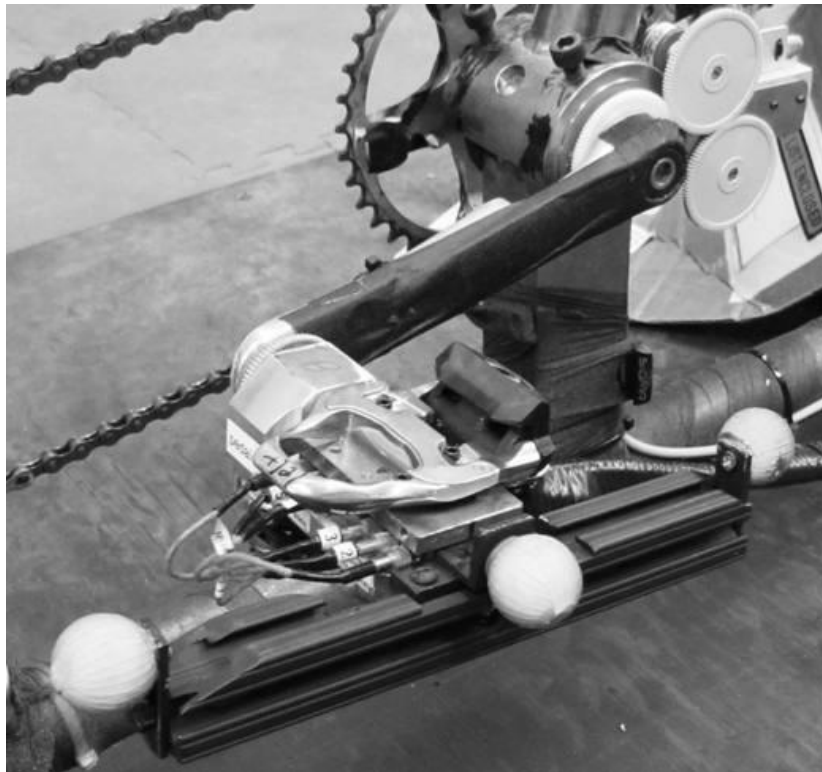


**Figure 80 - Dual element piezoelectric force pedals with the pedal interface and marker bracket shown.**

A static calibration trial was performed when the subject initially mounted the ergometer. The subject was asked to be still with the crank parallel to the ground for 10 seconds while data were collected. This information was used later to relate the static position of the greater trochanter marker (assumed to locate the center of hip joint rotation) to the sacrum and the ASIS markers. The greater trochanter marker may then be removed and its position determined by tracking the ASIS and sacrum markers.

The X-axis is defined as the longitudinal (anterior-posterior) axis of the cycle ergometer. The Z-axis is defined as the vertical (superior-inferior) axis of the cycle ergometer.

Data reduction was performed first with Peak Motus. Then the coordinate data and raw analog data were combined in custom written Matlab script (Matlab 2010b) to calculate the variables necessary for the uncertainty analysis (see below).

## **Kinematic models used**

### Ankle Joint

The kinematic model used for the ankle joint center of rotation (JCR) was based off Vaughan et al. (1999) and assumes a fixed joint center offset from the marker on the lateral malleolus of the ankle.

### Knee Joint

Two methods to calculate knee joint center were used. One assumes a fixed JCR going through the lateral epicondyle of the knee joint (Vaughan et al., 1999). The second method assumes the knee center moves along a path calculated from Smidt (1973) as the knee moves through its range of motion.

### Hip Joint

Four methods to locate the hip JCR were evaluated and described in Table 34. Data from Neptune & Hull (1995) were used to predict the variance of the bone pin and greater trochanter methods. The bone pin method was assumed to be the most accurate and thus the uncertainty in its location was based on the uncertainty in the motion system.

**Table 44 - Different assumptions on how to locate the hip joint center of rotation**

Method	Definition
Segment Length (SL) Method	Assumes a fixed JCR offset from the markers on the ASIS and Sacrum determined via a ratio to ASIS breath (Vaughan et al., 1999)
ASIS Method	Assumes a fixed JCR with offset determined via a static calibration trial relating the greater trochanter marker to the ASIS and sacrum markers. The hip JCR is then calculated based on the position of the ASIS and sacrum markers.
Bone Pin (BP) Method	Assumes a fixed JCR with the offset between the JCR and a marker array extending from a bone pin in the pelvis determined via radiograph (Neptune & Hull, 1995)
Greater Trochanter (GT) Method	Assumes a fixed JCR going through the greater trochanter marker

## Variables used for Uncertainty and Sensitivity Analysis

The necessary variables need to calculate sagittal plane joint moments during cycling, their definitions and other information are located in Table 35.

**Table 35 - Variable names to calculate joint moments via inverse dynamics**

Variable names	Definition	Obtained from
Limb Segment MOI	Mass moment of inertia (kg cm <sup>2</sup> ) of the limb segment in question	Zatsiorsky et al., 1990
Limb Segment Mass	Mass (kg) of the limb segment in question	Zatsiorsky et al., 1990
Limb Segment A	Limb Segment Angle	Calculated from marker coordinates
Limb Segment Ac	Angular acceleration of the limb segment (rad/s <sup>2</sup> )	Calculated as the second time derivative of the limb segment angle
COMAc z	Acceleration of the limb segment center of mass about the Z axis	Calculated as the second time derivative of the position of the center of mass
COMAc x	Acceleration of the limb segment center of mass about the X axis	Calculated as the second time derivative of the position of the center of mass
Limb Segment COM%	Location of the limb segment center of mass expressed as a percent of the limb segment length	Vaughan et al., 1999
Limb Segment L	Length (m) of the limb segment	Distance between joint centers and varies by JCR method
Pedal Fz	Force (N) about the Z axis	Measured via force pedals
Pedal Fx	Force (N) about the X axis	Measured via force pedals
Joint center to Force Application point	Distance from the calculated joint center to the point of force application (m)	Calculated from marker coordinates
Gravity	Acceleration due to gravity (m/s <sup>2</sup> )	Obtained from undergraduate physics lab experiment performed on campus

## Uncertainty and Sensitivity Analysis

A software package from Oracle called Crystal Ball (Fusion Edition, Release 11.1.2.0.00) embeds itself in Microsoft Excel and allows for RMC simulations for uncertainty and sensitivity analyses. Each variable were assigned a normally distributed probability distribution curve with an assigned standard deviation to define the range of the distribution curve. Each model were set to run 500,000 times and controlled to a 95% confidence level.

The motion capture system was calibrated in accordance with the manufacture specifications. The motion system calibration process would output the length of the one meter long calibration wand  $\pm$  the standard deviation. The standard deviation was 1.23mm and this was used as the uncertainty in the coordinate position of any marker. This was combined with the assumed uncertainty JCR position (Table 34) to calculate the uncertainty associated with calculating the limb segment angles needed for inverse dynamics. If there were insufficient information to determine the uncertainty of a measurement, a “standard assumption” of the standard deviation equal to 5% of the measurement was assumed sufficient.

The limb segment length and angles were calculated using basic trigonometry using the change in X and Z axes as two sides of the triangle. The uncertainty in the calculation is presented as one standard deviation from the mean in the output of the uncertainty model. This represents ~68% of the area under the distribution curve.

The uncertainties determined for the limb segment angles and lengths based on each JCR method were combined with uncertainties assumed for each variable used for the inverse dynamics model (Table 35). The joint moment for the ankle knee and hip joint were calculated in the sagittal plane using equations described by Brooker and Gregor (1994). The calculated joint moment vary throughout the crank cycle and at different joints. The average coefficient of variation (CoV) was used as the measure of

uncertainty in order to better compare across the calculated joint moments and the associated uncertainty in the output.

The relationship between uncertainty in thigh length and CoV in the hip joint moment calculation were determined by correlating those two variables together. A Pearson's correlation coefficient determined if this was a significant relationship.

**Table 36 - Uncertainty assigned to the X and Z axes for the JCR location to calculate uncertainty in limb segment angles**

<b>Method Name</b>	<b>Assigned Uncertainty (standard deviation of then normally distributed probability curve)</b>	<b>Rationale behind the assigned uncertainty</b>
Ankle Fixed JCR	± 2.9 mm	Uncertainty of marker position (1.23mm) plus uncertainty between fixed and moving ankle JCR (1.7mm) calculated from Rugg et al., (1990)
Knee Fixed JCR	± 16 mm	Uncertainty of marker position (1.23mm) plus uncertainty between fixed and moving ankle JCR (15mm) calculated from Smidt (1973)
Knee Moving JCR	± 1.23 mm	Uncertainty of marker position (1.23mm)
Segment Length (SL) Method	± 10% to the offset ratios listed in Vaughan et al., 1999	Twice the standard assumption to account for variability between the subjects used to derive these ratios and the current subject as well as variability in measurement of ASIS breath
ASIS Method	± 6.2 mm	Uncertainty of marker position on greater trochanter to actual hip JCR (5 mm) plus uncertainty of marker position (1.23mm)
Bone Pin (BP) Method	± 1.2 mm	Uncertainty of marker position (1.23mm)
Greater Trochanter (GT) Method	± 19.2 mm	Uncertainty of marker position (1.23mm) plus uncertainty between the greater trochanter marker and the hip joint (18 mm) calculated from Neptune & Hull (1995)

**Table 37 - Uncertainty assigned to each variable and the rationale behind the uncertainty used for the inverse dynamics model.**

<b>Variable name</b>	<b>Assigned Uncertainty</b>	<b>Rationale behind the assigned uncertainty</b>
Limb Segment MOI	± 5% of calculated value	Standard assumption
Limb Segment Mass	± 5% of calculated value	Standard assumption
Limb Segment A	Depends on model used	The uncertainty of this variable depended on the method used to determine JCR
Limb Segment Ac	± 9.6% of calculated value	Calculated in a separate uncertainty model using the uncertainty associated with segment length, segment mass, subject cadence
COMAc z	± 9.6% of calculated value	Calculated in a separate uncertainty model using the uncertainty associated with segment length, segment mass, subject cadence
COMAc x	± 9.6% of calculated value	Calculated in a separate uncertainty model using the uncertainty associated with segment length, segment mass, subject cadence
Limb Segment COM%	± 5% of calculated value	Standard assumption
Limb Segment L	± 3 mm	Measurement error associated with using a tape measure
Pedal Fz	± 1.5% of calculated value	Measurement error associated with this pedal system and outlined in Broker & Gregor 1990
Pedal Fx	± 1.5% of calculated value	Measurement error associated with this pedal system and outlined in Broker & Gregor 1990
Joint center to Force Application point	Varied based on limb segment and JCR model used but generally ± 2%	The uncertainty of this variable depended on the method used to determine JCR
Gravity	± 0.01 m/s <sup>2</sup>	Represents the standard deviation of the mean of 12 groups of undergraduate physics students calculating the acceleration due to gravity during a classroom lab experiment

## Results

### Uncertainty in limb segment length and angles based on JCR method

The distance between the pedal spindle and the ankle joint center was calculated as  $160 \pm 0.7\text{mm}$  and the foot angle was  $40 \pm 0.4$  degrees assuming a fixed ankle JCR.

The shank length and angle were affected by assuming a fixed or moving JCR (Table 36). The knee JCR assumption in combination with the hip JCR assumption also affected the calculation of thigh length and angle (Table 37).

**Table 38 - Uncertainty in shank length and angle based on JCR assumption**

JCR assumption	Uncertainty in Shank Length (mm)	Uncertainty in Shank Angle (degrees)
Fixed	10.3	0.91
Moving	1.8	0.42

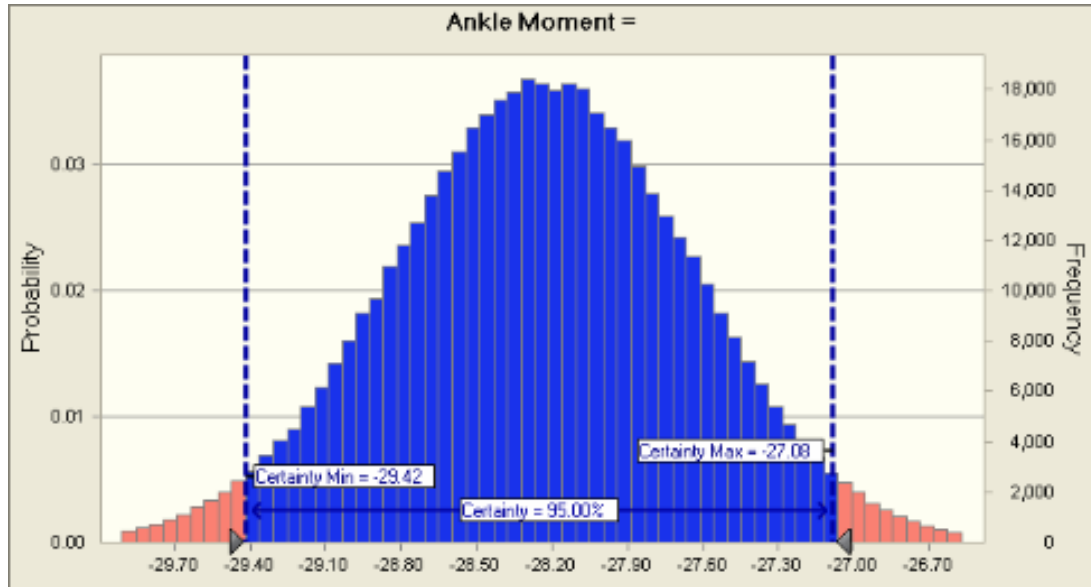
**Table 39 - Uncertainty in thigh length and angle based on knee and hip JCR assumptions. Note: the low uncertainty associated with the ASIS and Bone Pin methods when combined with the moving knee JCR assumption.**

	Uncertainty in Thigh Length (mm)		Uncertainty in Thigh Angle (degrees)	
	Fixed Knee JCR	Moving Knee JCR	Fixed Knee JCR	Moving Knee JCR
Hip JCR Method				
Segment Length (SL) Method	19.7	11.3	2.68	1.32
ASIS Method	16.5	2.69	2.38	0.47
Bone Pin (BP) Method	16.3	1.71	2.35	0.25
Greater Trochanter (GT) Method	20.3	16.0	3.36	2.42

### Uncertainty and sensitivity analysis results

Crystal Ball calculated ankle joint moment and the distribution of the all 500,000 model runs based on the uncertainty of each input variable (Figure 81). The ankle joint

moment had a coefficient of variation of 0.0211. Uncertainty associated with the pedal reaction force about the Z-axis accounted for 65.7% of the uncertainty in the ankle joint moment followed by foot angle 16.8% and the distance between the ankle joint center and the pedal spindle at 11.4%.



Statistics:	Forecast values
Trials	500,000
Base Case	-28.24
Mean	-28.24
Median	-28.24
Mode	—
Standard Deviation	0.60
Variance	0.36
Skewness	-0.0293
Kurtosis	3.00
Coeff. of Variability	-0.0211
Minimum	-31.24
Maximum	-25.57
Range Width	5.67
Mean Std. Error	0.00

**Figure 81 – An example of the output (Ankle moment) of the Crystal Ball software showing the distribution of the output as well as statistics describing the output.**

Assuming fixed knee JCR to calculate the knee joint moment resulted in a CoV of 0.089. The model was sensitive to shank angle (57.0%) and the shank length (27.8%). The moving knee JCR improved the CoV in the knee joint moment calculation to 0.047 and this model was most sensitive to shank angle (43.4%) and the ankle moment (24.2%). The uncertainty in the knee joint moment was only 1.2% sensitive to the uncertainty in the shank length when a moving knee JCR model is used.

The uncertainty in the hip joint moment calculation was affected by uncertainties in the hip and knee JCR assumptions made (Table 38) and those JCR assumptions also altered the sensitivity of those variables to uncertainty (Table 38).

**Table 40 - Uncertainty and sensitivity analysis results for the hip moment calculation based on different methods to calculated JCR**

Hip JCR Method	Coefficient of Variation		Most Sensitive Variable (%)		2nd Most Sensitive Variable (%)	
	Fixed Knee JCR	Moving Knee JCR	Fixed Knee JCR	Moving Knee JCR	Fixed Knee JCR	Moving Knee JCR
Segment Length (SL) Method	0.068	0.037	Thigh Angle (66.3)	Thigh Angle (55.6)	Thigh Length (15.2)	Thigh Length (17.3)
ASIS Method	0.061	0.022	Thigh Angle (64.4)	Knee Moment (41.2)	Knee Moment (18.2)	Thigh Angle (19.5)
Bone Pin (BP) Method	0.061	0.020	Thigh Angle (63.7)	Knee Moment (49.3)	Knee Moment (18.8)	Thigh Mass (19.7)
Greater Trochanter (GT) Method	0.080	0.057	Thigh Angle (75.4)	Thigh Angle (75.6)	Thigh Length (11.4)	Thigh Length (13.9)

There was a significant relationship between uncertainties in the thigh segment length and the hip joint moment ( $R = 0.97$ ) (Figure 82).

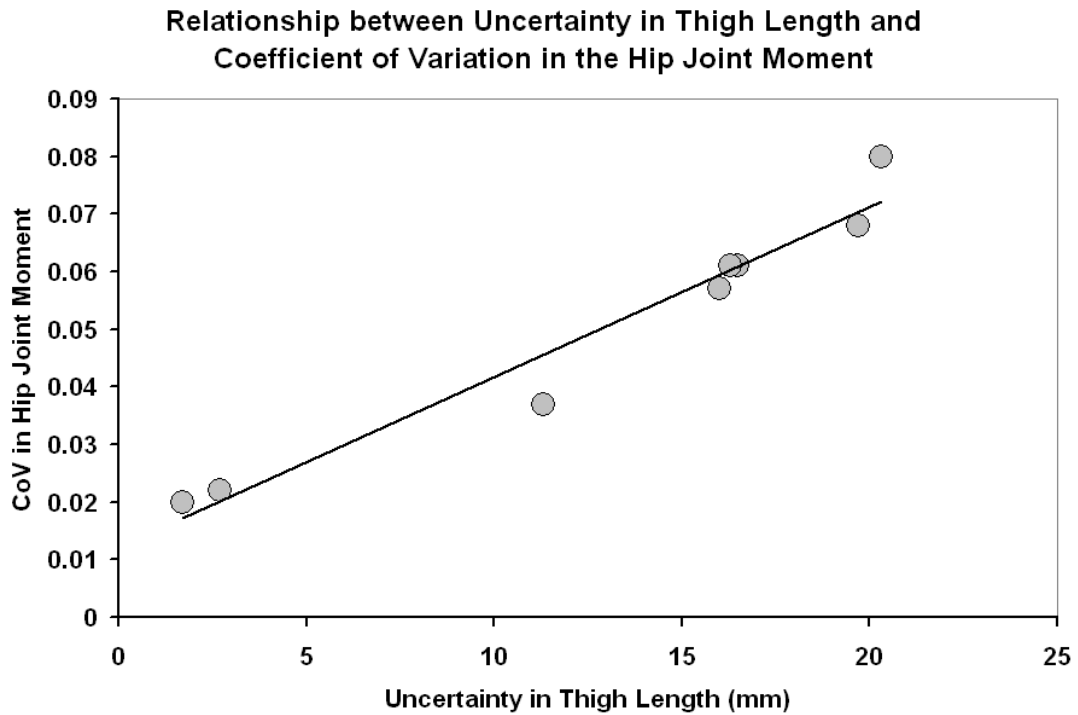


**Figure 82 - Relationship between uncertainty in thigh length and CoV in the hip joint moment calculation**

### Discussion

The major findings of the uncertainty and sensitivity analysis are 1) the fixed knee JCR increased uncertainty in the calculation of knee and hip joint moments 2) The method to calculate the hip JCR and knee JCR effected the hip joint moment and 3) the uncertainty in joint moment was related to the uncertainty in calculating limb segment length.

The assumption of a fixed ankle JCR for cycling appears reasonable given Rugg et. al., (1990) data showing relatively small variations between a fixed and moving JCR, the low CoV associated with the ankle moment calculation and the CoV for the ankle moment was largely due to the uncertainty in the reaction force measurement.

The use of a fixed knee assumption is typical for kinematic models used to calculate inverse dynamics (Vaughan et al., 1999, Broker & Gregor 1994) yet other researchers have shown the JCR of the knee joint is not fixed (Smidt 1973) and this can

have an effect of the calculation of joint moments (Holden & Stanhope, 1998). Our results also show the knee joint moment is affected by the additional error introduced by assuming a fixed knee center. The CoV in the knee moment was almost doubled when a fixed JCR was assumed. The sensitivity analysis revealed the uncertainty in the shank angle was the major driver of CoV for the knee moment yet it was less so when a moving knee JCR was assumed. In addition, the knee moment CoV was fairly insensitive to thigh length (also affected by knee JCR assumption). Taken together, these data suggest the moving knee JCR assumption should be preferred to calculate knee joint moments. The results of Smidt (1973) relate the knee JCR to the lateral epicondyle of the knee and could be used to design a formula to correct knee joint position calculated from the knee marker to actual knee JCR location.

Four methods to calculate hip JCR were evaluated with this model. The bone pin method demonstrated by Neptune & Hull (1995) in combination with a moving knee JCR assumption showed the lowest uncertainty to calculate thigh length, thigh angle and hip joint moment. However, implantation of a bone pin into the subject's pelvis is not practical for routine data collections. The ASIS method using a static calibration trail to determine the geometric relationship between the greater trochanter and the ASIS also demonstrated similar results to the bone pin method. This method can be easily incorporated into routine data collection protocols. Both the bone pin and ASIS methods demonstrate low CoV for the hip moment ( $< 0.025$ ) and the calculation was most sensitive to the knee moment not thigh angle. Therefore, it is recommended to use the ASIS method over methods relying on segment lengths or the greater trochanter marker to determine hip JCR. The combination of the ASIS method and a moving knee JCR assumption seems the most appropriate for subsequent hip joint moment calculation.

## **Conclusion**

A Random Monte Carlo simulation were preformed using Oracle Crystal Ball software to analyze the uncertainty and sensitivity of variables to calculate joint moments via inverse dynamics in the sagittal plane during cycling. Increasing uncertainty in determining the location of the joint center of rotation (JCR) increased uncertainty in the calculation of joint moments. However, it was not until uncertainty in JCR location exceeded 13mm that the joint moment was affected by greater than 5%. Therefore, it is concluded any method to locate the joint center within 13mm could be acceptable to calculate the joint moment. In order to minimize uncertainty associated with the calculation of joint moments it is recommended the researcher should 1) utilize a method to calculate a moving knee JCR based on the results of Smidt 1973 And 2) use the ASIS method to calculate the hip JCR and not to use a method that depends on estimation based on segment lengths (Vaughan et al., 1999) or tracking the greater trochanter marker during cycling.

## REFERENCES

- American College of Sports Medicine. (2006) *ACSM's Guidelines for Exercise Testing and Prescription*. 7th ed. Baltimore (MD):Lippincott Williams & Wilkins.
- Ansley L & Cangle P. (2009) Determinants of “optimal” cadence during cycling. *European J Sport Sci*. 9:61-85.
- Arbib MA, Bonaiuto JB, Jacobs S, Frey SH. (2009) Tool use and the distalization of the end-effector. *Psych Res*. 73:441-462.
- Baum BS & Li L. (2003) Lower extremity muscle activities during cycling are influenced by load and frequency. *J Electromyogr Kinesiol*. 13:181-190.
- Bieuzen F, Lepers R, Vercruyssen F, Hausswirth C, Brisswalter J. (2007) Muscle activation during cycling at different cadences: Effect of maximal strength capacity. *J Electromyogr Kinesiol*. 17:731-738.
- Broker JP & Gregor RJ. (1990) A dual piezoelectric element force pedal for kinetic analysis of cycling. *Int J Sports Biomech*. 6:394-404.
- Broker JP & Gregor RJ. (1994) Mechanical energy management in cycling: Source relations and energy expenditure. *Med Sci Sport Exerc*. 26:64-74.
- Broker JP & Gregor RJ. (1996) Cycling Biomechanics. In: Burke ER. (ed) *High-Tech Cycling 1<sup>st</sup> edition*. Champaign, IL: Human Kinetics, p. 145-166.
- Broker JP. (2003) Cycling Biomechanics: Road and mountain. In: Burke ER. (ed) *High-Tech Cycling 2<sup>nd</sup> edition*. Champaign, IL: Human Kinetics, p. 119-146.
- Brooks D. (2009) A static evaluation of transtibial prosthesis suspension. Unpublished MSPO Project, Georgia Institute of Technology, Atlanta, GA.
- Cappozzo A, Della Croce U, Fioretti S, Leardini A, Leo T, Maurizi M. (1994) Assessment and testing of movement analysis systems: spot checks. *Gait and Posture* 3:172.

- Chapman AR, Vicenzino B, Blanch P, Hodges PW. (2007) Leg muscle recruitment during cycling is less developed in triathletes than cyclists despite match cycling training loads. *Exp Brain Res* 181:503-518.
- Childers WL & Gregor RJ. (2008) Effect of cleat placement on muscle activation during cycling; A pilot study. *2<sup>nd</sup> Annual Serotta Cycling Symposium Proceedings*, Boulder, CO
- Childers WL, Hudson-Toole EF, Gregor RJ. (2009a) Activation changes in the Gastrocnemius muscle: Adaptation to a new functional role following amputation. *Med Sci Sport Exerc.* 41:S168.
- Childers WL, Kistenberg R, Gregor RJ. (2009b) The biomechanics of cycling with a transtibial amputation: Recommendations for prosthetic design and direction for future research. *Prosthet Orthot Int* 33(3):256-271.
- Childers WL, Kistenberg R, Gregor RJ. (2009c) Clinical Guidelines for Adapting the bicycle to Recreational Cyclists with Transtibial Amputation. *Proceeds of the AAOP 35th Annual Meeting and Scientific Symposium*, Atlanta, GA.
- Childers WL, Kistenberg R, Gregor RJ. (2010) Shortening the bicycle crank arm on the amputated side may reduce challenges faced by cyclists with uni-lateral transtibial amputation. *13th ISPO World Congress Proceedings*, Leipzig, Germany.
- Childers WL, Kistenberg R, Gregor RJ. (in press) Pedaling Asymmetries in Cyclists with Uni-lateral Transtibial Amputation: Effect of Prosthetic Foot Stiffness. *J Appl Biomech.*
- Childers WL, Kistenberg R, Gregor RJ. (in review) Pedaling Technique of Cyclists with Uni-lateral Transtibial Amputation. *Pros Orthot Int.*
- Convery P, Murray KD. (2000) Ultrasound study of the motion of the residual femur within a trans-femoral socket during gait. *Prosthet Orthot Int.* 24(3):226-232.
- Dingwell JB, Davis BL, Frazier DM. (1996) Use of an instrumented treadmill for real-time gait symmetry evaluation and feedback in normal and trans-tibial amputee subjects. *Prosthet Orthot Int.* 20:101-110.

- Dong H, Loomer P, Barr A, LaRoche C, Young E, Rempel D. (2007) The effect of tool handle shape on hand muscle load and pinch force in a simulated dental scaling task. *Appl Ergo.* 38:525-531.
- Erikson U, Lemperg R. (1969) Roentgenological study of movements of the amputation stump within the prosthetic socket in below-knee amputees fitted with a PTB prosthesis. *Acta Orthop Scand.* 40(4):520-529.
- Erickson MO, Nisell R, Arborelius UP, Ekholm J. (1985) Muscular activity during ergometer cycling. *Scand J Rehab Med.* 17:53–61.
- Fey NP, Silverman AK, Neptune RR. (2010) The influence of increasing steady state walking speed on muscle activity in below-knee amputees. *J Electromyogr Kinesiol.* 20:155-161.
- Fischer SL, Wells RP, Dickerson CR. (2009) The effect of added degrees of freedom and handle type on upper limb muscle activity during simulated hand tool use. *ergo.* 52(1):25-35.
- Gailey R & Harsch P. (2009) Introduction to triathlon for the lower limb amputee triathlete. *Prosthet Orthot Int.* 33(3):242-255
- Gardner SA, Martin JC, Martin DT, Barras M, Jenkins DG. (2007) Maximal torque- and power-pedaling rate relationships for elite sprint cyclists in laboratory and field tests. *Eur J Appl Physiol.* 101:287-292.
- Goldberg EJ, Requejo PS, Fowler EG. (2008) The effect of direct measurement versus cadaver estimates of anthropometry in the calculation of joint moments during above-knee prosthetic gait in pediatrics. *J Biomech.* 41:695-700.
- Gregor RJ, Cavanagh PR, LaFortune M. (1985) Knee flexor movements during propulsion: a creative solution to Lombard's paradox. *J Biomech* 18:307–316.
- Gregor, R. J., Komi, P. V., Jarvinen, M. (1987). Achilles tendon forces during cycling. *Int J Sports Med*, 8(Suppl.), 9 – 14.
- Gregor RJ, Broker JP, Ryan MM. (1991) The biomechanics of cycling. *Exerc Sport Sci Re.* 19:127–169.

- Gregor RJ, Fowler EG, Childers WL. (2011) Biomechanics of Cycling. In: Magee D, Manske R, Zachazewki J, Quillen W (ed). *Athletic and Sports Issues in Musculoskeletal Rehabilitation*. Elsevier Saunders, 187 – 216.
- Gregor RJ & Childers WL. (2011) Neuromechanics of Cycling. In: Komi PV. (ed) *Neuromuscular Aspects of Sport Performance, The Encyclopedia of Sports Medicine, An IOC Medical Commission Publication*. Wiley-Blackwell Pub. West Sussex, UK, 52 – 77.
- Heil DP, Derrick TR, Whittlesey S. (1997) The relationship between preferred and optimal positioning during submaximal cycle ergometry. *Eur J Appl Physiol* 75:160-165.
- Holden JP, Stanhope SJ. (1998) The effect of variation in knee center location estimates on net knee joint moments. *Gait and Posture*. 7:1-6.
- Hong JH, Mun MS. (2005) Relationship between socket pressure and EMG of two muscles in trans-femoral stumps during gait. *Pros Orthot Int*. 29(1):59-72.
- Hull ML & Gonzalez HK. (1990) The effect of pedal platform height on cycling biomechanics. *Int J Sport Biomech*. 6:1-7.
- Jaegers SMHJ, Arendzen JH, de Jongh HJ. (1996) An electromyographic study of the hip muscles of transfemoral amputees in walking. *Clin Orthoped Related Res*. 328:119-128.
- Juker D, McGill S, Kropf P. (1998) Quantitative intramuscular myoelectric activity of lumbar portions of the psoas and abdominal wall during cycling. *J Appl Biomech* 14:428-438.
- Kahle JT. (2002) A case study using fluoroscope to determine the vital elements of transfemoral interface design. *J Prosthet Orthot*. 14(3):121-126.
- Kapp SL. (2004) Visual Analysis of Prosthetic Gait. In Smith DG, Michael JW, Bowker JH. (Eds.), *Atlas of amputations and limb deficiencies: surgical, prosthetic and rehabilitation principles*. 3<sup>rd</sup> ed. (pp. 385-394). Rosemont, IL: American Academy of Orthopedic Surgeons.

- Kautz SA, Hull ML (1993) A Theoretical basis for interpreting the force applied to the pedal in cycling. *J Biomech* 26:155-165.
- Kautz SA, Brown DA, Van der Loos HFM, Zajac FE. (2002) Mutability of bifunctional thigh muscle activity in pedaling due to contralateral leg force generation. *J Neurophysiol*, 88:1308-1317.
- Kautz SA & Neptune RR. (2002) Biomechanical determinants of pedaling energetics: Internal and external work are not independent. *Exerc and Sport Sci Rev*, 30:159-165.
- Klodd E, Johansson JL, Farrell TR, Hanson WJ, Edell DJ, Faheem F. (2011) Electromyographic study of residual limb muscles of unilateral transfemoral amputees. *Proceeds of the AAOP 37th Annual Meeting and Scientific Symposium*, Orlando, FL.
- Korff T, Romer LM, Mayhew I, Martin JC. (2007) Effect of pedaling technique of mechanical effectiveness and efficiency in cyclists. *Med Sci Sports Exerc* 39:991-995.
- Kornecki S, Keibel A, Siemienski. (2001) Muscular co-operation during joint stabilization, as reflected by EMG. *Eur J Appl Physiol* 84:453-461.
- Kuo, A.D. (2001) A mechanical analysis of force distribution between redundant, multiple degree-of-freedom actuators in the human: implications for the central nervous system. In: Latash ML, Zatsiorsky VM. (ed) *Classics in Movement Science*. Champaign, IL: Human Kinetics, p. 663-663.
- Kristinsson O. (1993) The ICEROSS concept: a discussion of philosophy. *Pros Orthot Int*. 17:49-55.
- Laursen B, Sogaard K, Sjogaard G. (2003) Biomechanical model predicting electromyographic activity in three shoulder muscles from 3D kinematics and external forces during cleaning work. *Clin Biomech*. 18:287-295.
- Lafortune MA, & Cavanagh PR. (1983) Effectiveness and efficiency during bicycle riding. In H. K. Matsui & K. Kobayashi (eds), *Biomechanics VIII-B: International Series on Biomechanics* (pp. 928 - 936). Champaign, IL: Human Kinetics.

- Lilja M, Johansson T, Oberg T. (1993) Movement of the tibial end in a PTB prosthesis socket: A sagittal X-ray study of the PTB prosthesis. *Prosthet Orthot Int.* 17(1):21-26.
- Mizelle JC, Tang T, Pirouz N, Wheaton LA. (in press) Forming tool use representations: A neurophysiological investigation into tool exposure. *J Cognitive Neurosci.*
- Mornieux G, Stapelfeldt B, Gollhofer A, Belli A. (2008) Effects of pedal type and pull-up action during cycling. *Int J Sports Med.* 29:817-822.
- Murray JB. (2003) Efficiency of amputee cycling. Unpublished masters thesis. Univ of Colorado. Dept. of Integrative Physiology.
- Narita H, Yokogushi K, Shii S, Kakizawa M, Nosaka T. (1997) Suspension effect and dynamic evaluation of the total surface bearing (TSB) trans-tibial prosthesis: A comparison with the patellar tendon bearing (PTB) trans-tibial prosthesis. *Prosthet Orthot Int.* 21(3):175-178.
- Neptune RR & Hull ML. (1995) Accuracy assessment of methods for determining hip movement in seated cycling. *J Biomech.* 28(4):423-437.
- Neptune RR, Kautz SA, Hull ML. (1997) The effect of pedaling rate on coordination in cycling. *J Biomech.* 30(10): 1051-1058.
- Neptune RR & Hull ML. (1998) Evaluation of performance criteria for simulation of submaximal steady-state cycling using a forward dynamic model. *J Biomech Eng.* 120:334-341.
- Neptune RR & Herzog W. (2000) Adaptation of muscle coordination to altered task mechanics during steady-state cycling. *J Biomech.* 33(2):165-172.
- Nichols RT. (2002) Musculoskeletal mechanics: A foundation of motor physiology. In: Gandevia S, Proske U, Stuart DG. (ed) *Sensorimotor Control of Movement and Posture.* Kluwer Academic/ Plenum vol. XXX, p. 473-480.
- Newton RL, Morgan D, Schreiber MH. (1988) Radiological evaluation of prosthetic fit in below-the-knee amputees. *Skeletal Radiol.* 17(14):276-280.

- Norvell DC, Czerniecki JM, Reiber GE, Maynard C, Pecoraro JA, Weiss NS. (2005) The prevalence of knee pain and symptomatic knee osteoarthritis among veteran traumatic amputees and nonamputees. *Arch Phys Med Rehabil.* 86:487-93.
- Pierson-Carey CD, Brown DA, Dairaghi CA. (1997) Changes in resultant pedal reaction forces due to ankle immobilization during pedaling. *J Appl Biomech.* 13:334-346.
- Perry J. (1992) *Gait Analysis: Normal and Pathological Function.* Slack Inc. Thorofare, NJ.
- Powers CM, Rao S, Perry J. (1998) Knee kinetics in trans-tibial amputee gait. *Gait Posture.* 8:1-7.
- Prilutsky BI. (2000) Coordination of two- and one-joint muscles: functional consequences and implications for motor control. *Motor Control.* 4:1-44.
- Pruitt AL. (2004) *Andy Pruitt's complete medical guide for cyclists.* Boulder, CO: Velopress.
- Raasch CC, Zajac FE. (1999) Locomotor strategy for pedaling: Muscle groups and biomechanical functions. *J Neurophysiol* 82:515-525.
- Rossignol S. (1996) Neural Control of Stereotypical Limb Movements. In Rowell L. B. & Sheperd J. T. (ed), *Handbook of Physiology. Exercise: regulation and Integration of Multiple Systems, Section 12.* New York: Oxford Univ. Press. pp. 173-216
- Rouffet DM, Mornieux G, Zameziati K, Belli A, Hautier CA. (2009) Timing of muscle activation of the lower limbs can be modulated to maintain a constant pedaling cadence. *J Electromyogr Kinesiol* 19:1100-1107.
- Rugg SG, Gregor RJ, Mandelbaum BR, Chiu L. (1990) In Vivo moment arm calculations at the ankle using magnetic resonance imaging (MRI). *J Biomech.* 23(5):495-501.
- Ryan MM, Gregor RJ. (1992) EMG profiles of lower extremity muscles during cycling at constant workload and cadence. *J Electromyogr Kinesiol.* 2:69-80.

- Sadeghi H, Allard P, Prince F, Labelle H. (2000) Symmetry and limb dominance in able-bodied gait: a review. *Gait and Posture*. 12:34-45.
- Sanders JE, Karchin A, Ferguson JR, Sorenson EA. (2006) A noncontact sensor for measurement of distal residual-limb position during walking. *J Rehab Res & Develop*. 43(4):509-516.
- Sanderson DJ. (1990) The influence of cadence and power output on asymmetry of force application during steady-rate cycling. *J Human Mov Studies*, 19:1-9.
- Sanderson DJ, Martin PE. (1997) Lower extremity kinematic and kinetic adaptations in unilateral below-knee amputees during walking. *Gait and Posture*. 6:126-136.
- Sarre G & Lepers R. (2005) Neuromuscular function during prolonged pedaling exercise at different cadences. *Acta Physiologica Scandinavica*, 185:321–328.
- Sarre G, Lepers R. (2007) Cycling exercise and the determination of electromechanical delay. *J Electromyogr Kinesiol*. 17(5):617-621.
- Schmalz T, Blumentritt S, Reimers CD. (2001) Selective thigh atrophy in trans-tibial amputations: an ultrasonographic study. *Arch orthopaedic traum surg*, 121:307–312.
- Selles RW, Korteland S, Van Soest AJ, Bussmann JB, Stam HJ. (2003) Lower-Leg Inertial Properties in Transtibial Amputees and Control Subjects and Their Influence on the Swing Phase During Gait. *Arch Phys Med Rehabil* 84:569-577.
- Silverman AK, Fey NP, Portillo A, Walden JG, Bosker G, Neptune RR. (2008) Compensatory mechanisms in below-knee gait in response to increasing steady-state walking speeds. *Gait and Posture*. 28:602–609.
- Smidt GL. (1973) Biomechanical analysis of knee flexion and extension. *J Biomech*. 6:79-92.
- Soderberg B. (2003) Roetgen stereophotogrammetric analysis of motion between the bone and the socket in a transtibial amputation prosthesis: A case study. *J Prosthet Orthot*. 15(3):95-99.

- Ting LH, Raasch CC, Brown DA, Kautz SA, Zajac FE. (1998) Sensorimotor state of the contralateral leg affects ipsilateral muscle coordination of pedaling. *J Neurophysiol.* 80(3):1341-51.
- Ting LH, Kautz SA, Brown DA, Zajac FE. (1999) Phase reversal of biomechanical functions and muscle activity in backward pedaling. *J Neurophysiol.* 81:544 -551.
- Van Ingen Schenau GJ. (1989) From rotation to translation: Constraints on multi-joint movements and the unique action of bi-articular muscles. *Hum Move Sci* 8:301–337.
- Van Sickle Jr. JR, Hull ML. (2007) Is economy of competitive cyclists affected by the anterior–posterior foot position on the pedal? *J Biomech.* 40:1262-1268.
- Vaughan CL, Davis BL, O’Connor JC. (1999) *Dynamics of Human Gait 2<sup>nd</sup> ed.* Kiboho Pub.: Cape Town, South Africa.
- Wheeler JB, Gregor RJ, Broker JP. (1992) A dual piezoelectric bicycle pedal with multiple shoe pedal interface compatibility. *Int J Sport Biomech.* 8(3):251-258.
- Wood J, Papaioannou G, Fiedler G, Mitrogiannis C, Nianios G, McKinney R. (2011) Effect of elevated vacuum sockets on residual limb-socket motion in prolonged strenuous activities. *Proceeds of the AAOP 37th Annual Meeting and Scientific Symposium*, Orlando, FL.
- Winter DA, Sienko SE. (1988) Biomechanics of below-knee gait. *J Biomech*, 21:361–367.
- Zagorski JB, Zych GA, Latta LL, Finnieston AR. (1992) Orthotic design and application for functional treatment of tibial shaft fractures. *J Prosthet Orthot.* 4(3):126-136.
- Zatsiorsky VM, Seluyanov VN, Chugunova LG. (1990) Methods of determining mass-inertial characteristics of human body segments. In Chernyi G. G. & Regirer S. A., (Eds.), *Contemporary Problems of Biomechanics* (pp. 272-291), Boca Raton, FL: CRC.
- Zehr EP, Balter JE, Ferris DP, Hundza SR, Loadman PM, Stoloff RH. (2007) Neural regulation of rhythmic arm and leg movement is conserved across human locomotor tasks. *J Physiol.* 582:209-227.

## *Curriculum Vitae*

### **W. Lee Childers**

2305 Hosea Williams Dr., Atlanta, GA 30317  
(770)355-4184, lee@gatech.edu

---

#### **PUBLICATIONS**

---

Millard-Stafford M., **Childers W. L.**, Conger S. A., Kampfer A. J., Rahnert J. A. (2008) Recovery Nutrition: Timing and Composition after Endurance Exercise. *Current Sports Medicine Reports*. 7 (4) pg 193 – 201.

**Childers W.L.**, Kistenberg R., Gregor R.J. (2009) Biomechanics of cyclists with transtibial amputation. *Prosthetics and Orthotics International*. 33(3) 256-271.

**Childers W.L.**, Perell-Gerson K.L., Kistenberg R., Gregor R.J. (2009), Pedaling forces normalized to body weight in intact and uni-lateral transtibial amputees during cycling. In: van der Woude, L.H.V., Hoekstra, F., de Groot, S., Bijker, K.E., Dekker, R., van Aanholt, P.C.T., Hetinga, F.J., Janssen, T.W.J., Houdijk, J.H.P., editors. *Rehabilitation: Mobility, Exercise & Sports: 4th International State-of-the-Art Congress, Assistive Technology Series, Vol. 26*. IOS Press, Amsterdam, NL, 114 – 116.

Gregor R.J., Fowler E.G., **Childers W. L.** (2011) Biomechanics of Cycling. In: Magee D, Manske R, Zachazewki J, Quillen W, editors. *Athletic and Sports Issues in Musculoskeletal Rehabilitation*. Elsevier Saunders, 187 – 216.

Gregor R.J. & **Childers W. L.** (2011) Neuromechanics of Cycling. In: Komi P.V., editors. *Neuromuscular Aspects of Sport Performance, The Encyclopedia of Sports Medicine, An IOC Medical Commission Publication*. Wiley-Blackwell Pub. West Sussex, UK, 52 – 77.

**Childers W.L.**, Kistenberg R., Gregor R.J. (in press) Pedaling Asymmetry in Cyclists with Uni-lateral Transtibial Amputation and the effect of Prosthetic Foot Stiffness. *Journal of Applied Biomechanics*.

#### **PUBLICATIONS IN REVIEW or IN PROGRESS**

---

**Childers W.L.**, Kistenberg R., Gregor R.J. Pedaling Technique of Cyclists with Uni-lateral Transtibial Amputation. In review *Prosthetics Orthotics International*.

**Childers W.L.**, Perell-Gerson K., Gregor R.J. Method for Measuring Motion between the Residual Limb and the Prosthetic Socket during a dynamic task. Prepared for *Journal of Prosthetics and Orthotics*.

**Childers W.L.**, Finney D., Gregor R.J. Effectiveness of a Hinged Crank Arm for Cyclists with severe Knee Range of Motion Limitations. Prepared for *Journal Prosthetics and Orthotics*.

**Childers W.L.**, Thomas L.. Current Size and Growth of the US Lower Limb Prosthetic Market. Prepared for *Journal Prosthetics and Orthotics*.

#### **ABSTRACTS**

---

**Childers W. L.**, Kistenberg R., Gregor R. J. (2007) Pedaling asymmetry in uni-lateral transtibial amputee cyclists. *Southeastern Biomechanics Conference proceedings*, Duke University, Raleigh, NC.

**Childers W. L.,** Kistenberg R., Gregor R. J. (2007) Pedaling asymmetry in uni-lateral transtibial amputee cyclists and the effect of prosthetic foot stiffness. *12<sup>th</sup> ISPO World Congress Proceedings*, Vancouver, BC, Canada; pg 475.

**Childers W. L.,** Kistenberg R., Gregor R. J. (2008) Pedaling asymmetry in uni-lateral transtibial amputee cyclists; Implications for rehabilitation. *2<sup>nd</sup> Annual Serotta Cycling Symposium Proceedings*, Boulder, CO.

**Childers W. L.,** Gregor R. J. (2008) Effect of cleat placement on muscle activation during cycling; A pilot study. *2<sup>nd</sup> Annual Serotta Cycling Symposium Proceedings*, Boulder, CO.

**Childers W. L.,** Gregor R. J. (2008) Effect of seat tube angle on muscle activation during cycling; A pilot study. *2<sup>nd</sup> Annual Serotta Cycling Symposium Proceedings*, Boulder, CO.

**Childers W.L.,** Kistenberg R., Gregor R.J. (2008) Pedaling Asymmetry in Cyclists with Uni-lateral Transtibial Amputation and the effect of Prosthetic Foot Stiffness. *Proceeds of the AOPA National Assembly*, Chicago, IL.

**Childers W.L.,** Kistenberg R., Gregor R.J. (2009) Pedaling Asymmetry in Cyclists with Uni-lateral Transtibial Amputation and the effect of Prosthetic Foot Stiffness. *Proceeds of the AAOP 35<sup>th</sup> Annual Meeting and Scientific Symposium*, Atlanta, GA, USA, March 4<sup>th</sup> – 7<sup>th</sup>, 2009.

**Childers W.L.,** Kistenberg R., Gregor R.J. (2009) Clinical Guidelines for Adapting the bicycle to Recreational Cyclists with Transtibial Amputation. *Proceeds of the AAOP 35<sup>th</sup> Annual Meeting and Scientific Symposium*, Atlanta, GA, USA, March 4<sup>th</sup> – 7<sup>th</sup>, 2009.

**Childers W.L.,** Hudson-Toole E. F., Gregor R.J. (2009) Activation changes in the Gastrocnemius muscle: adaptation to a new functional role following amputation. *Medicine and Science in Sport and Exercise* 41:S168.

**Childers W.L.,** Kistenberg R., Gregor R.J. (2011) Motor Control of Persons with Amputation. *Proceeds of the AAOP 37<sup>th</sup> Annual Meeting and Scientific Symposium*, Orlando, FL, USA, March 18<sup>th</sup>, 2011.

**Childers W.L.,** Perell-Gerson, K.L., Gregor R.J. (2011) Method to Measure Motion Between the Residual Limb and the Prosthetic Socket. *Proceeds of the AAOP 37<sup>th</sup> Annual Meeting and Scientific Symposium*, Orlando, FL, USA, March 18<sup>th</sup>, 2011.

**Childers W.L.,** Gallagher T.P. Gregor R.J. (2011) Modeling Optimal Pacing Strategies for the Individual Pursuit. *Proceeds of the ACSM 58<sup>th</sup> Annual Meeting*, Denver, CO, USA, May 27<sup>th</sup> – 30<sup>th</sup>, 2011 (in press).

## INVITED PRESENTATIONS

---

Pedaling asymmetry in uni-lateral transtibial amputee cyclists. *Southeastern Biomechanics Conference*, Duke University, Raleigh, NC; April 20<sup>th</sup> 2007

Pedaling asymmetry in uni-lateral transtibial amputee cyclists and the effect of prosthetic foot stiffness. *12<sup>th</sup> ISPO World Congress*, Vancouver, BC, Canada; August 2<sup>nd</sup>, 2007

Pedaling asymmetry in uni-lateral transtibial amputee cyclists; Implications for rehabilitation. *2<sup>nd</sup> Annual Serotta Cycling Symposium*, Boulder, CO; January 30<sup>th</sup>, 2008

Effect of cleat placement and seat tube angle on muscle activation and pedaling kinetics. *2<sup>nd</sup> Annual Serotta Cycling Symposium*, Boulder, CO; January 30<sup>th</sup>, 2008

Biomechanics of Cyclists with Amputation. *1<sup>st</sup> Annual Getting2Tri National Training Camp*, Atlanta, GA; March 15<sup>th</sup>, 2008

Pedaling Asymmetry in Cyclists with Uni-lateral Transtibial Amputation and the effect of Prosthetic Foot Stiffness. *AOPA National Assembly*, Chicago, IL; September 13<sup>th</sup>, 2008

Pedaling Asymmetry in Cyclists with Uni-lateral Transtibial Amputation and the effect of Prosthetic Foot Stiffness. Thranhardt lecture series of the AAOP 35<sup>th</sup> Annual Meeting and Scientific Symposium, Atlanta, GA, USA, March 5<sup>th</sup>; 2009

Clinical Guidelines for Adapting the bicycle to Recreational Cyclists with Transtibial Amputation. AAOP 35<sup>th</sup> Annual Meeting and Scientific Symposium, Atlanta, GA, USA; March 6<sup>th</sup>, 2009

Biomechanics of Cyclists with Amputation; Factors to improve Performance. 2<sup>nd</sup> Annual Getting2Tri National Training Camp, Atlanta, GA; March 20<sup>th</sup>, 2009

Pedaling forces normalized to body weight in intact and uni-lateral transtibial amputees during cycling. 4th International State-of-the-Art Congress "Rehabilitation: Mobility, Exercise & Sports", Amsterdam, NL; 7<sup>th</sup>, 2009

Activation changes in the Gastrocnemius muscle: adaptation to a new functional role following amputation. ACSM 56<sup>th</sup> Annual Meeting, Seattle, WA, USA, May 29<sup>th</sup>; 2009

Biomechanics of Cycling with an Amputation: Recommendations for the Clinician and Direction for Future Research. New England chapter of AOPA Annual Meeting, Manchester, NH, USA; October 15<sup>th</sup>, 2009

Biomechanics of Cyclists with Amputation; Factors to improve Performance. 3<sup>rd</sup> Annual Getting2Tri National Training Camp, Atlanta, GA; March 19<sup>th</sup>, 2010

Biomechanics of Cycling for Bike Geeks; Going from Zero to Hero with the turn of a Hex Key. Georgia Institute of Technology, Atlanta, GA; January 18<sup>th</sup>, 2010

The Current Size and Future Trends of the US Prosthetic Market. Hanger Educational Fair, Reno, NV, Feb 4<sup>th</sup>, 2011.

Motor Control of Persons with Amputation. *Proceeds of the AAOP 37<sup>th</sup> Annual Meeting and Scientific Symposium*, Orlando, FL, USA, March 18<sup>th</sup>, 2011.

Method to Measure Motion Between the Residual Limb and the Prosthetic Socket. *Proceeds of the AAOP 37<sup>th</sup> Annual Meeting and Scientific Symposium*, Orlando, FL, USA, March 18<sup>th</sup>, 2011.

Modeling Optimal Pacing Strategies for the Individual Pursuit. *Proceeds of the ACSM 58<sup>th</sup> Annual Meeting*, Denver, CO, USA, May 27<sup>th</sup> – 30<sup>th</sup>, 2011 (in press).

---

## VOLUNTEER WORK

---

Cycling for People with Amputation. 1<sup>st</sup> Annual Getting2Tri National Training Camp, Atlanta, GA; March 15<sup>th</sup>, 2008

Bob Gailey's Amputee Running Clinic. Amputee Coalition of America National Meeting, Atlanta, GA June 21<sup>st</sup>, 2008

Cycling for People with Amputation. 2<sup>nd</sup> Annual Getting2Tri National Training Camp, Atlanta, GA; March 20<sup>th</sup>, 2009

Bob Gailey's Amputee Running Clinic. Amputee Coalition of America National Meeting, Atlanta, GA June 20<sup>th</sup>, 2009

Amputee Bicycling Fitting Clinic. Walter Reed Army Medical Center, Washington DC, February 24<sup>th</sup>, 2010

Cycling for People with Amputation. 3<sup>rd</sup> Annual Getting2Tri National Training Camp, Atlanta, GA; March 19<sup>th</sup>, 2010